University of East Anglia

Synthesis of novel symmetrical and unsymmetrical aza BODIPY analogues.

Budur Nuwayji Alanazi

A thesis submitted to: School of chemistry, University of East Anglia

in fulfilment of the requirements for the degree of Doctor of Philosophy

March 2023

Declaration

The research described in this thesis is, to the best of my knowledge, original except where due reference is made.

Budur N Alanazi

2023

Abstract

This thesis is focused on the expansion of the synthetic study of aza (dibenzo) BODIPY analogues. It describes a more detailed investigation of the formation of the precursor aminoisoindolines using reaction of alkyl and benzyl acetylenes with bromo benzamidine under microwave conditions. Treating the amidine with 1-hexyne under Sonogashira copper-free cross coupling reaction conditions led to unexpected formation of the six-member ring compound, 3-butyl isoquinoline-1-amine was isolated in 31% yield. However, using aryl acetylene in the synthesis of the precursor aminoisoindolines successfully produced the required 5-member ring compounds (aminoisoindolines) in good yield. Therefore, a variety of new symmetrical and unsymmetrical aza BODIPYs and their precursors aza (dibenzo) dipyrromethenes bearing electron withdrawing or electron donating substituents have been smoothly synthesised and isolated in good yield. Initially the synthesis of unsymmetrical analogues was achieved using simple mixed condensation reactions. Approximately statistical mixtures were produced when the precursor aminoisoindolenes were electronically similar. However, when they were different, the reaction favoured the formation of the two symmetrical derivatives. Consequently, a new synthetic procedure has been developed to control the synthesis of unsymmetrical analogues by converting of the amino group of one aminoisoindoline into good leaving groups such as triflate or tosylate. This successfully led to favour formation of the unsymmetrical aza (dibenzo) dipyrromethenes with reaction yields of up to double those obtained via the mixed condensation synthetic method (50% - 64%).

Complexation of symmetrical and unsymmetrical aza (dibenzo) dipyrromethenes with $BF_3.OEt_2$ was successfully optimized by treating the mixture with TMS-Cl to remove the fluoride ion which led to shift the equilibrium towards the target aza BODIPYs with remarkable improvement in the outcome.

The final part of the thesis describes attempts to cyclise aza dipyrromethenes to form porphyrin-like macrocycles. Unfortunately, these attempts were unsuccessful due to a combination of low reactivity and isomerisation of the precursors in the presence of any metal.

This thesis is dedicated to my beloved mother.

Acknowledgements

First and foremost, I would like to give thanks to the almighty Allah for giving me the strength, knowledge, and the ability to complete this project satisfactorily.

I would also like express my deepest gratitude to my supervisor, Prof. Andrew N. Cammidge for his unlimited support during my PhD. I am very grateful to him for his advice, invaluable supervision and patience he has given me during the past years.

I would also like to extend my thanks to Dr. Isabelle Fernandes for her time, advice and support. Also, I would like to thank Prof. Richard Stephenson, and Dr. Maria Paz Muñoz-Herranz for their valuable comments. I would also like to acknowledge Dr. David Hughes, and Dr Atheer Madlool for their help in the X-Ray crystallography service. I would also thank the examiners Prof. Jon Preece (University of Birmingham), and Dr Rianne Lord (UEA) for their time.

A special and massive thanks to my beloved husband, Mr Khalid for all his love, kindness, and unlimited support that he has shown to me during the last years, he was always stood by my side through the good times and bad. There are no adequate words to thank him, I will be grateful for him forever. I am exceedingly grateful to my little angels Rivanna, Omar, and Mishaal, they are the greatest gift from Allah to me, they are always bringing joy to my life, and taught me to always smile.

I am also deeply grateful to my parents, and my brothers and sisters for their unconditional love, and continuous encouragements, they have been always close to me despite the distance.

I would like to acknowledge all the past/current members of Cammidge's group, I deeply appreciate the time that we worked together at the lab, and the experience they shared with me during the last four years.

I am very grateful to the Princess Nourah Bint Abdul Rahman University for the opportunity to study in the UK, and the Embassy of Saudi Arabia for the funding of my PhD degree.

List of abbreviations

Abs	Absorption
aq.	Aqueous
Ar	aromatic/ aryl
AcOEt	ethyl acetate
b.p	boiling Point
BINAP	2,2′-bis(diphenylphosphino)-1,1′-binaphthyl
Bu	butyl
Conc.	Concentrated
°C	Celsius
d	doublet
dd	doublet of doublets
DBU	1,8-diazabicyclo [5.4.0] undec-7-ene
DCM	Dichloromethane
DMF	N, N-dimethylformamide
DMSO	Dimethyl sulfoxide
eq.	Equivalent
h	Hour
Hz	Hertz
IR	Infrared
J	coupling constant in NMR spectroscopy
λ	lambda (wavelength)
m	Multiplet
MALDI	matrix assisted laser desorption ionisation
m.p	melting point
Me	Methyl
mmol	milli mole
mol	Mole
MS	mass spectrometry
MW	Microwave
OMe	Methoxy
OPh	Phenoxy

OTf	triflate, trifluoro methane sulfonate
PE	petroleum ether
PDT	photodynamic therapy
Ph	Phenyl
ppm	parts per million
py	Pyridine
Rf	retention factor
rt	room temperature
s	Singlet
SubTBDAP	Sub tri benzo di aza porphyrin
TBDAP	Tetra benzo di aza porphyrins
TBTAP	Tetra benzo tri aza porphyrin
t	Triplet
t-Bu	tertiary butyl
THF	Tetrahydrofuran
TLC	thin layer chromatography
UV/Vis	Ultraviolet/Visible spectroscopy
δ	chemical shift in parts per million (ppm)
ε	molar extinction coefficient
λ	Wavelength

Contents

list of figures

list of schemes

List of tables

Chapter 1: Introduction and Literature review

1.0. Introduction of BODIPYs

BODIPY (4-bora-3a,4a-diaza-s-indacene)[1, 2] is a class of fluorescent dyes also referred to as boron dipyrrin or boron dipyrromethene.[3] This class of compounds was first reported by Treibs and Kreuzer in 1968.[1] However, it was towards the end of the 1980s that it began to attract attention and by 1990s was a booming and successful area of research.[4] A range of physical and chemical properties of BODIPY dyes make them excellent for optimal laser performance.[5] They are chemically robust, have a high thermal resistance, low photodegradation and high solubility in most organic solvents [5, 6] Moreover, they possess an interesting photophysical signature.[7] They usually display strong absorption in the visible region and bright fluorescence spectral bands often in the green-yellow part of the visible spectrum.[8] Their absorption and emission bands tend to be relatively sharp resulting in creating pure colours with molar absorption approaching 10^5 M^{-1} cm^{-1},[8] high fluorescence quantum yields, and excellent photochemical stabilities,[9] in addition to facile synthesis and structural versatility.[10] BODIPY cores consist of two pyrrole units linked via a methine bridge at the 2 position as well as via a boron atom co-ordinated to each of the pyrrole nitrogen heteroatoms, structure **2** (Figure 1.1).[11, 12] The IUPAC name and the numbering system of the BODIPY structure **2** is based on the s-indacene structure **3** (Figure 1.1, **A**) and not dipyrromethene **1** which it resembles. As in the related porphyrin structures the *meso*-position refers to the central 8-position.[13] Figure 1.1 **A** shows the numbering system for BODIPY structures, which was derived from indacene. This numbering system differs to that used for dipyrromethenes, however the α, β, and *meso* positions are defined in the same way.[13]

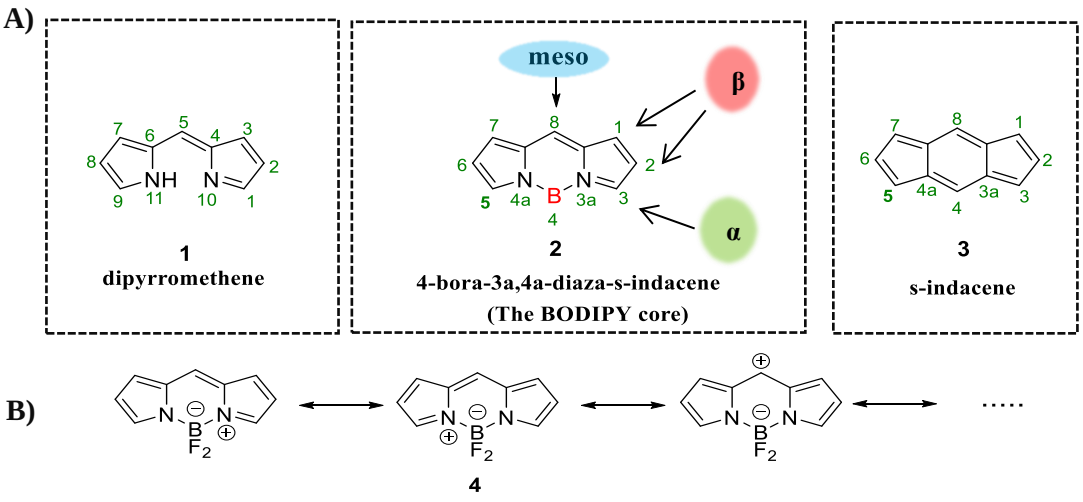

Figure 1.1: A) Structure of dipyrromethene, IUPAC numbering, and **B)** the resonance of the BODIPY core.[14]

The formal structure of a BODIPY dye is a complex, composed of a central disubstituted electron-deficient boron surrounded by a monoanionic dipyrromethene ligand. The boron dipyrrin core is overall neutral but contains a formal positive charge delocalized over the ring structure while the formal negative charge locates on the boron atom.[7] Thus, it is formally a betaine compound **4** (Figure 1.1, **B**) however unlike most betaines it relatively nonpolar in nature hence the formal charges are not depicted on the structures, it is possible to explain the reactivity of the BODIPY core by using the resonance structures (Figure 1.1, **B**).[14] The BODIPY parent core, known as "the little sister of porphyrin", is a particular intriguing structure as the boron difluoride BF_2 complexes a fragment of a hybrid porphyrin macrocycle.[15]

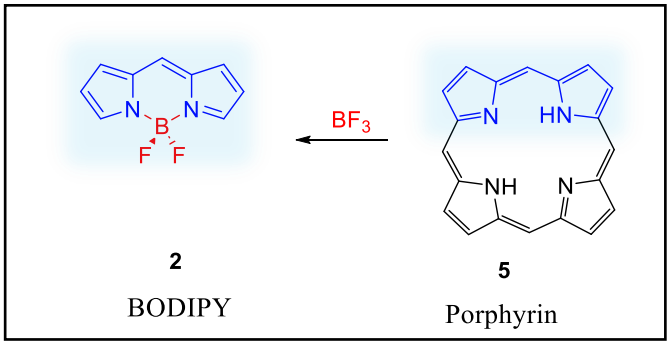

Figure 1.2: Structure of BODIPY **2** and Porphyrin unit **5**.

The absorption and emission wavelengths for classical BODIPY chromophores lie in the range 470–530 nm.[11] This limits their application as activity in the far-red or NIR region would be more useful in a number of applications including biological imaging. Also, BODIPY derivatives have some undesirable characteristics for many applications in biotechnology, particularly their small Stokes of approximately 10 - 30 nm.[11] A variety of strategies have therefore been developed to access BODIPYs that emit in the far-red or NIR region, and to obtain BODIPY dyes with large Stokes shifts and high quantum yields by a range of structural modifications of the BODIPY core.[11, 16] These include, replacement of the meso-carbon of the BODIPY by a nitrogen atom to form the analogous aza-BODIPY dyes (Figure 1.3 **A**).[17] In addition to a variety of extensions of the π conjugation such as functionalization of α-positions of the pyrrole rings by introduction of diaryl substituents, vinyl, styryl and aryl ethynyl substituents at the α-positions 3, 5 position of the BODIPY unit.[18] However, it should be noted that some of these changes decreased the fluorescence quantum yields and this may be attributed to nonradiative energy loss due to spinning motions about the C-aryl single bonds[19] (i.e. a possible rationale for this is that energy loss because of the rotation about the C-aryl

single bonds of the aromatic substituents).[19] Furthermore some systems such as the bis-styryl derivatives decreased the (photo)- chemical stability as they are prone to photooxidation[20] (example is shown in Figure 1.3 **B)**. An example or a different modification, rigidification of rotatable moieties, is shown in Figure 1.3 **C**.[21] Functionalization of 3,5 position with electron donating substituents (push) group on the BODIPY unit (behaving as electron deficient (pull) group) causes push−pull effect within the molecule (Figure 1.3 **D**).[22] Another modification strategy has been developed towards the extension of the π conjugation by the annulation of aryl moieties on the pyrrole ring.[23] Depending on the position of the aromatic ring fusion, i.e. [b]-bond or [c]-bond, two isomeric structures can be identified (Figure. 1.3 **E** and **F**). This not only alters the absorption but also provides a more rigid aromatic core.[20]

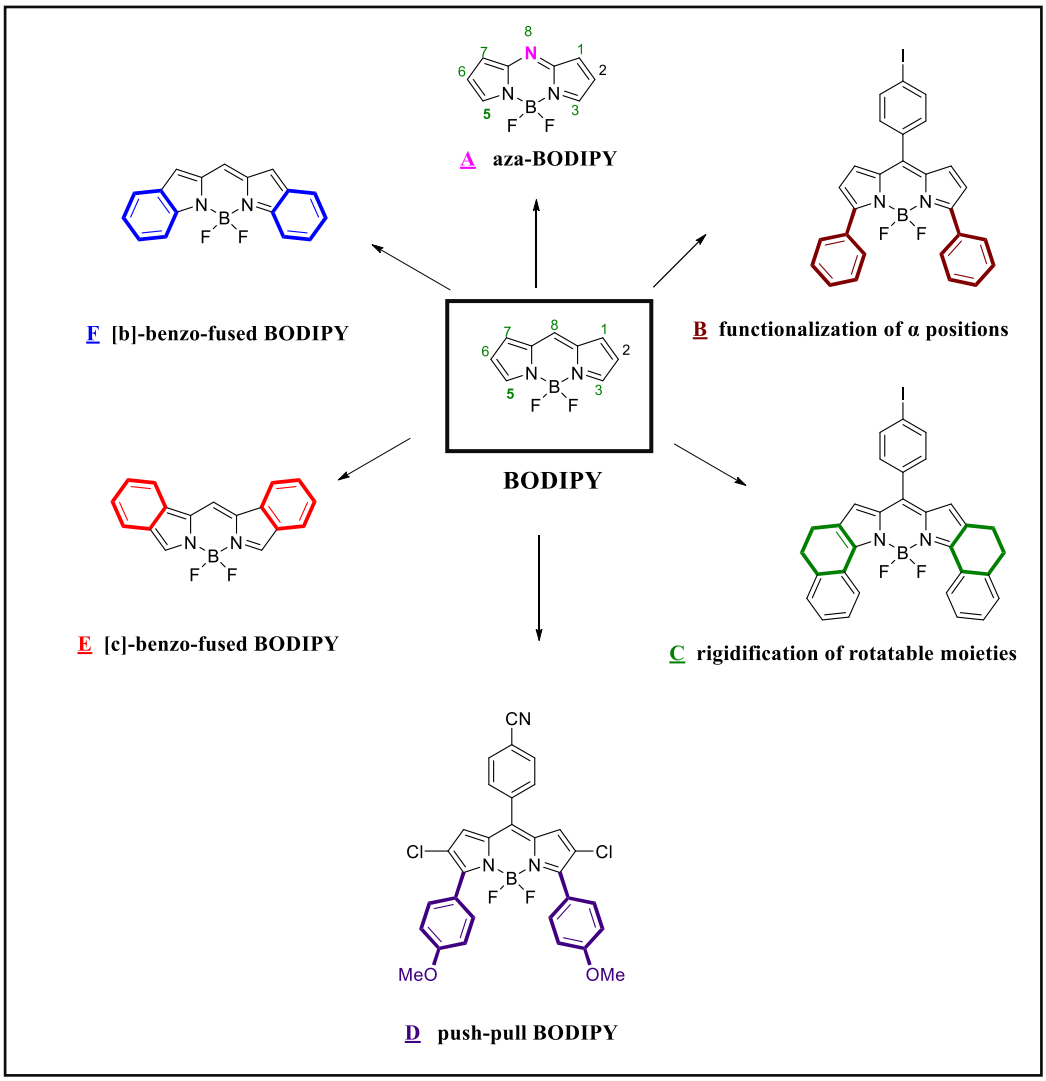

Figure 1.3: Modification examples to BODIPY unit.

Table 1.1 illustrates some examples from the literature that demonstrate the effect of structural modification of BODIPY derivatives on the absorption and emission wavelengths.[20, 23]

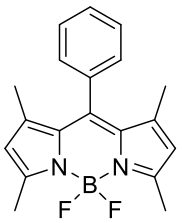	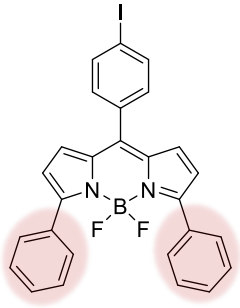	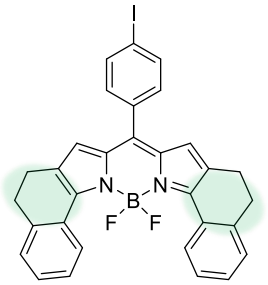
λ_{max} abs = 498 nm MeOH λ_{max} em = 508 nm MeOH	λ_{max} abs = 555 nm $CHCl_3$ λ_{max} em = 588 nm $CHCl_3$	λ_{max} abs = 634 nm MeOH λ_{max} em = 588 nm MeOH
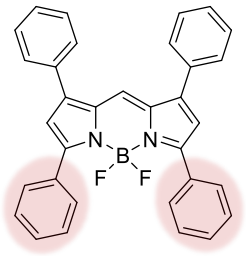	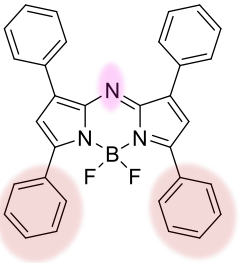	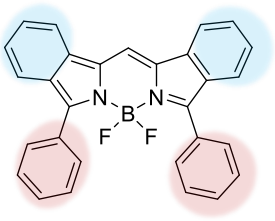
λ_{max} abs = 564 nm MeOH λ_{max} em = 593 nm MeOH	λ_{max} abs = 650 nm $CHCl_3$ λ_{max} em = 672 nm $CHCl_3$	λ_{max} abs = 634 nm MeOH λ_{max} em = 658 nm MeOH
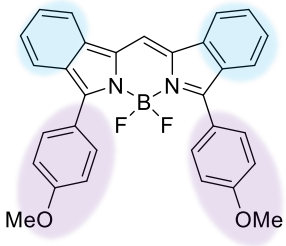	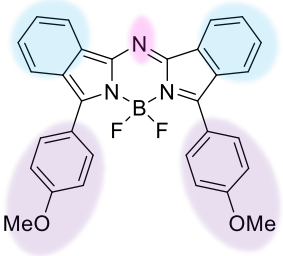	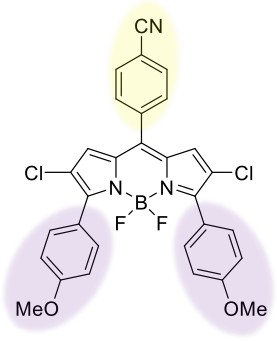
λ_{max} abs = 658 nm toluene λ_{max} em = 690 nm toluene	λ_{max} abs = 718 nm CH_2Cl_2 λ_{max} em = 756 nm CH_2Cl_2	λ_{max} abs = 609 nm toluene λ_{max} em = 650 nm toluene

Table 1.1: Absorption and emission wavelengths of BODIPY derivatives from the literature.[20, 23]

1.1. Synthesis of BODIPYs

The original synthesis of BODIPYs was an unexpected discovery by Treibs and Kreuzer.[1] They found that the acylation of 2,4-dimethyl pyrrole **6** with acetic anhydride (Ac_2O) using boron trifluoride diethyl etherate ($BF_3.OEt_2$) as a Lewis acid catalyst, resulted in the formation of two brightly fluorescent compounds, products **9** and **10**, in a low yield of 7 % and 9 % respectively, as shown in Scheme 1.1.[1] The low yield was due to an insufficient amount of $BF_3.OEt_2$ and the occurrence of over acylation which led to a mixture of products rather than the desired 2 acyl pyrrole **7**.[1] However, the authors improved their yields by first forming and isolating dipyrromethene **8**, followed chelating this ligand using a large excess of $BF_3.OEt_2$ in the presence of an excess of triethylamine, which acted as a base.[1]

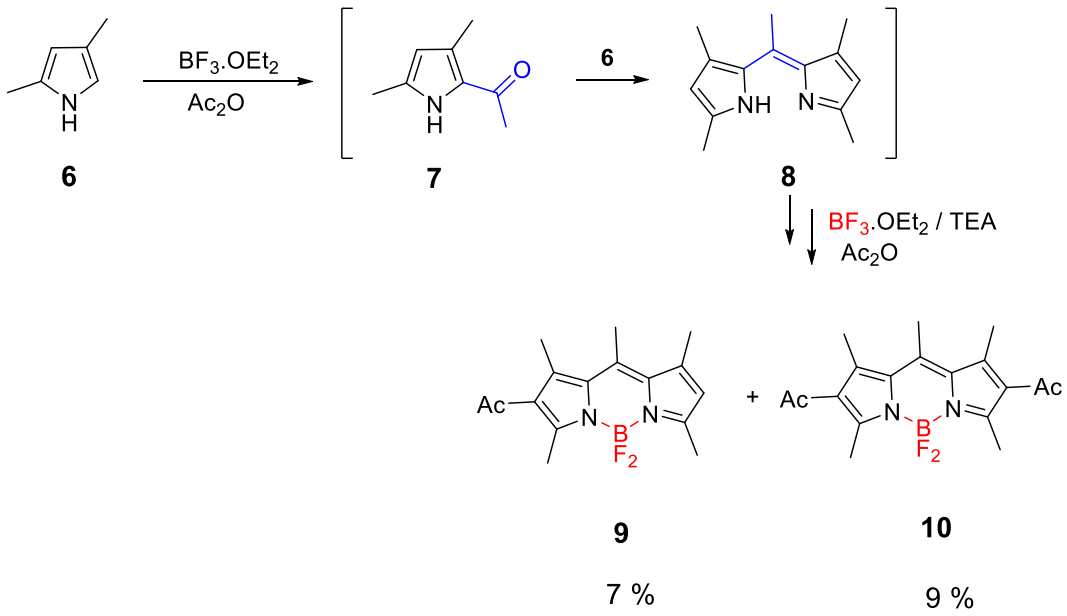

Scheme 1.1: Synthesis of the first BODIPY dyes **9** and **10** by Treibs and Kreuzer.[1]

Thus, the first step in the standard synthesis of the BODIPY unit begins with the preparation of the corresponding dipyrromethene. Two distinct synthetic approaches have been adapted from porphyrin chemistry to form this ligand.[1, 13] The first approach can be seen in Scheme 1.2; it starts with an acid-catalysed condensation of pyrrole **11**

with an aldehyde **12** forming a dipyrromethene **13**.[24] Typically, pyrrole is used as the solvent, so it is in excess, in order to prevent polymerization.[25] An alternative more convenient water based system, the HCl-catalysed synthesis of 5-aryl dipyrromethane **13** that does not require the use of large excess of pyrrole has also been reported.[26] Since this protocol does not require a large excess of pyrrole it is better suited for the large-scale synthesis. Additionally water is an inexpensive and environmentally benign ('green') solvent compared to pyrrole.[14] As dipyrromethanes **13** are unstable and sensitive to light, air, and acid, it is best to use them immediately upon preparation. Treatment of dipyrromethane **13**, with an oxidant such as 2,3-dichloro-5,6-dicyano-1,4-benzoquinone (DDQ) or the milder 2,3,5,6-tetrachloro-1,4-benzoquinone (p-chloranil), yields dipyrromethene **14** (dipyrrin).[27, 28]

It should be noted with this method that there are only a few cases where the aldehyde in the first step is not aromatic or heteroaromatic, since this reaction tends to fail with nonaromatic aldehydes.[27] On the other hand, numerous aromatic aldehydes ArCHO **12** are commercially available, making this approach a popular method for introducing aromatic functionalities at the *meso*-carbon.[14] The target boron dipyrrin dye **15** is obtained by treating dipyrrin **14** with an excess of base and $BF_3.OEt_2$.[27] All three reactions can be conducted sequentially, purifying after each step, or in a one-pot procedure, by the stepwise addition of the reagents to the reaction mixture. Unfortunately, the latter strategy results in lower yields although it is operationally easier.[14]

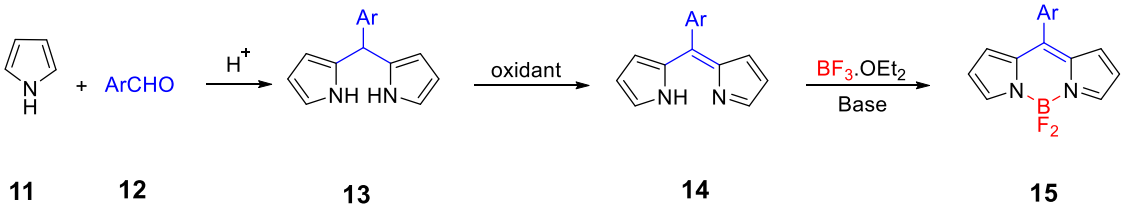

Sheme 1.2: Synthesis of BODIPY **15** by an acid-catalysed condensation of pyrrole **11** with an aromatic aldehyde **12**, followed by oxidation and boron complexation.[14]

The alternative is the second approach that involves the acid-catalysed condensation of a 2-acylpyrrole **18** with a pyrrole **16** that is unsubstituted at its 2-position.[14] Under these acidic conditions, the dipyrrinium salt **19** is initially formed followed by deprotonation of salt **19** with base and fluoroboration with $BF_3.OEt_2$ to yield BODIPY dye **20** (Scheme 1.3).[29] A key contrast with the previous procedure is that it is not limited to an aryl

group, (the substituent that ends up at the meso-position is not limited to an aryl group); hence, a larger range of boron dipyrrins can be made using this approach.[14] Additionally this allows for the synthesis of unsymmetrical boron dipyrrins such as **20** ($R_1 \neq R_2$) [30] via the condensation of two different pyrrole moieties alongside symmetrical dipyrrinium salts such as **19** ($R_1 = R_2$, Scheme 1.3) via a similar procedure.[14] As shown in Scheme 1.3, the acylation and condensation of a 2-unsubstituted pyrrole **16** are done consecutively, forming in situ 2-acylpyrrole **18** that immediately reacts further to symmetrical dipyrrinium salt **19** (Scheme 1.3).[14] Moreover, the acylating agent **17** used in this reaction can be varied it can be either an acid chloride [31, 32] acid bromide,[33] anhydride ,[34] or ortho ester.[35] Burgess and Wu discovered an alternative to forming symmetrical dipyrrinium salts such as **19** ($R_1 = R_2$). They serendipitously discovered that in the presence of phosphorous oxytrichloride ($POCl_3$) pyrrole-2-carbaldehyde derivatives **21** self-condense. Treatment with excess base and $BF_3.OEt_2$ yielded BODIPY **20**.[36]

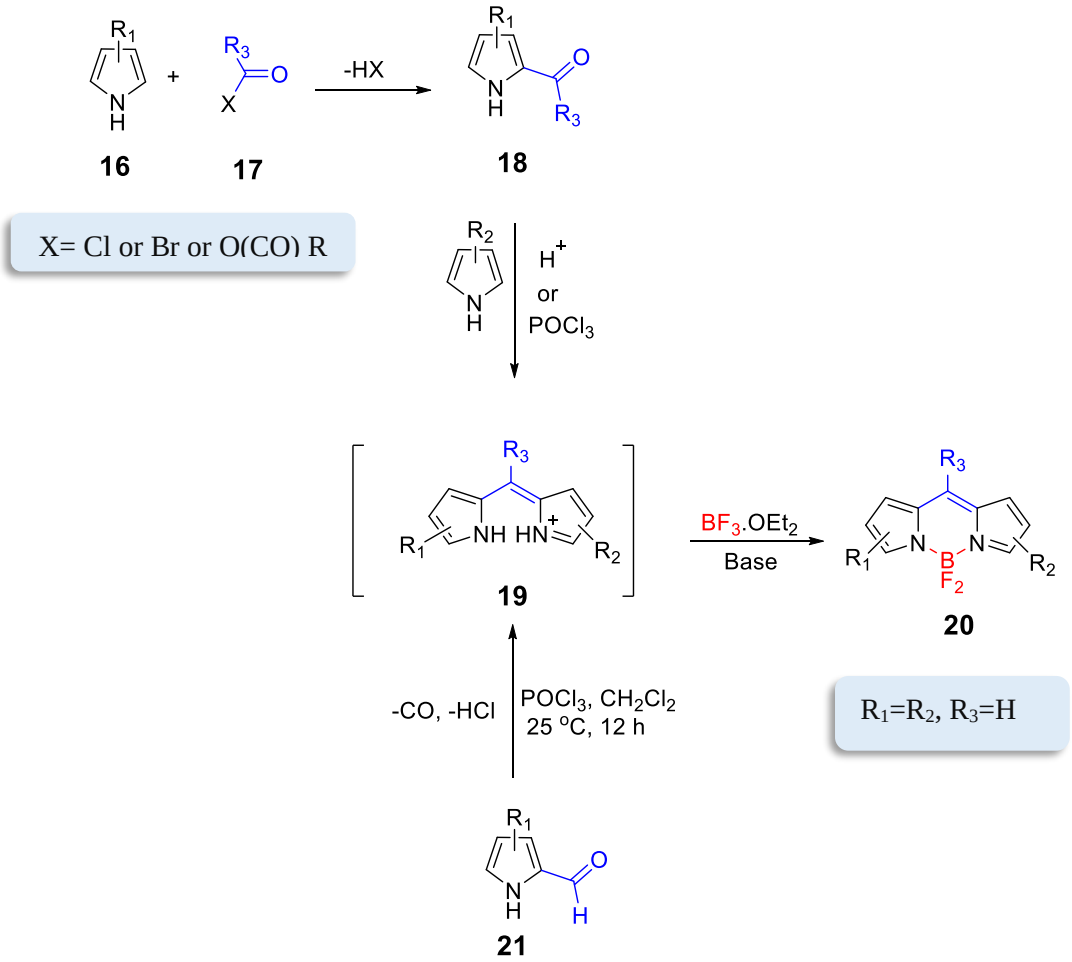

Scheme 1.3: Formation of dipyrrinium salts **19** and BODIPY dyes **20** by condensation of 2-acylpyrroles **18** and 2-unsubstituted pyrroles **16**.[14]

1.2. Synthesis of benzo fused BODIPY fluorophores

Kang and Hangland reported the first diisoindole BODIPYs in 1995.[37] Their synthetic pathway uses the Paal– Knorr synthesis; this depends on the condensation of 2-acylacetophenone **24** with ammonia or ammonium salts[38] followed by treatment with Et_3N and $BF_3.OEt_2$. This afforded the corresponding benzo fused BODIPY **26**.[20] The 2-acylacetophenone **24** is synthesised by reacting of *o*-hydroxy-acetophenone derivatives with N-arylhydrazones, then treated with lead(IV) salt (Scheme 1.4).[39]

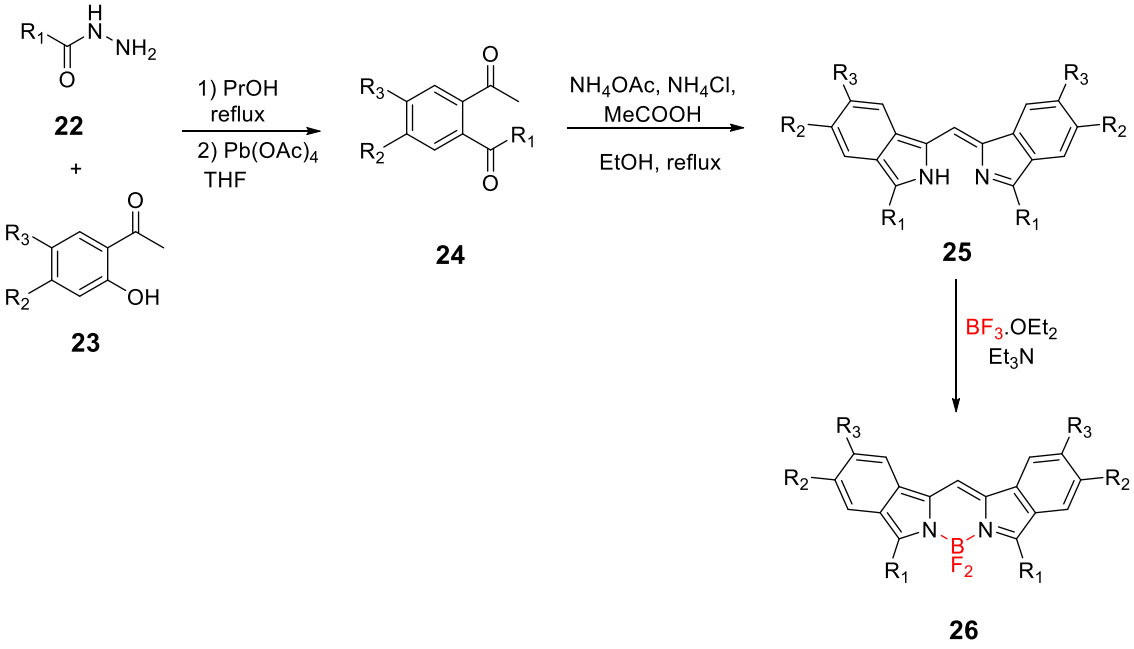

Scheme 1.4: Synthesis of diisondole -BODIPYs **26** by Kang and Haugland using the Paal–Knorr strategy.[39]

Following this methodology symmetrical BODIPYs analogues can be formed in good yields,[20] whereas condensation of different 2-acylacetophenone precursors produced unsymmetrical diisoindole BODIPYs in lower yield.[20] Also, during this strategy various dibenzo dipyrrins with a hydrogen atom in the meso position can be synthesised and examples are shown in Figure 1.4.[20]

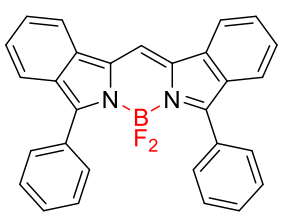

λ_{max} abs = 634 nm

λ_{max} em = 658 nm

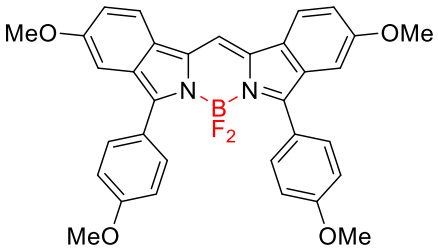

λ_{max} abs = 673 nm

λ_{max} em = 704 nm

Figure 1.4: Examples of diisondole -BODIPYs using the Paal–Knorr strategy.[20]

In the late nineties (1998) Ono and co-workers published synthetic procedures to synthesise diisoindole BODIPYs. They started with formation of a masked isoindole **30** instead of ordinary isoindole via Diels Alder reaction by reacting cyclopentadiene or cyclohexadiene with β-sulfonyl nitroethylene followed by a Barton Zard reaction with ethyl isocyanoacetate.[40]

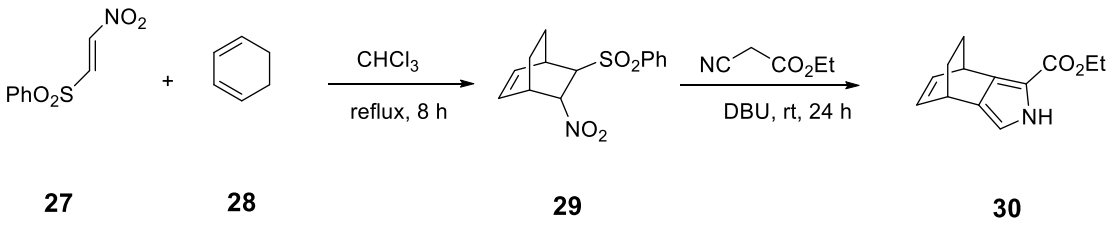

27 **28** **29** **30**

Scheme 1.5: Synthesis of a ‘‘masked’’ isoindole **30**.[40]

The alternative masked isoindoles could be synthesised in good yield because they have more stability during the separation and purification on silica gel and in acidic or basic solutions compared with simple isoindoles moieties.[20] This methodology supplements the Barton Zard strategy that proved difficulty in synthesis of simple isoindoles due to poor electrophilicity of the nitrobenzene.[40] Following this procedure diisoindole BODIPY can be synthesised through four steps initiated from the masked isoindole.[18] After reducing the ester by $LiAlH_4$, it was reacted with acyl chloride followed by adding Et_3N and $BF_3.OEt_2$ producing BODIPY **32** with fused bicyclo [2.2.2] octadiene units. Finally, it was converted to BODIPY **33** by retro Diels Alder reaction.[18]

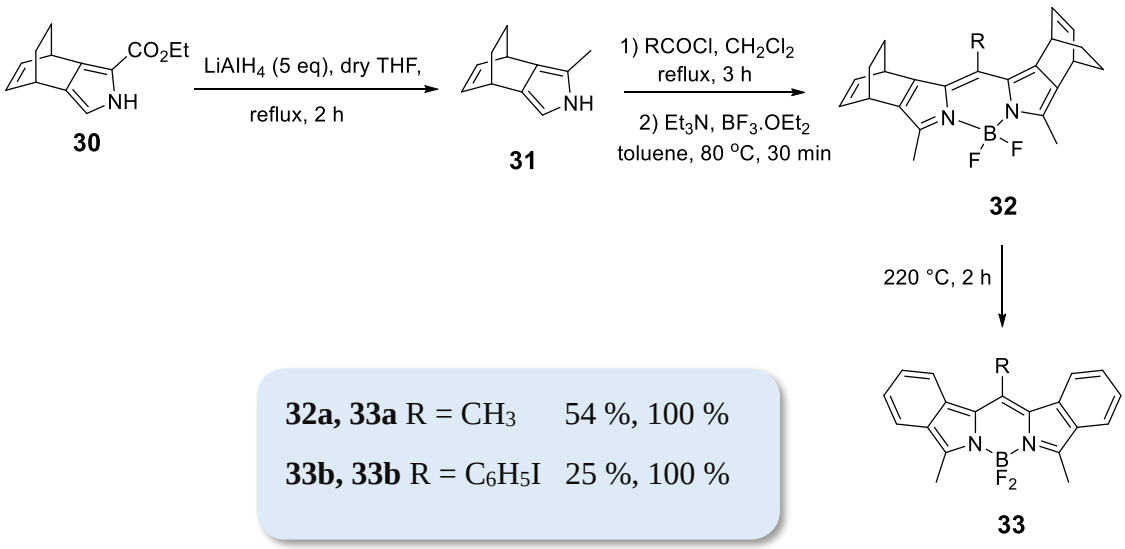

Scheme1.6: Synthesis of diisoindole-BODIPYs by a retro Diels–Alder reaction.[18]

Because of the extended π conjugation, all the resulting derivatives of diisoindole BODIPYs showed increase in the intensity of absorption which almost doubled.[20] Also, these BODIPY dyes exhibited absorption and emission maximum wavelength that showed a bathochromic shift around 70 to 80 nm compared with the corresponding non benzo fused BODIPYs.[20]

compound	λ_{max} abs	λ_{max} em	Example of non-benzo fused BODIPY
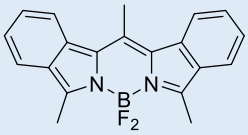 **33 a**	558 nm	564 nm	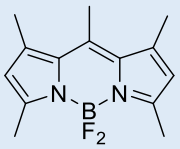 λ_{max} abs = 493 nm λ_{max} em = 519 nm
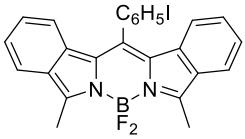 **33 b**	561 nm	569 nm	

Table 1.2: Absorption and emission wavelengths of benzo fused BODIPYs **33a**, and **33b** compared with non-benzo fused BODIPY.[18]

1.3. Synthesis of a different Class of π-Extended BODIPY derivatives

Recently, a new class of π-extended BODIPY derivatives have garnered interest. The structures are directly relevant to the aza analogues (reported earlier by our group)[41] that are the subject of this research and thesis. Jiao et al, extended the π-conjugation beyond the dipyrromethene unit, resulting in a more rigid framework which is significantly different from classical BODIPYs in their electronic configuration.[42] They are accessed by the facile condensation of aldehyde and pyrrole in aqueous solution in the presence of HCl, for example see Scheme 1.7. In spite of the low yields this is a facile one pot reaction using commercially available reagents hence can furnish significant quantities of the extended BODIPY (100 mg in a single experiment). They explored the use of a slight excess of the mesitaldehyde (1.0 equivalent) with pyrrole (0.7 equivalent) in a H_2O: MeOH (3:1) solvent system in the presence of catalytic HCl.[42] The product could be directly observed by thin-layer chromatography (TLC). Unlike with dipyrromethene, there was no need for oxidation and the product was used directly for further complexation with $BF_3{\cdot}OEt_2$ to provide the extended BODIPY **35**.[42] Extended BODIPY **35a** was obtained in 10 % yield, while a similar condensation of 2,6-dichlorobenzaldehyde and pyrrole in a H_2O: THF (5:1) mixture gave extended BODIPY **35b** in 7 %. The crystal structure analysis of **35b** further confirmed the unique π-extended dipyrromethene core structure.[42] The two α-vinyl double bonds both adopt an *E* configuration. Both π-extended BODIPYs displayed intense absorption and moderate emission with maxima around 565 and 620 nm, respectively, and showed interesting reactivity toward various nucleophiles such as phenethylamine.[42]

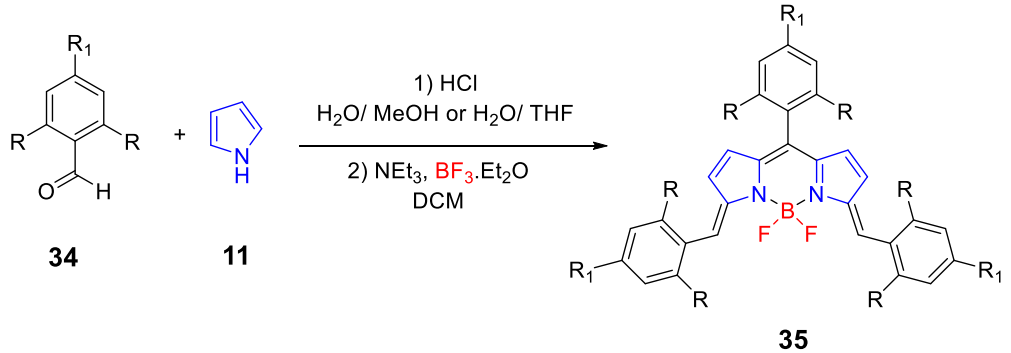

34a R = R_1 =CH_3

34b R = Cl, R_1= H

35a R = R_1 = CH_3 10 %

35b R = Cl, R_1= H 7 %

Scheme 1.7: Synthesis of Ex-BODIPYs **35a** (in H_2O: MeOH), and **35b** (in H_2O: THF).[42]

1.4. Introduction to aza BODIPYs and their precursor aza dipyrromethenes

A subset of BODIPY structures is known as aza-BODIPYs. In this group the methine carbon atom in position 8 is replaced with a strongly electron-withdrawing imine nitrogen (Figure 1.5). Aza dipyrromethene **36**, the key precursor to aza-BODIPY **37**, were reported in the 1940s, but were not extensively researched.[43] However, the drive to find compounds with far-red or NIR region led to increased research into the application of aza dipyrromethenes over the last few decades.[44] O'Shea and co-workers have reported that the aza-BODIPYs modification to the BODIPYs core effectively red shifted the absorption properties whilst conserving the extinction coefficients, fluorescence intensity and photostability.[45] As a result the aza-BODIPY dyes can form efficient sensitizers for photodynamic therapy (PDT).[46, 47]

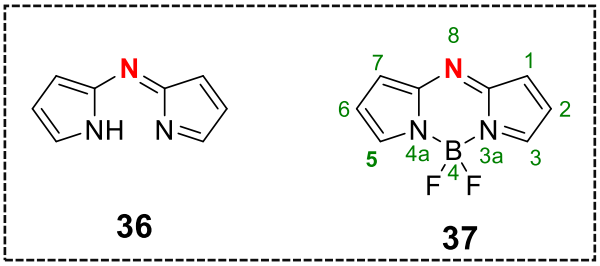

Figure 1.5: Aza dipyrromethene unit **36** and the corresponding aza-BODIPY core **37**.

1.5. Applications

As previously mentioned with BODIPYs, aza-BODIPY dyes and their various sub-structures have a wide variety of applications ranging from laser dyes to labelling reagents, chemo sensors to fluorescent switches.[9] However a key area of application is in photodynamic therapy (PDT).[48] PDT is a non-invasive process that is used to treat malignant and premalignant diseases.[48] The process is via the action of three components that result in targeted cellular and tissue damage.[48] Firstly the photosensitiser accumulates within a tumour. In the second stage it is then irradiated with a suitable low energy light such that it doesn't damage healthy body tissue.[48] Finally upon irradiation the photosensitiser is excited, it can then transfer its excited state energy to the tumour via generation of a singlet oxygen, thus leading to the death of the tumour.[43] The singlet oxygen generated has the ability to react with most organic molecules, as a result of the spin-allowed nature of these procedures.[48] Thus, this singlet

oxygen generation is a key process and a photosensitiser that can quantitatively generate singlet oxygen is required in PDT.[48] Many photosensitisers that have been cleared for medical use still suffer from some key flaws such as low absorption in the near infra-red region, which decreases its efficiency, and toxicity which results in unwanted side effects. However it has been found that BODIPY and aza-BODIPY structures have more favourable properties as a photosensitiser as they address these issues due to their significant fluorescence quantum yield and for example high photostability.[49] As mentioned earlier aza-BODIPY structures, due to the red-shifted absorption properties when compared to BODIPY structures, have particular importance as photosensitisers for PDT.[46, 47]

1.6. Synthesis of aza dipyrromethenes

The synthetic strategies to prepare aza dipyrromethenes were first reported by Rogers 1943.[50] He attempted a Leuckart reaction by heating ammonium formate with 4-nitro1,3-diphenylbutan-1-one **38** under solventless conditions wherein unexpectedly an intense blue colour was observed. A similar result was observed when 4-oxo-2,4-diphenyl butane nitrile **40** was used as substrate (Scheme 1.8)[51] giving **39** as ‘‘a new chromophoric system, having a formal relationship to the phthalocyanines’’.[51] However, possibly due to the success of phthalocyanines as blue dyes, aza dipyrromethenes were not investigated in much detail for a further 50 years.[52] Due to the limited analytical instrumentation at that time, which were limited to melting points, elemental analysis, and molecular weight determinations, it was not easy to determine the structural assignment of the resulting coloured compound.[52]

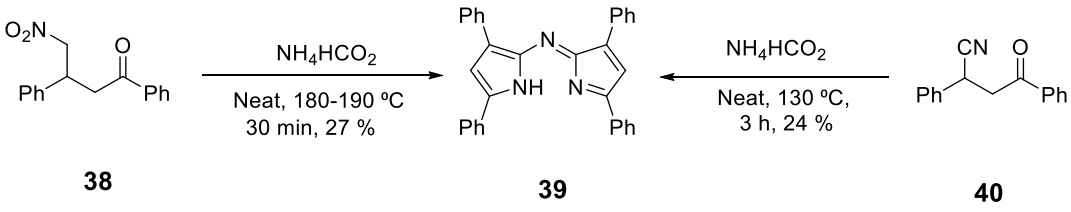

38 **39** **40**

Scheme 1.8: Synthetic strategies to aza dipyrromethenes **39** formation developed by Rogers.[50]

Through the degradation reactions and re-synthesis published by Rogers the resulting product **39** was characterised.[50] Degradation reaction includes heating of **39** with hydriodic acid to form 2,4-phenyl pyrrole **41**. Then 2,4-phenylpyrroles **41** were converted into their corresponding 5-nitroso derivatives **42**, at room temperature reaction with sodium nitrite in EtOH/aq HCl; the nitrosation reaction occurred

selectively at the unsubstituted α-pyrrole position to produce the desired product **42**.[11, 53] Then it was condensed with a second molecule of 2,4-phenylpyrrole **41** under high temperature in acetic acid to confirm aza dipyrromethene structure **39** (Scheme 1.9).[11, 53] Further, reduction of compound **42** in the presence of Adams's catalyst H_2, PtO_2, led to generation of 5-amino-2,4-diphenyl pyrrole **43** which oxidised upon exposure to air, then self-condensed with the loss of ammonia producing aza dipyrromethene **39** in low yield.[51, 52]

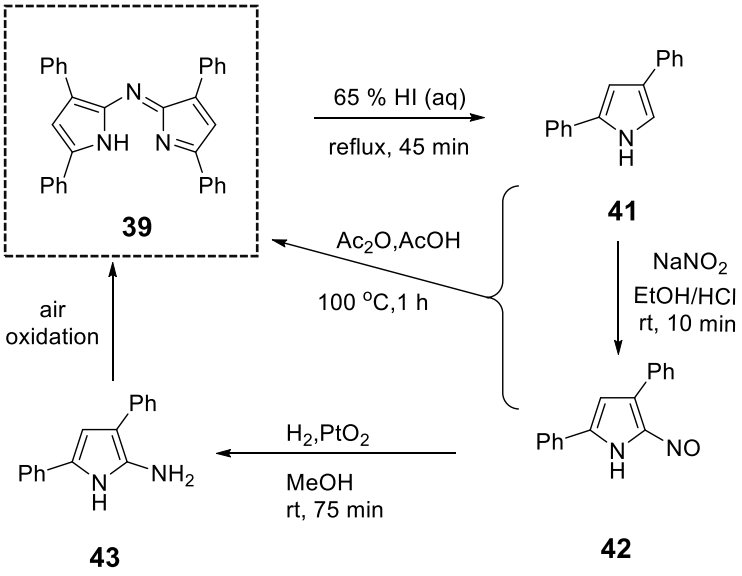

Scheme 1.9: The cycle of degradation and resynthesis of tetra aryl aza dipyrromethenes compound **39**.[51, 52]

The synthesis is most facile when there are four phenyl substituents, however it is possible to obtain the diphenyl products **44** (Figure 1.6) by following the procedure described in Scheme 1.9, starting with 2-phenyl pyrrole.[11]

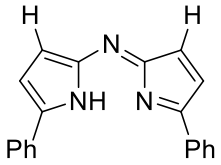

44

Figure 1.6: Structure of diphenyl aza dipyrromethene **44**.

It was not until the 1990's that the first reactions of aza dipyrromethenes with boron electrophiles were reported (Scheme 1.10).[53, 54] For example treatment of 3,5-tetraphenyl aza dipyrromethene **39** with $BF_3.OEt_2$ resulted in the formation of aza-BODIPY **45** Unfortunately, this method did not yield the less substituted aza-BODIPY **46** after treatment of the corresponding aza-dipyrromethene **44** with boron trifluoride.[54]

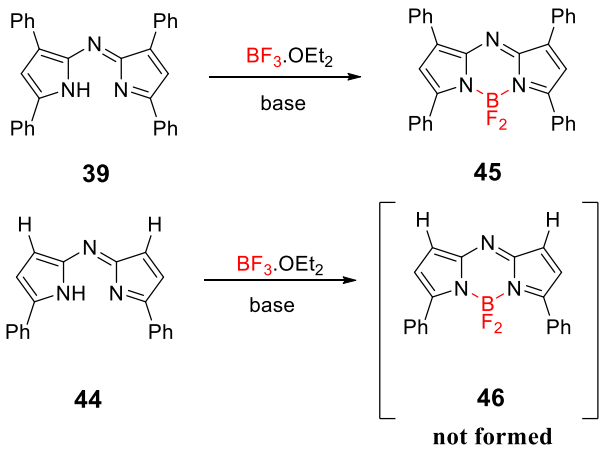

Scheme 1.10: First synthetic procedure in the formation of aza-BODIPY dyes.[11]

Later, O'Shea group has optimised this synthetic route by using different ammonium sources. The reaction performed by heating of 4-nitro1,3-diphenylbutan-1-one **47** with ammonium acetate instead of ammonium formate in either ethanol or butanol as solvents under reflux. This was smoothly performed, led to a significant development in the outcome yield. However, it was observed that use of alcohol solvents usually causes the aza dipyrromethenes to precipitate from the reaction mixture, thus, enabling easier isolation and enhanced yields.[46] Using mild condition such as replacing of formate with acetate led to improve the reaction outcome, by following this procedure several derivatives of aza dipyrromethene have been synthesized in moderate yield ~ (25%-50%) as described in Scheme 1.11.[46] However, using compound **47** as starting material allowed the synthesis of aza dipyrromethenes with only two different aryl substituents.[52]

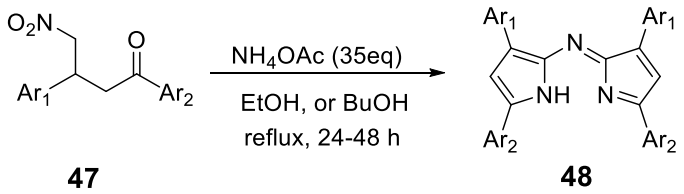

compound	*Ar_1*	*Ar_2*	*Time/h*	*Yield %*
48a	Ph	Ph	48h	42 %
48b	Ph	p-OMePh	24h	47 %
48c	p-OMePh	Ph	48h	48 %
48d	p-BrPh	Ph	48h	24 %

Scheme 1.11: General route to formation of aza dipyrromethene **48**.[52]

Scheme 1.12 shows a possible mechanism for formation of the aza dipyrromethene core from the nitromethane adducts. Initially pyrrole **A** is formed, this is then nitrosylated *in situ* to give **B** which then condenses with another molecule of the pyrrole (Scheme 1.12).[11]

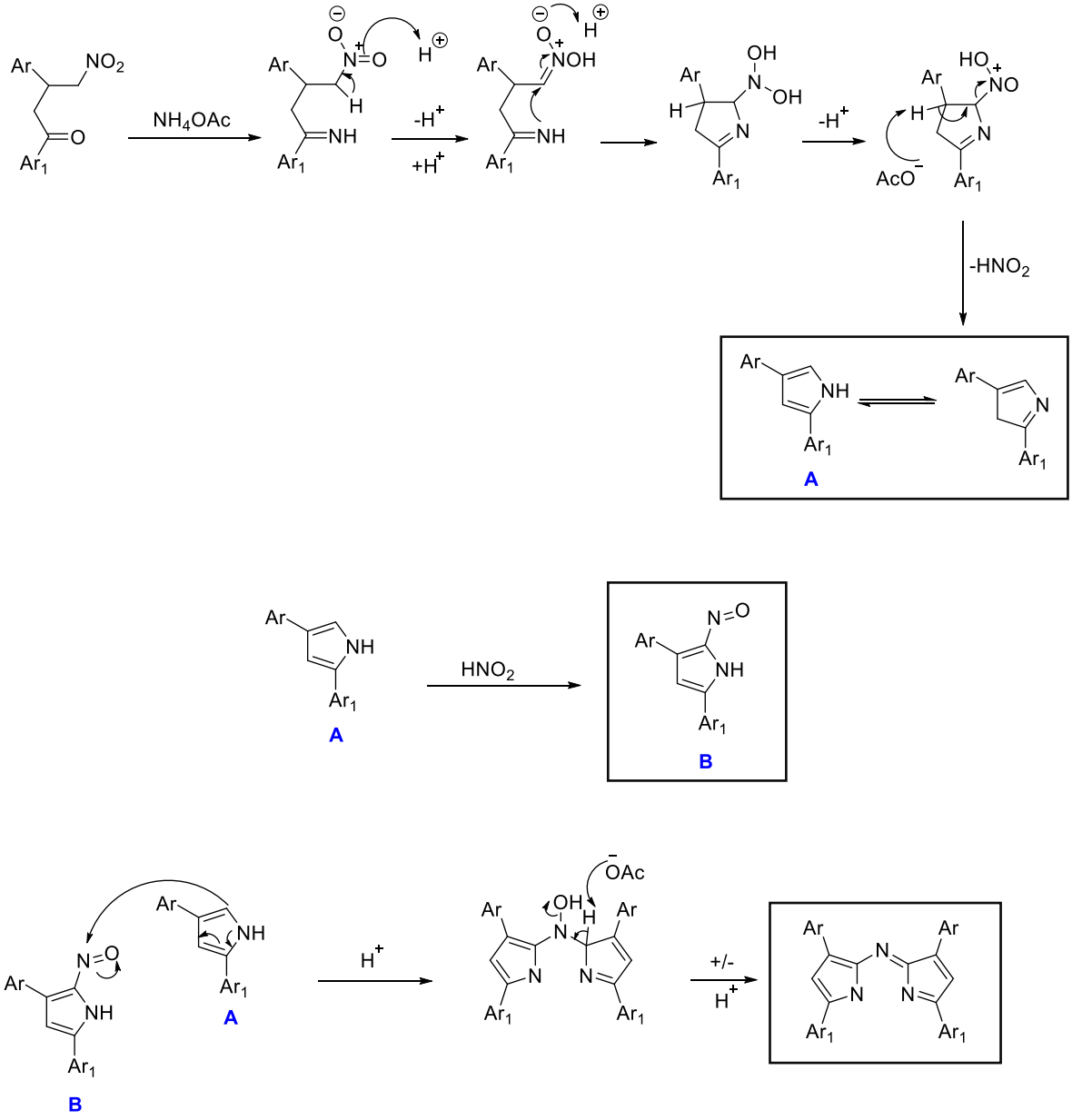

Scheme 1.12: Synthetic mechanism of aza dipyrromethene from nitro butyrophenones.[11]

Another approach has been developed in order to synthesise unsymmetrical aza dipyrromethenes by condensing diaryl pyrroles and nitroso diaryl pyrroles in acetic

anhydride/acetic acid mixture at 100 °C.[55] Work up by cooling the reaction mixture with ice then extraction with DCM, and purified by slow evaporation of a chloroform solution at room temperature giving the pure aza dipyrromethene **51** as dark blue material in good to excellent yields (Scheme 1.13).[55] Following this approach led to synthesise derivatives of aza dipyrromethene with one to four different substituted aryl rings depending on the pyrrole building blocks.[55]

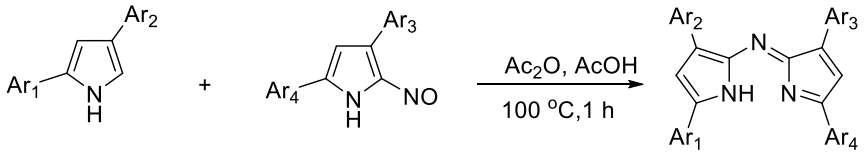

49 **50** **51**

compound	*Ar_1*	*Ar_2*	*Ar_3*	*Ar_4*	*Yield %*
51a	Ph	Ph	$pMeNC_6H_4$	Ph	35 %
51b	Ph	Ph	$p\text{-}BrC_6H_4$	Ph	92 %
51c	Ph	Ph	$p\text{-}Et_2NCH_2C_6H_4$	Ph	94 %
51d	$p\text{-}MeOC_6H_4$	Ph	Ph	$p\text{-}MeOC_6H_4$	72 %
51e	Ph	$p\text{-}FC_6H_4$	$p\text{-}Et_2NCH_2C_6H_4$	$p\text{-}MeOC_6H_4$	88 %
51f	Ph	$p\text{-}FC_6H_4$	Ph	$p\text{-}MeOC_6H_4$	94 %

Scheme 1.13: Synthetic strategy to formation of unsymmetrical aza dipyrromethene.[55]

Moreover, it has been observed that the addition of strongly electron donating groups along with the increase in conjugation provides a means to further increase the red shifting of the fluorescence emission.[44] This has been demonstrated with the addition electron donating groups on the para position of the 5-Ar substituents which led to increased extinction coefficients and red shifts in the absorption maximum.[11] Figure 1.7 shows examples from the literature demonstrating the effect of adding electron donating groups on the 5-positions of Aryl substituents on the absorption and emission. In Figure 1.7**B**, installation of the electron donating groups (NMe_2) on the para phenyl substituents led to increase the absorption and emissions by 149 nm compared with non-

phenyl substituents **(**Figure 1.7**A**).[3, 56] The increase of the absorption and emission properties in these motifs led to properties as effective photosensitizers and agents of photodynamic therapy, like photofrin or protoporphyrin.[57]

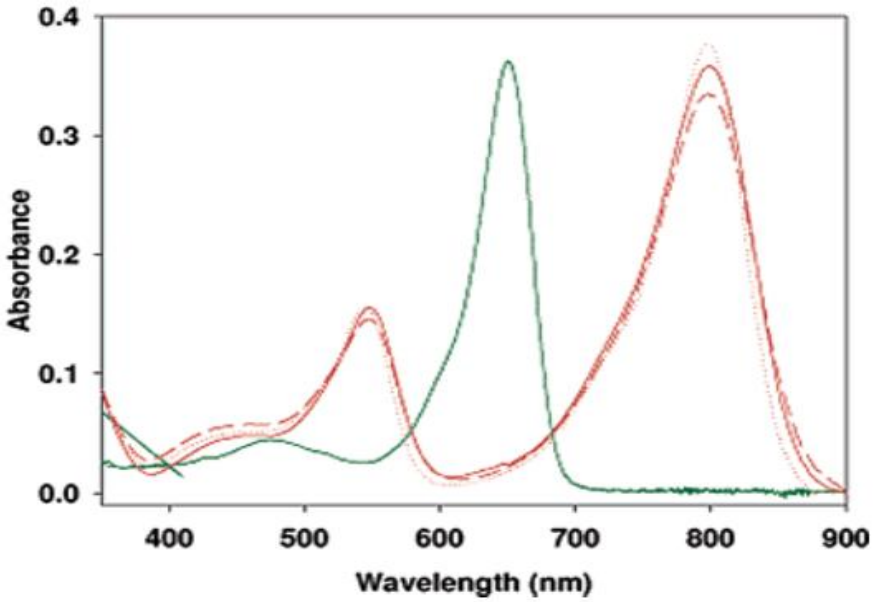

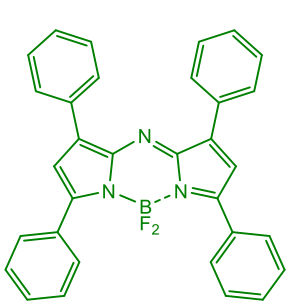

A

λ_{max} abs = 650 nm

λ_{max} em = 672 nm

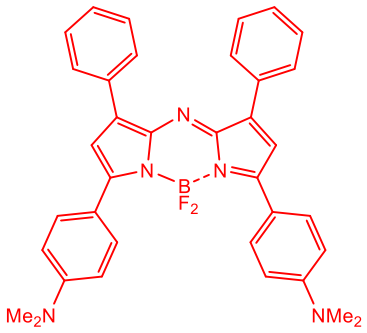

B

λ_{max} abs = 799 nm

λ_{max} em = 823 nm

Figure 1.7: A selection of aza-BODIPY structures showing the effect of electron donating groups on the absorption and emission properties, and the absorption spectra of **A** in $CHCl_3$ (green λ_{max} 650 nm), and **B** in $CHCl_3$ (solid red line λ_{max} 799 nm), ethanol (dashed red line λ_{max} 799 nm), and toluene (dotted red line λ_{max} 798 nm), (conc. 4×10^{-6} M).[56]

1.7. Synthesis of benzo-fused aza BODIPYs

A variety of modifications have been explored to optimize the aza-BODIPY scaffolds in order to further shift the absorption and emission properties towards the far red and NIR region.[58,59] Vollman reported the first synthesis of benzo fused aza dipyrromethenes in 1972 by the reaction of phthalonitrile with 2.5 equivalents of aryl magnesium bromides, at room-temperature in dry benzene. By using steam distillation and recrystallisation from pyridine , benzo fused aza dipyrromethenes were isolated in low to moderate yield.[60]

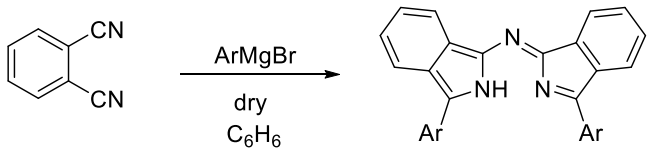

52 **53**

53a Ar = phenyl 34 %

53b Ar = 4-CH_3 phenyl 24 %

53c Ar = 4-OCH_3 phenyl 7 %

Scheme 1.14: Synthesis of benzo fused aza dipyrromethene by Vollman.[47, 60]

To date a number of novel ring-fused aza-BODIPY scaffolds have been reported.[61] These fused ring systems are identified as [b]-fused, and/or [c]-fused (fusion at the β sites), aza BODIPYs depending on the bonds involved in annulation of the aromatic group onto the pyrrole ring, or boron-fused where the ring fusion is via intramolecular B-O ring formation (Figure.1.8).[61] These fused ring derivatives can be classified into four key groups as shown in Figure 1.8.[61]

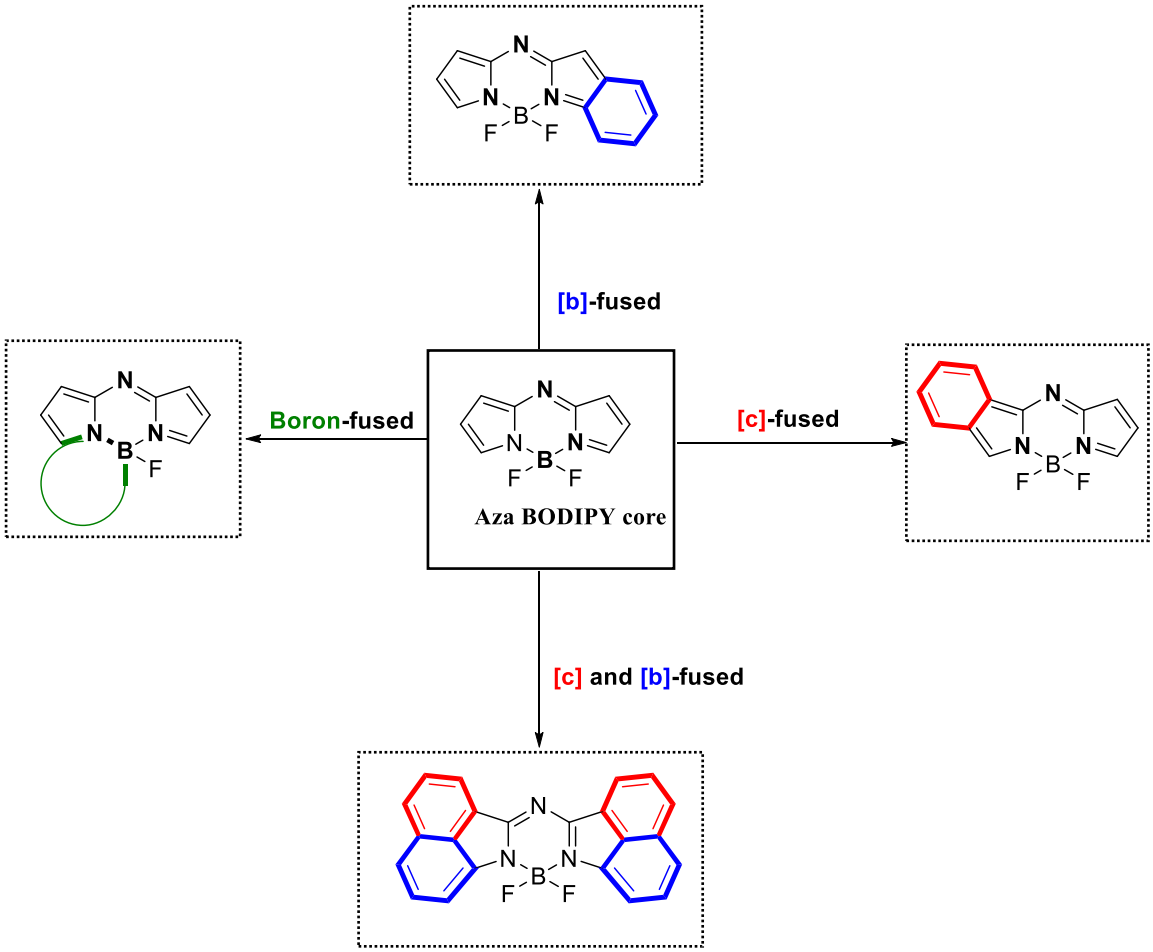

Figure1.8: Type of the ring-fused aza-BODIPY analogues.[61]

1.7.1 Synthesis of [b]-fused aza dipyrromethenes and aza-BODIPYs from ring-fused pyrroles

The first report of the conformationally restricted six-membered ring-fused aza-BODIPYs was by Carreira and co-workers in 2005.[47] By simply replacing 2,4-diaryl pyrroles with stable ring-fused pyrrole precursors **54**, they developed a convenient synthetic route to constructed [b]-fused aza dipyrromethene **55** and aza-BODIPY **56** (Scheme 1.15).[47] Since then, their reported preparation of [b]-fused aza-BODIPYs **56** by direct cyclization of substituted pyrroles has become a popular method that furnishes the desired products in good to excellent yields 76 %.[61] However, the precursors themselves, the fused pyrroles, require a multiple-step synthesis. Hence it limits the effectiveness of this strategy to conveniently access a diverse range of ring-fused aza BODIPYs (Scheme 1.15).[47]

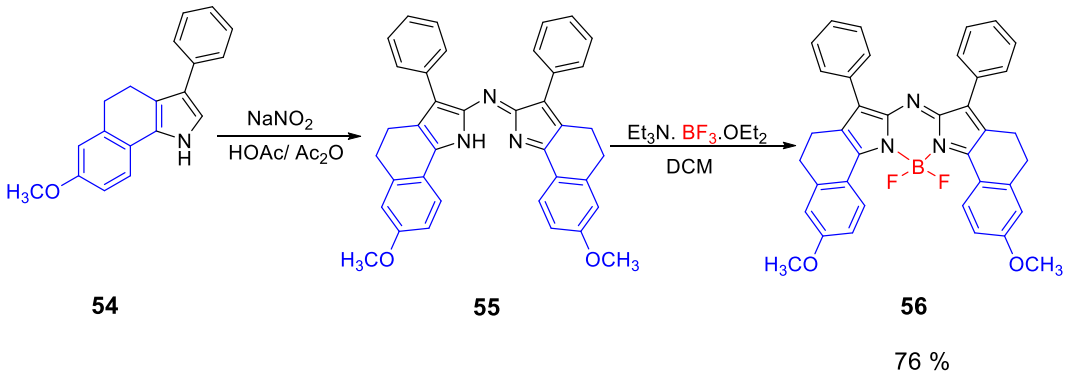

Scheme 1.15: Synthesis of [b]-fused aza dipyrromethene **55** and aza-BODIPY **56**.[47]

1.7.2 Synthesis of [c]-fused (fusion at the β sites) aza dipyrromethenes and aza-BODIPYs

1.7.2.1 From phthalonitrile and their derivatives

In 2008, Lukyanets and Kobayashi reported the synthetic method to synthesise [c]-fused aza-BODIPYs (Figure 1.8), following Vollman procedure as mentioned previously. Reaction of phthalonitrile **52** with aryl magnesium bromides in dry benzene at room temperature for 1 h, steam distillation and recrystallization from pyridine and methanol provided [c]-fused aza dipyrromethenes **53a** and **53d** in moderate yields, 28 % and 27 % respectively (Scheme 1.16).[44] Following chelation by treatment with BF_3OEt_2, the resulting [c]-fused aza-BODIPYs **57a** and **57d** were obtained in good yields.[44] As expected, these exhibited significant shift in the absorption and fluorescence spectra. The fused aza dipyrromethenes **53a** and **53d** displayed intense absorption bands at 653 nm and 658 nm respectively.[44] Thus they exhibit a red-shift analogous to that observed in the spectra of aza dipyrromethenes systems with extended π-conjugated.[62,63] The fluorescence spectra of **53a** and **53d** exhibit emission at 701 nm, and 705 nm respectively. Complexation to the corresponding aza-BODIPYs increased the red-shift further.[44] The fused aza-BODIPY moieties **57a** and **57d** exhibit intense absorption at 715 nm, and 724 nm respectively alongside intense emission at 736 nm, and 749 nm respectively.[44] Thus they have an expanded scope for application most notably, the

application of the ring-fused aza-BODIPY **57a** as potential donor unit for NIR-absorbing organic solar cells.[64]

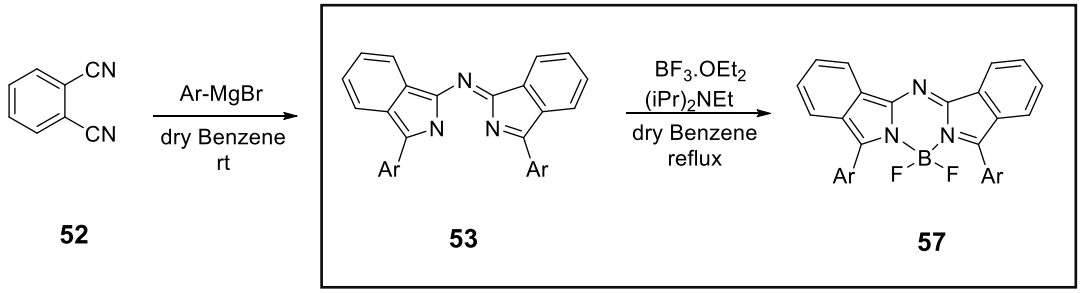

52 **53** **57**

53a Ar = phenyl 28 %

53d Ar = 4-*tert*-butylphenyl 27 %

57a Ar = phenyl 70 %

57d Ar = 4-*tert*-butylphenyl 73 %

Scheme 1.16: Formation of benzo fused aza-BODIPY **57** from phthalonitrile.[44]

The ready availability of the starting materials, (phthalonitriles and their derivatives), and aryl magnesium bromides either commercially or via a facile synthesis make this strategy very attractive.[61] Thus this has proved itself to be an efficient strategy to access a number of symmetric aromatic [c]-fused aza-BODIPYs with additional aryl substituents at the 3,5- positions.[61] Nonetheless as noted by Gresser et al, in 2011, the high reactivity of Grignard reagent limited the substrate scope of this method as it led to a number of side products.[65] Gresser and co-workers were able to overcome this to some extent by modifying the reaction conditions to limit side products and optimise yield. They found the use of one equivalent of phenyl Grignard reagent in diethyl ether at 20 ℃ followed by reaction in formamide instead of using water steam distillation furnished the desired products in better yields.[65] Scheme 1.17 shows the suggested mechanism which involves reacting of phthalonitrile with phenyl Grignard, then evaporating the solvent produced crude, likely to be the magnesium salt of 1-arylisoindoylimines **58**. Heating of the resulting material with formamide under reflux for a few minutes gave the activated amine species **59** which could be easily converted to compound **60**. Condensation of compounds **59** and **60** following by loss of ammonia, led to give the desired benzo fused aza dipyrromethene **53**. Under these conditions the yield of **53** was increased from 28 %, to 55 %. Finally the aza-BODIPY **57** was also successfully prepared in good yields 78 %.[65]

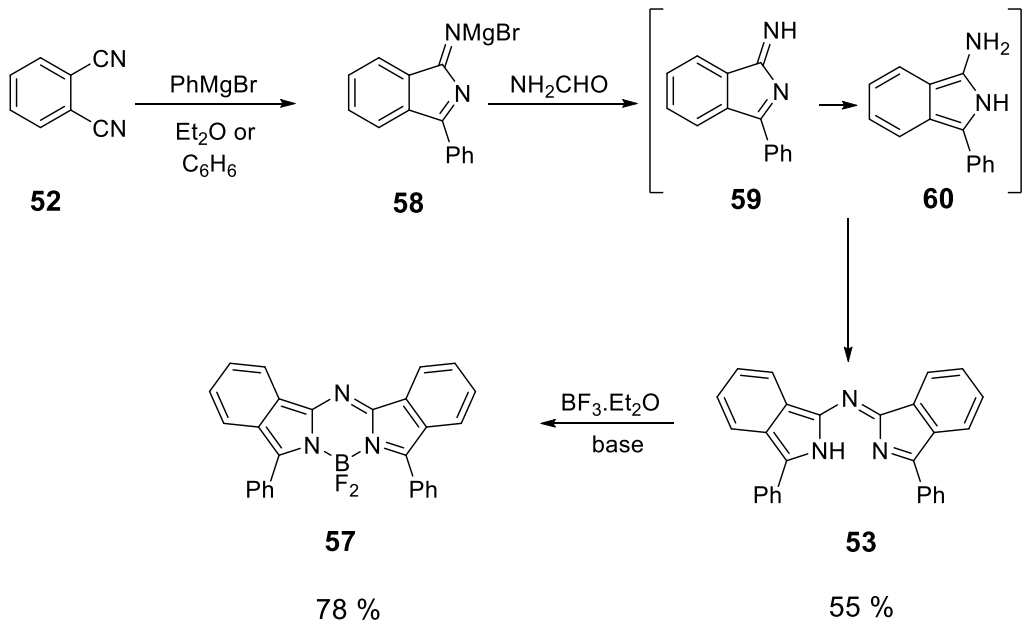

Scheme 1.17: Synthesis of benzo-fused aza-dipyrromethene **53** and its BF_2 complexes **57**.[65, 66]

Another successful application inspired by this route is the synthesis of the ring-expanded aza-BODIPY dye **62** by Mack et al (Scheme 1.18).[67] Here, 1,2-dicyanoacenaphthylene **61** which was prepared using the methods of Rieke and co-workers[68] was used as a synthetic precursor to furnish the NIR absorbing ace naphthalene-fused ring in 54 % yield (Scheme 1.18). This ace naphtho-fused aza-BODIPY **62** is particularly suitable for application in solar cells due to its relatively wide ranging absorption band at 628 nm.[67]

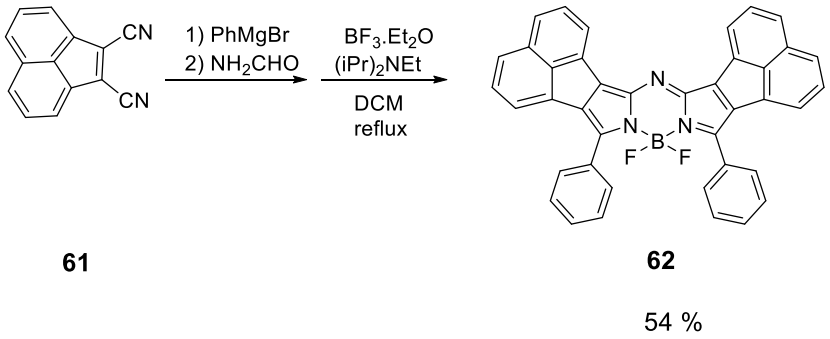

61 **62**

54 %

Scheme 1.18: Synthesis of ace naphthalene-fused aza-BODIPY **62**.[67]

A number of benzo fused aza-BODIPY dyes were synthesized using this route including the first chiral aza-BODIPY derivatives. One featured a binaphthyl substituent **63**, **64** [69] and another benzo-fused aza-BODIPY **65** with *tert*-butyl dimethyl silyl groups at the phenyl substituents.[70]

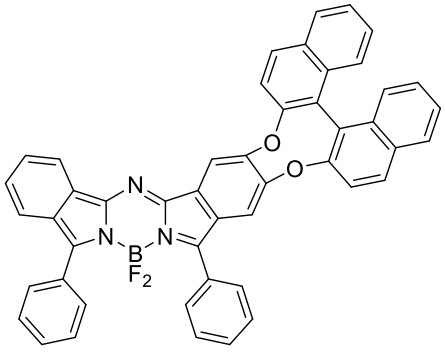

63

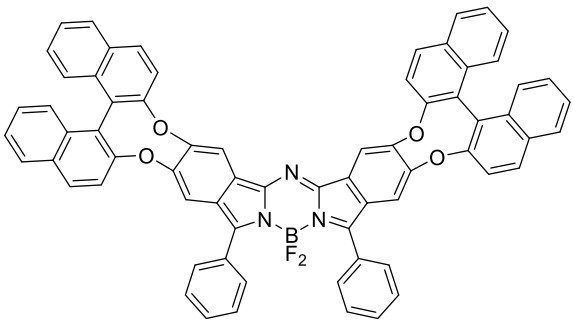

64

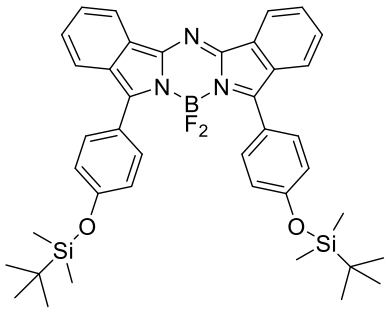

65

Figure 1.9: Derivatives of benzo fused aza-BODIPYs.[69, 70]

The first synthesis of unsymmetric aza diisoindolylmethenes and their BF_2 complexes was reported by Shen and co-workers (Scheme 1.19).[71] Treatment of phthalonitrile with a solution of potassium *tert*-butoxide in dry dimethylformamide (DMF) at 0 °C for 3 h produced compound **66** in 79 % yield. This unsymmetrical compound, containing an amine group on one side, was subsequently treated with dimethylamine in tetrahydrofuran (THF) to form compound **67** in 69 % yield. Treatment of **67** with $BF_3.Et_2O$ under basic conditions in dichloromethane resulted in the formation of BF_2 -chelated complex **68**.[71]

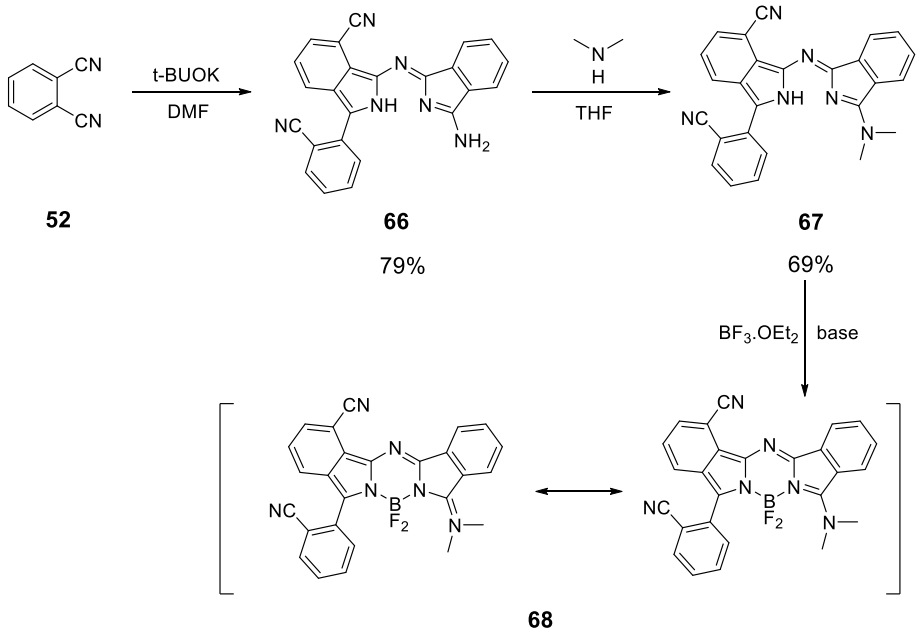

Scheme 1.19: Synthesis of unsymmetrical benzo-annulated aza BODIPY **68**.[71]

The postulated mechanism for the formation of **66** includes deprotonation of phthalonitrile at the *ortho* position of the CN group using potassium *tert*-butoxide in DMF initiates the reaction.[72] The phthalonitrile anion acts as a nucleophilic reagent to attack the cyano moiety of a second phthalonitrile molecule, this then leads to the formation of C-C bond.[72] This is followed by a further nucleophilic reaction and finally two electrons reduction process to furnish the aza diisoindolymethene with an amino group on one side.[72] It should be noted that in this mechanism the activation of C-H bond in phthalonitrile by the concomitant formation of anion with potassium *tert*-butoxide is the key step. This versatile method has been extended to furnish other benzo-fused aza-BODIPY derivatives, such as *tert*-butyl or *tert*-butyl thiol (**69**, **70**, and **71**) (Scheme 1.20).[71]

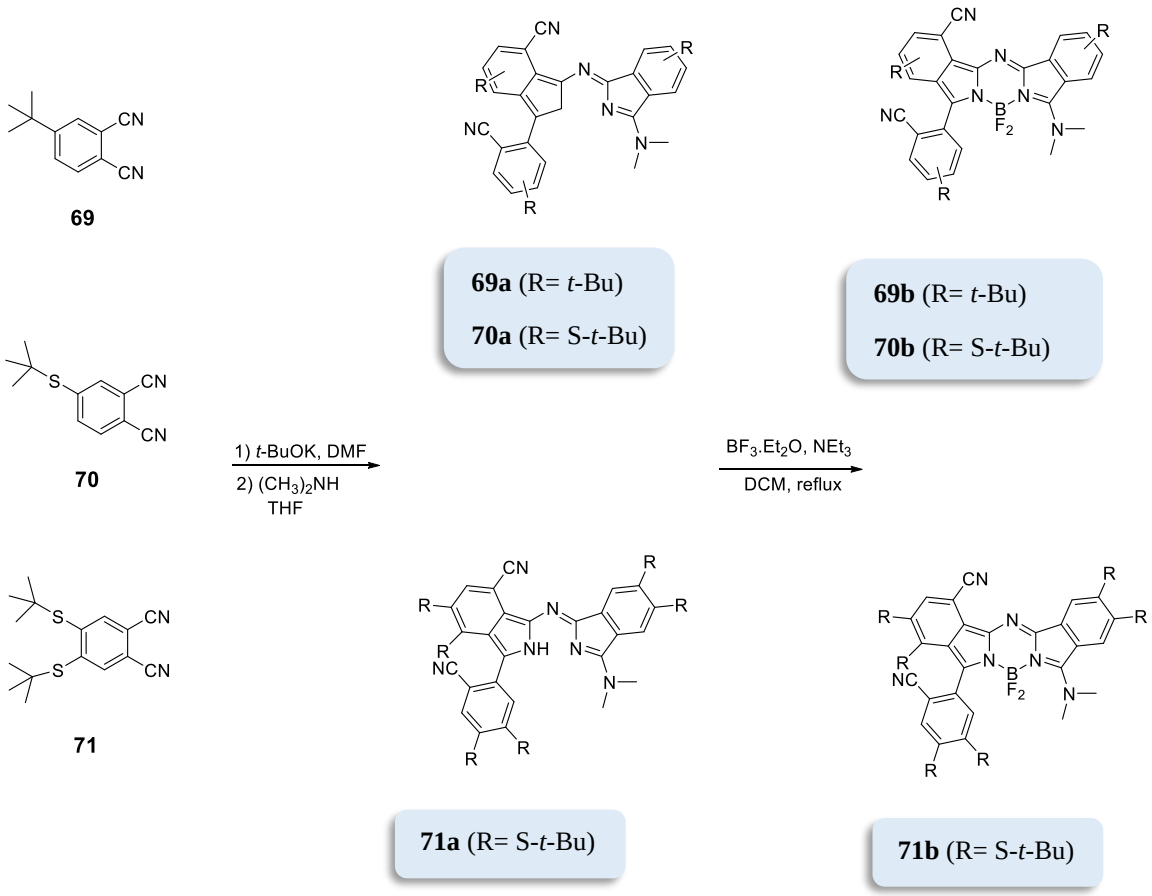

Scheme 1.20: Synthesis of derivatives of aza-diisoindolymethene from mono and bis substituted phthalonitrile.[71]

Another synthetic strategy has been used to synthesise a variety of benzo fused aza dipyrromethenes from benzonitriles with different functional group such as benzene, benzonitrile and thiophene (Scheme 1.21 inset).[73] In this process a molecule of the benzonitrile is lithiated by LDA in the *ortho*-position to the cyano group at low temperature to form **73**.[73, 74] Subsequent coupling with the second molecule of benzonitrile leads to the formation of the intermediate **74** (Scheme 1.21). Condensation of the intermediate **74** after reduction with formamide led to produce the benzo fused aza dipyrromethenes.[73] Unfortunately, as a result of the low solubility of the corresponding aza-BODIPYs, the BF_2 complexes could not be obtained with the exception of the compound **75**. It was successfully converted to the corresponding aza-BODIPY **76** after the treating with $BF_3.OEt_2$. They could obtain zinc(II) complexes of the benzo fused aza dipyrromethenes which demonstrated strong absorption in the 621–653 nm region and these had no detectable fluorescence.[73]

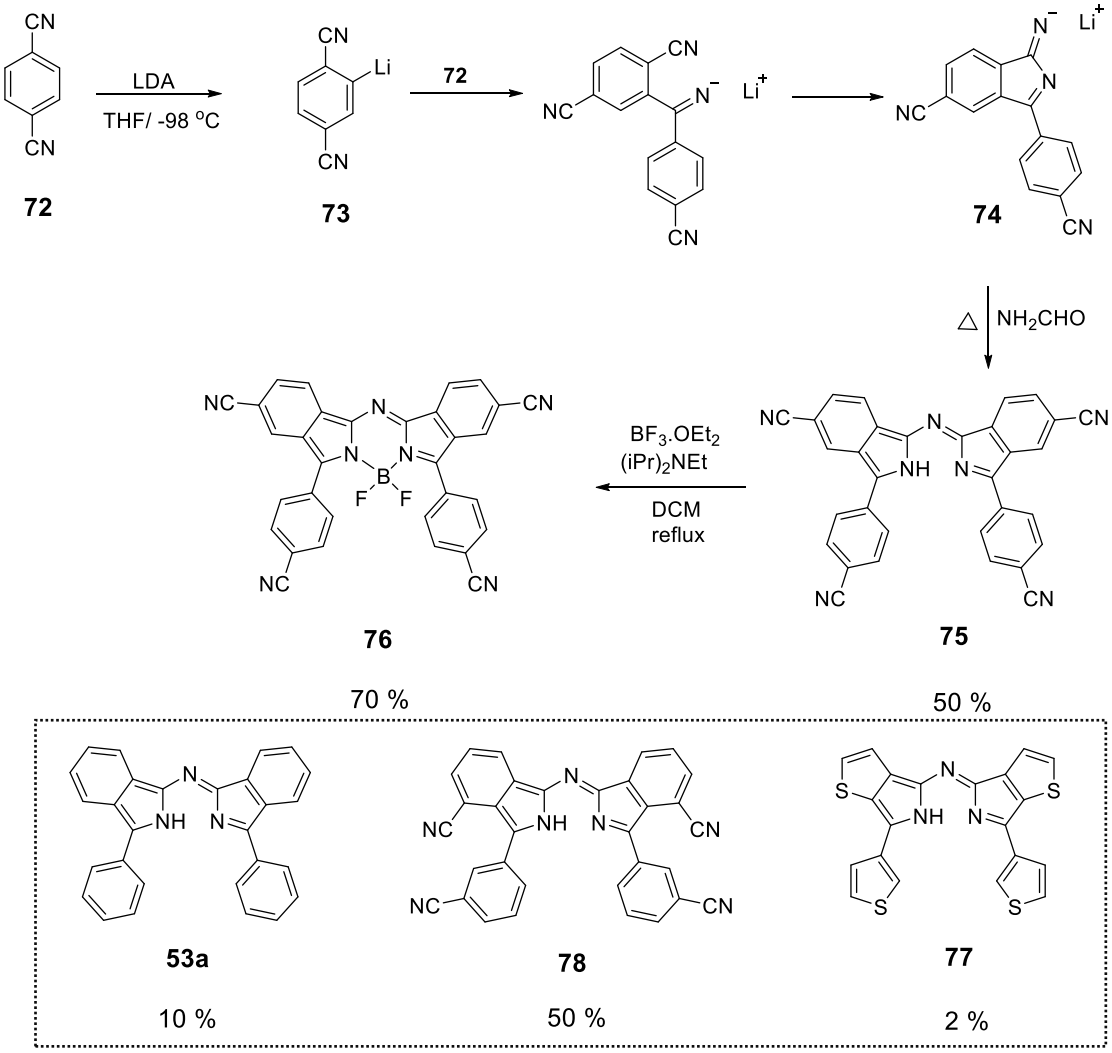

Scheme 1.21: Formation of benzo-fused aza dipyrromethenes by reacting of *ortho*-lithiated nitriles with benzonitrile.[73]

Our group has reported a straightforward synthetic pathway for a new type of aza (dibenzo) dipyrromethenes and the corresponding aza-BODIPY derivatives via the aminoisoindoline precursors.[41] The synthesis of the aminoisoindolines starts with the precursor amidine **79** under palladium catalysed cross coupling with a variety of arylacetylenes and furnishes a number of aminoisoindolines.[75] The aminoisoindolines **80** and **81** undergo efficient self-condensation to form the π extended aza (dibenzo) dipyrromethene derivatives **81** and **82**.[41] Typically the aminoisoindolines **80** and **81** were heated under reflux in toluene for 2 h, and the products were isolated by crystallization from dichloromethane and methanol to obtain deep red crystals of aza (dibenzo) dipyrromethene derivatives **82** and **83**. The straightforward treatment of aza (dibenzo) dipyrromethene precursors **82** and **83** with $BF_3 \cdot OEt_2$ furnished the corresponding aza (dibenzo) BODIPY analogues **84** and **85** in moderate yield (Scheme 1.22).[41]

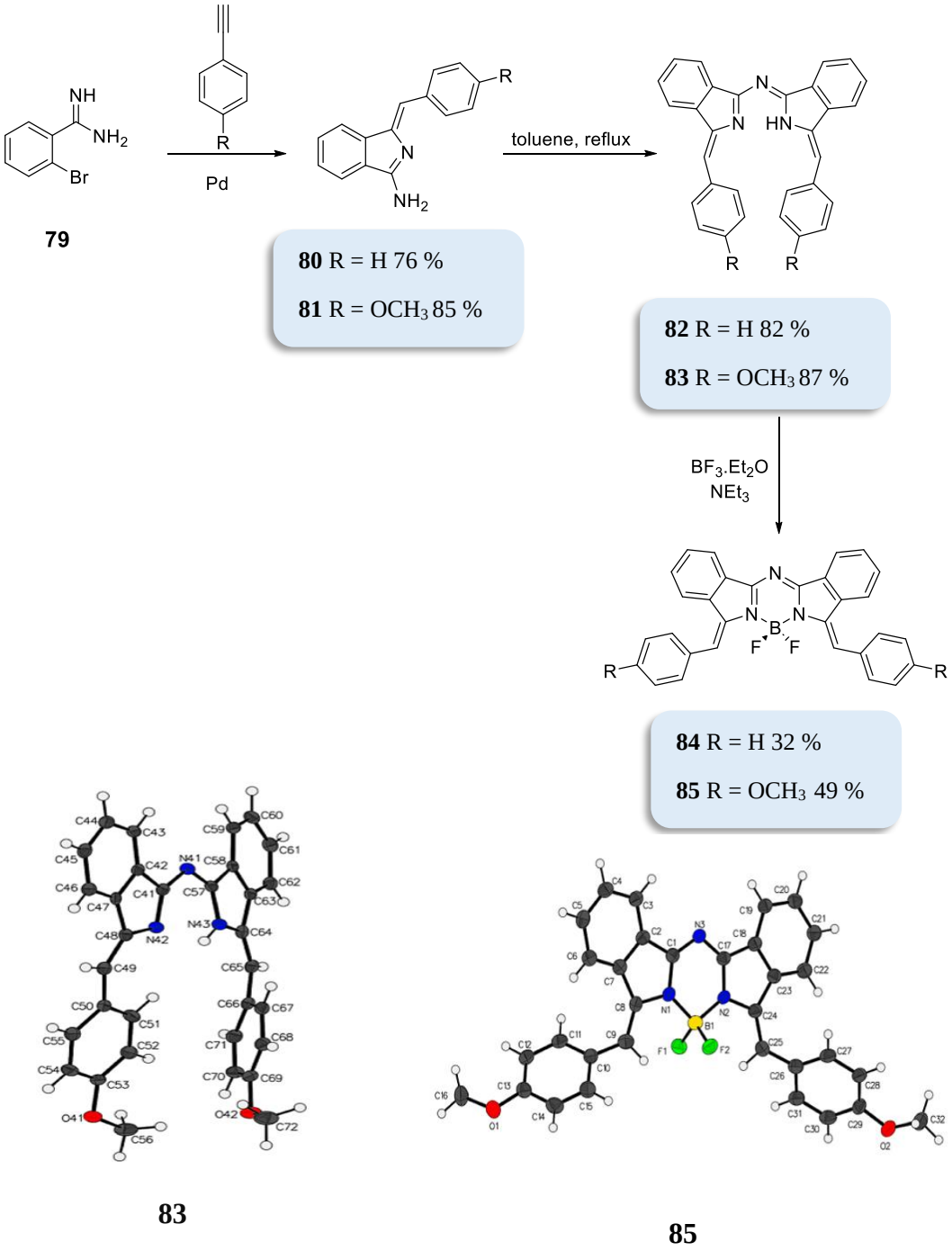

Scheme 1.22: Synthesis of aza BODIPYs from aminoisoindolines and X-ray crystal structure of compound **85**.[41]

Furthermore, X-ray crystallography and analysis of **82** and **83**, showed that the same *Z,Z* configuration present in the starting material was reproduced in the aza (dibenzo) dipyrromethene products.[41] However, it is immediately apparent from the crystal structure of **85** (Scheme 1.22), that the aza BODIPY analogues display the opposite of the configuration of their precursors i.e., the *E,E* configuration. However, this may solely be a result of the crystal packing and solid-state interactions favouring in this case

the *E,E* configuration.[41] The photophysical properties of these analogues are promising. Aza (dibenzo) dipyrromethenes exhibited a relatively broad profile in the visible region with a maximum at 465 nm in dichloromethene.[41] Addition of further conjugation via the introduction of 4-methoxy substituents in **83** led to shift the absorption to 491 nm, as observed in similar classical BODIPYs.[65] Analogous to their precursors, boron complexes **84** and **85** show absorption maxima at 439 and 469 nm, respectively, (Figure 1.10) supporting a similar trend of the substituent effect. However, unlike their precursors **82** and **83**, they show fluorescence with significant Stokes shifts of around 90 nm, albeit with low quantum yields (**84** ~ 5 %, **85** ~ 0.5 %).[41]

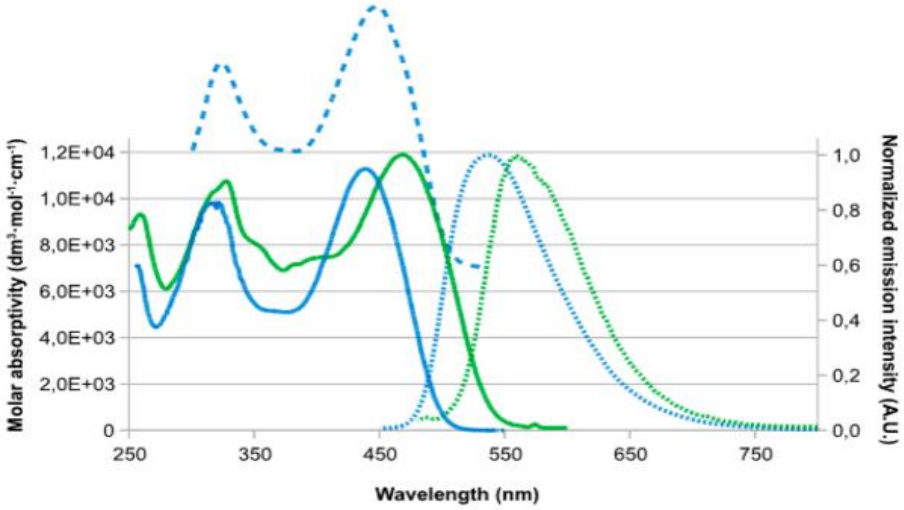

Figure 1.10: UV−vis absorption spectra for compound **84** (blue solid line), and compound **85** (green solid line), and normalized fluorescence emission (blue dotted line) spectra of **84** and for **85** (green dotted line), in DCM and the excitation spectrum of **84** (dashed line, λ_{max} em = 537 nm).[41]

1.7.3 Synthesis of [b] and [c] fused aza dipyrromethenes and aza BODIPYs

1.7.3.1 From benzo [c, d] indole-2-amine

Synthesis of [b] and [c]-fused aza dipyrromethenes and aza-BODIPYs from benzo [c, d] indole-2-amine provides an alternative route for building ring-fused aza dipyrromethenes and their corresponding aza-BODIPYs.[76] The first reported of naphtho [c] and [b] fused aza-BODIPYs was by Vasilenko and co-workers in 1986 using 2-benz-[c,d] indolamine hydroiodide and 2-(methylthio)benz[c,d]-indole-hydroiodide (Scheme 1.23 inset).[77] Subsequently in 2015 Kobayashi and Shimizu reported the use of a Schiff-

base reaction involving titanium tetrachloride to catalyse this reaction. This allowed them to access the benzo[c,d]indole- containing-aza-BODIPY skeleton **86** by a facile treatment of commercially available benzo[c,d] indole-2(1H)-one (lactam) **88** and heteroaromatic amine **87**, with titanium tetrachloride in triethylamine.[76] Then $BF_3.Et_2O$ was added to the reaction mixture producing compound **86** in 41 % yield. (Scheme 1.23).[76] The aza-BODIPY **86** demonstrated strong fluorescence in solution and showed good solid-state emission.[76] However, the absorption and emission is centred at around 540 nm, which is not ideal for potential applications as a NIR dye.[76] Following this synthetic pathway compound **90** was successfully achieved by reacting diketopyrrolopyrrole (DPP) **89** as the starting material with heteroaromatic amine **87** in 1.0 % yield. In comparison to **86** the dimer **90** exhibited a significantly red-shifted absorption maximum at 747 nm which is more suitable for NIR applications. So far these remain the only two synthetic strategies towards fused aza-BODIPY structures utilizing benzo [c, d] indole-2-amine.[76, 77]

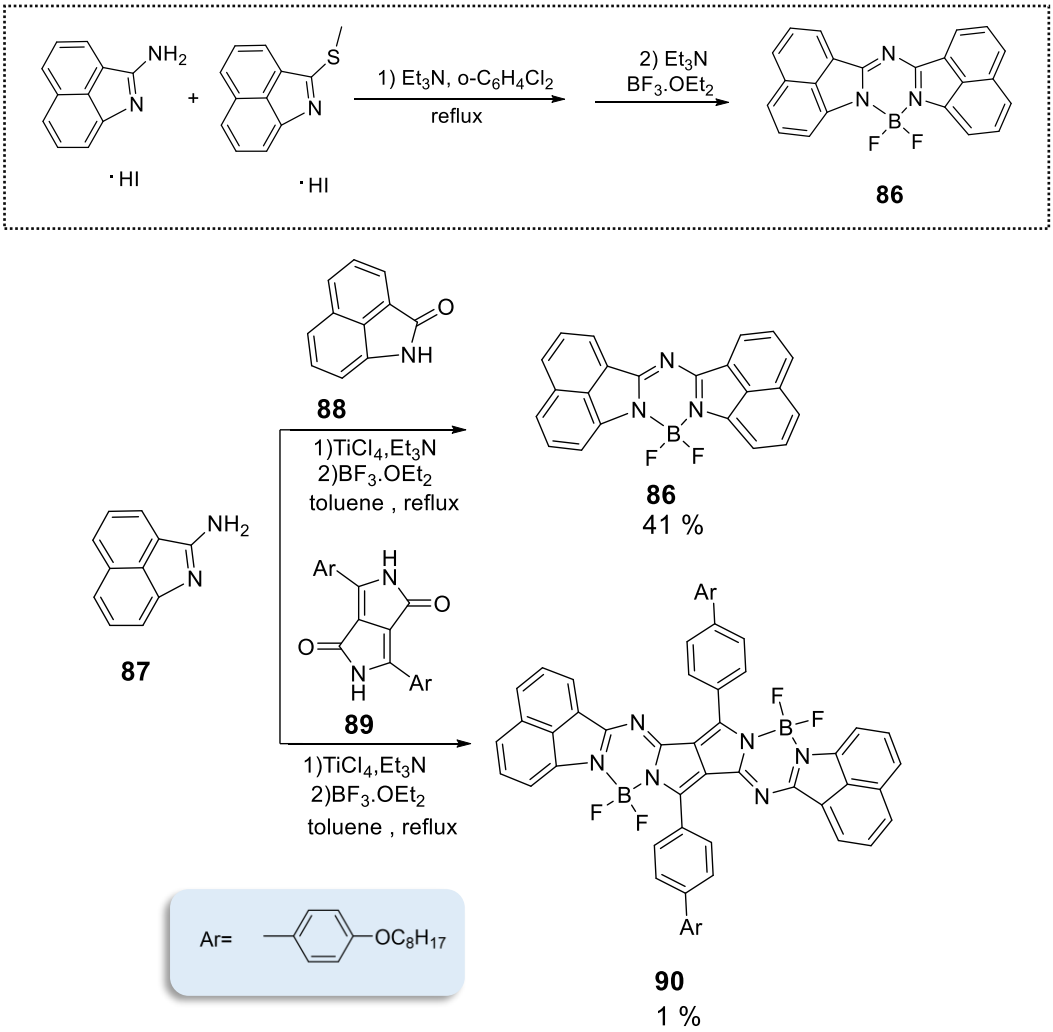

Scheme 1.23: Synthesis of aza-BODIPYs **86** and **90** from benzo [c, d] indole-2-amine.[76 ,77]

1.7.3.2 Postmodifications of ring-fused aza-BODIPYs

The final route towards [b] and [c]-fused aza dipyrromethenes and aza-BODIPYs is via postmodification of ring-fused aza-BODIPY dyes.[61] Large numbers of aza-BODIPY chromophores, in particular tetraphenyl and hexaphenyl aza BODIPYs, are readily available via facile synthesis.[61] Thus, further annulation onto these pre-synthesised cores provides a promising strategy to access various ring-fused aza-BODIPYs with extended π -conjugation, that complements the three strategies previously discussed.[61] A number of ring-fused aza-BODIPYs have been reported recently via post functionalization of the parent aza-BODIPY chromophores.[78, 79, 80] In particular Jiao and co-workers have reported efficient postfunctionalisation strategies primarily of tetraphenyl and hexaphenyl aza-BODIPY derivatives, typically using regioselective intramolecular oxidation reactions or palladium catalysed C–H activation followed by intramolecular coupling reactions.[78, 79, 80] This route of annulation of tetraphenyl or hexaphenyl substituted aza-BODIPYs provided access to [b]-fused **92**, and [b], [c]-fused **91** derivatives in moderate yields.[78, 79]

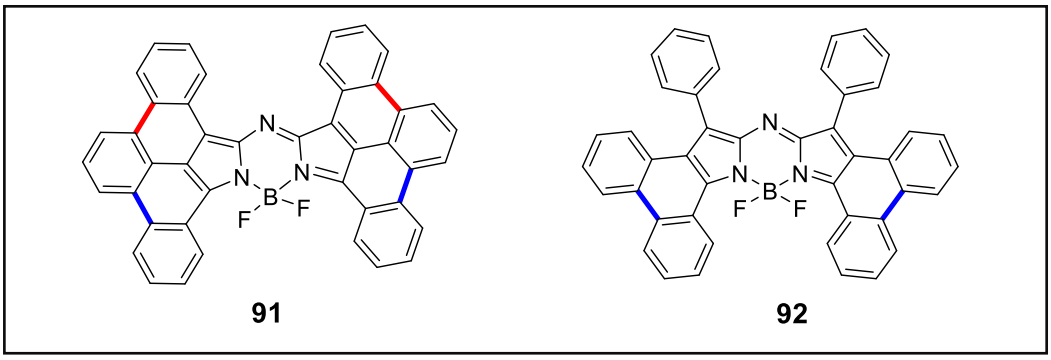

Figure 1.11: Structures of [b]-fused aza BODIPY **92** and fully fused system **91**.

In 2017 Jiao, Hao and co-workers reported the preparation of three novel [b] fused aza-BODIPYs **96 a-c** including an interesting nine-ring fused structure (Scheme 1.24).[78] Regioselective bromination of aza BODIPY **93**, using a literature procedure, led to 2,6-dibromo aza BODIPY **94** in nearly quantitative yield (Scheme 1.24). Suzuki coupling of 2,6-dibromo aza BODIPY **94** with an aromatic boronic acid was followed by an iron(III) chloride mediated intramolecular oxidative aromatic coupling which led the desired ring fused aza-BODIPYs **96 a-c**. The oxidative ring fusion reaction proved to be highly regioselective with qualitative isolated yields over 93 %, and none of the [c] fused product, or any other fused derivatives were observed.[78]

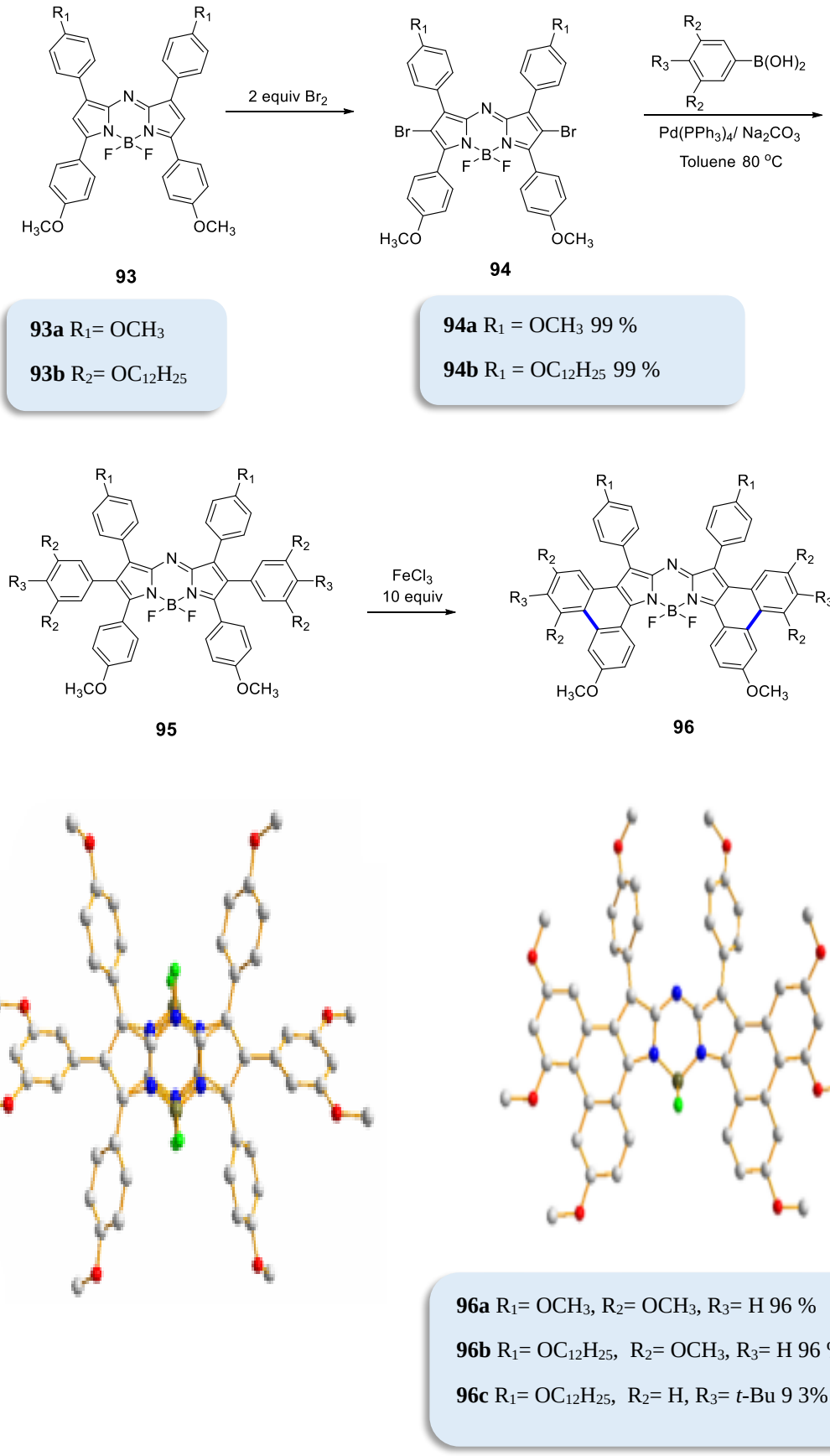

Sheme 1.24: Regioselective formation of [b]-fused aza BODIPYs via postmodification of ring-fused aza-BODIPYs, and X-ray crystal structures of compounds **95a** and **96a**.[78]

The resultant aza-BODIPYs **95 a-c** show nearly identical strong absorption centred at around 683 nm and moderate fluorescence emission centred at 716 nm, respectively, in toluene. Compounds **96 a-c** show absorption at around 790 nm and fluorescence emission centred at 807. In comparison with **95 a-c**, this ring fusion brings more than 100 nm red-shift in both the absorption and emission bands.[78]

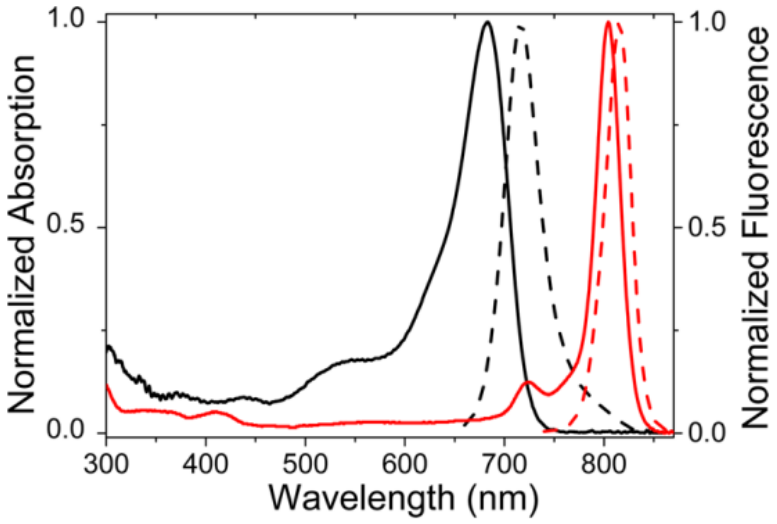

Figure 1.12: UV- vis absorption spectra or compound **95a** (black solid line), and compound **96a** (red solid line), and fluorescence emission spectra (dotted lines) of **95a** (black) and **96a** (red) in toluene.[78]

Attempts to form the fully fused system **91** via treatment of compound **95a** with a large excess of $FeCl_3$ led mainly to the product **96a-c** instead of the fully fused product (Scheme 1.24).[78] Varied conditions of oxidants, solvents, temperatures, and light irradiation did not lead to further fusing of **96a-c** to generate the expected [b],[c] fused product.[78] Jiao, Hao and co-workers reported the successful synthesis of the [b],[c] fused aza BODIPY **99** (Scheme 1.25) from the oxidative ring-fusion reaction of hexaphenyl aza BODIPYs .[80] In analogous porphyrin systems Osuka [81] and Gryko [82] had both demonstrated that the electron-rich directing groups were conclusive for the successful oxidative ring fusion.[80] Thus Jiao, Hao and co-workers rationalized that the addition of the electron-rich directing groups on a specific phenyl group of hexaphenyl aza BODIPYs would be able to activate it for efficient oxidative annulation and thus form the [b], [c] fused **99**. Hence, **97** which bears two methoxy (electron rich directing)

groups on the *meta*-positions of 1,7 phenyls was prepared. Suzuki coupling reactions of aza dipyrromethene **97** with 4-*tert*-butylphenyl boronic acid followed by complexation with $BF_3.Et_2O$ yielded the desired product **98a** in 65 % (Scheme 1.25).[80] In this reaction compound **97** underwent Suzuki coupling reaction instead of its corresponding boron complex due to formation of some BF_2 decomposition products. Treatment **98a** with 40 equivalents of $FeCl_3$ gave the desired fully fused **99a** in 11 % yield. Halving the amount of $FeCl_3$ to 20 equivalents, gave the corresponding [b] ring-fused product **100a** in 31 % yield. To activate the system towards formation of [b], [c] ring fused systems they synthesized **98b** and **98c** with two additional methoxy groups on the *meta*-positions of 2,6-phenyls. Applying the same reaction conditions as to **98b** and **98c** led to the corresponding [b], [c] ring fused aza-BODIPYs **99b** and **99c** in 19 % and 41 % yields respectively (Scheme 1.25).[80] As expected, compound **98b** and **98c** demonstrated higher reactivity; they required only 20 equivalents of $FeCl_3$ to initiate oxidative ring-fusion reaction to form the fully annulated system.[80] As mentioned previously the [b], [c] fusion results in an over 100 nm red-shift compared to the parent in the absorption spectrum. Hexaphenyl aza BODIPYs **98 a-c** showed absorption maxima at 675, 684, and 674 nm, respectively, which were red-shifted to 787, 808, and 791 nm, respectively in **100 a-c**. Notably the [b],[c] fused **99 a-c** showed a further red shift, with near-infrared absorption in the range 826 – 878 nm and emission in the range 832 – 907 nm.[80] Figure 1.13 shows the UV-Vis absorption and fluorescence emission spectra of compounds **98a**, **99a** and compound **100a**.[80]

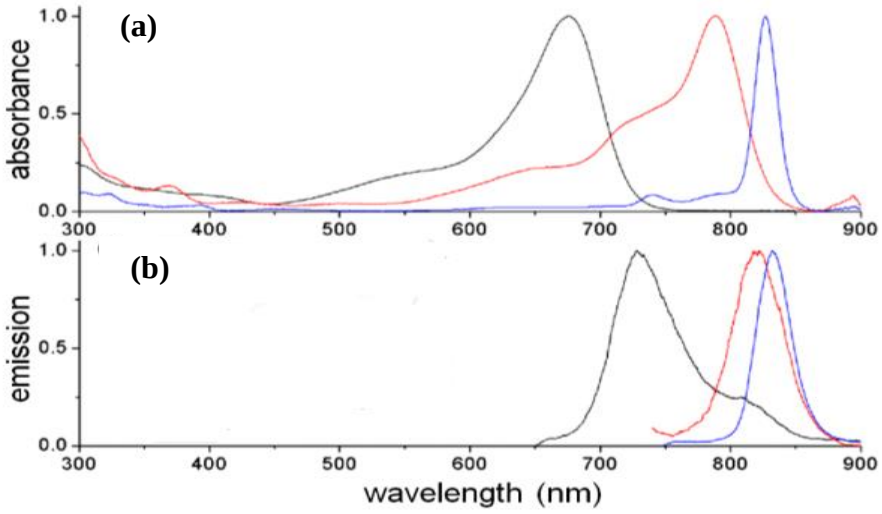

Figure 1.13: UV-vis absorption **(a)**, and fluorescence emission **(b)** spectra of compound **98a** (black lines), compound **100a** (red lines), and compound **99a** (blue lines) in toluene.[80]

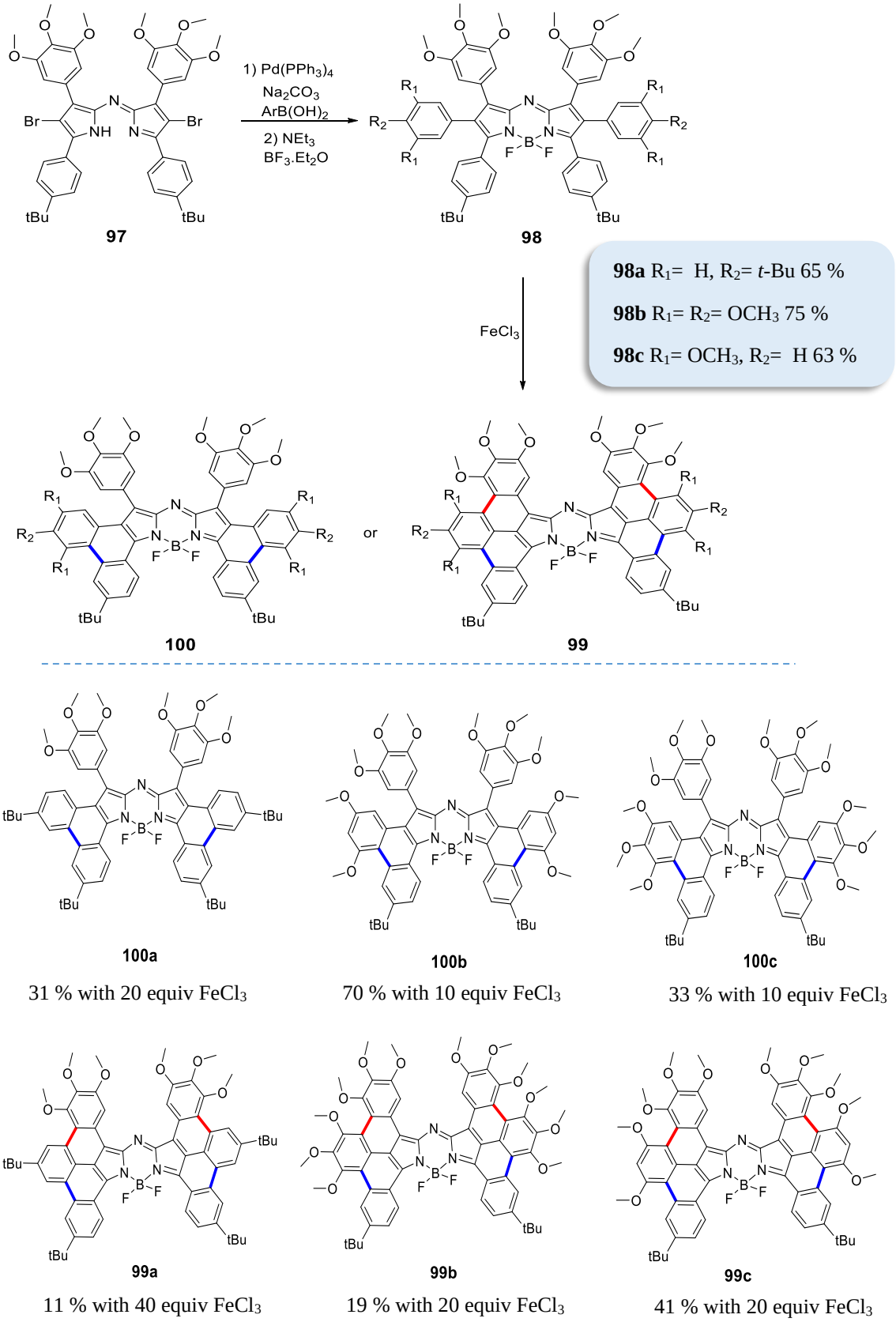

Scheme 1.25: Results of ring-fused aza-BODIPYs depending on the equivalents of $FeCl_3$ used.[80]

Applying the concept of using electron rich methoxy groups to direct the oxidative cyclisation, later in 2017 Jiao, Hao and co-workers reported the synthesis of [c] fused

aza BODIPYs. They used an analogous strategy to previously described i.e. bromination followed by Suzuki coupling and palladium catalysed intramolecular C−H activation reaction.[79, 83] However, oxidative annulation still generated exclusively [b]-fused compound **103** in 87 % yield (Scheme 1.26).[79] Bromination of hexaphenyl aza BODIPY **102** led to dibromo hexaphenyl aza BODIPY **104** in 82 % yield. The regioselectivity can be explained by the three electron rich directing methoxy groups on the 1,7-phenyls of aza BODIPY compound **104**, $Pd(OAc)_2$ catalysed intramolecular C−H activation of dibromo hexaphenyl aza BODIPY **104** led to the [c]- fused isomer **105** in 46 % yield. (Scheme 1.26). This compound **105** showed absorption at 745 nm whereas the unfused precursor to **102** absorptions at 694 nm. This 51 nm red-shift is lower than that achieved via the corresponding b fused ring systems.[79]

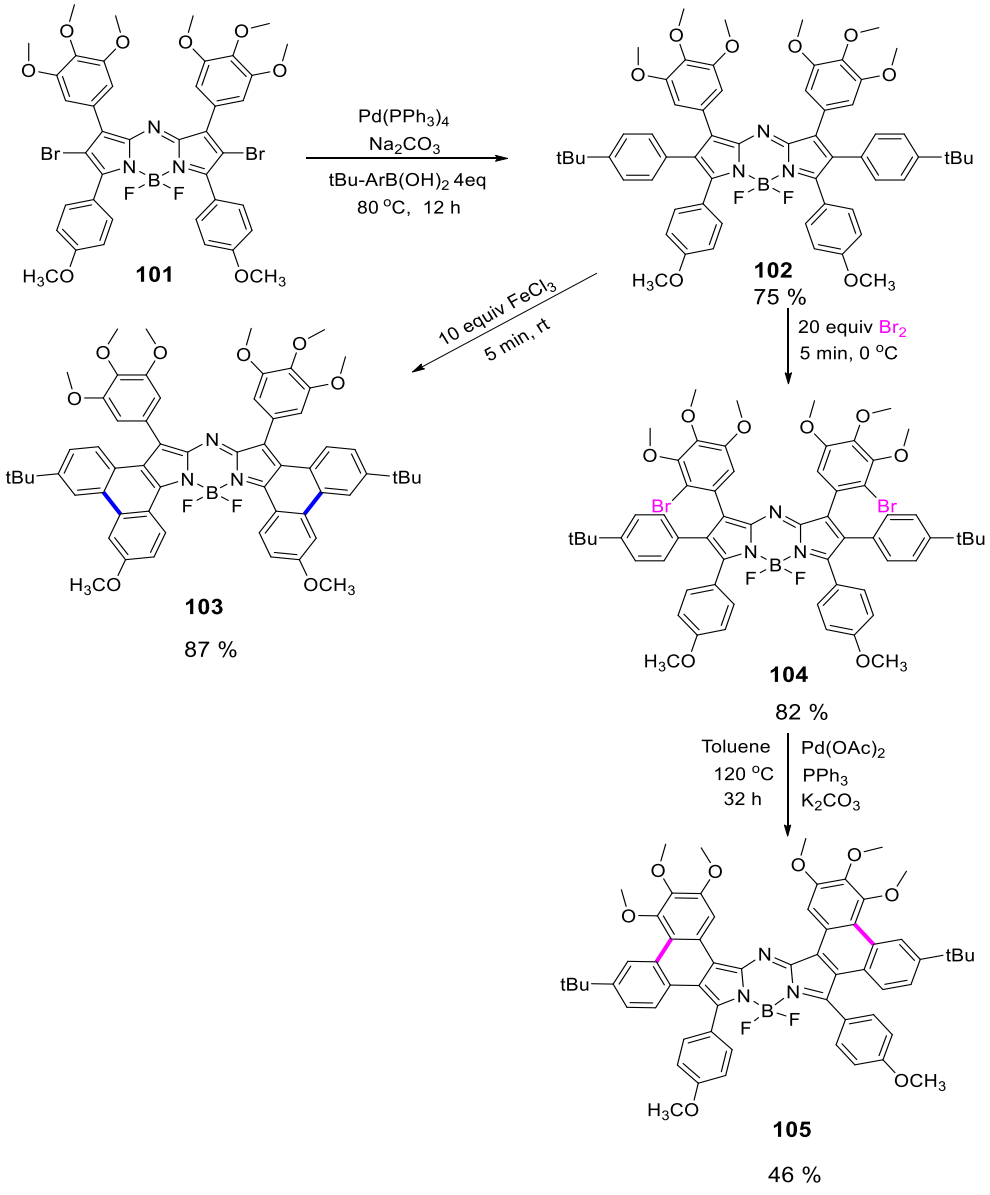

Scheme1.26: Synthesis of fused aza BODIPYs **103** and **105**.[79]

1.8. Boron fused aza-BODIPYs

A number of boron fused aza-BODIPYs have been prepared primarily using a brominating agent to cause demethylation of a methoxy substituent followed by spontaneous cyclisation.[61] For example O'Shea et al reported the synthesis of boron fused aza-BODIPYs **107 a-d** from the tetra aryl-substituted aza-BODIPYs precursors **106 a-d**, which in turn can be synthesized in four steps from commercially available materials.[84] Treatment of the tetra aryl-substituted aza-BODIPYs **106 a-d** with BBr_3 resulted in demethylation of the methoxy groups to the corresponding bisphenols followed by spontaneous cyclization to give the corresponding boron fused **107 a-d** in 21 to 61 % yield. However, the methoxy and methylamine substituted **106 e** and **106 f** did not yield any products. They also observed that prolonging the reaction time or amount of BBr_3 led to further bromination on the benzene and pyrrole rings. These compounds were also isolated and analysed. As expected, the restrictions caused by the B-O bonds led to a shift in **107 a** absorption by 86 nm and in its emission maxima by 58 nm compared to the unfused parent compound **106 a**.[85]

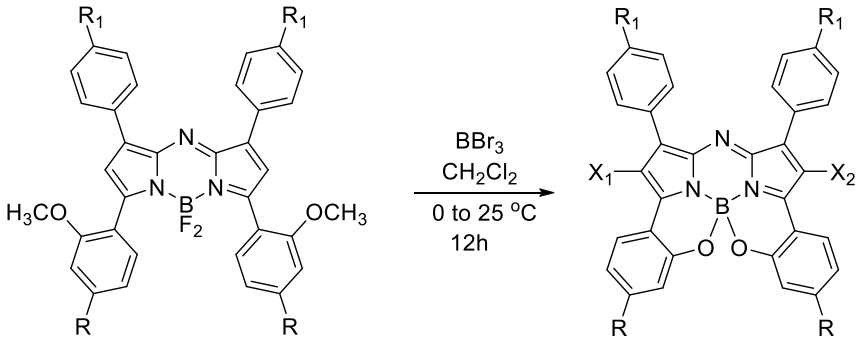

106 a-d **107 a-f**

	a	b	c	d	e	f
R	**H**	**H**	**H**	**H**	**OMe**	**NMe_2**
R¹	**H**	**Br**	**Br**	**Br**	**Br**	**Br**
X¹	**H**	**H**	**Br**	**Br**	**H**	**H**
X²	**H**	**H**	**H**	**Br**	**H**	**H**
Yield (%)	**62**	**36**	**41**	**21**	**n/a**	**n/a**

Scheme 1.27: Synthesis of boron fused aza BODIPYs **107 a-d**.[85]

1.9. Aim of the Project

In recent years, the investigation of BODIPYs has attracted many researchers due to their interesting photophysical properties. They exhibit absorption bands close to the NIR region, which led to increased research into their applications. The first synthesis of the precursor azadipyrromethenes in our group was achieved during the development of a new synthetic strategy towards new classes of *meso*-aryl tetrabenzotriazaporphyrins (TBTAPs). However, later our group developed new straightforward synthesis pathways to access this new type of azadipyrromethene from self-condensation of aminoisoindolines under reflux, then converting to the corresponding aza BODIPYs. Aminoisoindolines were smoothly achieved by reacting a 2-bromo amidine with aryl acetylene via copper-free Sonogashira cross-coupling, followed by a cycloismerization reaction under microwave irradiation .[75] The resulting aza BODIPYs bear structural similarity to the traditional aza BODIPYs, but differ significantly in the electron configuration leading to notably different absorption and emission properties (Figure 1.14).[41]

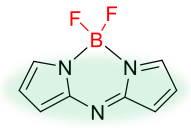

traditional aza BODIPYs

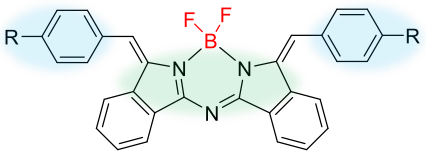

aza BODIPYs in the Cammidge group previous work

Figure 1.14: Traditional aza BODIPY structure, compared with the resulting aza BODIPY in Cammidge group's previous work.

The bond arrangement in the traditional aza BODIPY is not possible in the resulting structure due to presence of the external units (phenyl methylene) at the α position and benzo fusion at the β position on the aza BODIPY structure (Figure 1.14). Building on this work, this project aims to investigate the scope of the processes, starting with extension to alkyl and benzyl acetylenes, alkylated aminoisoindolines and use as the precursors in the synthesis of aza (dibenzo) dipyrromethenes and the corresponding aza-BODIPYs, to access aza BODIPYs that have similar π systems to that found in the traditional aza BODIPYs. To achieve this aim, 1-hexyne was selected for the synthesis of alkyl aminoisoindoline, which is the key intermediate in the synthesis of the main

target. The resulting structure is expected to change the chemistry significantly by an oxidation reaction with loss of two hydrogens as described in Figure 1.15.

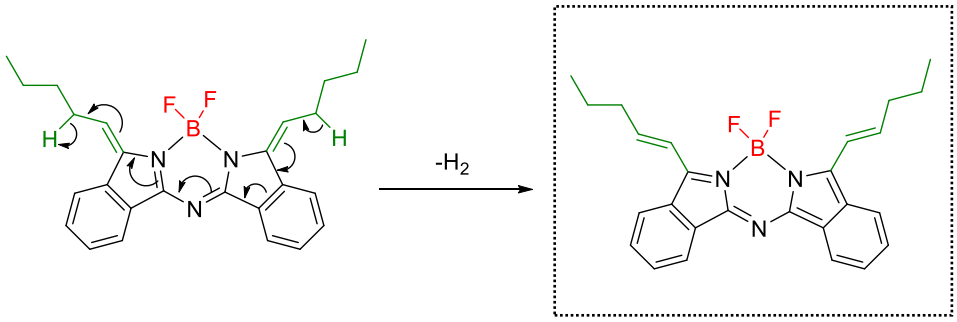

Figure 1.15: Target structure.

The second aim is investigating the reactivities and electronic effects of different derivatives (such as donor and acceptor substituents), and alternative aryl units on the synthesis and properties of these molecules. and investigate whether a synthetic strategy could be developed to efficiently give unsymmetrical derivatives. There are no unsymmetrical derivatives reported to date and the investigation of electronic effects has not been investigated.

The last aim is investigating the extension of π conjugated system on the aza dipyrromethenes either by ring fusion reactions of the parent aza BODIPYs, or formation of the macrocycle structures from the aza (dibenzo) dipyrromethene derivatives.

Chapter 2: Results and Discussion

2.1 Attempted syntheses of alkyl aza (dibenzo) dipyrromethenes (ADBDP)

Aza (dibenzo) dipyrromethenes are precursors to a subset of BODIPY analogues. In this class of compounds, the methine carbon at the *meso* position is replaced with strongly electron withdrawing nitrogen atom as we mentioned in the introduction chapter. Several modifications have been published to optimize the aza-BODIPY scaffolds in order to further shift the absorption and emission properties towards the far red and NIR region.[58,59] In 2014 our group has published a new class of conjugated boron aza (dibenzo) dipyrromethenes and its precursors aza (dibenzo) dipyrromethenes through relatively straightforward synthetic procedure from readily available aminoisoindoline derivatives.[41] In this synthetic pathway the aminoisoindolines are the key intermediate which can be smoothly accessed from 2-bromobenzoamidine **79** as described in Scheme 2.1. Heating of aminoisoindolines **80** and **81** under reflux in toluene at 120 °C produces the π-extended aza-(dibenzo) dipyrromethene derivatives **82** and **83** in good yield. Aza (dibenzo) dipyrromethene derivatives smoothly converted to the corresponding aza BODIPYs **84** and **85** by treating with $BF_3.OEt_2$ in the presence of TEA as a base in dry DCM (Scheme 2.1).

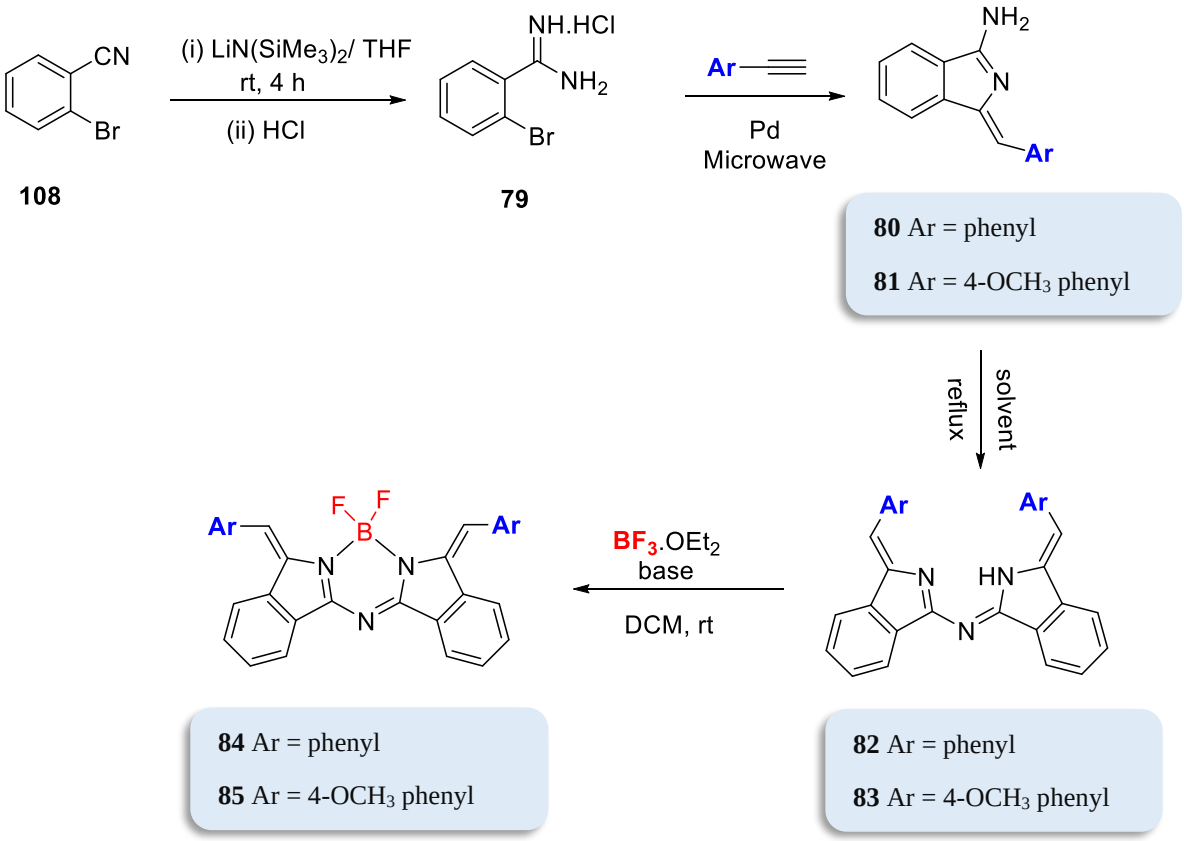

Scheme 2.1: The full synthetic route towards aza BODIPYs **84**, and **85** and their precursors (ADBDPs) **82**, and **83**.[41]

The resulting structures include modifications on the parent core such as, replacement of the carbon atom on the methine bridge (*meso*-carbon) with nitrogen, extended the π conjugation system via benzo fused the pyrrole rings at the β position on the ADBDP unit, and functionalization of pyrrole units at the α position via conjugation to a benzene ring.[44] There is contrasting spectroscopic behaviour when comparing the resulting molecule with traditional BODIPY derivatives, presumably as a result of the local aromaticity that is preserved in the benzene rings giving a different electronic structure to that found in BODIPYs, they display absorption in the visible region with a maximum ~ 465 nm in DCM.[41]

Based on the success of this strategy this project aims to investigate the scope of this process and extend this strategy to furnish a range of aza (dibenzo) dipyrromethanes (ADBDP), and the corresponding aza-BODIPYs that could have interesting properties and applications. A key stage to achieve this aim would involve extending the copper free Sonogashira coupling to alkyl and benzyl acetylenes. This seemingly simple structural modification is expected to change the chemistry significantly due to the potential tautomerism of the intermediate and its subsequent impact on the electronic configuration of the BODIPY unit (Figure 2.1).

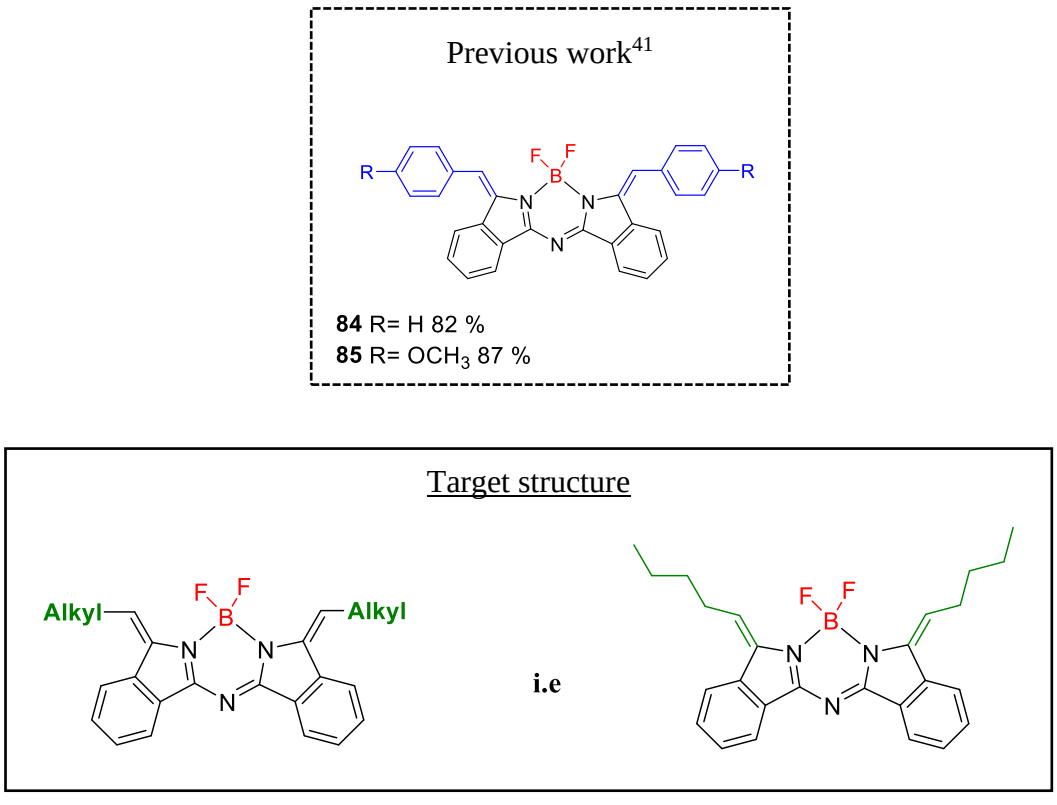

Figure 2.1: Target structure of alkyl aza BODIPY.

2.1.1 Attempted syntheses of alkyl aminoisoindolines for use in the synthesis of aza (dibenzo) dipyrromethenes (ADBDP) and aza BODIPYs and competing formation of aminoisoquinolines.

Aminoisoindoline derivatives have been used as key intermediates in the synthesis of aza BODIPYs and its precursor ADBDP. Previously our group has published successful synthesis of aminoisoindoline derivatives following the procedure reported by Hellal and Cuny[75] as mentioned in the introductory section. This led us to consider extending it to embark on the formation of aminoisoindoline derivatives starting with extension to alkyl and benzyl acetylenes as the key intermediates in the synthesis of aza-BODIPYs (Scheme 2.2).

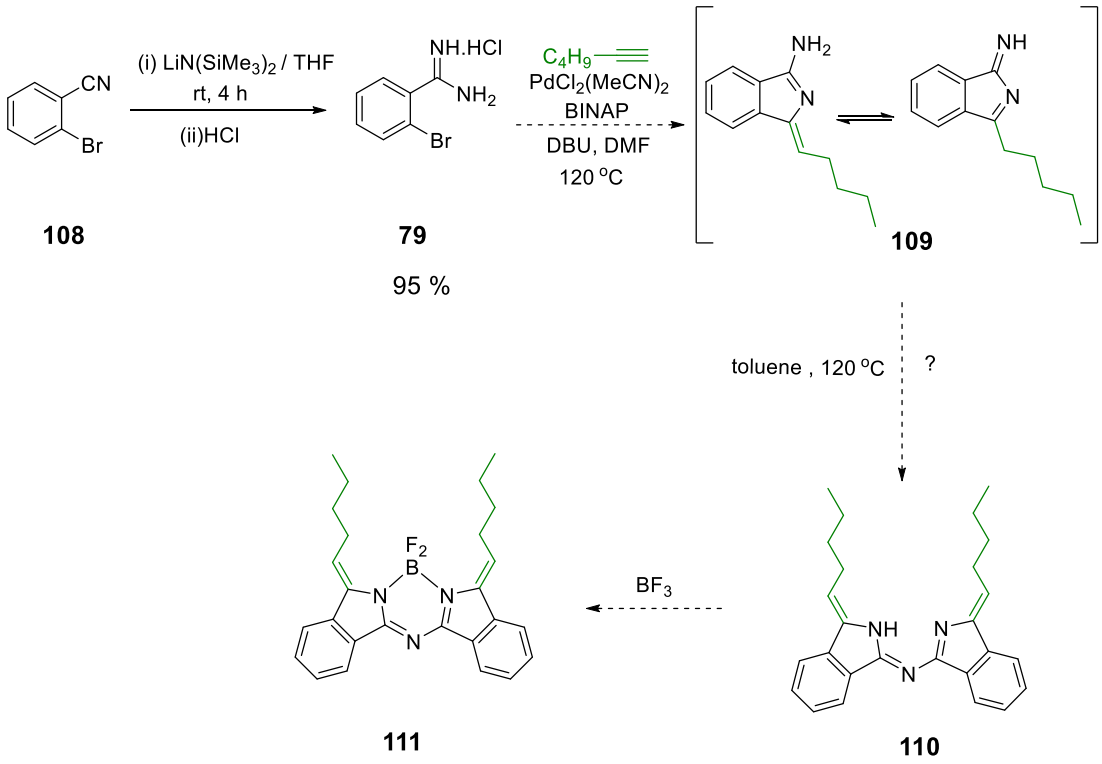

Scheme 2.2: Outline plan toward hexyl aminoisoindoline **109** and its corresponding aza (dibenzo) dipyrromethene **110** and aza BODIPY **111** using 1-hexyne.

The first stage in the formation of the aminoisoindoline derivatives begins by following the procedure published by the Meijere group for the synthesis of amidine **79**, by converting 2-bromobenzonitrile **108** to its corresponding 2-bromobenzamidine hydrochloride **79**. [86] Consequently 2-bromobenzonitrile **108** was treated with a solution of lithium bis(trimethylsilyl)amide in dry THF, and the mixture left stirring under

nitrogen at room temperature for 4 h. Then the mixture was quenched with a solution of HCl (5N) in isopropanol to obtain 2-bromobenzimidamide hydrochloride **79** as a white sold in 95 % yield. Compound **79** was characterised by ^{1}H-NMR spectroscopy where N-H protons are clearly visible as broad peaks at 9.49 ppm and 9.25 ppm (Figure 2.2). The spectra matched the published ^{1}H-NMR spectrum for compound **79**.

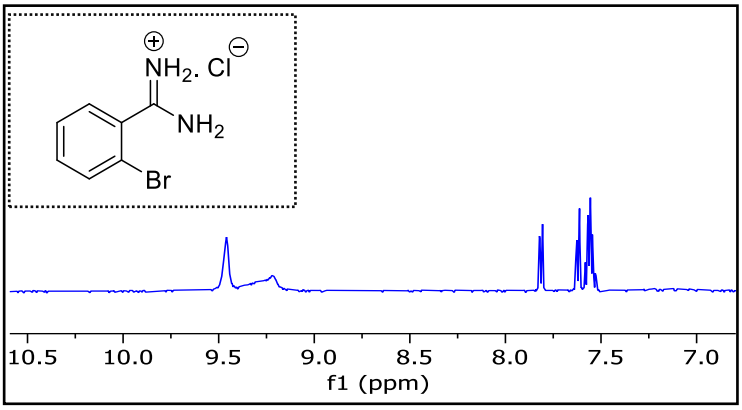

Figure 2.2: ^{1}H-NMR spectrum of 2-bromobenzimidamide hydrochloride **79.**

The mechanism of formation of compound **79** includes a nucleophilic attack by the nitrogen bis trimethylsilyl anion (stabilized by a lithium cation) at the partially positive carbon atom of the nitrile group. Acid work up removes the trimethylsilyl groups yielding 2-bromobenzamidine **79** (Scheme 2.3).

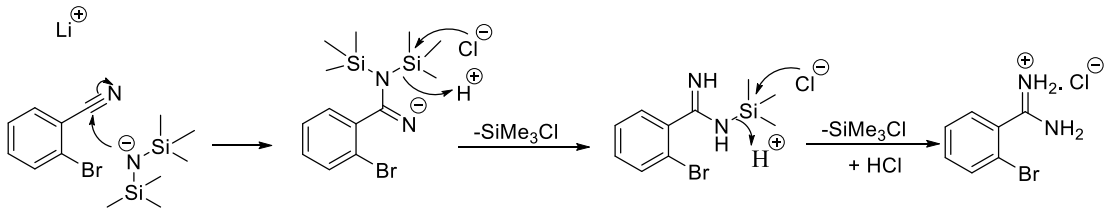

Scheme 2.3: Formation mechanism of compound **79.**

The next stage was based on the procedure developed by Hellal and Cuny, which involves synthesis of the aminoisoindolines using aryl acetylene derivatives.[75] The starting material **79** underwent a palladium catalysed copper-free Sonogashira cross-coupling followed by a cycloismerisation reaction under microwave irradiation to give aminoisoindolines in good yield.[75] In this pathway the copper was replaced by an amine

as a base. As in Sonogashira cross coupling the unfavourable homocoupling of the terminal alkyne was formed. In the original procedure the one-pot reaction was accomplished by reacting amidine, phenyl acetylene, catalytic amounts of palladium and BINAP as ligand, in the presence of DBU as a base. The reaction was carried out in DMF as the solvent, and this mixture was placed in a microwave vial then irradiated under microwave at 120 ºC for 1 h. After that the mixture was separated and washed with a saturated solution of $NaHCO_3$ and purified by column chromatography and crystallised from DCM: PE (1:1) giving the pure aryl aminoisoindolines as yellow crystals in good yield.[75] ^{1}H-NMR spectrum of aminoisoindoline compounds illustrates the characteristic vinyl proton at ~ 6.65 ppm confirming that this one pot reaction is stereo selective producing the *(Z)*–isomer as major product.[78] The suggested copper-free Sonogashira reaction mechanism is illustrated in (Scheme 2.4). The first step of the mechanism involves oxidative addition of the aryl halide to the active catalyst $[Pd^{(0)}L_2]$, to form the four-coordinated palladium complex. The acetylene ligand consequently coordinates to palladium metal followed by deprotonation of the ligated alkyne occurs through the action of a base, DBU. Then *trans*/*cis* isomerization and reductive elimination occur stepwise reforming the catalytic species $[Pd^{(0)}L_2]$ ready to start a new cycle.[87]

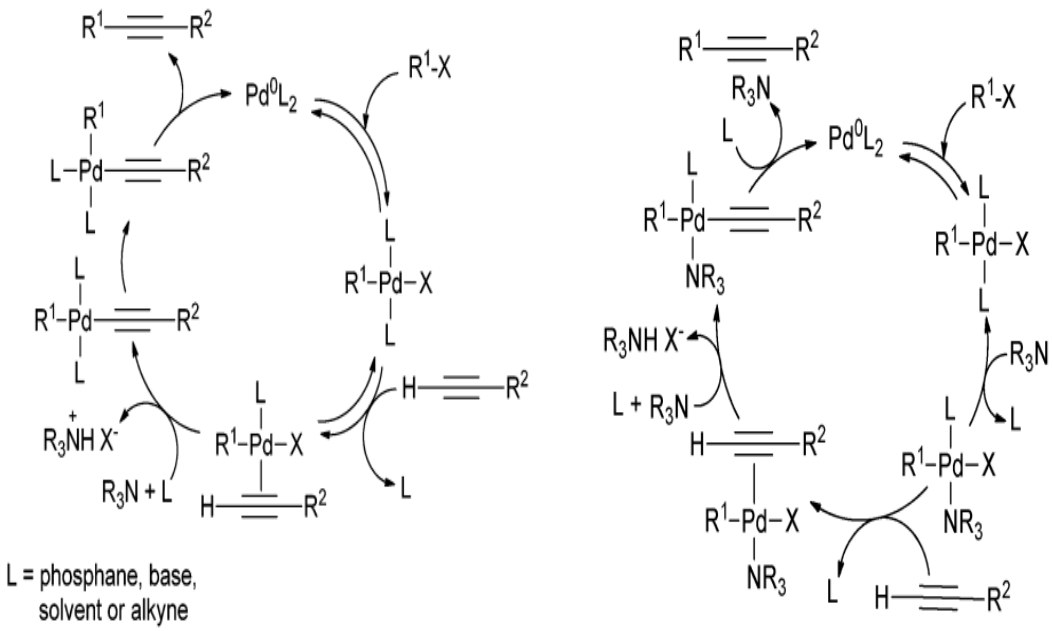

Scheme 2.4: Suggested copper-free Sonogashira cross-coupling reaction.[87]

The mechanism described above was commonly preferential if the amine is a less good ligand than the alkyne for the palladium(II).[88] In the case of synthesis of aryl aminoisoindoline, coupling is immediately followed by a regioselective 5-exo-dig cycloismerization domino reaction to give the final product. The suggested mechanism includes three steps clarified in Scheme 2.5. The reaction is initiated by coordination of the palladium catalyst to the alkyne, followed by the loss of HCl. Finally, protonation recovers of the catalyst.

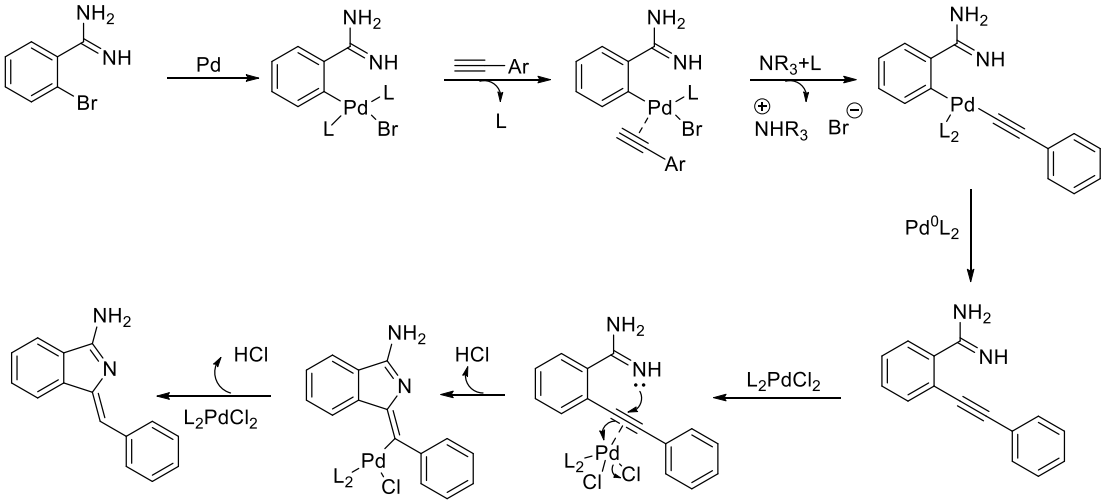

Scheme 2.5: Suggested mechanism for the 5-exo-dig cyclodimerization.

Accordingly, in order to achieve the alkyl aminoisoindoline compound **109**, 1-hexyne was selected due to it is availability and likely solubility to the final compound. Attempting to synthesise compound **109** following the identical conditions as described above. A product with the expected (*m/z* 200) mass was isolated. However, the ^{1}HNMR spectra of the resulting compound demonstrated that the expected aminoisoindoline **109** was not formed. A new singlet of 1H appeared at 6.84 ppm instead of the expected triplet peak for the alkene proton in the target compound (labelled *****, Figure. 2.3). Which reasoned this corresponds to the newly formed C-H proton, formed via cyclisation to yield a different ring system. The alkyl chain gives a characteristic set of peaks starting with a triplet integrating to two protons corresponding to alkyl proton followed by the rest of peaks giving 2H, 2H multiplets, and 3H triplet respectively at correspondingly lower values.

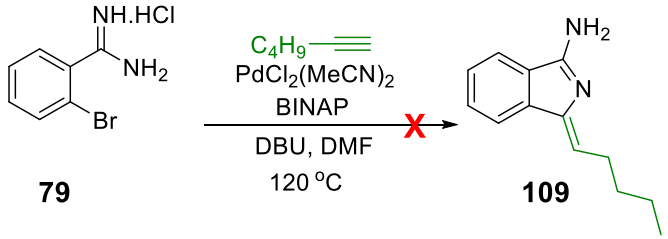

Scheme 2.6: Unsuccessful synthesis toward alkyl aminoisoindoline **109.**

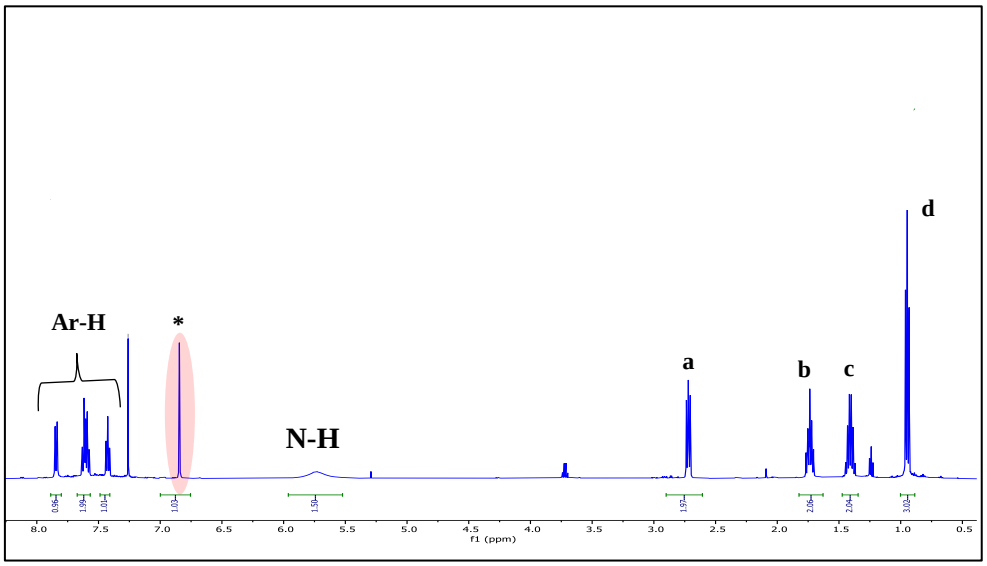

Figure 2.3: ^{1}H-NMR spectrum of the resulting product from reacting of amidine **79** with 1-hexyne under microwave condition.

It was suspected that the cyclisation might be occurred in different way producing the 6-member ring compound. On close inspection of the literature, it found this has been observed before, as in some cases, the competition between 5 and 6 membered ring compounds (isoindoline and isoquinoline) have been observed to vary depending on conditions used. Fortunately, the resulting crystals were suitable for X-ray crystallography and, as expected, it confirmed the structure assignment for 3-n-butyl-isoquinolin-1-amine, which crystallises to form H-bonded pairs of molecules as shown in Figure 2.4. The results, performed and analysed by our collaborator Dr David Hughes, show that all the non-hydrogen atoms of the isoquinoline rings of the resulting molecule form a good planar array; the carbon atoms of the *n*-butyl group lie close to this plane and show an all-*trans* chain. One of the amino H atoms forms a good hydrogen bond to the N atom of a neighbouring molecule, and this bonding is repeated about a centre of symmetry, thus forming an eight-membered ring which links the pair of molecules in a dimer unit. Structural data and tables are given in the Appendix.

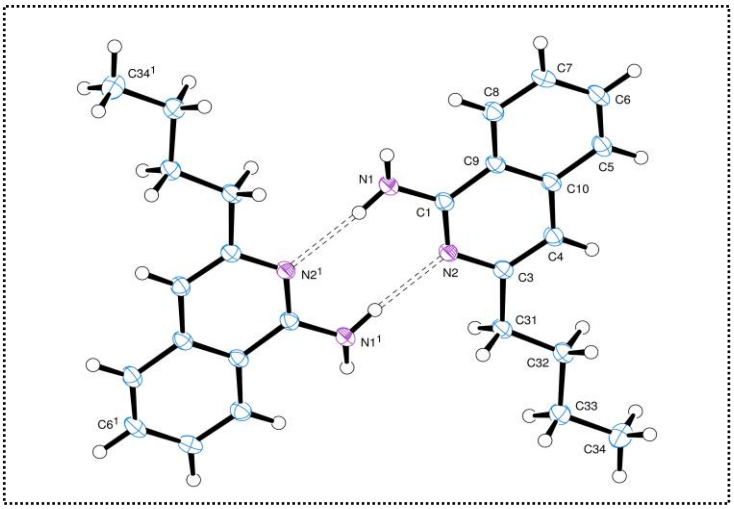

Figure 2.4: Crystal structure of 3-butyl isoquinoline -1-amine compound **112.**

Using 1-hexyne failed to produce the desired aminoisoindoline **109** however, the isomeric isoquinoline **112** was isolated in 31% yield. Subtle changes in reaction conditions and the starting alkyne clearly affect chemical control in the formation of 5 versus 6 membered rings. The suggested mechanism of this reaction includes a nucleophilic attack where an amine group attacks on the triple bond to give 6-endo dig cyclisation compound (Scheme 2.7 inset).[89]

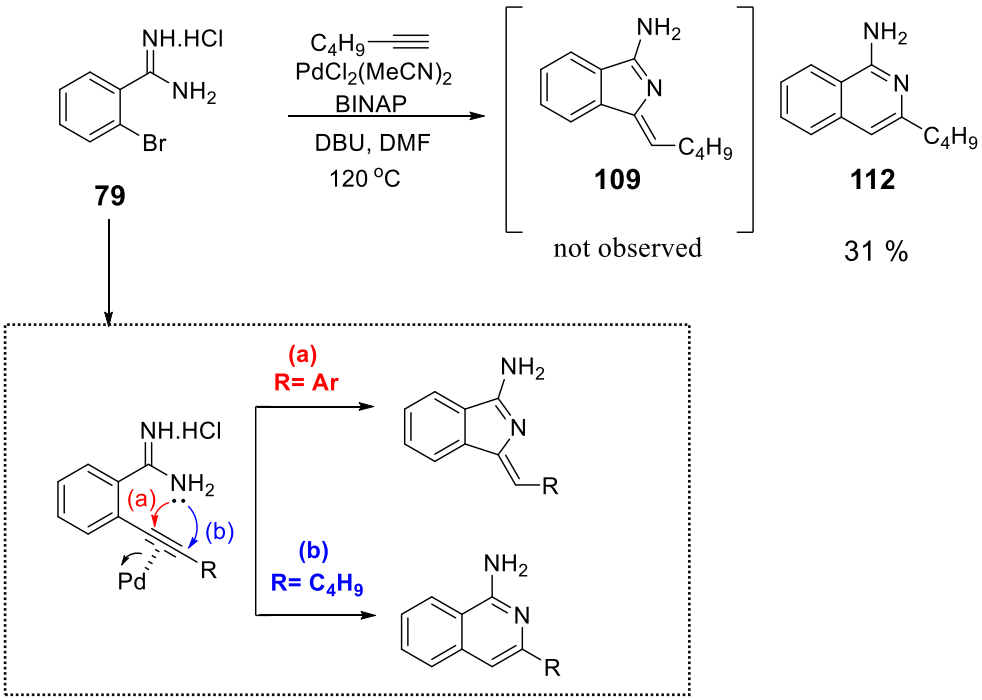

Scheme 2.7: Synthesis of compound **112**.

2.2 Introduction to isoquinoline

Isoquinoline (2-azanaphthalene) is composed of a benzene ring fused to a pyridine ring (Figure 2.5). It is an important heterocyclic system and a structural isomer of quinoline.[90]

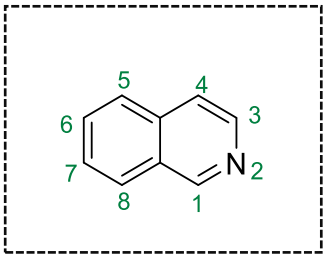

Figure 2.5: Structure of isoquinoline core.

Isoquinoline was initially extracted from coal tar in 1885 by Hoogewerf and van Dorp.[90] In 1914, Weissgerber reported a faster route by selective extraction of coal tar, exploiting the fact that isoquinoline is more basic than quinoline, followed by fractional crystallization of the acid sulfate.[91] More recently the synthesis of isoquinolines has attracted considerable attention given the wide range of biological activities exhibited by isoquinoline derivatives.[92] Of the many reported routes the transition metal catalysed route to construct the isoquinoline core is particularly significant.[93] As compared to the classical synthetic methods, such as the Pomeranz-Fritsch reaction, which is mostly subjected to harsh condition such as using strong acids, or performed the reaction under multiple steps which effects the resulting yield, while the transition metal catalysed route requires milder conditions.[94] In particular, the palladium catalysed methodology have garnered the most attention because of the considerable role that palladium plays in carbon−carbon bond coupling[95] and annulation reactions of alkynes.[96]

Recently, 2-alkynylbenzonitriles have been used as precursors for the construction of the isoquinoline or isoindoline derivatives through aminative 6-endo-dig and 5-exo-dig cyclization, respectively. In these cases, competition between 5 and 6 membered ring formation has been observed to vary depending on conditions used. Moreover, 2-alkynylbenzonitriles precursor would lead to the products without elimination or formation of any side products hence have the potential to attain 100 % atom economy in this case.[97] For example, 1-aminoisoquinoline (Table 2.1 **E**) have been successfully formed by the reaction of secondary amines with 2-alkynylbenzonitriles, under solvent-free condition and using copper-based catalysts. Here it is clear that the secondary amines influence the regioselectivity of the reaction i.e. they favour 6-endo-dig

cyclization as opposed to the 5-exo-dig.[97] However, attempting this annulation with primary aliphatic amines and secondary aromatic amines generated a complex mixture.[97] On the other hand, other catalysts such as triflates of Zn, favoured the formation of 1-aminoisoindoles via 5-exo-dig cyclization.[97] Nonetheless, it should be noted that it has also been reported under different conditions, the use of zinc as a catalysts with this precursor favours 6-endo-dig resulting in naphthalene amino esters.[98] Thus, it appears both the catalyst and reaction conditions impact the product formed. Rare earth catalyst such as lanthanides have also been used to catalyse sequential addition/annulation reaction of secondary amines with 2-alkynylbenzonitrile derivatives,[99] resulting in a tandem procedure for the preparation of aminoisoindoline (Scheme 2.8). The authors Pengqing and Yinlin suggest that the reaction is initiated by deprotonation of the amine by the lanthanide catalyst, resulting in coordination to form Ln-N species **A** and a sequential insertion of CN triple bond to the Ln N species to furnish lanthanide-amidinate intermediate **B**. This is followed by *cis*-addition of Ln N bond to C-C bond leading to cyclization, resulting in intermediate **C**. Finally the desired aminoisoindoline is obtained via protonation of **C** with another amine.[99]

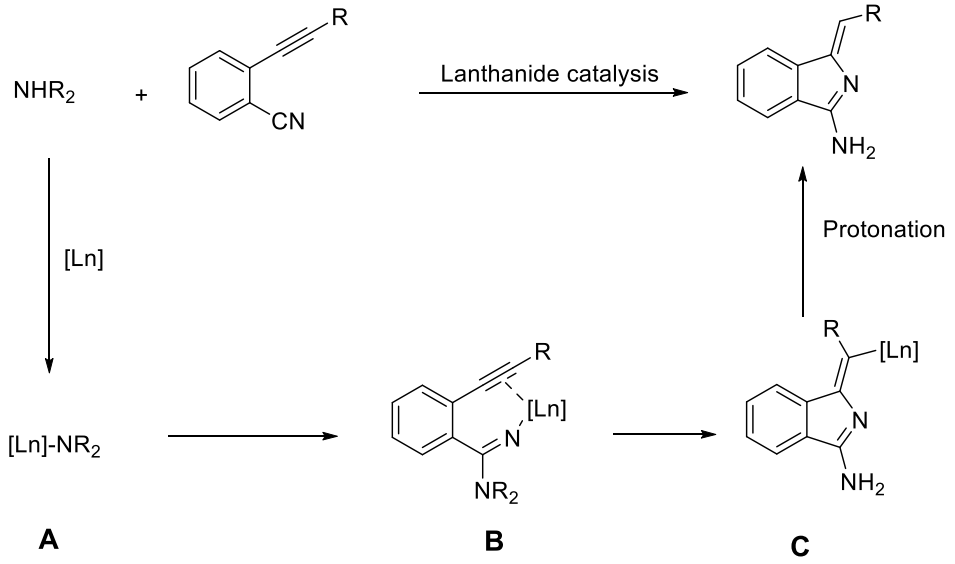

Scheme 2.8: Synthesis of aminoisoindoline by using rare earth catalyst and secondary amine.[99]

Additional synthetic procedures have been published by Xien Shen, this includes reaction of 2-alkylbenzonitrile with aliphatic amines in the presence of a catalytic amount of $Ti(NMe_2)_4$, in toluene or benzene.[100] This has shown excellent

regioselectivity with regards to the 5-exo-dig cyclization for the preparation of substituted aminoisoindolines. Moreover only *Z* isomers were isolated as the final products.[100] Table 2.1 gives a comparative summary of the four different catalysts discussed above and the resulting products.

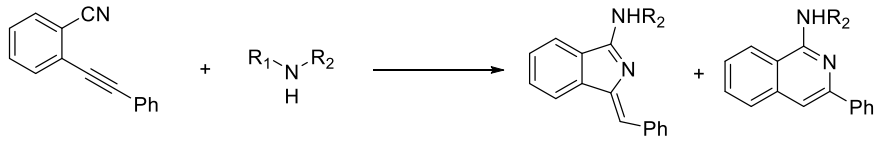

D E

	NHR_2	solvent	Time/h	temperature	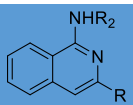	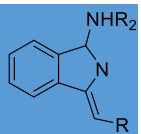
CuOTf·PhMe	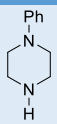	Solvent free	24 h	120 °C	62 %	20 %
$Zn(OTf)_2$	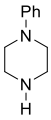	Solvent free	24 h	120 °C	8 %	76 %
$La[N(SiMe)_2]_3$		Toluene	6 h	25 °C	0 %	97 %
$Ti(NMe_2)_4$	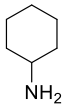	C_6D_6, or toluene	18 h	115 °C	0 %	95 %

Table 2.1: Comparative summary of synthesis of aminoisoindolines and amino isoquinolines using different catalysts.

Yang et al, have reported a strategy for the one-pot synthesis of isoquinoline from 2-alkynylbenzaldehyde as shown in scheme 2.9.[101] This includes reacting of 2-bromo arylaldehydes with a range of terminal acetylenes under standard Sonogashira coupling conditions. They found that replacing of copper catalyst by a combination of 2 mol % of $Pd(OAC)_2$ and 4 mol % of PPh_3 led to doubling the yield. DMF was used as the solvent, KOAc as the base and microwave irradiation as the heating source. After completion of palladium-catalysed coupling, ammonium acetate was used as an ammonia source for the imination step.[101]

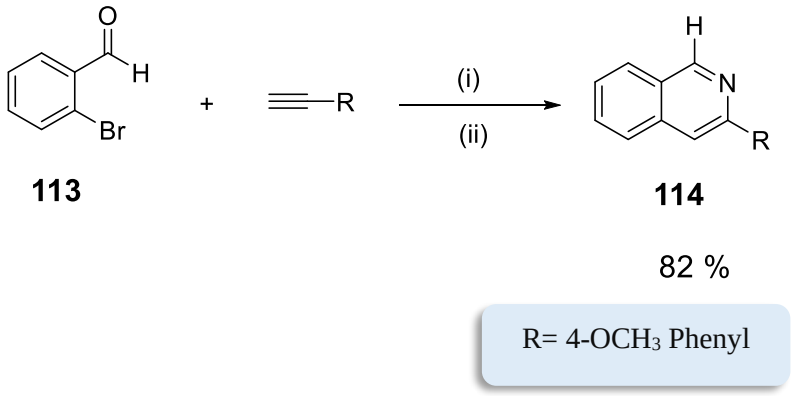

(i) $Pd(OAc)_2$, PPh_3, KOAc, microwave, 80 ℃, 1 h, DMF

(ii) NH_4OAc, microwave, 150 ℃, 2 h

Scheme 2.9: Synthesis of isoquinolines by microwave-assisted One-Pot reaction from 2-alkynylbenzaldehyde.[101]

Another reported route for the formation of the 1-aminoisoquinolines from 2-Alkynylbenzamides is by using gold(III) catalyst in the presence of ammonium acetate (Scheme 2.10).[102] This synthetic route starts with the coupling of 2-bromobenzamides with terminal alkynes under Sonogashira cross coupling condition to produce the corresponding 2-alkynylbenzamides **115**. The 1-aminoisoquinolines **116** are produced after coordination of the gold(III) catalysts to carbon – carbon triple bond in the alkyne which results in the regioselective 6-endo-dig cyclization in 92 % yield.[102]

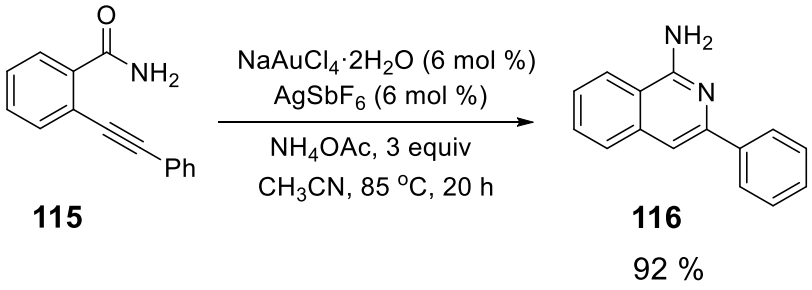

Scheme 2.10: Synthesis of isoquinolines **116** from 2-alkynylbenzamides by using gold(III) catalyst.[102]

2.3 Synthesis of 2-hexynalbenzonitrile and use it as precursor in the synthesis of alkyl aminoisoindoline.

The unexpected result led to identifying useful conditions to 6-endo-dig regioselectivity which could have application for forming interesting isoquinoline units. However, in order to obtain the target, the desired alkyl aminoisoindoline **109**, another route has to devise. This synthetic pathway includes three steps as described in Scheme 2.11. The first step starts with changing the amidine to its precursor 2-bromobenzonitrile to produce the corresponding 2-hexylbenzonitrile **117** which could be accomplished according to the literature under Sonogashira cross coupling reaction.[99] The next step involved treating 2-hexylbenzonitrile **117** with a solution of lithium bis(trimethylsilyl) amide in dry THF to produce the corresponding 2-hexylbenzoamidine **119**. The final step was applying microwave heating conditions using Pd catalyst, hoping this might allow the formation of the desired alkyl aminoisoindoline **109**.

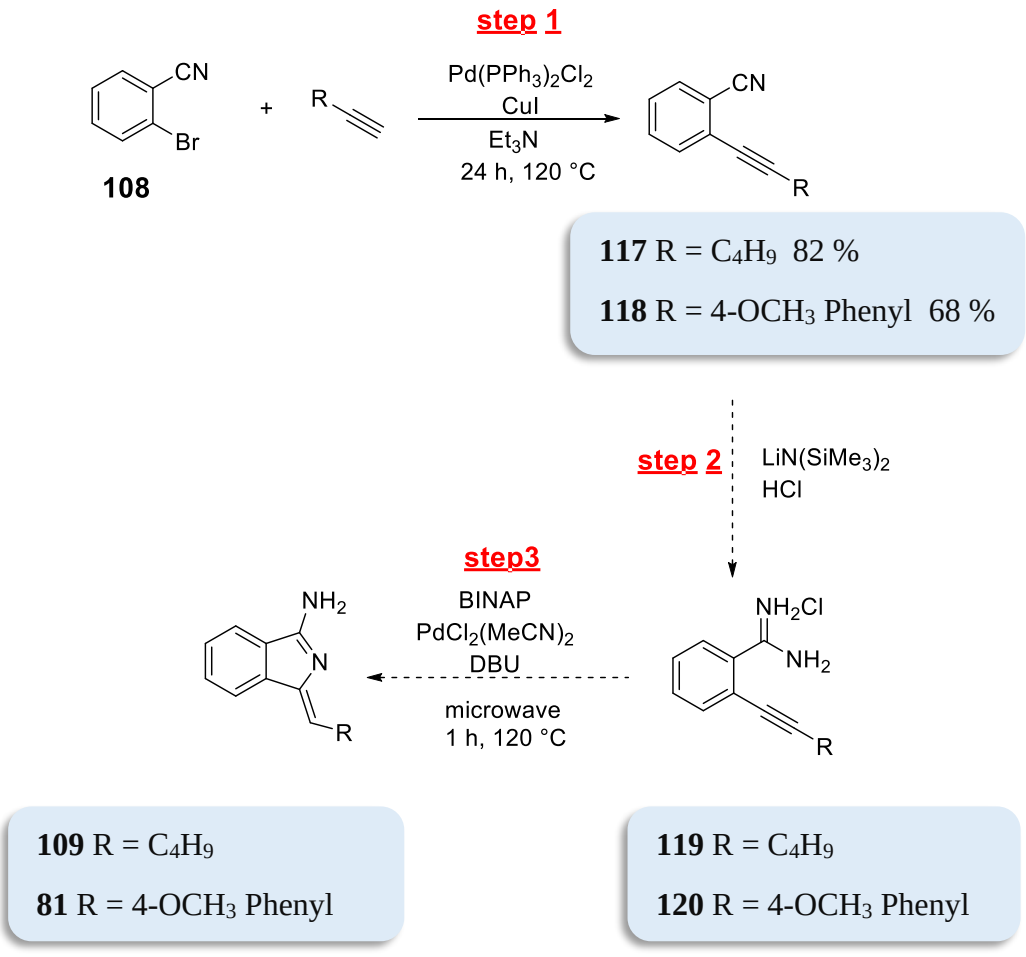

Scheme 2.11: Outline of suggested pathway to formation of compound **109**.

This plan was inspired by the suggestion that the mechanism for the formation of aryl aminoisoindolines involved the aryl ethynyl amidine as the intermediate before the cyclisation step as described earlier. So, the next decision was to start synthesising 4-methoxy phenyl ethynyl amidine **120** directly to ensure the effectiveness of the synthesis, and as the resulting 4-methoxy phenyl aminoisoindoline **81** could be easily identified due to its availability from previous synthesis. Compound **118** was successfully synthesised via a Sonogashira cross coupling, it was the first fraction that eluted from the column chromatography and was isolated as white crystals in good yield, 68 % (Scheme 2.11). The ^{1}H-NMR spectrum of compound **118** as shown in Figure 2.6 showed doublet at 6.91 ppm with coupling constant J = 7.8 Hz for the protons in the phenyl ring labelled **a**, the other phenyl protons appeared as a doublet overlapped with other signal refer to the benzene ring protons labelled **b**, benzene ring protons appeared in the expected aromatic region. The methoxy protons clearly appear as a singlet peak at δ 3.84 ppm. MALDI-MS spectrum showed a clear peak at *m/z* 233 confirming **118** was formed.

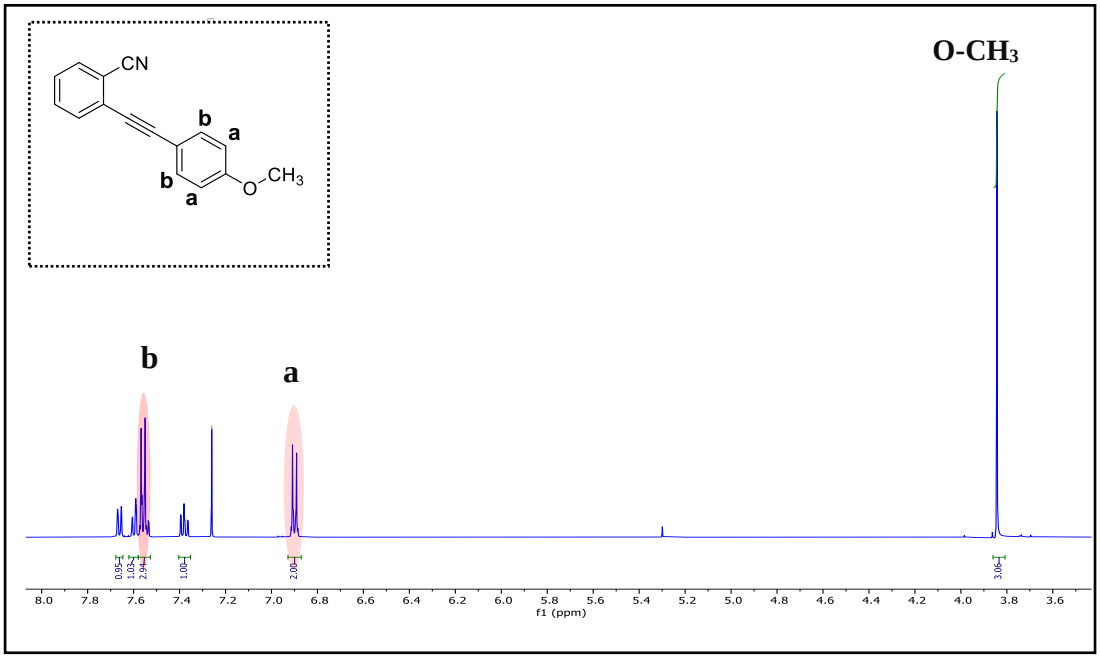

Figure 2.6: ^{1}H-NMR spectrum of compound **118**.

For the next step, treating compound **118** with a solution of lithium bis(trimethylsilyl) amide in dry THF, led to the production of compound **120** in excellent yield 80 %. The structure of compound **120** was confirmed by NMR spectroscopy and X-ray diffraction analysis as shown in Figure 2.7. As expected, the ^{1}HNMR spectrum retains the same features present in the precursor nitrile but they are shifted slightly and the N-H signals

are not observed, most likely due to exchange in the CD_3OD solvent. The crystal structure confirmed the product, but the data (appendix) were of low quality so additional analysis of the structure was not undertaken.

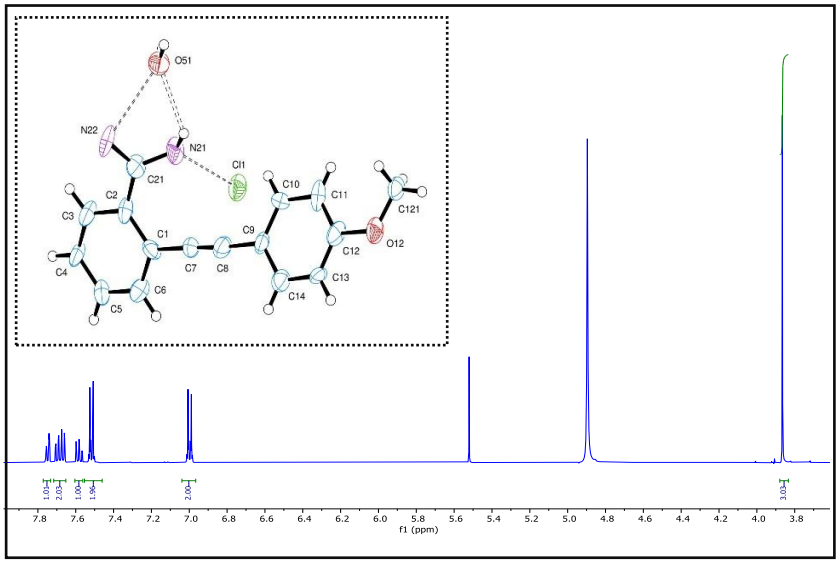

Figure 2.7: ^{1}H-NMR spectrum and X-ray crystal structure of compound **120**.

In the final step, compound **120** underwent a cycloismerisation reaction, following a microwave assisted protocol developed by Hellal and Cuny.[75] Compound **120** was treated with catalytic amounts of palladium catalyst and BINAP as ligand, in the presence of DBU as base and employing DMF as the solvent for the reaction. The mixture was irradiated under microwave heating at 120 ºC for 1 h, after which an aqueous work up was performed, and recrystallisation with DCM: PE to give the pure aminoisoindoline **81** as yellow crystals in 65 % yield. Thus, this pathway to the synthesis of 4-methoxy phenyl aminoisoindoline **81** has confirmed that compound **120** is an intermediate in the one pot reaction, this provides evidence that supports the proposed reaction mechanism.

Then, moving to the first step was applied using 1-hexyne under normal Sonogashira condition, compound **117** was produced in excellent yield 82 % (Scheme 2.11). Compound **117** was characterised using ^{1}H-NMR and ^{13}C-NMR spectroscopy and demonstrated all signals as in the reference.[103] The next step involved synthesis of 2-hexyl benzamidine hydrochloride **119** by treating of 2-hexylbenzonitrile **117** with a solution of lithium bis(trimethylsilyl)amide in dry THF (Scheme 2.12). The mixture was quenched with a solution of HCl (5N) in isopropanol then it was diluted by H_2O and extracted by ethyl acetate. The resulting product was separated by using several

column chromatography. A product with molecular weight 366 was isolated. The ^{1}H NMR spectroscopy indicates a butyl and propyl chains, and the aromatic region showed this compound has two benzene rings as shown in Figure 2.8. While the Infrared spectra showed a nitrile CN group, alkyl, alkene and NH functional groups.

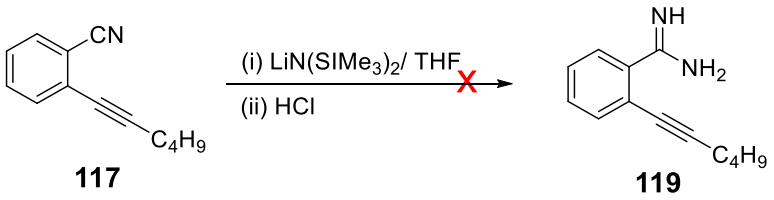

Scheme 2.12: Unsuccessful attempt to synthesis of compound **119**.

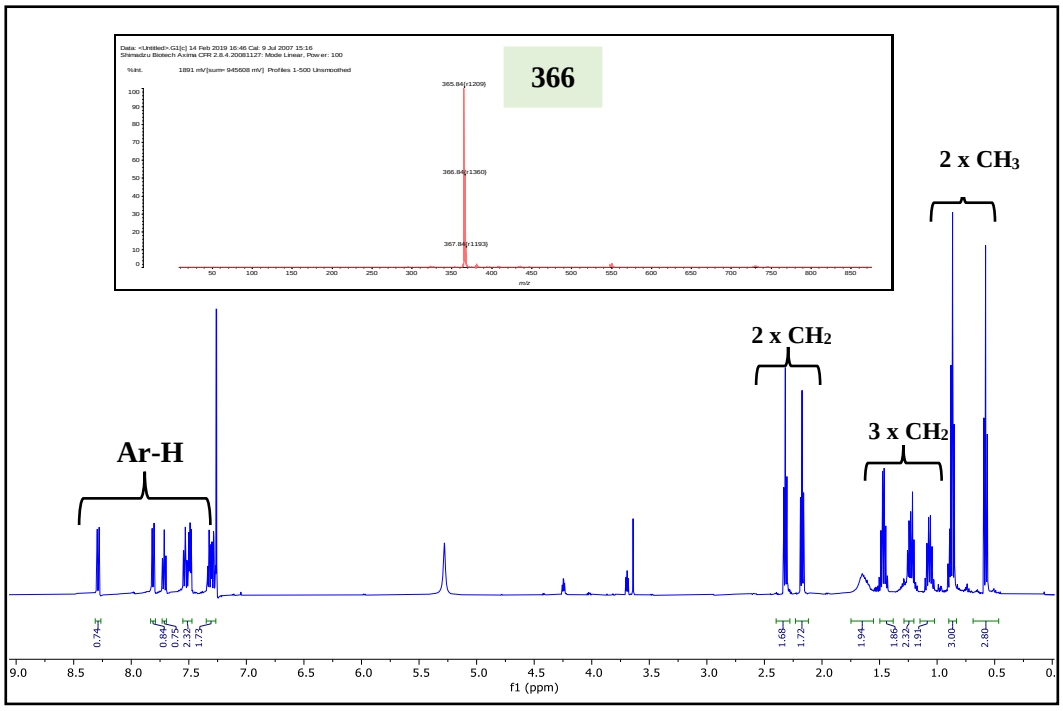

Figure 2.8: ^{1}H-NMR spectrum and MLADI mass spectra of the resulting compound with molecular weight 366.

Our explanation was the reaction with the strong base led to the starting material being deprotonated on the position * as shown in Scheme 2.13, then reacting with itself to give the suggested structure shown in the Scheme 2.13.

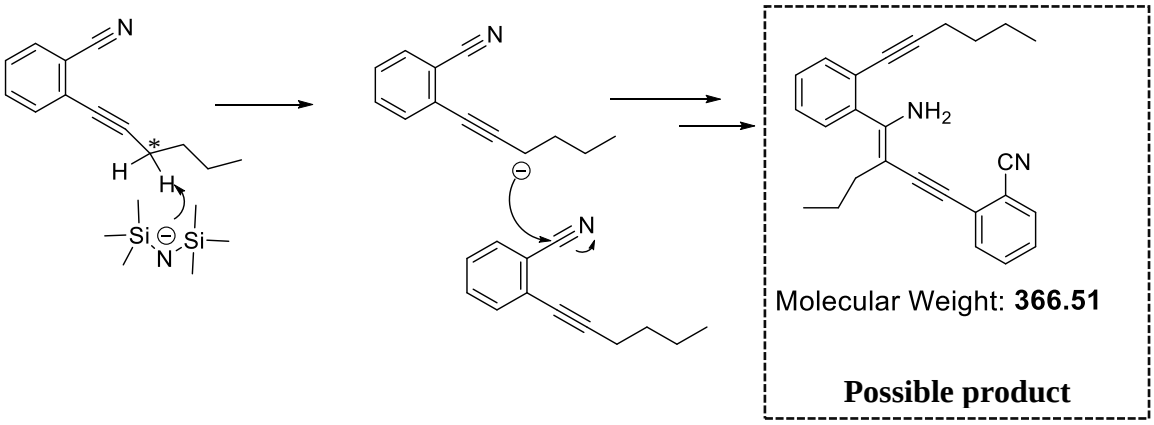

Scheme 2.13: Suggested resulting structure resulting from the reaction between compound **5** and lithium bis(trimethylsilyl)amide in THF.

There are a few literature methods published for converting nitriles to the amidines. Pavel and his co-workers had synthesised *para*-substituted aryl amidines following a development based on the Pinner amidine synthesis.[104] In this synthesis *para*-substituted aryl amidines were synthesised by three methods as described in the Scheme 2.14.

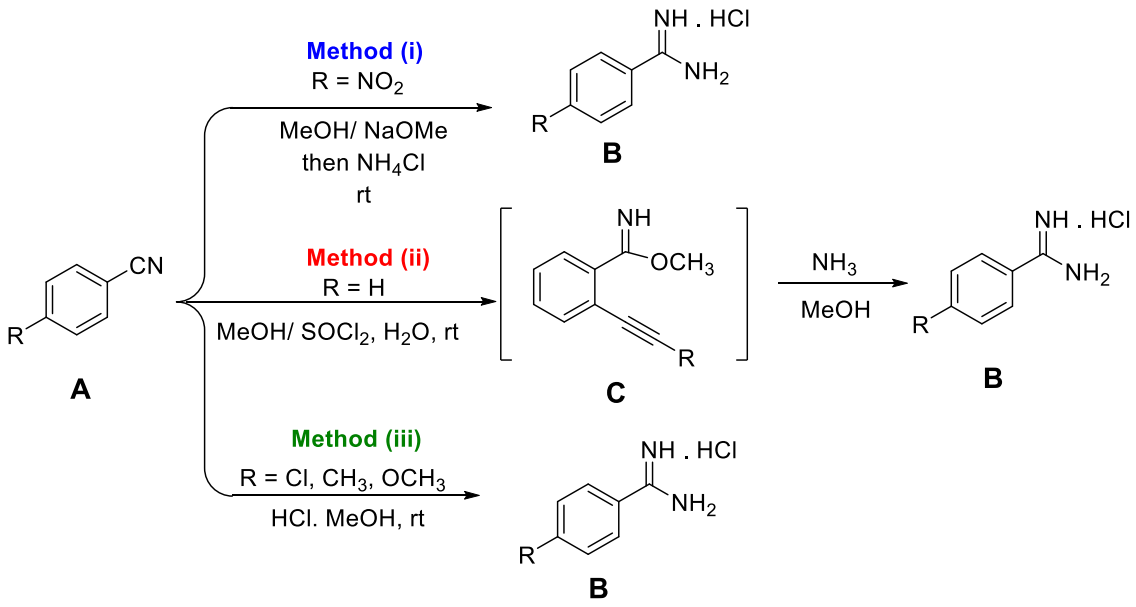

Scheme 2.14: Synthesis of 4- substituted aryl amidines.[104]

Method **(i)** as shown in Scheme 2.14 involved treatment of compound **A** with the sodium methoxide as the base in methanol at room temperature, followed by adding of dry ammonium chloride. Pavel et al, had proven that the use of basic conditions are more suitable for nitriles with electron withdrawing group substituents, while for nitriles

with electron donating substituents the acidic condition is the preferred method.[104] Following this method was unsuccessful in the formation of 2-alkyl benzo amidine **119**, the starting material remained unreacted. The second method **(ii)** was then attempted (Scheme 2.14). This involves treatment of compound **a** with thionyl chloride in methanol at room temperature, then after the formation of the intermediate methyl imidate hydrochloride **C**, methanolic ammonia solution is added in one portion.[104] Unfortunately, this method too did not produce the target product. This may be due to the equilibrium reaction between the starting material and the intermediate compound during the process and with the presence of thionyl chloride, the reaction shifts to the starting material. The third method reported method **(iii),** includes treatment of nitriles with HCl in methanol at room temperature. This method was not attempted because in case of hexyl benzonitrile the triple bond will likely undergo electrophilic addition converting to the alkene under these conditions.

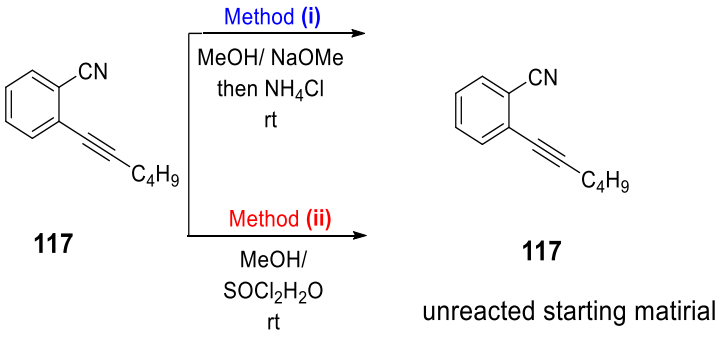

Scheme 2.15: Synthesis attempts of formation of compound **119**.

As previously mentioned, the synthesis of aminoisoindolines by the lanthanide-catalysed tandem intermolecular cross-disinsertion reaction of 2-alkynylbenzonitriles and secondary amines have been recently reported (Scheme 2.16).[99]

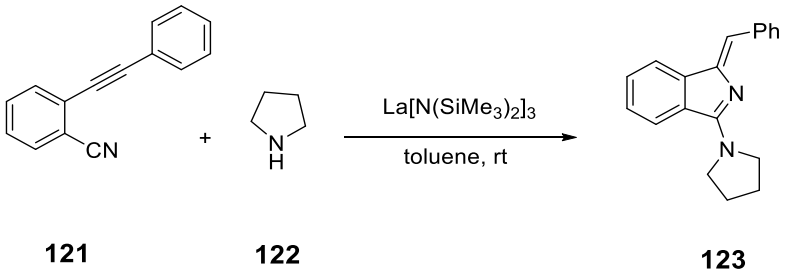

Scheme 2.16: Synthesis of aminoisoindoline from 2-phenylalkynylbenzonitrile.[99]

Inspired by these works, it was decided to follow this synthetic procedure. Compound **117**, with piperidine as the base (due to its availability in the lab), in the presence of

lanthanide catalyst such as lanthanum bis(trimethylsilyl)amide, was stirred in toluene at room temperature. TLC showed starting material remained even when doubled the equivalence of the amine or attempted heating the mixture under reflux. Unfortunately, these were unsuccessful conditions to produce the desired alkyl aminoisoindoline. Using alternate lanthanide sources like lanthanum(III) acetylacetonate hydrate or replacing the amine with bis(trimethylsilyl)amine did not help to convert the starting material towards the target product. The final attempt was made using palladium as a catalyst and BINAP as a ligand to assist the cyclisation but unfortunately starting material did not react. It is not clear why these reactions were unsuccessful in our hands, but it is to be noted that in the procedure that we followed[99] the authors do not report any examples with piperidine, (lit examples use pyrrolidine). There might be some subtle influence of the secondary amine on these reactions. Therefore, it was decided to not investigate it further.

Then, replacing the 1-hexyne with 3-phenyl-1propyne **124** was attempted, with the idea that the aromatic substituent influences the electronic properties of the alkyne thus favouring the 5-exo-dig cyclisation required. The reaction was performed following the procedure reported by Hellal and Cuny as explained earlier.[75] TLC for the crude showed complicated mixture of spots and MALDI-TOF mass spectrum showed no significant peak corresponding to our desired compound **125**, as such the crude was not analysed further.

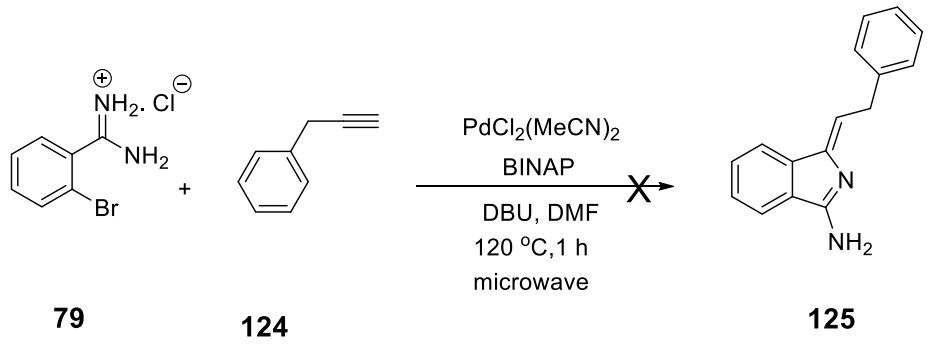

Scheme 2.17: Unsuccessful attempt to synthesis of compound **125**.

2.4 Alternative syntheses using different terminal acetylenes.

All the previous attempts towards aminoisoindolines using alkyl acetylene unfortunately were unsuccessful. Therefore, synthesis of aminoisoindoline using an acetylene ester was the next target, by following the synthetic protocol which has been

discussed earlier.[75] Unfortunately, using the ethyl propiolate **126** failed to give the target product **127**. TLC showed a complicated mixture, and most of 2-bromobenzoamidine **79** remained unreacted. This might be due to the fast formation of the acetylene homocoupling compound. Trace amounts of other compounds were also isolated by several separations via column chromatography. ^{1}H-NMR spectroscopy of the resulting product indicates two unsymmetrical benzene rings as well as a N-H proton (Figure 2.9). ^{13}C-NMR showed clear peaks for the C=N and C=O. No additional analysis was performed due to the poor generated yield. Accordingly, we suggest that the reaction started with coupling of the acetylene in the bromo position of the amidine compound followed by amination reaction by the other amidine molecule to give the intermediate **128** which might have cyclised to provide compound **129** as shown in Scheme 2.18.

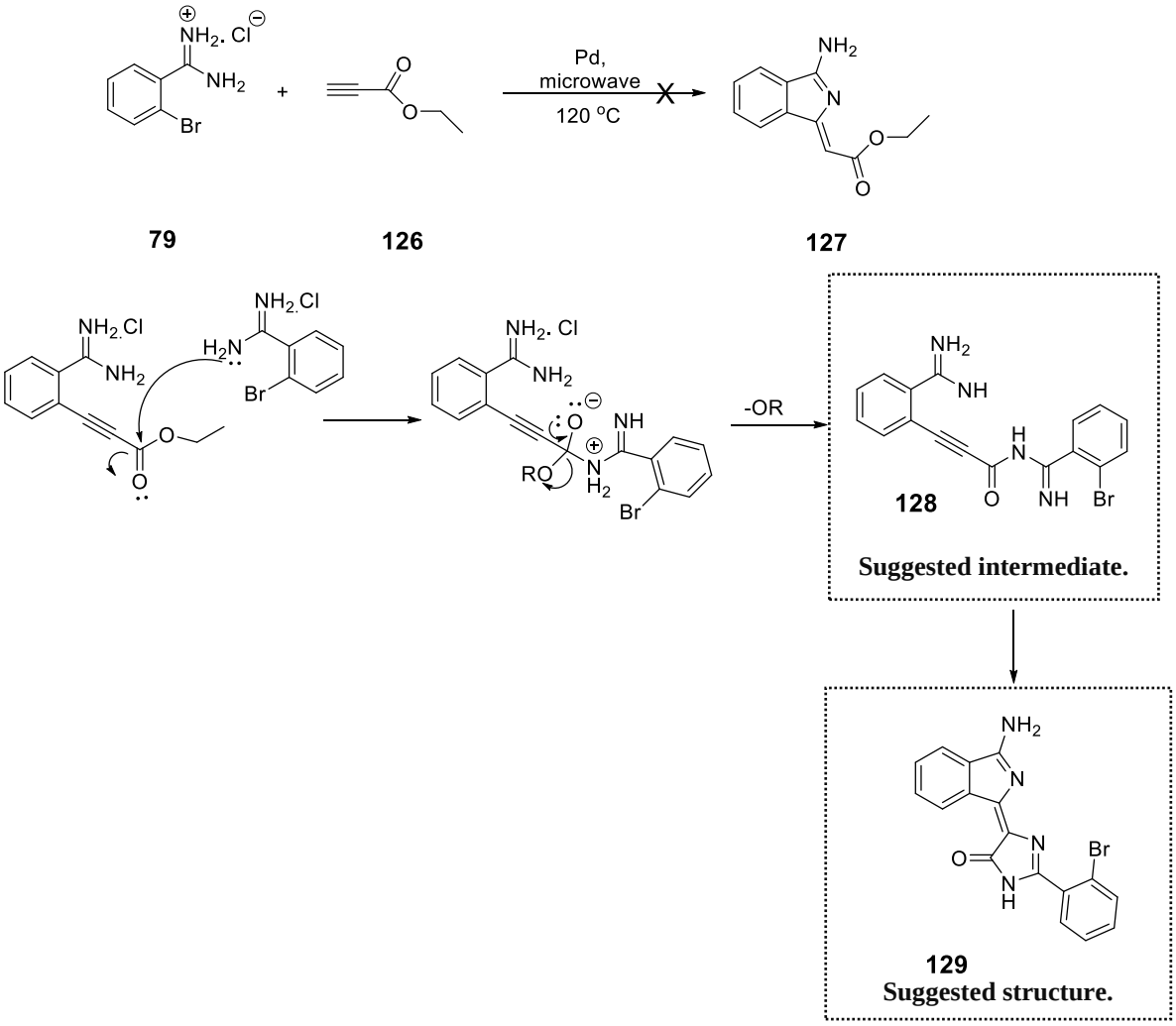

Scheme 2.18: Suggested resulting structures from the reaction between 2-bromobenzoamidine and ethyl propiolate.

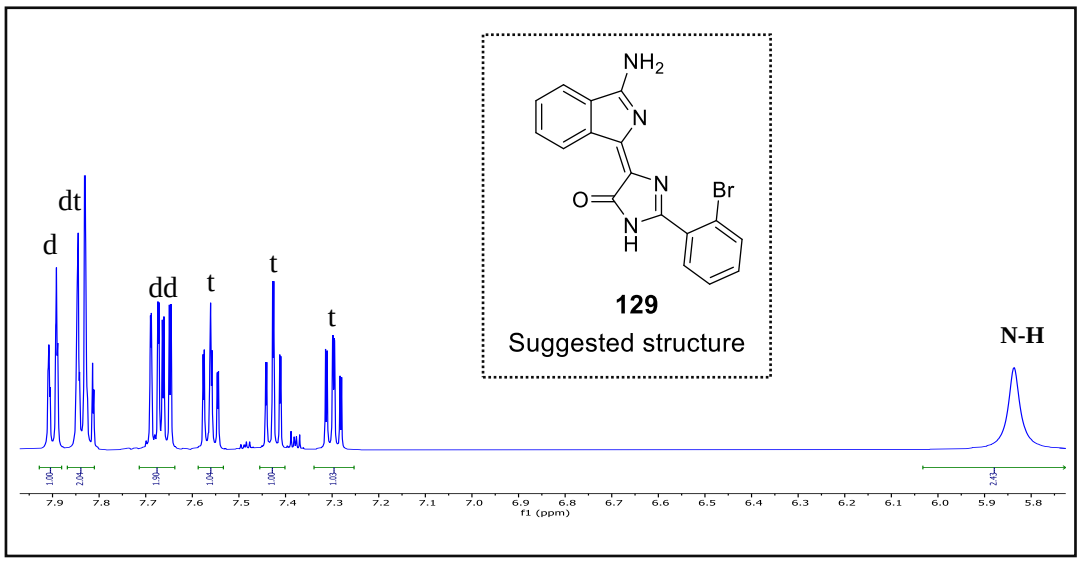

Figure 2. 9: ^{1}H-NMR spectrum of product from the reaction between 2-bromobenzoamidine and ethyl propiolate.

In order to obtain the target product, the standard Sonogashira cross coupling reaction was followed starting with 2-bromobenzonitrile **108**. Unfortunately, this reaction was unsuccessful, most of the 2- bromobenzonitrile remained unreacted and 1,6-diethyl 2,4-hexadienedioate **132** was isolated as a yellow oil in 30 % yield. An explanation is that the ester acetylene homocoupling compound seems to be produced first, then reduced to the corresponding alkene (either *cis* or *trans*), due to effect of the Pd catalyst as shown in Scheme 2.19.

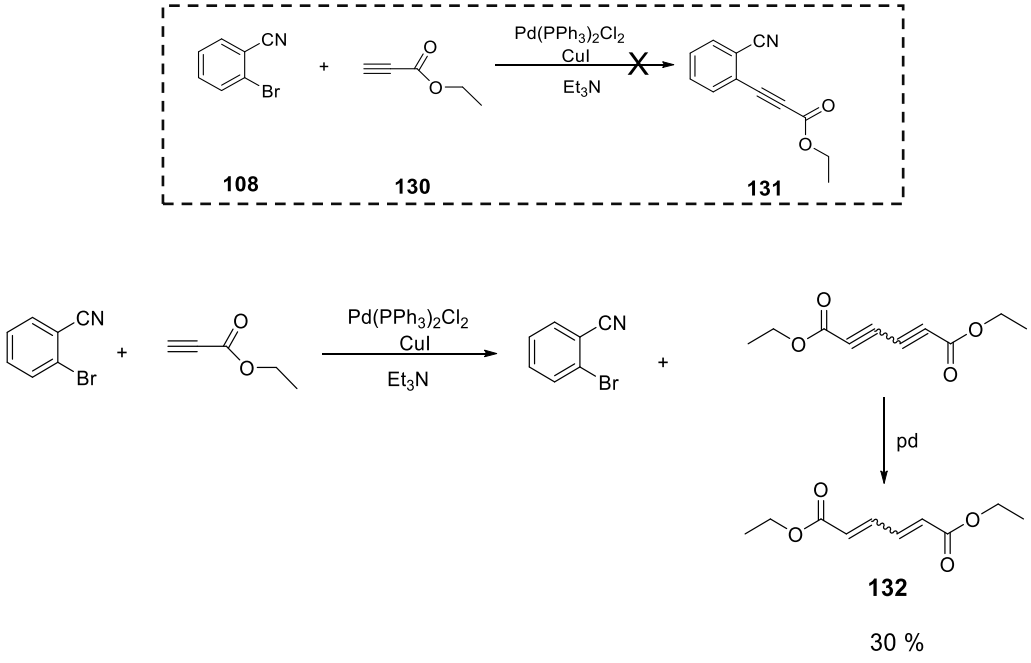

Scheme 2.19: Attempt to synthesise compound **131** using Sonogashira cross coupling reaction.

Formation of compound **132** was confirmed by ^{1}H-NMR spectroscopy. Two doublets appeared at 7.57 ppm and 5.65 ppm with coupling constant J = 12 Hz in addition to ethyl chain protons at 4.20 ppm and 1.29 ppm respectively.

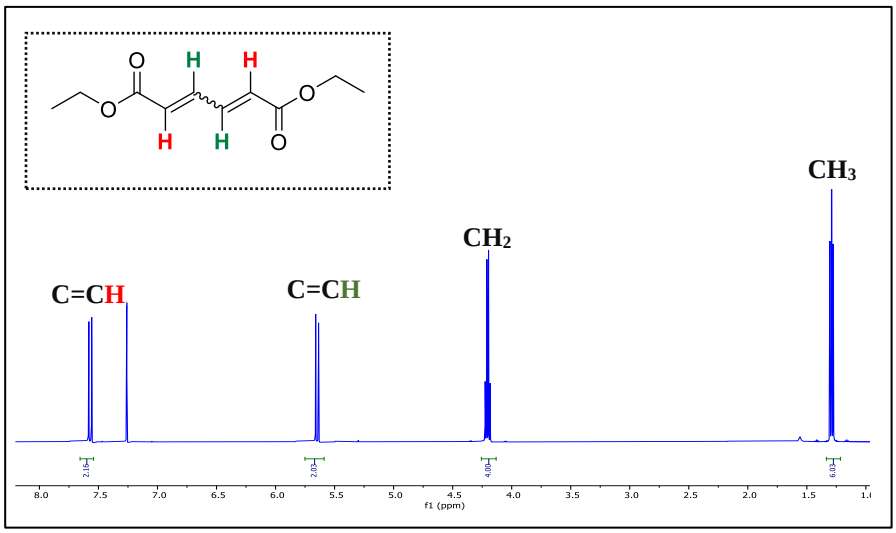

Figure 2. 10: ^{1}H-NMR spectrum of compound **132**.

Then the reaction was repeated by replacing the ethyl ester with an aromatic acetylene ester to allow for easy monitoring by TLC. Also, it was assumed this might assist the successful coupling at the bromo position in the amidine compound to give the required intermediate followed by the cyclisation to give the target aminoisoindoline compound **134**. Therefore, 2-bromobenzoamidine **79** was reacted with 2-naphthyl propiolate **133** under microwave condition. This reaction failed to give the target product, the major resulting compound was naphthol **135**, this was confirmed by ^{1}H-NMR spectroscopy. While the other compound **136** showed two doublet peaks at 6.5 ppm J = 7 Hz and at 8.03 ppm J = 7 Hz which indicate those peaks for the *cis* alkene protons, in addition a broad singlet peak around 10 ppm which must be N-H or O-H this confirmed by treating the sample with deuterium oxide. Four protons for the benzene ring appeared in the aromatic region. ^{13}C-NMR indicates 10 carbons of which one of them was a carbonyl carbon and appeared at 162 ppm (Figure 2.11). Fortunately, this compound gave suitable crystals for X-ray diffraction analysis confirmed the structure assignment for 2-(2-bromophenyl)-4(3H)-pyrimidinone **136** (Scheme 2.20 inset). We are awaiting full analysis from our crystallography collaborator.

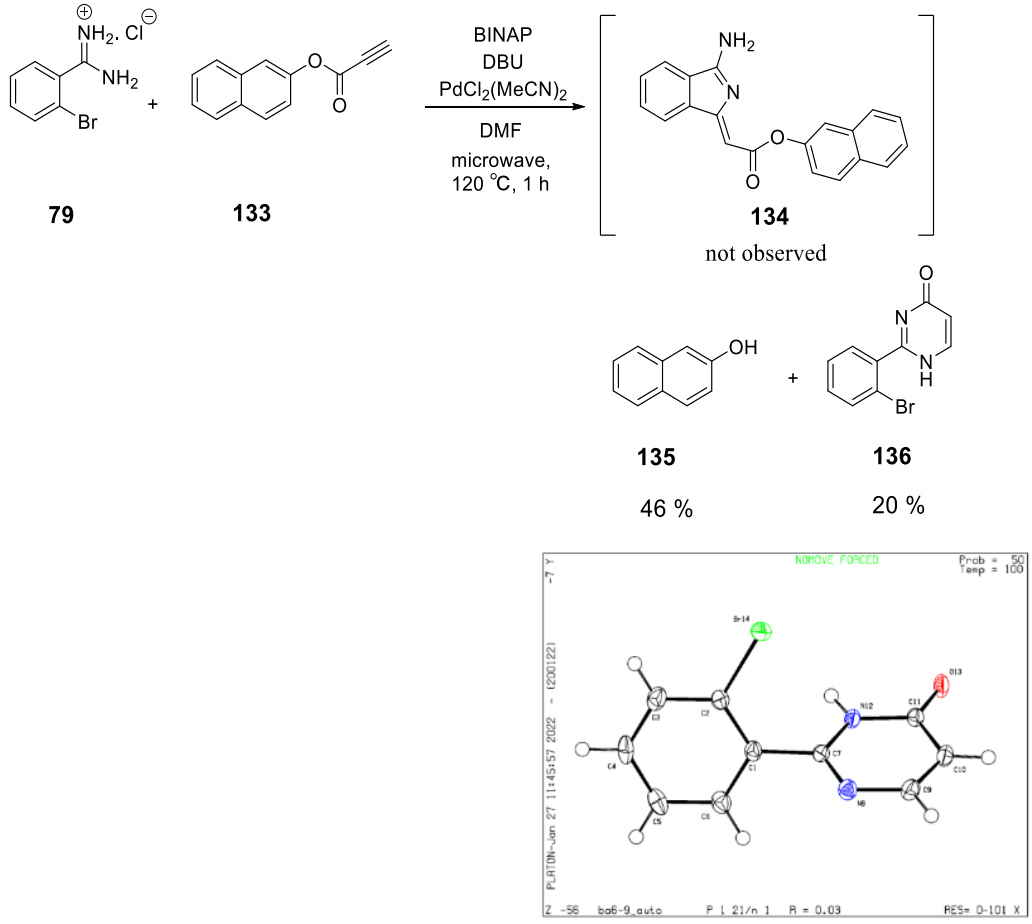

Scheme 2.20: Resulting compounds **135** and **136** from reaction of amidine **79** and 2-naphthyl propiolate under microwave condition, and Xray crystal structure of **136**.

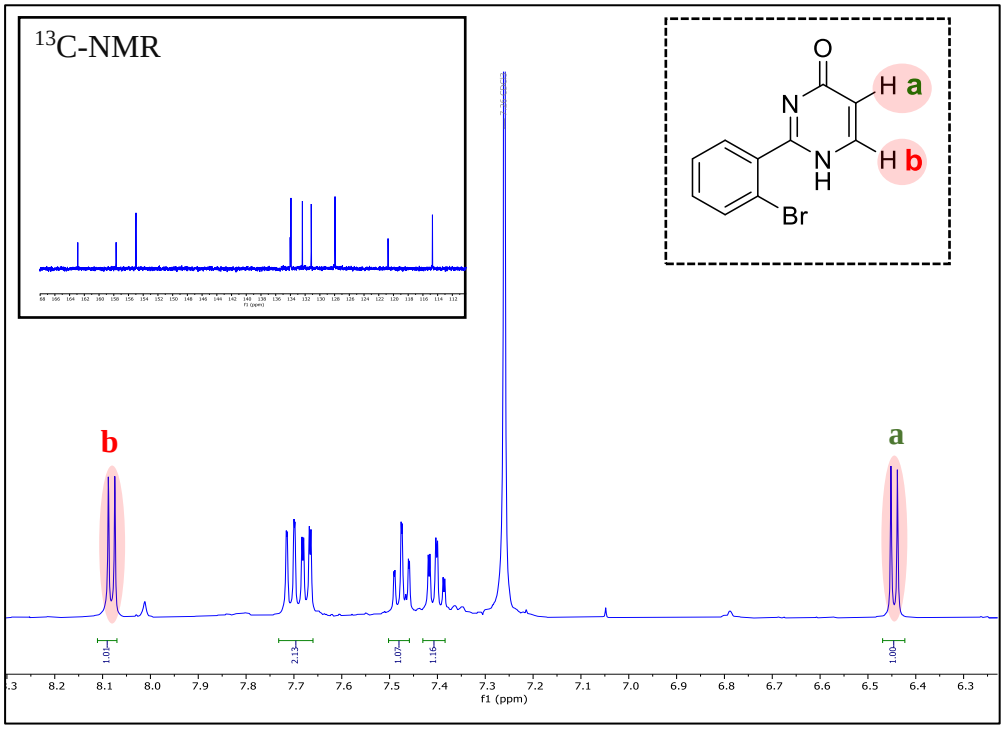

Figure 2. 11: ^{1}H-NMR and ^{13}C-NMR spectrum of compound **136**.

The proposed explanation for this reaction is that the lone pair on the amine amidine initiates the coupling by attacking the partially positive carbon on the carbonyl of the 2-naphthyl propiolate compound followed by the cyclisation to produce compound **136** in 20 %. The resulting naphthoxide is protonated during the workup to give the naphthol **135** in 46 % yield.

2.5 Symmetrical and unsymmetrical aza (dibenzo) dipyrromethenes (ADBDP)

With the lack of success in formation of aminoisoindolines using alkyl terminal, the attention was turned to synthesise aminoisoindolines using aryl acetylenes and focus on expanding the range of derivatives available and investigating the reactivities and electronic effects of different derivatives (such as donor and acceptor substituents). Cammidge group has already synthesised and published the successful synthesis of aminoisoindolines using aryl acetylene derivatives, and the resulting aminoisoindolines were used as the intermediates in the synthesis of aza-BODIPYs, TBTAPs and SubTBDAPs (Scheme 2.21).[41]

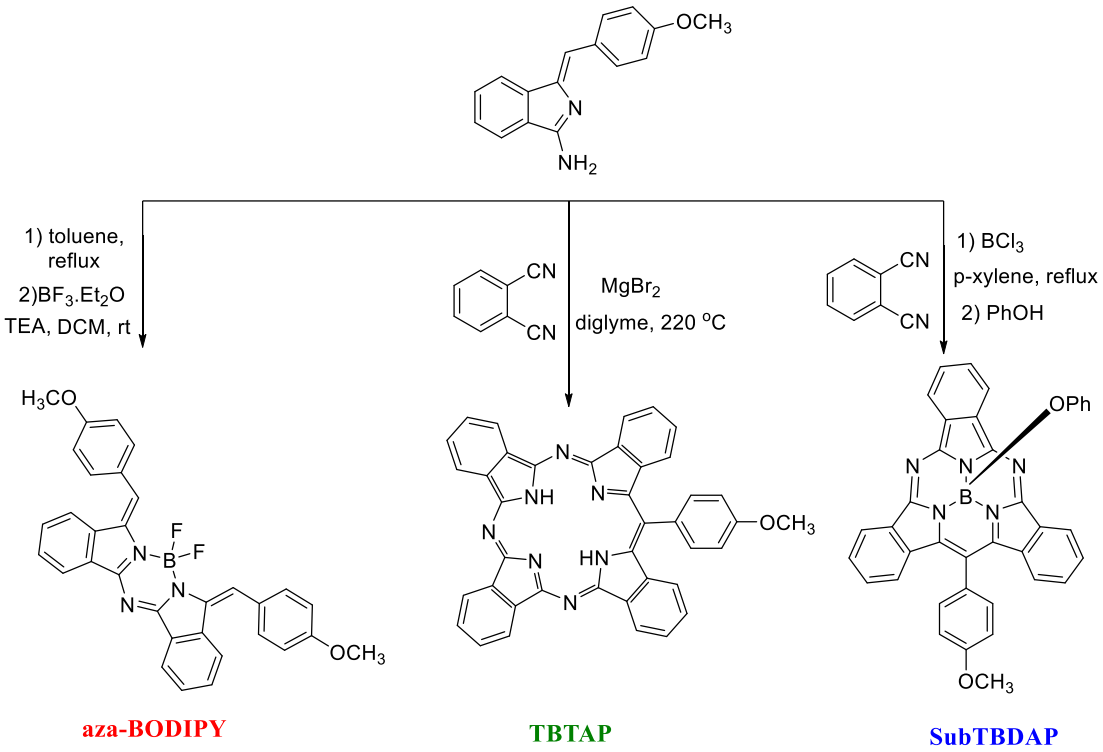

Scheme 2.21: Synthesis of aza-BODIPYs, TBTAPs and SubTBDAPs from aminoisoindolines.[41]

The synthesis of symmetrical aza (dibenzo) dipyrromethene derivatives can be accomplished smoothly by heating aminoisoindoline derivatives in toluene under reflux at 120 °C.[41] As stated previously this class of compounds is relatively under explored. However, this project aimed to investigate the effects of electron withdrawing, electron donating, and alternative aryl units on the synthesis and properties of these molecules and investigate whether a synthetic strategy could be developed to efficiently give unsymmetrical derivatives. There are no unsymmetrical derivatives reported to date and the investigation of electronic effects has not been investigated.

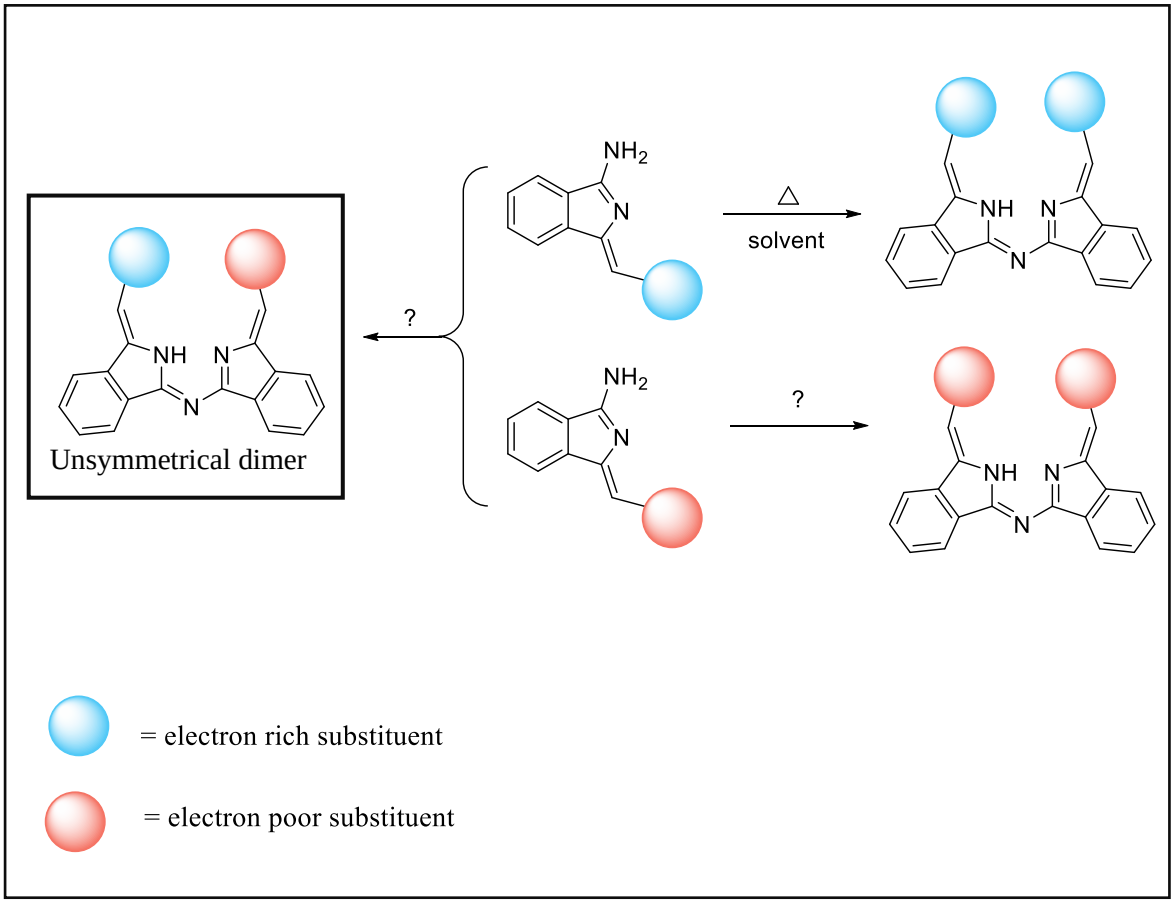

Scheme 2.22: Structures of the symmetrical and unsymmetrical aza (dibenzo) dipyrromethenes.

2.5. 1 Selection of aminoisoindolines precursors

The synthesis of new aminoisoindoline compounds were carried following the general condition that published by Hellal and Cuny.[75] Amidine **79** was reacting with a commercially available 3-methoxy phenyl acetylene, in the presence of catalytic amounts of bis(acetonitrile)palladium(II) chloride and BINAP as ligand, DBU was added as a base, and DMF as the solvent. The reaction mixture was irradiated under

microwave at 120 ºC for 1 h. Workup by quenching the reaction with ethyl acetate then washing the mixture with a saturated solution of $NaHCO_3$, purified by crystallisation from DCM: PE (1:1) giving the pure 3-methoxy phenyl methylene aminoisoindoline **137** as yellow crystals in good yield. The reaction was also performed using different aryl acetylenes such as (4-methoxy phenyl acetylene, and 4-pentyloxy phenyl acetylene) they both succeeded in converting the amidine **79** to the aminoisoindoline derivatives **81** and **138** in good yield ≥ 70 %.

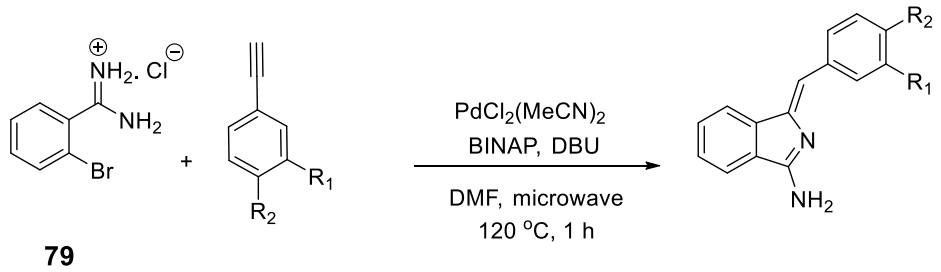

79

137 R_1= OCH_3 , R_2 = H

81 R_1=H , R_2 = OCH_3

138 R_1=H , R_2 = OC_5H_{11}

Scheme 2.23: Synthesis of aminoisoindoline compounds **137**, **81** and **138**.

Figure 2.12 shows stack ^{1}HNMR spectrum of compound **137** and compound **81** in deuterated chloroform. In both spectra the alkene proton is clearly appear as a singlet peak at 6.72 ppm and 6.75 ppm in compounds **137** and **81** respectively. A broad singlet corresponding to the proton on the 3-methoxy phenyl ring in compound **137** appeared at 7.83 ppm labelled **a,** other phenyl protons in compound **137** appeared as doublet of doublet at 6.83 ppm labelled **b**, in addition to doublet and triplet signals at 7.56 ppm and 7.30 labelled **d** and **c** respectively. While in compound **81** the 4-methoxy phenyl protons labelled **a1** and **b1** appear as doublets at 8.08 ppm and 6.94 ppm with coupling constant *J* = 8.8 Hz. Methoxy protons appears in both spectra as a singlet at 3.89 ppm and 3.83 ppm in **137** and **81** respectively. The analysis confirmed that the 5-exo-dig cyclisation was successful, and this one pot reaction is stereo selective producing the (*Z*)–isomer as the isolated product. The other aryl aminoisoindolines (4-pentyloxy

phenyl methylene aminoisoindoline) **138** was also fully characterised by ^{1}H-NMR, ^{13}C-NMR, MALDI- TOF mass spectrometry, and as expected showed similar characteristic peaks for the aminoisoindoline with variations only observed at the aryl substituent.

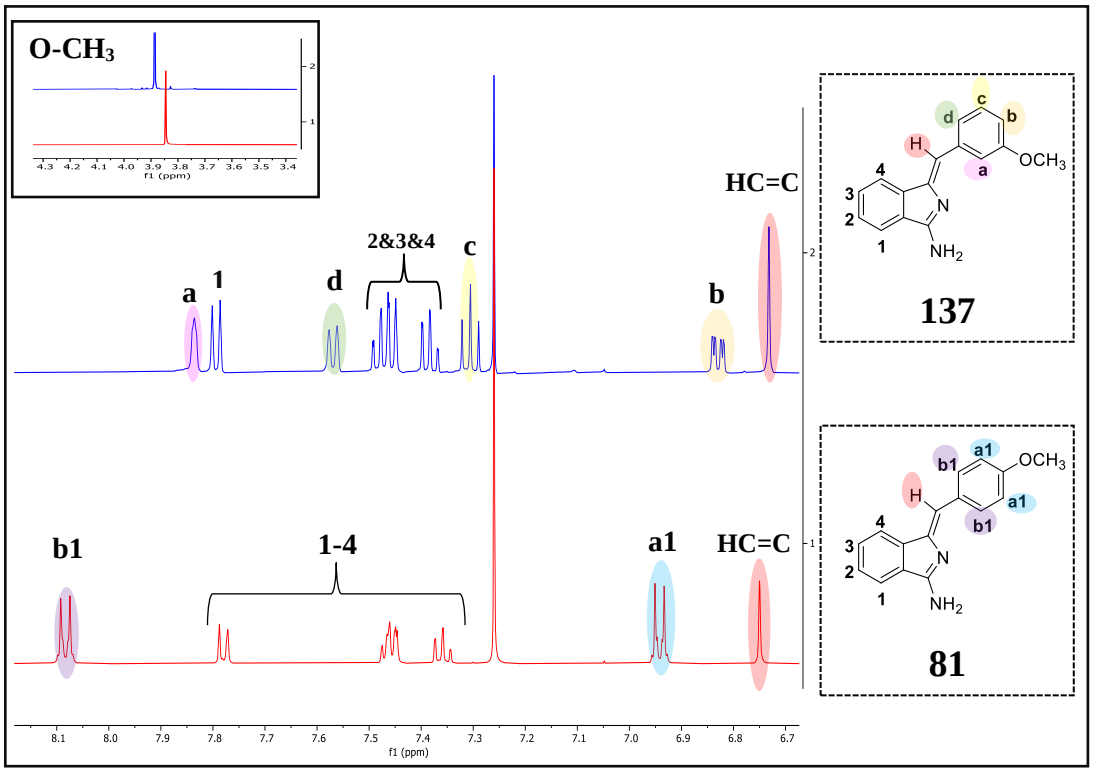

Figure 2. 12: ^{1}H-NMR spectrum of compounds **137** (blue colour) and **81** (red colour).

Next, the focus was on the synthesis of aminoisoindolines bearing electron withdrawing substituents. It was expected this would affect the electronic properties in the target ADBDP and aza-BODIPY molecules. 4-Nitro and 4-cyano substituents were selected due to their high electron withdrawing ability via both resonance and inductive effects. Following the identical procedure reported by Hellal et al., a solution of 1-ethynyl 4-nitro benzene **139** and DBU in dry DMF was added to a mixture of amidine **79**, BINAP and $PdCl_2(MeCN)_2$. The mixture was then irradiated in a microwave reactor at 120 °C for 1 h (Scheme 2.24).

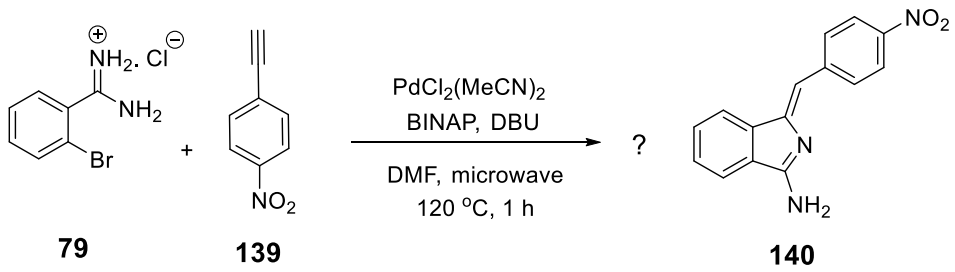

79 **139** **140**

Scheme 2.24: Synthesis attempt to formation of compound **140**.

Unfortunately, this reaction yielded a very complicated reaction mixture, the products obtained could not be isolated pure in spite of several chromatographic separations. The major fraction obtained contained only two spots by TLC, but unfortunately it could not be purified further nor suitable crystals for X-ray diffraction obtained. It was suspected that one of these compounds is the aminoisoindoline **140** so, another strategy has been applied in order to isolate the components of the mixture. By treating the mixture with p-toluene sulfonyl chloride in the presence of Et_3N in dry DCM, it was expected that formation of the corresponding aminoisoindoline tosylate compound might lead to easier separation. Unfortunately, no reaction occurred. The ^{1}H-NMR spectra of the mixture shows two singlet peaks at 7.05 ppm, and 6.79 ppm corresponding to the alkene protons in both compounds, as well as 16 protons on the aromatic region for the presence of two phenyl substituents and two core benzene rings.

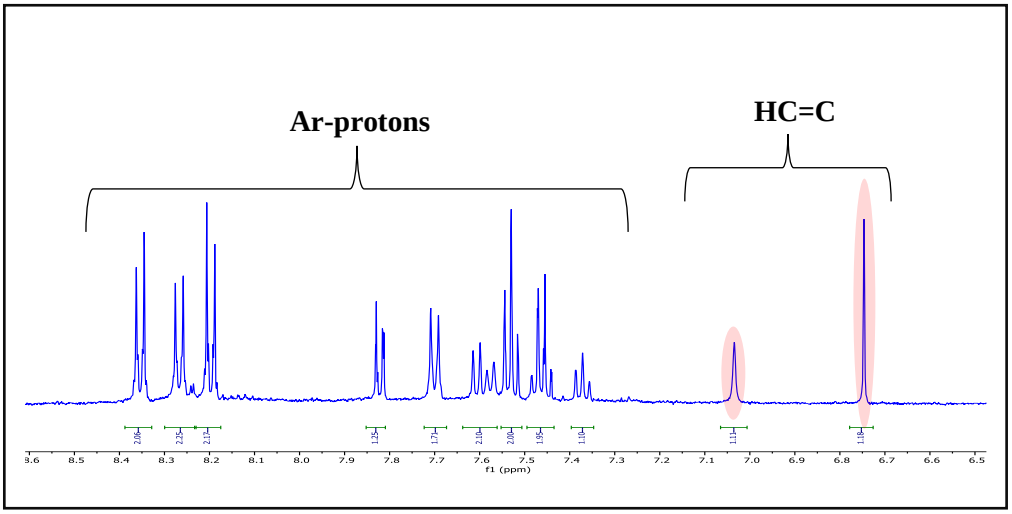

Figure 2. 13: ^{1}H-NMR spectrum of the resulting mixture from the reaction of amidine **79** and 1-ethynyl 4-nitro benzene under microwave condition.

As mentioned previously competition between formation of 5 and 6 membered ring compounds (isoindoline and isoquinoline) can occur depending on the reaction condition used, they have been observed in the literature. For example, reacting 2-[(4-nitrophenyl)ethynyl] benzonitrile **141** with secondary amine **142** in the presence of CuOTf. PhMe as a catalyst in toluene at 120 ℃ can access both the aminoisoindoline **144** and aminoisoquinoline **143** in a ratio of 1:1 as illustrated in Scheme 2.25.[97]

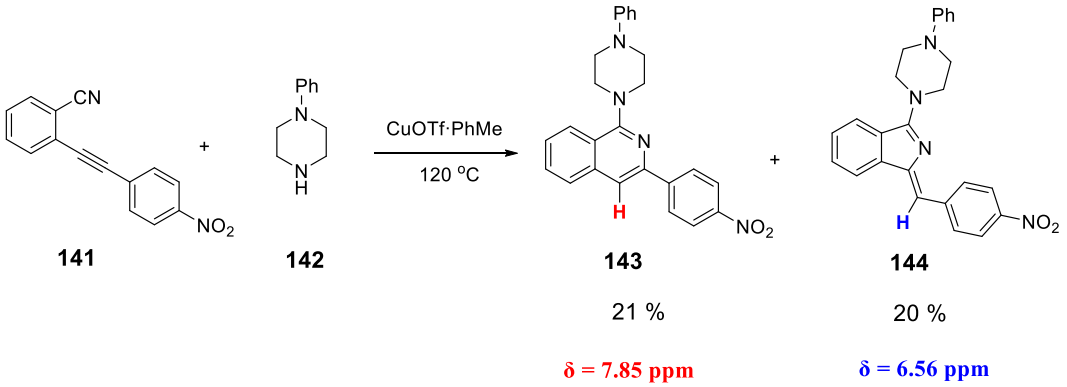

Scheme 2.25: Competition between formation of aminoisoquinoline **143** and aminoisoindoline **144**.[97]

Comparing between the ^{1}H-NMR spectrum for compound **143**, compound **144** and the mixture spectrum, the alkene singlets in the compound **143** and **144** appeared at 7.85 ppm and 6.56 ppm respectively, this was close to the chemical shift for the two singlet peaks in the ^{1}H-NMR spectrum for the mixture obtained. The singlets appeared at 7.05 ppm and 6.79 ppm. However, there is no conclusive evidence for the outcome of this reaction due to other possibilities. The reaction also, might result in a mixture of *E* and *Z* aminoisoindoline isomers **140** and **145**.

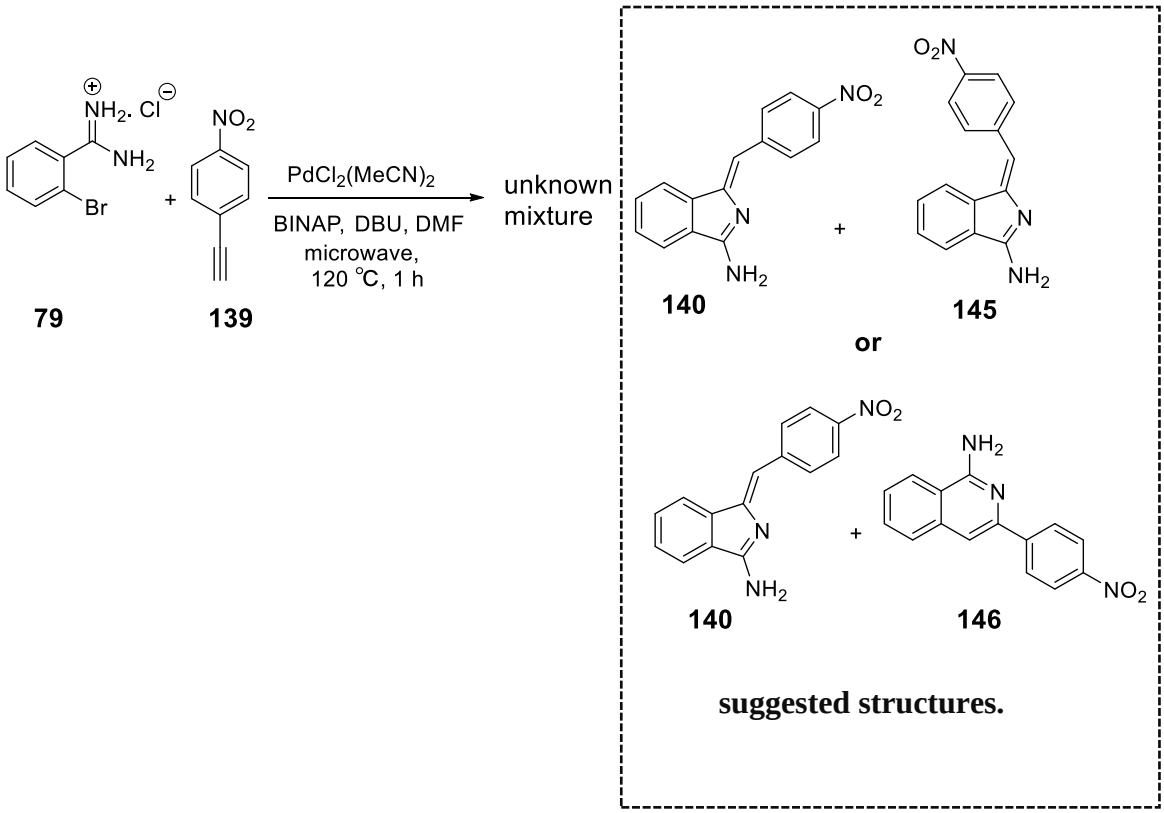

Scheme 2.26: Attempted formation of compound **140** from the reaction of amidine **79** and 1-ethynyl 4-nitro benzene under microwave condition.

After unsuccessful formation of 4-nitro phenyl methylene aminoisoindoline **140** following the microwave conditions, an alternative stepwise route was attempted (Scheme 2.27). Synthesis of the intermediate 4- nitro amidine **151** was the next target, then it would undergo cyclisation reaction using palladium(II) catalyst under microwave conditions, this might be producing the desired product **140**. The intermediate **151** can be accomplished via three steps as shown in Scheme 2.27. Firstly, 2-bromobenzonitrile **108** was treated with dimethyl ethynyl carbinol **147** under Sonogashira conditions to produce the corresponding compound **148** in excellent yield.[103] Then compound **148** was subjected to the reported modified Sonogashira coupling with 1-idol-4- nitrobenzene **149** in the presence of $PdCl_2(PPh_3)_2$, CuI, and Bu_4NI in a heterogeneous mixture of toluene and aqueous NaOH under nitrogen at 80 °C for 24 h.[105] Yeung et al., found this procedure was very effective to reduce the amount of the resulting homo-coupling compound and assist to increase the target compound yield by more than 23 % compared with the outcome when the normal

Sonogashira condition performed.[105] Following this procedure compound **150** was obtained in good yield. In the third step, compound **150** was treating with LiTMS in dry THF produced the corresponding amidine **151** in low yield. Figure 2.14 shows stacked ^{1}H-NMR spectra of both **150** and **151** in deuterated methanol, they both display set of peaks for all of the phenyl and benzene protons.

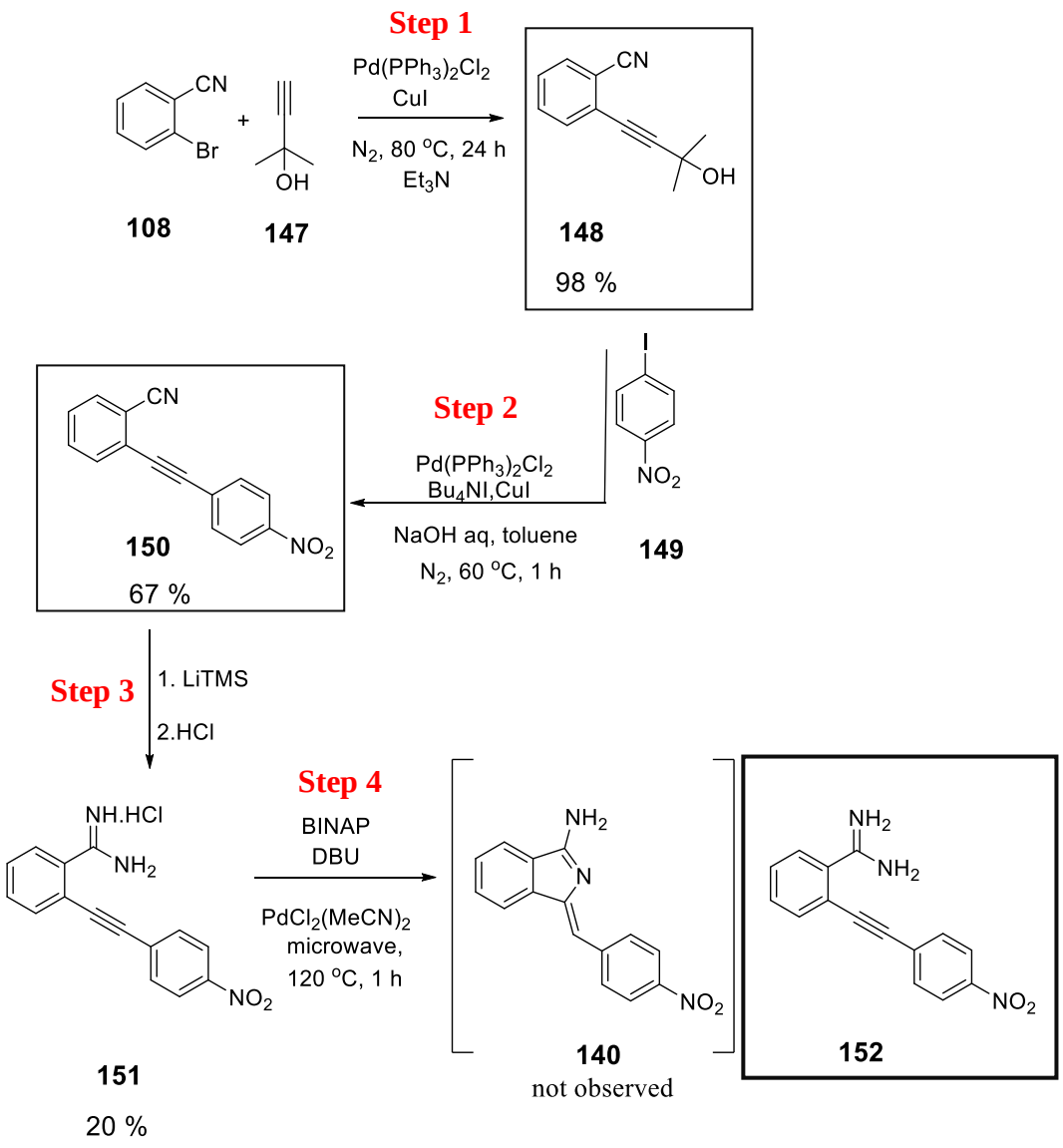

Scheme 2.27: Stepwise synthesis route toward compound **140**.

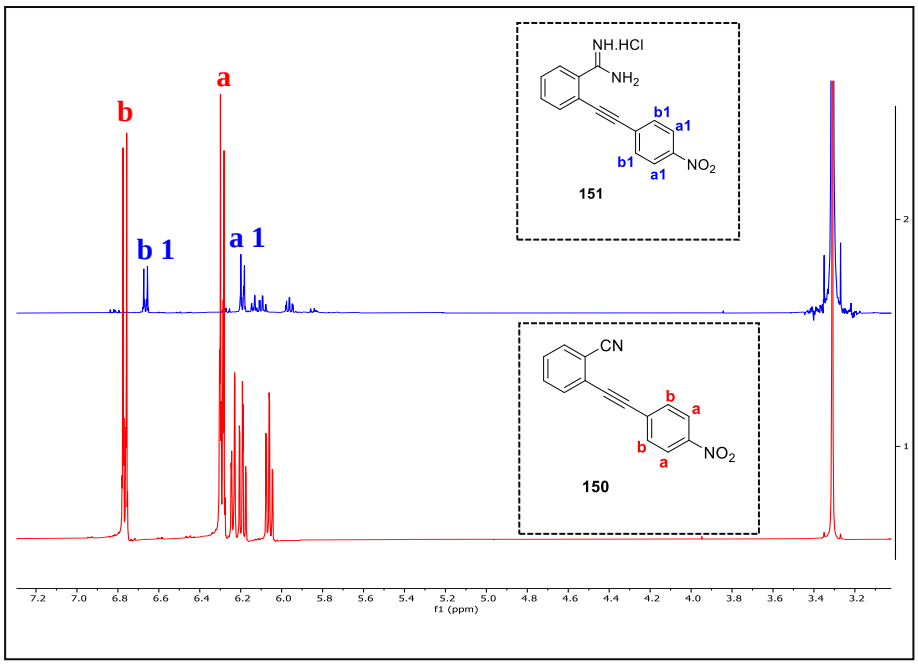

Figure 2. 14: ^{1}H-NMR spectrum of compounds **150** (red colour) and **151** (blue colour).

After the intermediate **151** has been successfully synthesis, it underwent a microwave irradiation in the presence of Pd(II) catalyst. Unfortunately, this reaction was poor, giving a complicated mixture that was difficult to separated and analyse. The major product formed **152** which was separated by several columns and isolated in poor yield. The ^{1}HNMR spectra of compound **152** indicates that the intermediate amidine hydrochloride salt **151** converted to the free amidine **152** (Figure 2.15).

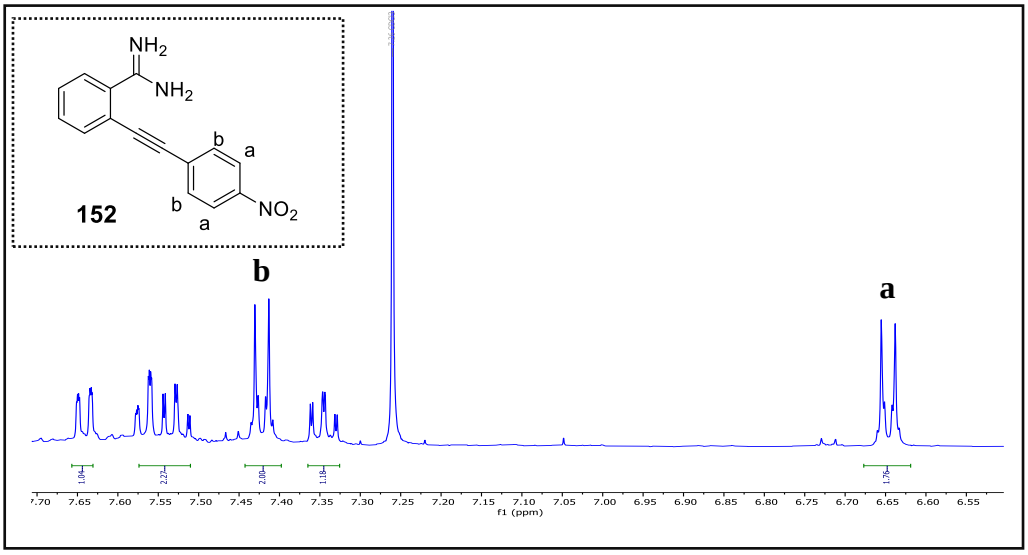

Figure 2.15: ^{1}H-NMR spectrum of compound **152** in deuterated chloroform.

Therefore, the attention was switched to the 4-cyano derivative. Using of 4-ethynyl benzonitrile **153** under the microwave conditions that are described above led to the successful synthesis of the corresponding 4-benzonitrile methylene aminoisoindoline **154** in 65 % yield.

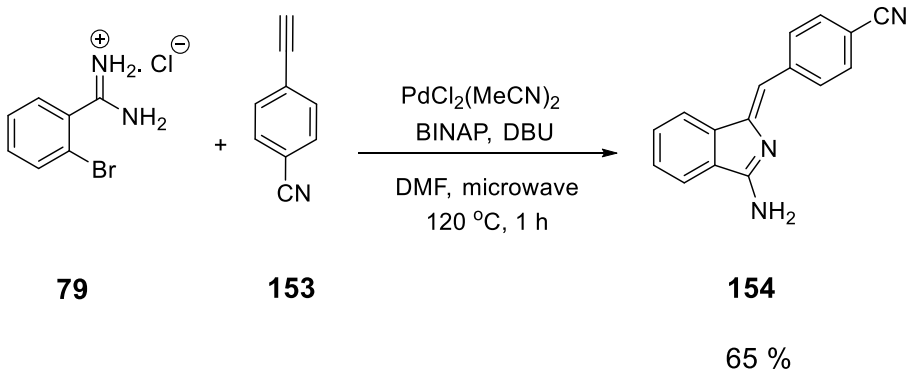

Scheme 2.28: Synthesis of compound **154**.

The structure of product **154** was confirmed by ^{1}HNMR spectroscopy which showed the alkene proton appears as a singlet at 6.8 ppm and the set of peaks of the 4-cyno phenyl and benzene ring protons in the aromatic region (Figure 2.16). MALDI- TOF mass spectrometry showed a clear peak at *m/z* 245confirming that compound **154** was formed.

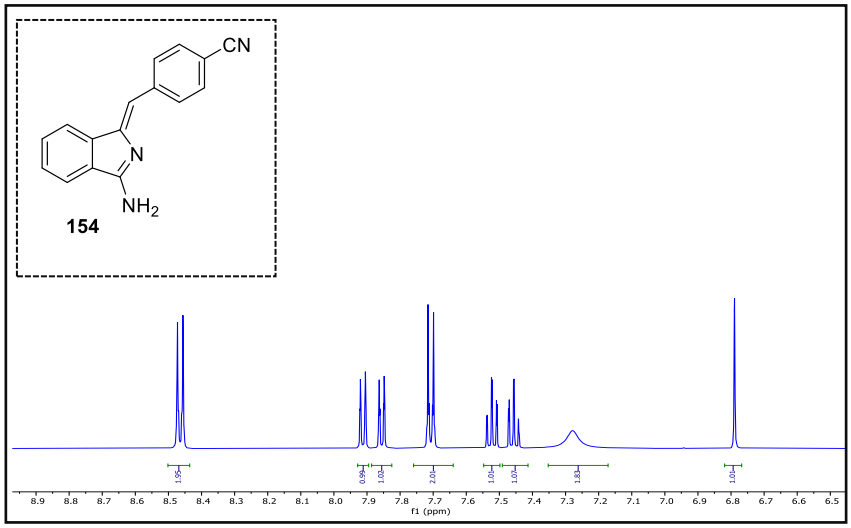

Figure 2. 16: ^{1}H-NMR spectrum of compound **154**.

Table 2.2 summarises the derivatives of aryl acetylene used to synthesise aminoisoindolines and their outcomes. All aminoisoindoline compounds were furnished easily and fast, they were isolated in good yield, except when we used 1-ethynyl-4-nitrobenzene, where the reaction produced an inseparable mixture.

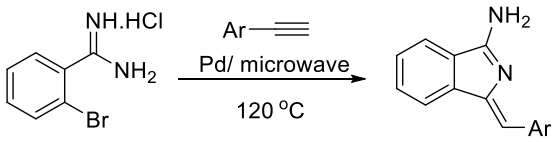

2

Entry	Ar	Resulting product	Yield%
1	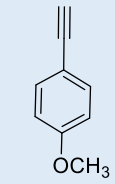	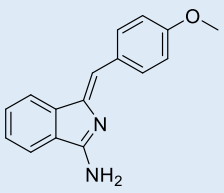 **81**	74 %
2	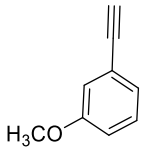	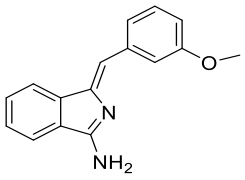 **137**	72 %
3	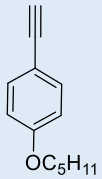	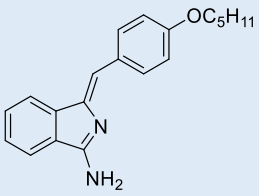 **138**	73 %
4	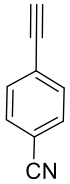	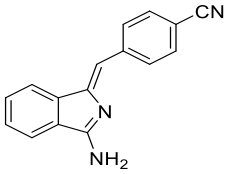 **154**	65 %
5	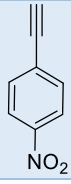	Unknown products	-

Table 2.2: Summary of the synthesis of aminoisoindoline derivatives.

2.5.2 Synthesis of symmetrical aza (dibenzo) dipyrromethenes (ADBDP) from self-condensation of aminoisoindolines.

The synthesis of aza (dibenzo) dipyrromethenes via dimerization (self-condensation) of aminoisoindolines has been previously reported by our group.[41] The aminoisoindoline derivatives were initially refluxed in toluene at 120 ºC for 2-24 h, until the aminoisoindoline is completely consumed. This reaction was reproducibly carried out using different aminoisoindolines with donor and acceptor substituents. These self-condensation reactions gave the required symmetrical compounds as red crystals in good to excellent yield averaging 60-80 %. The likely mechanism of this reaction includes a nucleophilic attack where an amine group of one molecule attacks the partially positive carbon between the two nitrogens on the other molecule followed by extrusion of ammonia and tautomerisation of the resulting structure resulting in the target symmetrical ADBDPs.

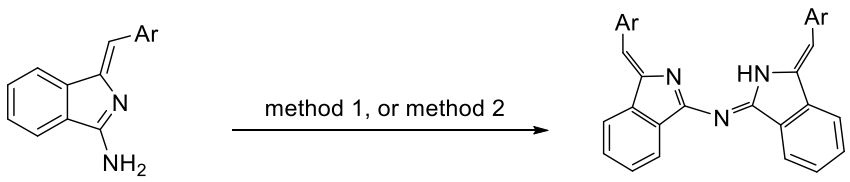

Method 1 = toluene, 120 ℃, 24 h

(83 Ar = 4-OCH_3 phenyl**, 155** Ar = 3-OCH_3 phenyl**, 156** Ar = 4-OC_5H_{11} phenyl)

Method 2 = diglyme, 200 ℃, 24 h

(157 Ar = 4-CN phenyl)

Scheme 2.29: Synthesis of aza (dibenzo) dipyrromethenes.

Using toluene as the solvent was not a good choice for the synthesis of compound **157** because it was unable to dissolve the starting material **154**, which remained unreacted during the reaction for a long period of time then started to dimerise after 24 h. Therefore, the solvent was replaced with diethylene glycol dimethyl ether (diglyme) and heated at 200 ℃. After 2 h the colour of the solution changed to a red colour and TLC showed formation of the desired product **157**. The reaction was left to continue for

over 24 h until the starting material was almost consumed. All the aza (dibenzo) dipyrromethene compounds were purified by column chromatography eluting with DCM, followed by recrystallisation with 1:1 DCM and MeOH to produce red crystals in good yield. Compounds **155** and **157** gave crystals suitable for X-ray crystallography which confirmed these structures and showed that the configuration of the alkene double bonds were *Z, Z* as shown in Figure 2.17. The crystallography results, performed and analysed by UEA collaborator Dr David Hughes, are similar for the two structures **155** and **157**. Compound **157** is representative, and the data show all the bonds in the chain of N (2) -C (1) – N (41) – C (21) – N (22) are very similar, at *ca* 1.34 Å, suggesting delocalisation. However, the amino nitrogen atoms are different - the hydrogen on N (2) comes up strongly in early difference maps while the hydrogen on N (22) appears weaker. It is assumed that there is only one hydrogen atom here, shared unequally between the two nitrogen atoms. After refinement, the ratio of hydrogen (2):H (22) is *ca* 0.64:0.36. Both these hydrogen atoms are involved in hydrogen bonds to the opposite nitrogen atom in the molecule.

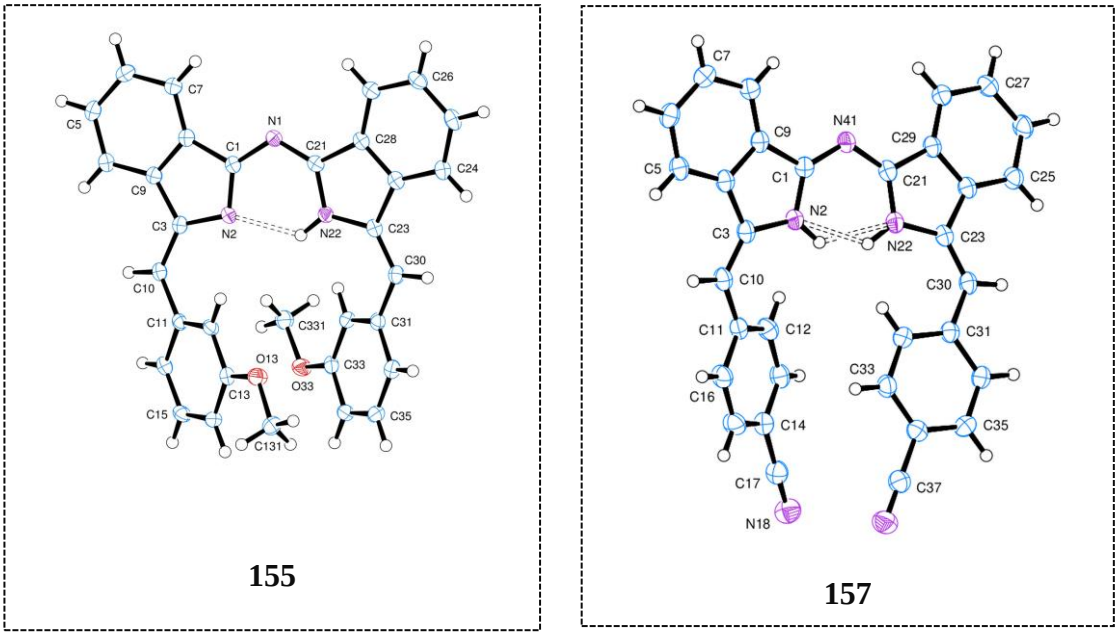

Figure 2.17: Crystal structures of compounds **155** and **157**.

These aza (dibenzo) dipyrromethene derivatives were further characterized by NMR spectroscopy and MALDI-TOF mass spectrometry to confirm their identity. The

[1]HNMR spectra of compound **157** is shown below (Figure 2.18). The key characteristic peak for the amine protons is observed at 13.35 ppm. The vinyl (C=CH) proton is seen as a singlet, integrating to two protons at 7.0 ppm. Moreover, the aromatic region shows eight protons of the isoindoline benzene rings and the phenyl groups. The other aza dipyrromethene compounds **83**, **155**, and **156**, were also fully characterised by [1]HNMR, [13]CNMR, MALDI-TOF mass spectroscopy and as expected showed similar characteristic peaks for the desired compounds with variations only observed at the aryl substituents.

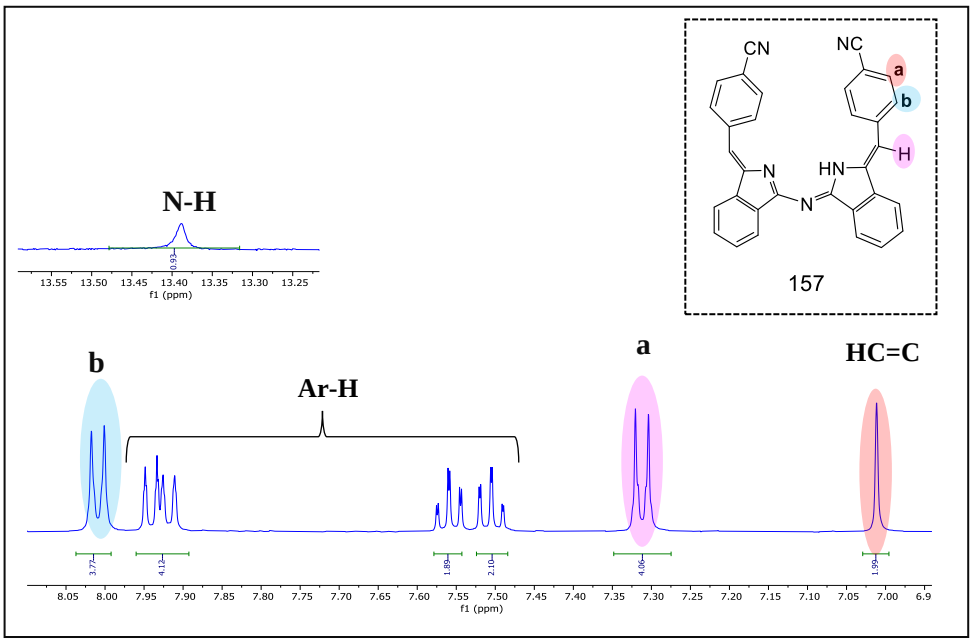

Figure 2. 18: [1]H-NMR spectrum of compound **157**.

Table 2.3 summarises the synthesis of symmetrical aza dibenzo dipyrromethene derivatives isolated from smooth and efficient self- condensation producing the desired compounds in good yield.

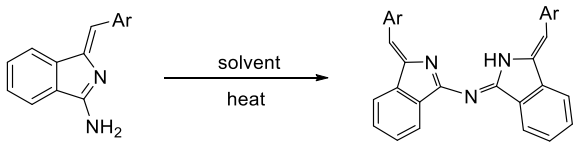

Ar	solvent	Time and temperature	Resulting compound	Yield %
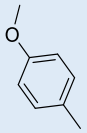	toluene	24 h 120 °C	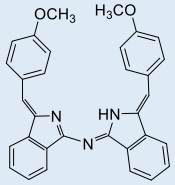 **83**	82 %
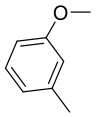	toluene	24 h 120 °C	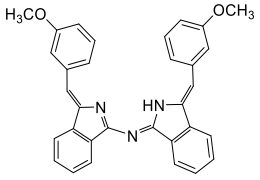 **155**	84 %
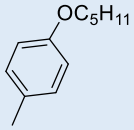	toluene	24 h 120 °C	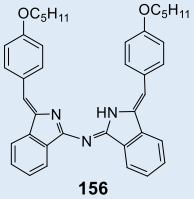 **156**	80 %
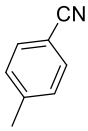	toluene	48 h 120 °C	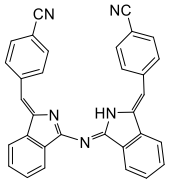 **157**	40 %
	diglyme	24 h 200 °C		60 %

Table 2.4: Summary of the synthesis of aza (dibenzo) dipyrromethene derivatives.

During the separation of all these derivatives a side product was noticed, it was the first fraction eluted from the column chromatography and was green in colour. The amount isolated of this fraction was very small, nonetheless a concentrated sample of it were collected over the course of several reactions, during formation of compound **156**. The ^{1}HNMR spectrum for this fraction was unclear, and MALDI-TOF mass spectrometry gave three main ion peaks. One of them at *m/z* 835 indicates it could contain a TBDAP-$(OC_5H_{11})_2$ molecular structure **158** as shown in Figure 2.19. We were unable to purify this fraction further. Previously in our group when other aza dipyrromethene derivatives were synthesised we had made similar observations. However, this was not an important issue to investigate extensively due to the trace yields that were collected. Moreover,

previously in our group experiments were carried out re-subjecting the aza dipyrromethenes to the formation of TBTAPs reaction conditions ($MgBr_2$, diglyme, 220 °C), but no more than trace hybrid macrocycles were observed.[106]

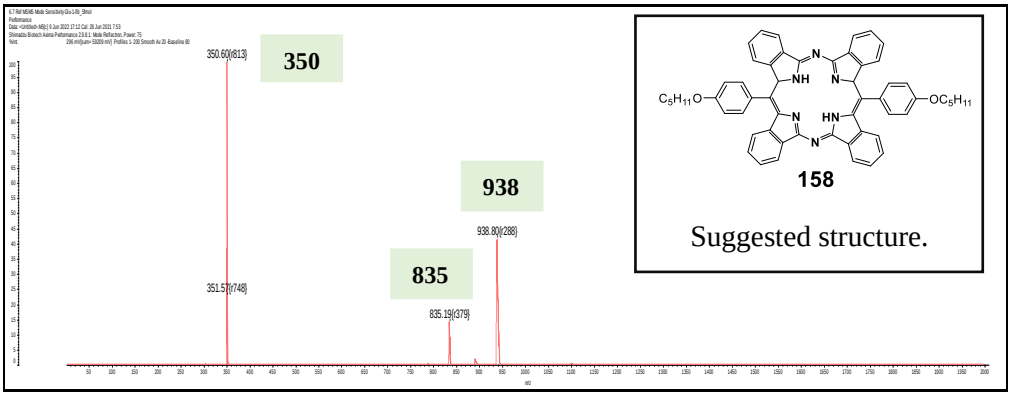

Figure 2. 19: MALDI-TOF mass spectrum of the green fraction isolated from synthesis of **156**.

2.5.3 Synthesis of unsymmetrical aza (dibenzo) dipyrromethenes (ADBDPs).

Unsymmetrical aza (dibenzo) dipyrromethene derivatives had not yet been investigated, and such systems could present interesting properties. In particular, systems bearing complementary donor and acceptor fragments are expected to show valuable modified properties. We started the investigation following the standard procedure i.e., heating a 1:1 mixture of 3-methoxy phenyl methylene aminoisoindoline **137** and 4-methoxy phenyl methylene aminoisoindoline **81** using toluene as the solvent at 120 °C. Following this reaction by TLC showed a major red spot corresponding to the aminoisoindoline dimerization products as well as two other minor spots close to the baseline which refer to the starting materials. The red dimers were isolated and the ^{1}HNMR spectrum proved the product to be a mixture of the symmetrical and unsymmetrical condensation products, as expected. Closer analysis of the ^{1}HNMR spectrum of the resulting mixture showed a total of four singlet peaks refer to the methoxy protons appearing in the range of 3.61 ppm - 3.70 ppm, two of them overlapping at 3.61 ppm. Vinyl protons appear as sets of four singlets overlapping at 6.75 ppm and 6.80 ppm, this indicates formation of symmetrical and unsymmetrical aza (dibenzo) dipyrromethene compounds (Figure 2.20). They demonstrated yields of 1: 1.76: 1 for compounds **83**, **159** and **155** respectively, based on NMR integrations for the isolated mixture. The obtained compounds had very similar chromatographic mobility which led to difficult separation, even after exploring a range of solvents systems.

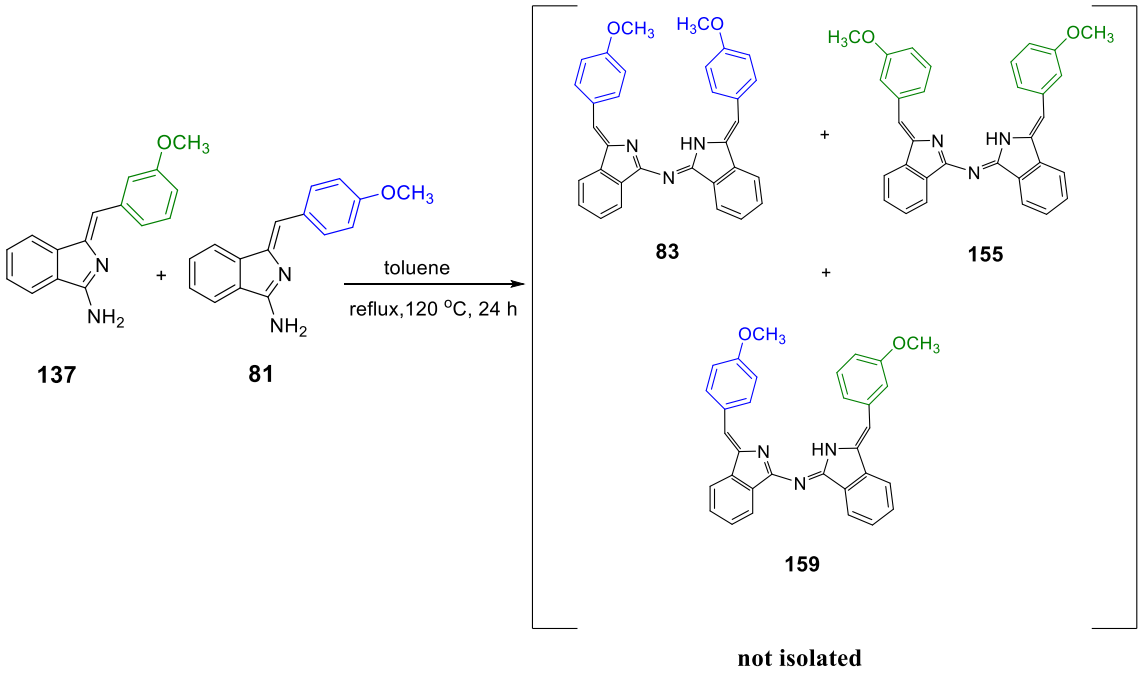

Scheme 2.30: Mixed condensation reaction forming symmetrical aza dipyrromethenes **83, 155**, and unsymmetrical-aza dipyrromethene **159.**

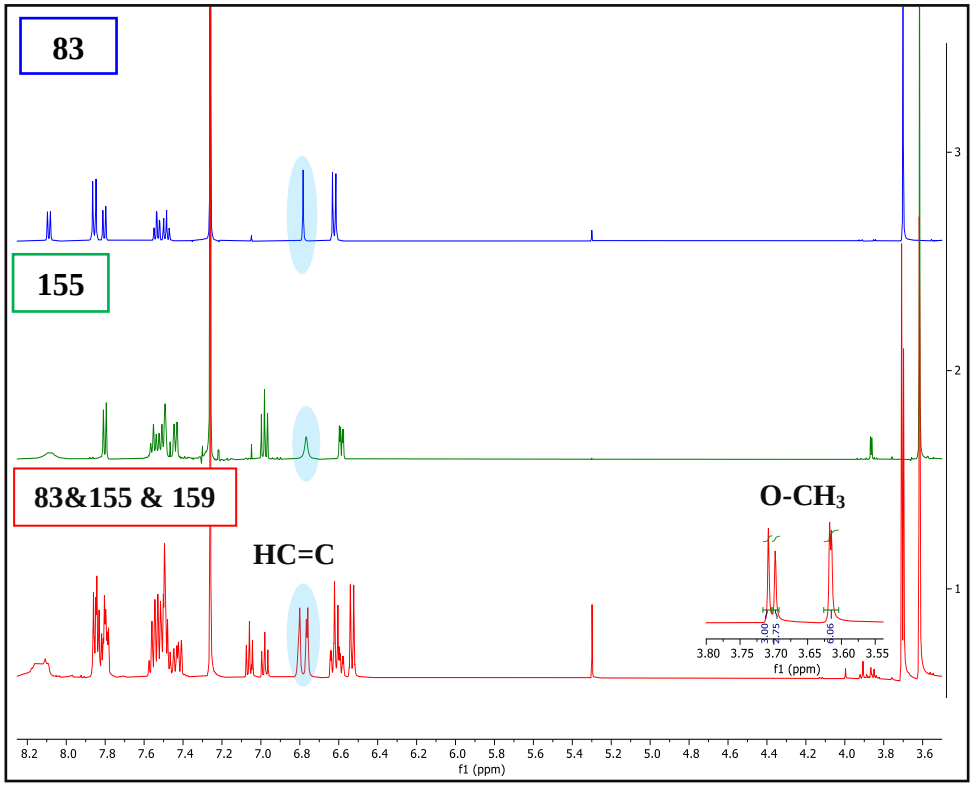

Figure 2.20: ^{1}HNMR spectrum of the mixture of symmetrical and unsymmetrical aza dipyrromethenes (red colour) compared with ^{1}HNMR spectrum of the compounds **83** (blue colour), and **155** (green colour).

MALDI-TOF mass spectrometry was not helpful due to the identical mass of both compounds and no further analysis was performed. So, the focus was turned to dimerisation of other aminoisoindoline derivatives that would be separable. As such, 4-pentyloxyphenyl methylene aminoisoindoline **138** was selected to be used with 4-methoxyphenylisoindolene **81**, refluxing at 120 °C in toluene. TLC revealed the formation of three major products, later confirmed by MALDI mass spectrum to be the self-condensation products for symmetrical and unsymmetrical aza dipyrromethene compounds. Purification of the mixture by column chromatography gave three of aza (dibenzo) dipyrromethenes, 4-methoxyphenyl-aminoisoindolene self-condensation product **83** (30 %), 4-pentyloxyphenyl aminoisoindolene self-condensation product **156** (2 7 %), and the target unsymmetrical product **160** (44 %).

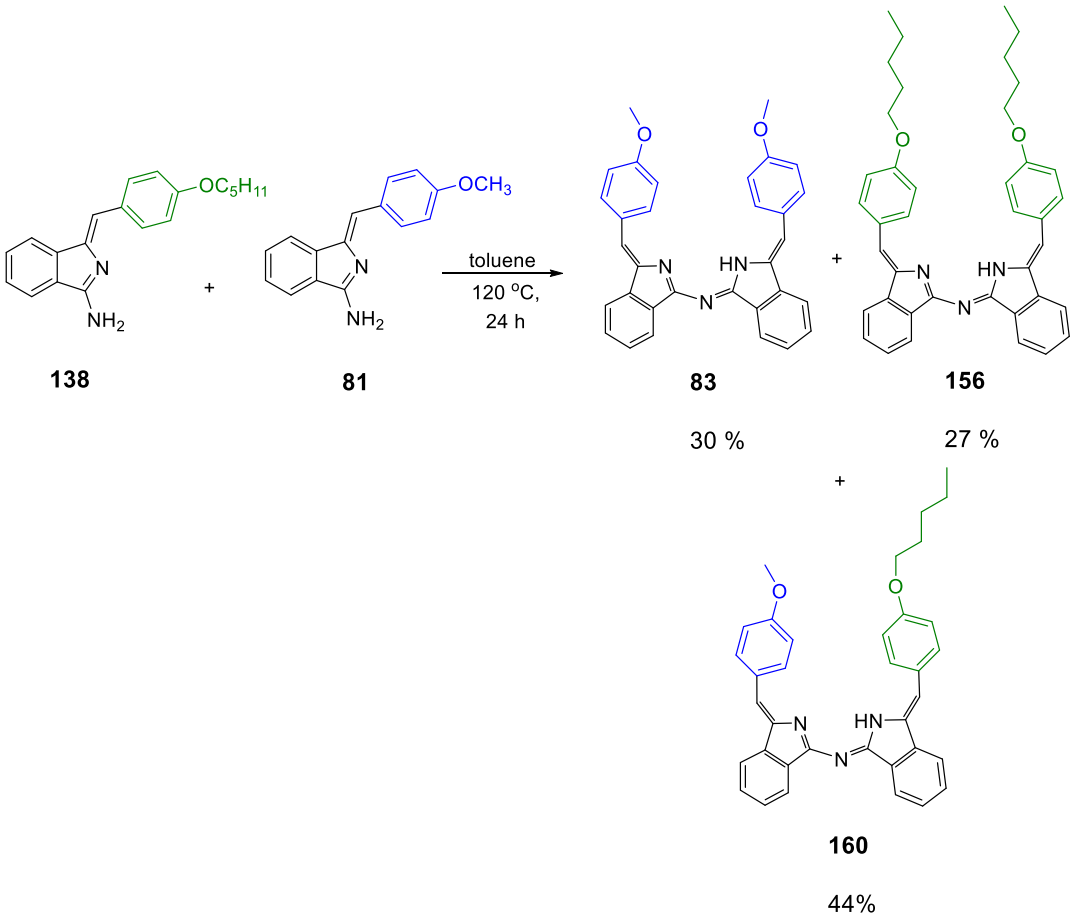

Scheme 2.31: Formation of symmetrical aza (dibenzo) dipyrromethenes **83** and **156**, and unsymmetrical aza dipyrromethene **160**.

The ^{1}HNMR spectrum in deuterated acetone for **160** showed all signals corresponding to both methoxy and pentyloxy protons. The alkene peaks appear as a singlet integrating to two protons. The aromatic protons for the phenyl and isoindoline benzene rings appeared as expected in the range between 6.6 ppm - 8.0 ppm.

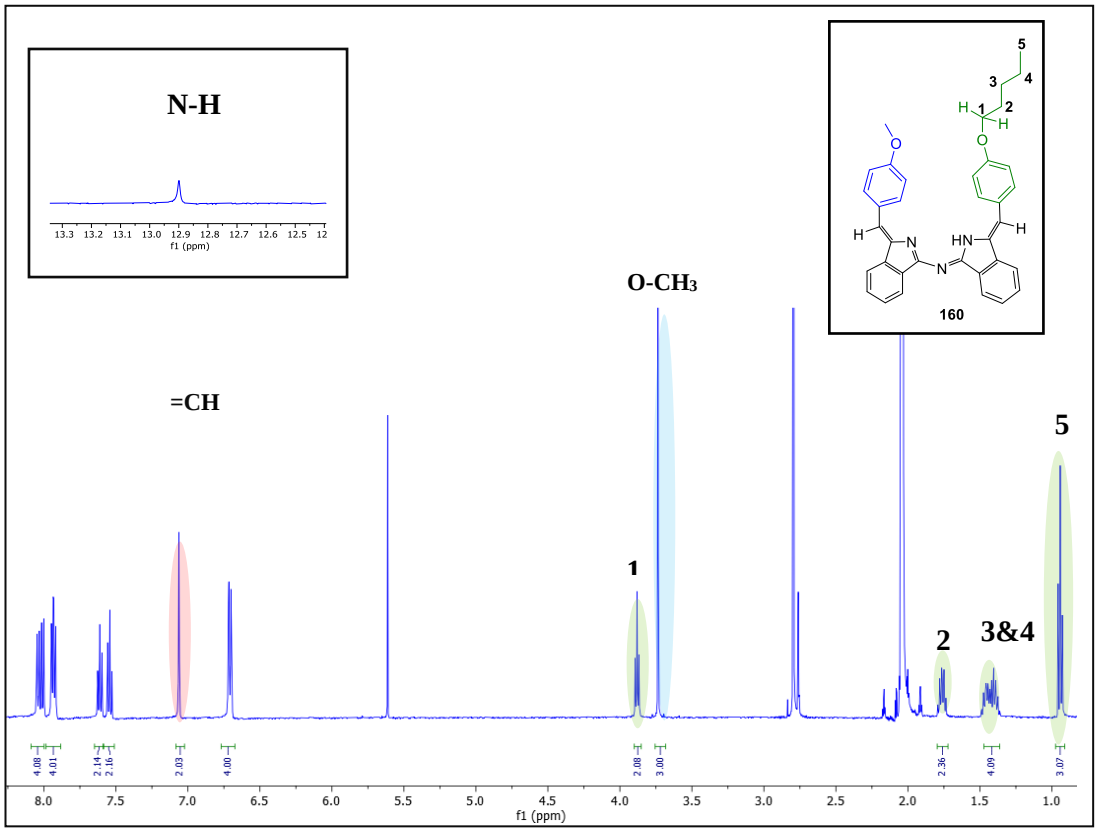

Figure 2.21: ^{1}HNMR spectrum of compound **160**.

Condensation of similar electronic components was expected to produce an approximately statistical mixture of compounds. It was reasoned if one component was electron rich and one was electron poor, then we might be able to favour one unsymmetrical product. This was assumed in the mechanism one component behaves as a nucleophile, therefore favoured by addition of electron rich substituent, whereas the second component behaves as an electrophile, therefore favoured by addition of electron withdrawing substituent, and that might lead to formation of unsymmetrical dimer (Scheme 2.32).

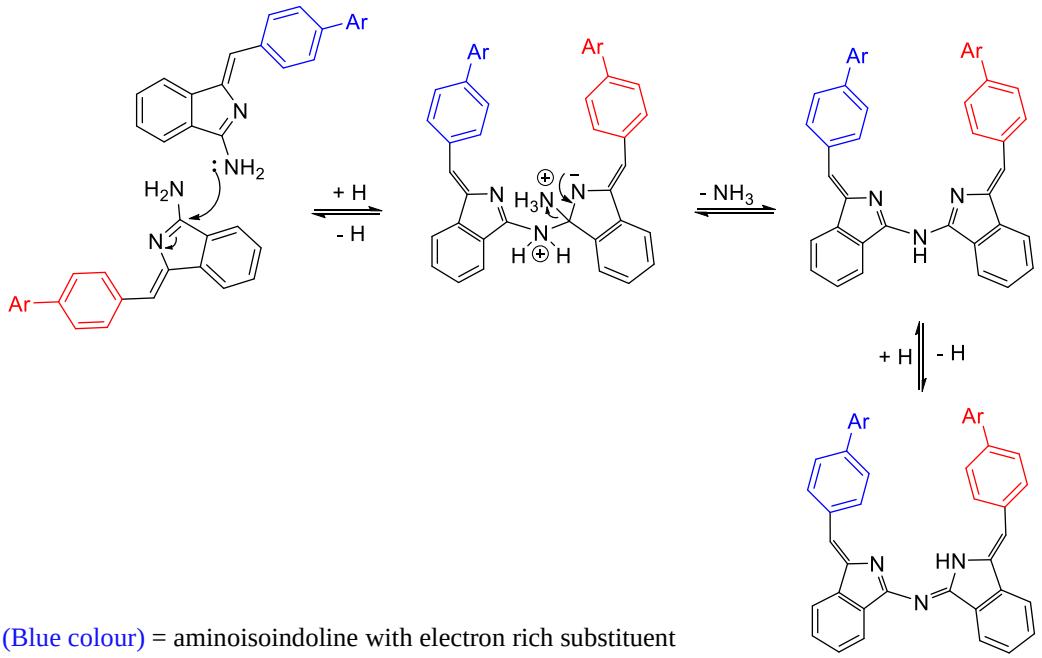

(Blue colour) = aminoisoindoline with electron rich substituent

(Red colour) = aminoisoindoline with electron poor substituent

Scheme 2.32: Suggested mechanism for formation of unsymmetrical aza (dibenzo) dipyrromethenes (ADBDPs).

Condensation of electron poor 4-cyano substituted aminoisoindoline **154** (prepared as previously described) with the 4-methoxyphenylisondoline compound **81** was therefore examined. The reaction was monitored by TLC. After a few hours it was observed formation of a new red spot, and the reaction was left longer due to presence of large amount of starting materials still unreacted. After 24 h reflux the red spot has become the major component. Another red spot has also formed, refers to symmetrical di cyano aminoisoindoline dimer **157** (the reference was already available from previous preparation). Also, there was a minor spot close to the baseline which corresponded to the starting material **154**. After separation of the mixture and analysis by ^{1}HNMR spectroscopy, the first red spot was found not to be a single compound but rather a mixture of 4-methoxy aminoisoindoline dimer **83** and the target unsymmetrical product **161.** They had very similar chromatographic mobility which led to difficult separation.

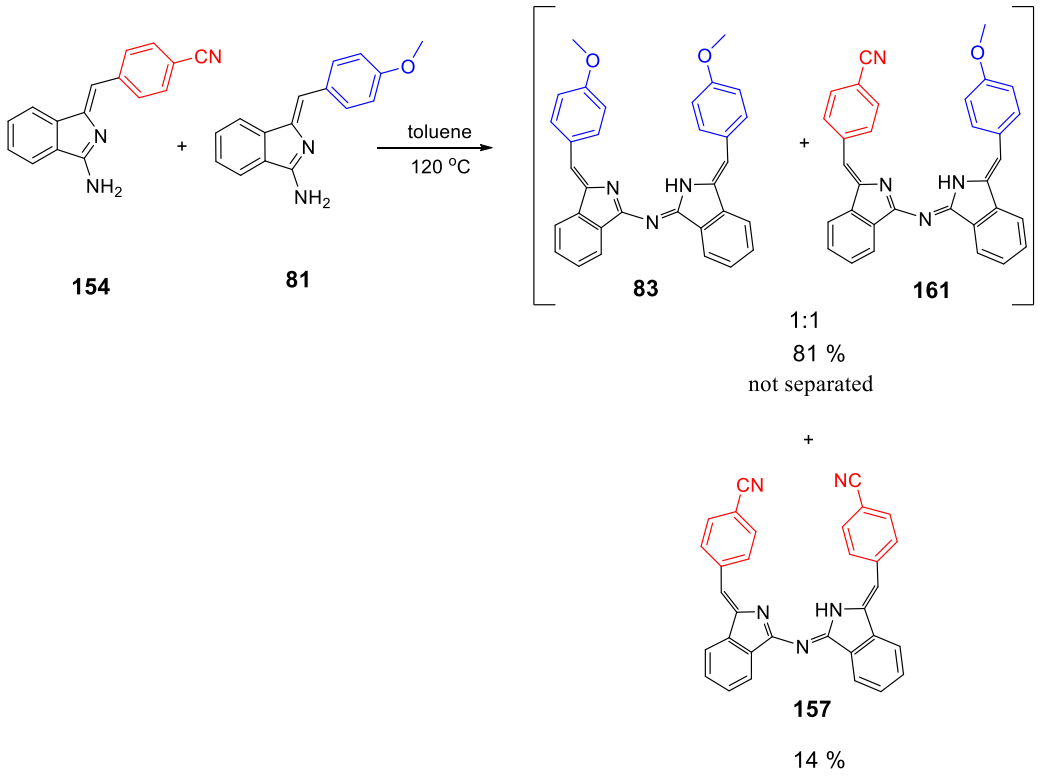

Scheme 2.33: Mixed condensation reaction formatting of symmetrical aza dipyrromethenes **83**, **157**, and unsymmetrical aza dipyrromethene **161**.

During this reaction the formation of compound **157** was very slow and the outcome yield was poor, the explanation is that the aminoisoindoline with electron rich substituent **81** is more reactive than the aminoisoindoline with electron poor substituent **154**. So, in the first step compound **81** initiates the reaction by reacting either with itself, producing the symmetrical ADBDP **83** or with compound **154** to produce the unsymmetrical **161**. Therefore, when compound **81** was consumed, and only compound **154** remains, then it started the self-condensation reaction producing the symmetrical ADBDP **157**. Another suggestion for the low yield of compound **157** is that the slow step in the reaction mechanism could be loss of ammonia and the protonation might be less favoured if the substituent is electron withdrawing leading to slow formation of compound **157**. Also, as mentioned earlier, compound **154** is poorly soluble in toluene so, it is formed later in the reaction. Figure 2.22 illustrates comparison between ^{1}HNMR spectrum of compound **83** and the resulting mixture of 83 and **161** in deuterated acetone. As shown, there were two singlets at 3.79 ppm and 3.74 ppm indicating the presence of the methoxy group in symmetrical and unsymmetrical dimers. There were three singlets appear at 7.13 ppm, 7.10 ppm and 7.07 ppm which refer to the vinyl protons (C=C-H),

multiplet at 6.70 ppm integrating to four protons refer to the phenyl protons in both symmetrical and unsymmetrical dimers. From the NMR integration, they demonstrated the yield ratio **1:1** for the compound **83** and compound **161** respectively. While compound **157** was isolated in low yield 14 %. MALDI-TOF mass spectrum for the first fraction confirmed presence of two products with two ion peaks at *m/z* 477 and *m/z* 480, which correspond to the target product **161** and 4-methoxy phenyl aminoisoindoline self-condensation product **83**.

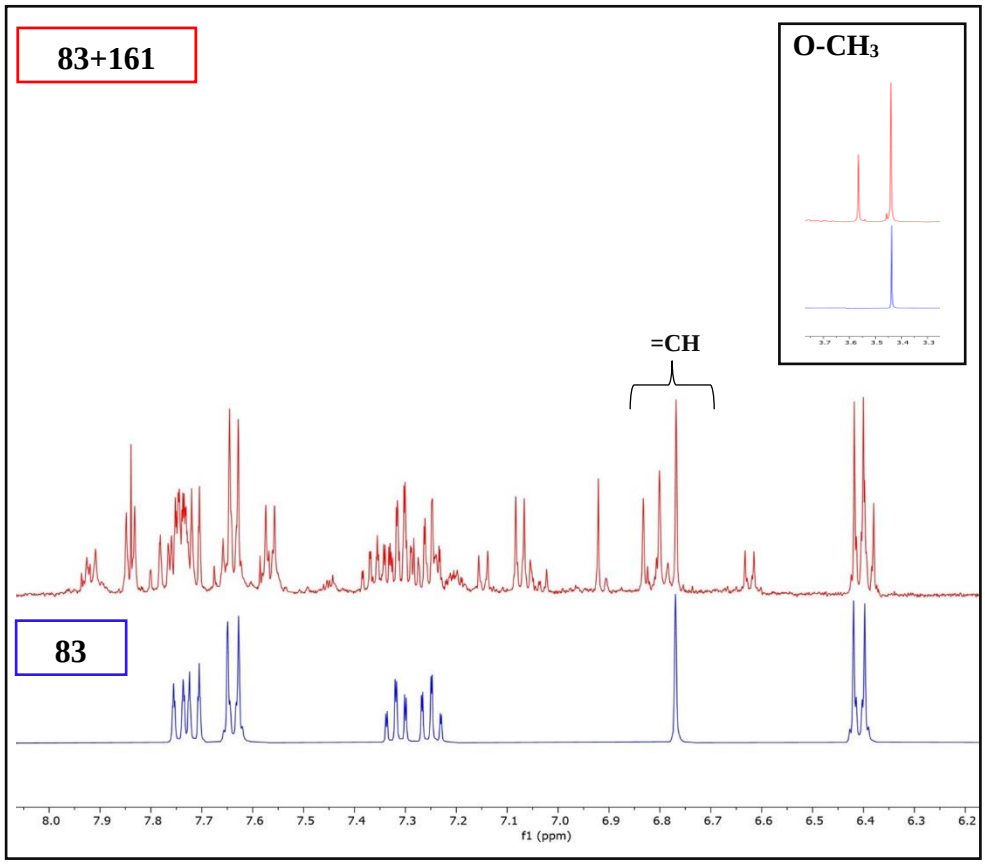

Figure 2.22: ^{1}HNMR spectrum of the mixture symmetrical aza dipyrromethene **83** (blue colour), and the mixture of symmetrical **83** and unsymmetrical aza dipyrromethene **161** (red colour).

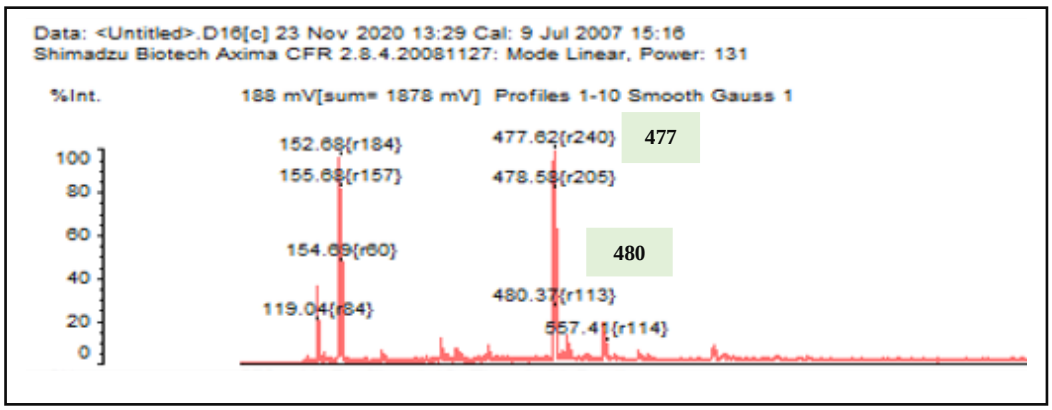

Figure 2.23: MALDI-TOF spectrum of the crude mixture.

In order to make separation possible, 4-methoxy phenyl methylene aminoisoindoline **81** was replaced by the 4-pentyloxy phenyl methylene aminoisoindoline **138**. However, the similar issue was also encountered, and the TLC showed two red spots were very close to each other. MALDI-TOF mass spectrum for this fraction confirmed the presence of two products with *m/z* 536 and *m/z* 597 molecular weights which correspond to the target product **162** and 4-pentyloxy aminoisoindoline self-condensation product **156** (Figure 2.24).

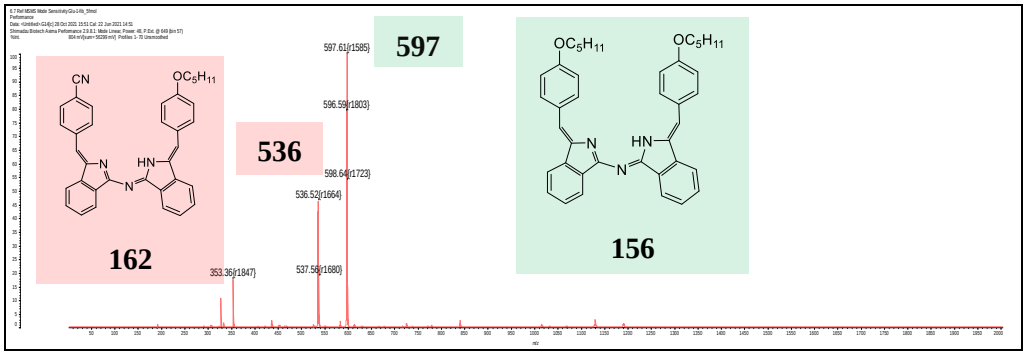

Figure 2.24: MALDI-TOF mass spectrum of the crude mixture.

These products were difficult to isolate, trace amount of compound **156** remained inseparable from the mixture in spite of applying several solvent systems. Compound **157** was also observed on the TLC, it was isolated from the column chromatography in low yield. The ^{1}HNMR spectra of the first fraction (Figure 2.25) showed two sets of the pentyloxy chains demonstrating presence of two products, three singlets at 6.81 ppm, 6.78 ppm and 6.71 ppm correspond to the vinyl protons (C=C-H) in the symmetrical and unsymmetrical dimers. Multiplet at 6.61 ppm integrating to four protons which supports the presence of two pentyloxy phenyl protons in both symmetrical and unsymmetrical dimer. A doublet at 7.22 ppm with coupling constant J = 8.7 Hz corresponds to the cyano phenyl protons.

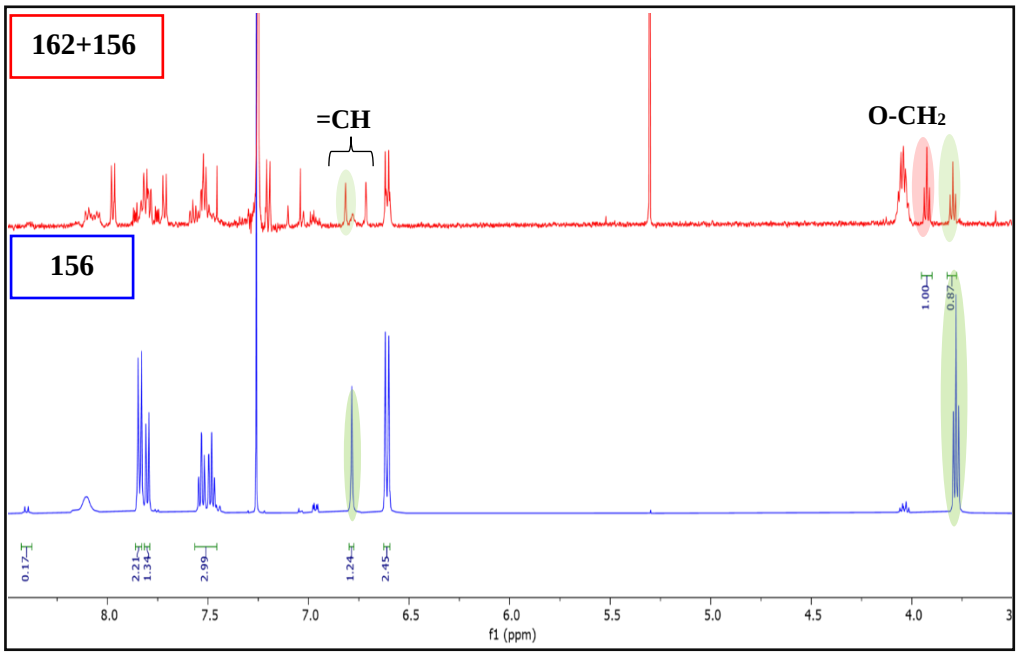

Figure 2.25: [1]HNMR spectrum of symmetrical aza dipyrromethene **156** (blue colour), and the mixture of symmetrical **156**, and unsymmetrical aza dipyrromethene **162** (red colour).

2.6 Controlled synthesis of unsymmetrical derivatives.

Although operationally simple, this synthetic procedure was not an efficient method to synthesise the unsymmetrical aza (dibenzo) dipyrromethenes as the isolation of products was impossible. Moreover, the symmetrical derivatives from the electron rich component were generally observed in the close proportion to that of the unsymmetrical product. This indicated the higher reactivity of electron rich derivatives. To overcome this issue, it was looked to design a method to prevent formation of the symmetrical aza (dibenzo) dipyrromethenes and improve the yield of unsymmetrical dimers. Therefore, it was investigated conversion of the amino group of one aminoisoindoline into good leaving group by converting to the corresponding tosylate. The 4-alkoxy phenyl aminoisoindolines **81** and **138** were chosen as substrates to investigate tosylate methodology, due to their rapid self-condensation, producing the symmetrical compounds that are difficult to separate from the unsymmetrical dimers. Compounds **81** and **138** were treated with p-toluene sulfonyl chloride (Ts-Cl) in the presence of TEA[107] (Scheme 2:34).

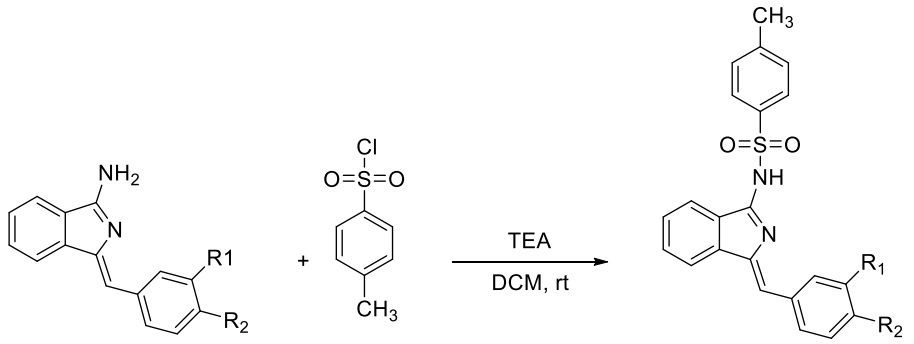

137 R_1= OCH_3, R_2 = H

81 R_1= H, R_2 = OCH_3

163 R_1= OCH_3, R_2 = H

164 R_1=H, R_2 = OCH_3

Scheme 2.34: Synthesis of compound **163** and compound **164**.

The mixture was stirred at room temperature in dry DCM and the reaction monitored by TLC. Conversion to a new product was observed in both cases. Work up led to isolation of pure materials whose spectroscopic data were consistent with the formation of a tosylate. However, there are in theory two possible sites (nitrogens) that can undergo tosylation, and ^{1}HNMR spectroscopy cannot differentiate between them. Fortunately, crystals suitable for X-ray crystallography were obtained for **163** and **164**, and the crystal structures (Figure 2.26) clearly prove that tosylation has occurred on the desired nitrogen. The crystallography results, performed and analysed by UEA collaborator Dr David Hughes, are again similar for the two structures **163** and **164**. However, in structure **164** the hydrogen atom on N (11), is clearly identified.

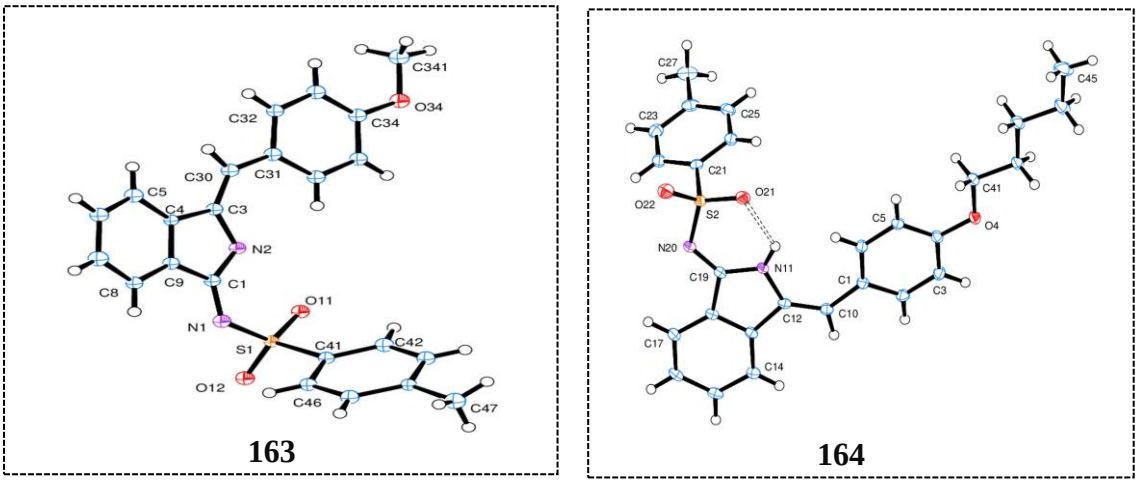

Figure 2.26: X-Ray structure for compound **163** and compound **164**.

Figure 2.27 illustrates the ^{1}H-NMR spectrum of compound **163**. The spectrum confirmed that the Ts group is indeed coupled on the amine group of the 4-methoxy phenyl methylene aminoisoindoline, as it is clear to observe presence of Ts group protons appeared as doublet at 7.47 ppm overlapped with another doublet refers to the isoindoline benzene ring with coupling constant J = 8.2, 6.0 Hz, in addition to doublet at 7.29 ppm with coupling constant J = 8.0 Hz. Methyl group protons appeared as a singlet at 3.88 ppm. The aminoisoindoline set peaks appeared at the expected range between 7.00 ppm -7.90 ppm (Figure 2.27). Compound **164** was also fully characterised by ^{1}H-NMR, ^{13}C-NMR, MALDI- TOF mass spectrum and as expected showed similar characteristic peaks for the desired compound.

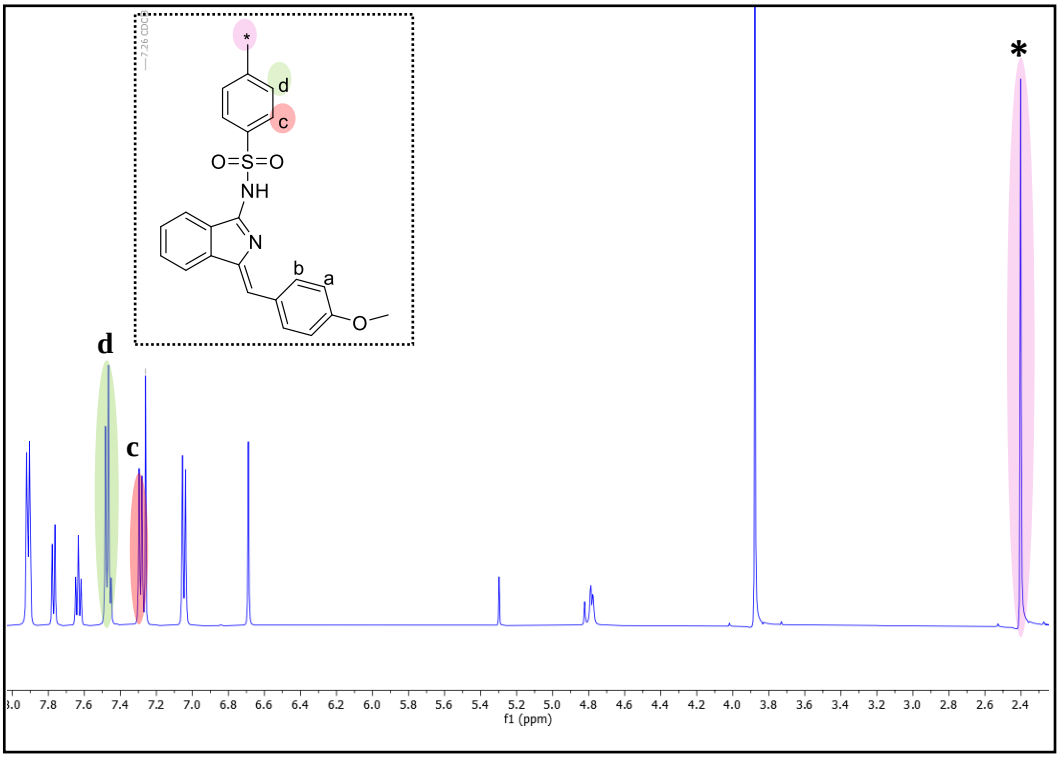

Figure 2.27: ^{1}HNMR spectrum of compound **163**.

Our working assumption for the reaction mechanism, it was suggested a tosylation of **163** or **164** followed by a nucleophilic reaction. It was postulated in the key step the amino group of one component behaves as a nucleophile while on the second component it behaves as a leaving group due to the tosylation. It was suggested that the tosylation of the amine (amidine) would simultaneously reduce the nitrogen nucleophilicity and improve its ability to act as a leaving group. After compounds **163**

and **164** were isolated, they were tested by refluxing each separately in toluene at 120 °C in order to detect whether the Ts group would be removed under the condensation reaction condition. The reaction was monitored frequently by TLC over 8 h, indicating that no dimerisation reaction occurred. This test was also carried out using p-xylene at 140 °C, and once more there was no changes observed of the tosylate products. Accordingly, after the evidence had made that Ts group was effective in protecting of NH group on the 4-alkoxy phenyl methylene aminoisoindoline tosylate derivatives **163** and **164**, which subsequently underwent condensation reaction with 4-cyano substituted aminoisoindoline **154** (Scheme 2.35). Therefore, the amine group on the compound **154** acts as a nucleophile attacking the partially positive carbon between the two nitrogens on the 4-alkoxy phenyl aminoisoindoline tosylate derivatives **163** and **164** followed by loss of the Ts group and tautomerisation of the resulting structure to obtain the target unsymmetrical aza dipyrromethenes **161** and **162**. This route was successful to furnish the unsymmetrical aza dipyrromethenes **161** and **162** with remarkable improvement of the reaction yields to those obtained via the mixed condensation synthetic method. In both pathways compound **157** produced in low yield ≤ 24 %.

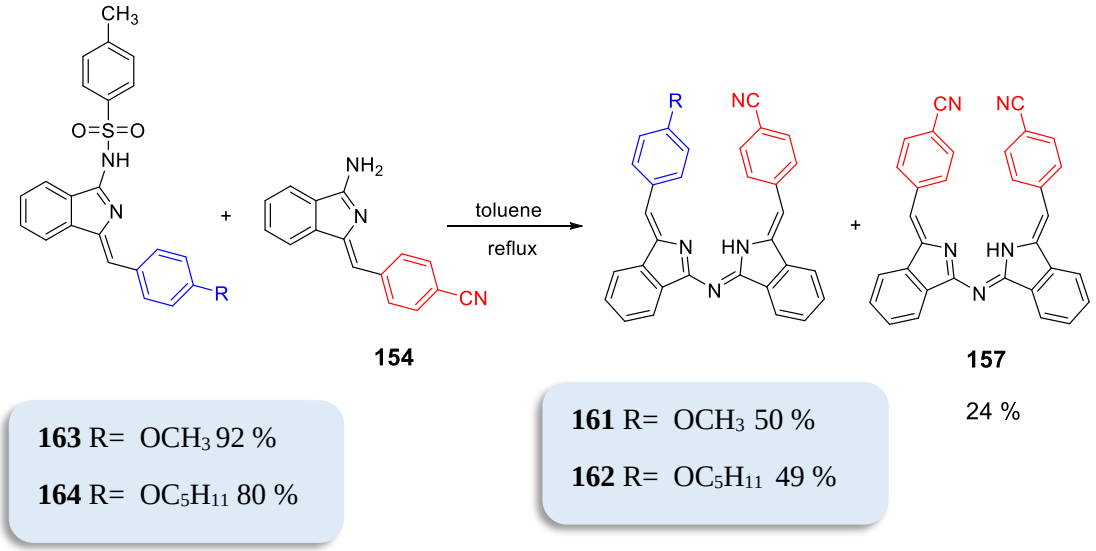

Scheme 2.35: Synthesis of unsymmetrical aza (dibenzo) dipyrromethenes (ADBDPs) **161** and **162** via aminoisoindolines tosylate **163** and **164**.

Compounds **161** and **162** were analysed by ^{1}H-NMR spectroscopy and they both displayed similarities in their ^{1}H-NMR spectra, the only difference was in the methoxy protons and pentaloxy chain protons. Figure 2.28 shows the ^{1}H-NMR spectrum of compound **161**, vinyl (C=CH) protons appeared as two singlets at 7.0 ppm and 6.9 ppm

confirming a break of the symmetry in the aza dipyrromethene. MALDI- TOF mass spectrum showed the expected ion peaks for both compounds confirming their structures.

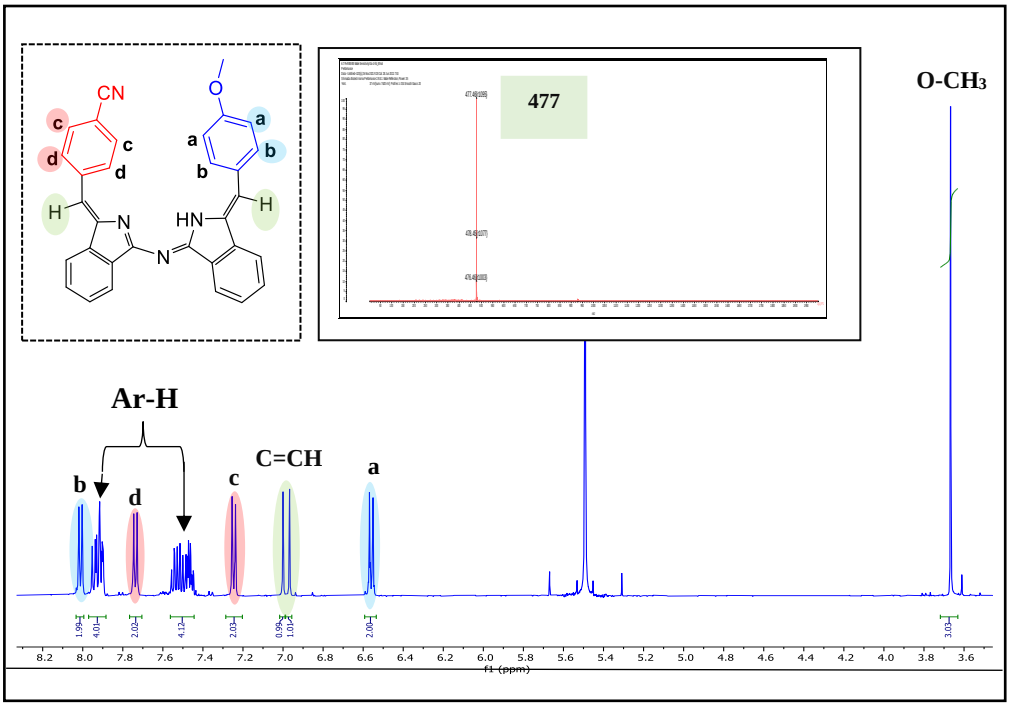

Figure 2.28: [1]HNMR spectrum and MALDI-TOF mass spectrum of compounds **161**.

The improvement in yield is because the protection of the amino functional group with Ts group prevented formation of symmetrical self-condensation of aminoisoindolines, whose formation leads to decrease in the yield of the unsymmetrical dimers and an impossible separation. With the optimized condition in hand, we turned our attention to investigate this strategy further by converting of amino group in the 4-methoxy phenyl aminoisoindoline **81** into a better leaving group. This was easily achieved by reacting **81** with trifluoromethanesulfonic anhydride under nitrogen in the presence of pyridine at -20 °C in dry DCM.[108] The work up and isolation of the crude mixture followed by column chromatography led to the isolation of pure materials whose spectroscopic data were consistent with formation of a triflate aminoisoindoline **165**. Crystals suitable for X-ray diffraction was eventually grown from a mixture of 1:1 DCM and PE**,** and analysis showed that the triflate group coupled at the desired nitrogen (Figure 2.29). The crystallography results, again performed and analysed by UEA collaborator Dr David Hughes, shows the isoindole group forms the central plane of the molecule. The

normal to the phenyl group is rotated 14.3 ° from that of the isoindole group and the SO_2-CF_3 group provides the only significantly displaced atoms from the major planar units. The pyrrole hydrogen atom was recognised in difference maps and forms a good intramolecular hydrogen bond with O (121), (Figure 2.29 **A**). Molecules are stacked, principally through the π π interactions between overlapping isoindole rings, in columns parallel to the *a* axis, (Figure 2.29 **B**, and **C**), with interplanar distances of 3.000 and 3.319 Å, either side of the isoindole plane. The phenyl ring partially overlaps its symmetry neighbour on one side at a distance of 3.59 Å; there are no π π interactions on the opposing side.

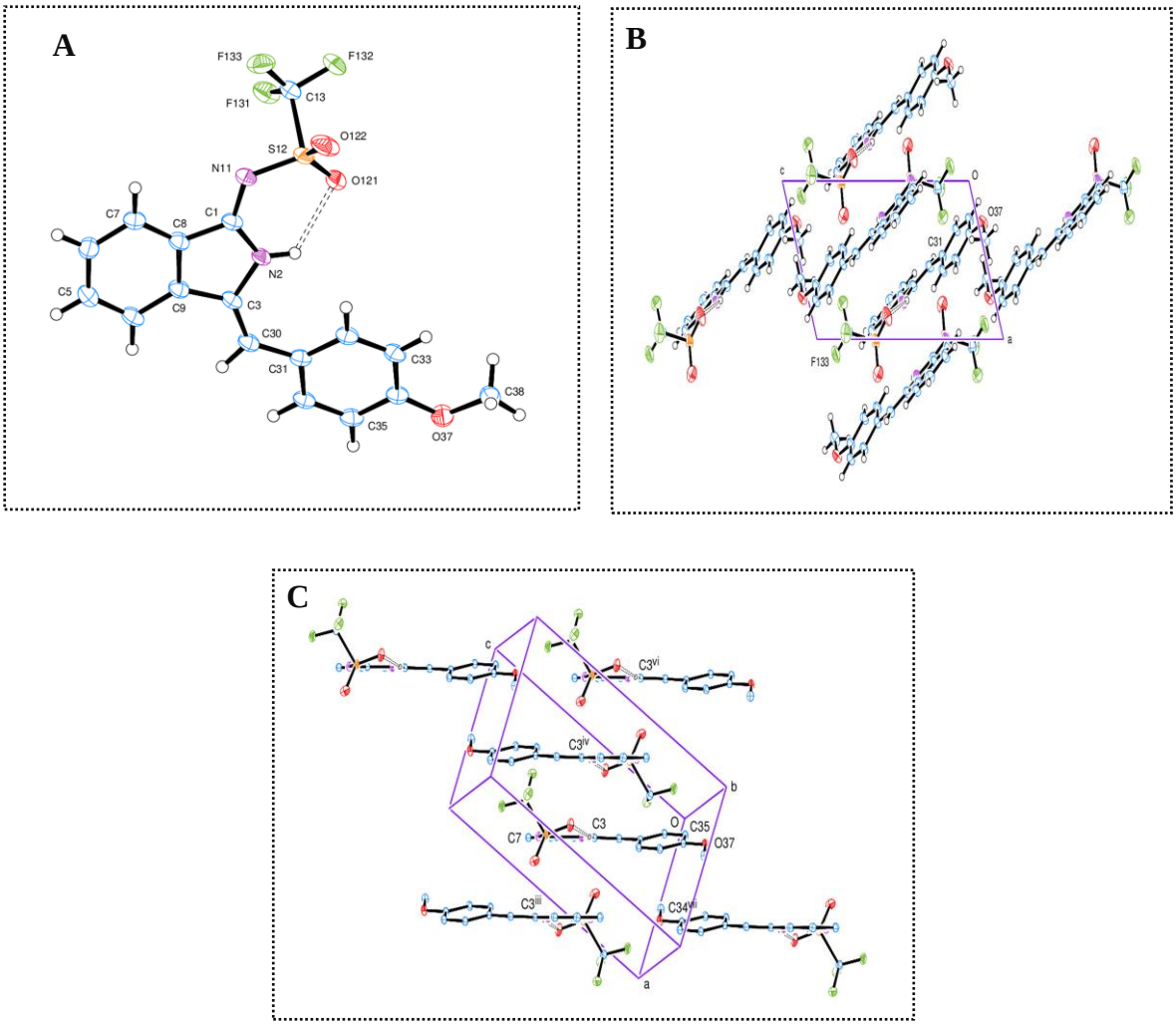

Figure 2.29: X-Ray structure for compound **165**.

Therefore, to detect whether the triflate group would be removed under the dimerisation condition, compound **165** was examined by refluxing in toluene at 120 °C, and TLC showed no dimerisation reaction had occurred. So, compound **154** was added to the solution, after 24 h unsymmetrical dimer **161** was isolated in 64 % yield (Scheme 2.36). The increase in the unsymmetrical outcome indicates that the triflate group is a better leaving group than the tosylate.

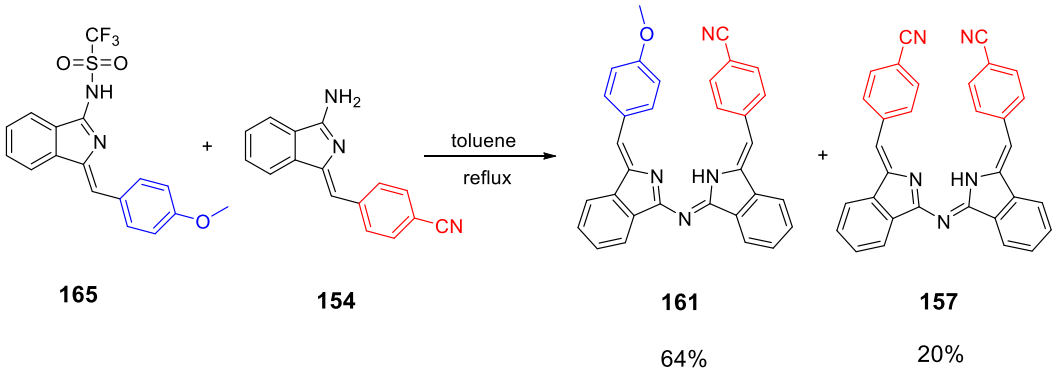

165 **154** **161** 64% **157** 20%

Scheme 2.36: Synthesis of unsymmetrical aza (dibenzo) dipyrromethene (ADBDP) **161** from triflate aminoisoindoline **165**.

Table 2.4 summarises the reactions carried out using this synthetic procedure and the resulting yields of the symmetrical and unsymmetrical aza dipyrromethenes using tosylate and triflate aminoisoindolines. In terms of comparing the resulting yield of the unsymmetrical dimer **161** in both reactions, the one using the 4-methoxy phenyl aminoisoindoline triflate showed an increase of 14 % compared to the tosylate. However, there was not much difference in the yield observed when 4-methoxyphenyl aminoisoindoline **81** was condensed with 4-pentaloxy phenyl aminoisoindoline, either with tosylate group or the triflate group, which indicates that they have almost equal influence. Also, the reactivity of the aminoisoindolines with electron donating substituents on the phenyl ring led to the self-condensation of the 4-alkoxy phenyl aminoisoindolines, producing the symmetrical 4-alkoxy aminoisoindoline dimers in a convergent yield.

Reactant 1	Reactant 2	Solvent & time	Result 1	Result 2	Results3
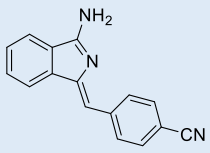 **154**	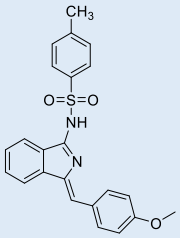 **163**	toluene, reflux, 24 h	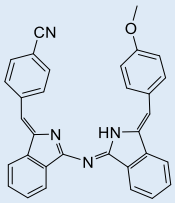 **161** 50 %	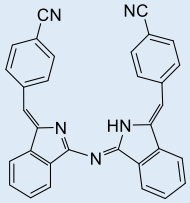 **157** 24 %	unreacted **163** 17 %, and **154** traces
	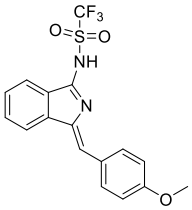 **165**	toluene, reflux, 24 h	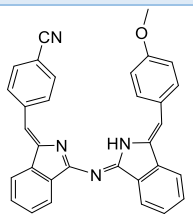 **161** 64 %	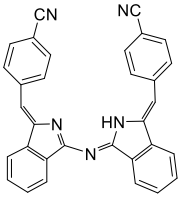 **157** 20 %	unreacted **165** 15 %, and **154** traces
	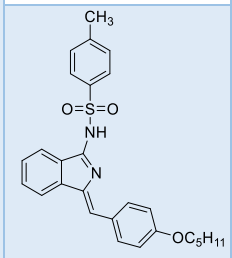 **164**	toluene, reflux, 24 h	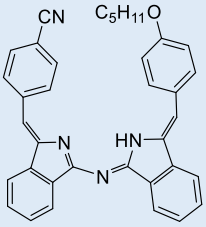 **162** 49 %	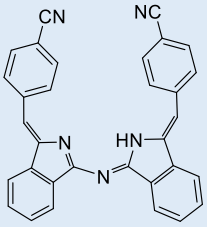 **157** 23 %	unreacted **164** 17 %, and **154** traces
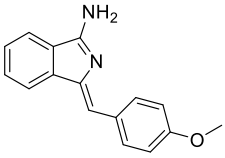 **81**	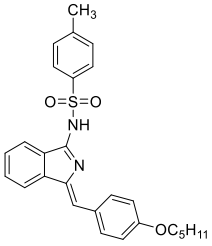 **164**	toluene, reflux, 24 h	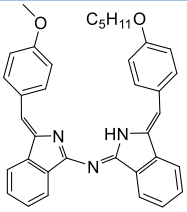 **160** 51 %	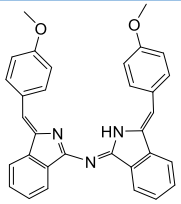 **83** 41 %	traces of the SMs
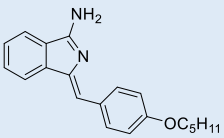 **138**	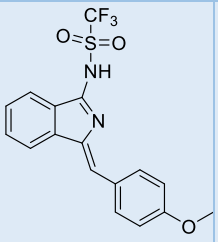 **165**	toluene, reflux, 24 h	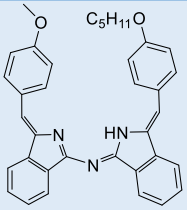 **160** 49 %	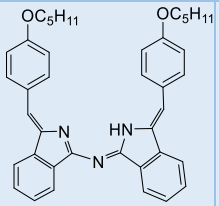 **156** 39 %	traces of the SMs

Table 2.4: Summary of the formation of unsymmetrical aza dipyrromethenes using tosylate and triflate aminoisoindolines.

2.7 Complexation of symmetrical and unsymmetrical aza (dibenzo) dipyrromethenes (ADBDPs) using boron trifluoride diethyl etherate.

Previously, our group had isolated aza BODIPY-OPh **168** as a side product during the formation of the Sub-TBDAP hybrids **166** as shown in Scheme 2.37. This one pot reaction was done in two steps, the first step was by refluxing of phenyl methylene aminoisoindoline **80** with phthalonitrile in the presence of BCl_3 as the boron template for the macrocyclisation process, in p-xylene for 3 h. In the next step, the B-Cl fragment was replaced with stable B-OPh moieties by adding excess of phenol to the reaction vessel.[109] In this reaction aza BODIPY-OPh **168** was isolated as a side product, the major product was SubPc-OPh **167**, while the target boron subtribenzodiazaporphyrin (SubTBDAP) **166** was obtained as pink-red solid in 15 % yield.[109]

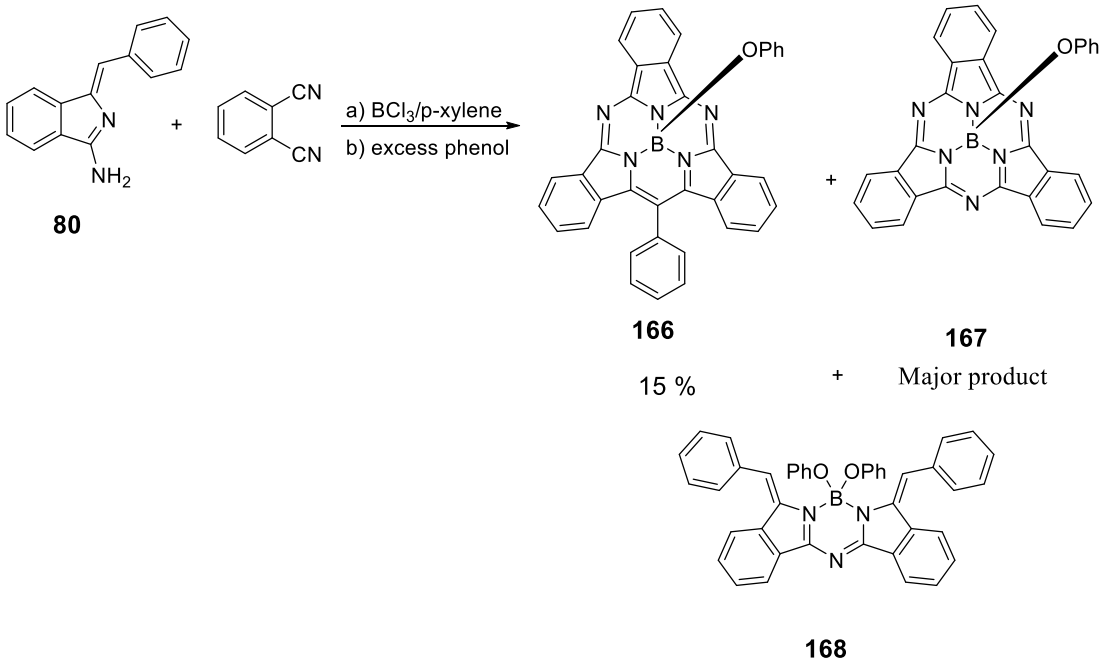

Scheme 2.37: Formation of aza BODIPY-OPh **168** as a side product during synthesis of Sub-TBDAP hybrids.[109]

Our group were able to control synthesis of aza BODIPYs-OPh compounds in one single reaction step, by irradiating aminoisoindoline derivatives and triphenyl under microwave in p-xylene at 220 ℃ for 1 h. High temperature was required to stop the equilibrium formed between the dimer (boron free), and the desired product (boron complex) **168**, and to allow aminoisoindoline **80** to fully convert to the target aza

BODIPYs. Following this synthetic pathway, compounds **168** and **170** were isolated as either yellow solid in 41 % yield or a red solid in 14 % yield respectively (Scheme 2.38).[110]

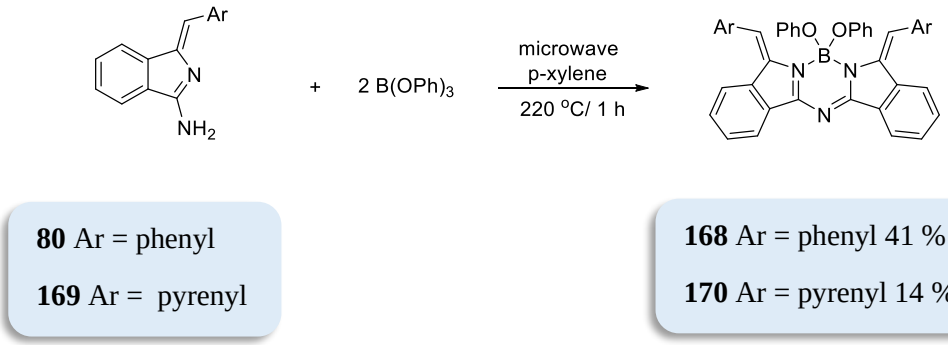

80 Ar = phenyl

169 Ar = pyrenyl

168 Ar = phenyl 41 %

170 Ar = pyrenyl 14 %

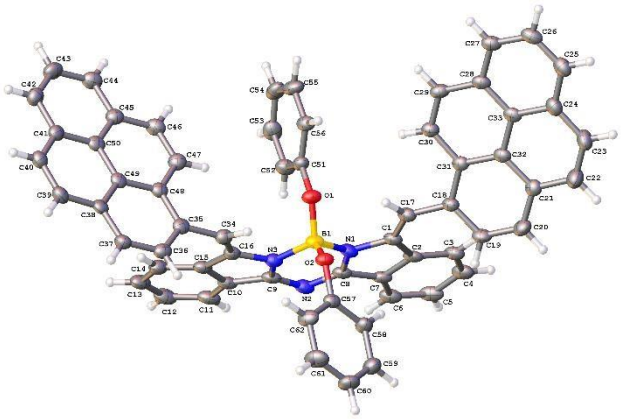

Scheme 2.38: Synthesis of aza BODIPYs-OPh compounds **168** and **170** under microwave irradiation, and X-ray crystal structure of compound **170**.[110]

Our group has isolated compound **168** as a single isomer with *E, E* configuration, this assignment was strongly supported by ^{1}HNMR spectrum which demonstrated a set of signals for a single compound with a singlet peak referring to the alkene proton at 8.36 ppm. Also, ^{11}B-NMR spectrum showed one singlet at 2.34 ppm confirming presence of one single isomer. In contrast they isolated compound **170** as a mixture of isomers, this indication was based on the ^{1}H-NMR spectrum which showed two different sets of signals, and the ^{11}B-NMR showed two singlets at 2.76 ppm and 1.80 ppm, this strongly supported presence of two isomers, they favoured the *E, E* configuration in a ratio (4:1). Eventually, crystals were grown from 1:1 DCM and MeOH as the crystallisation system, producing suitable crystals for X-ray diffraction demonstrating the *E, E* configuration (Scheme 2.38 inset). Therefore, the reaction was repeated following a

similar microwave condition at 180 ºC with 4-methoxy phenyl methylene aminoisoindoline **81** as the starting material. TLC after 1 h showed two major spots. The first spot was orange in colour, and it was suspected this to be the boron complex. The other was red and refers to the dimer **83** (reference was available from previous preparation). The reaction was left longer in order to give it more chance to be completely consumed, but the reaction was not completed even after 8 h reflux. Then the mixture was cooled down, and PhOH was added, to prove the equilibrium, and drive the reaction back toward the dimer **83**. As we expected, after 1 h reflux, TLC showed two red spots very close to each other referring to the dimer isomers, and the orange spot had disappeared.

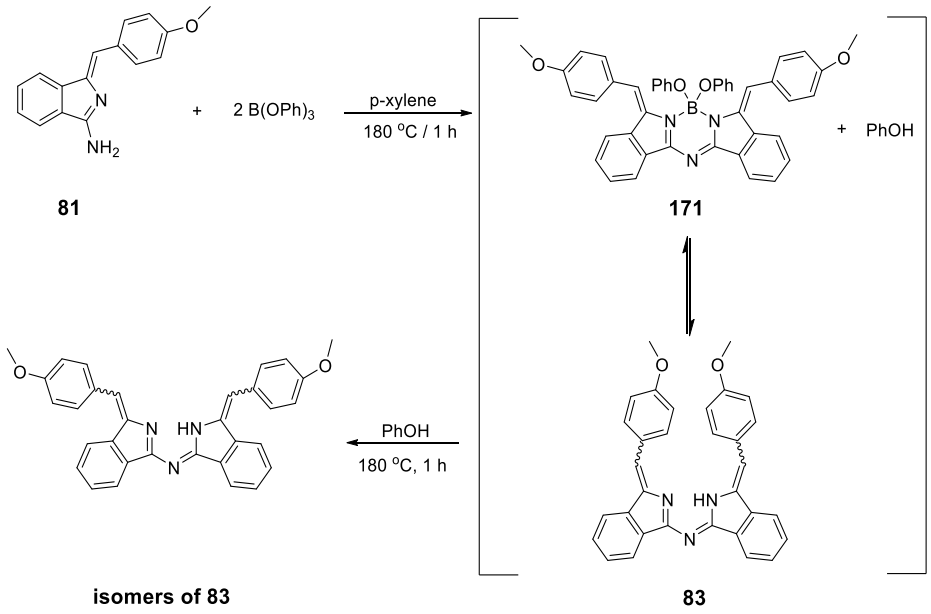

Scheme 2.39: Clarification of the chemical equilibrium between compounds **83** and compound **171**.

Complexation of aza (dibenzo) dipyrromethenes (ADBDPs) with $BF_3.OEt_2$ is more common, and our group has synthesised aza BODIPYs derivatives by straightforward synthetic procedure.[41] Compounds **82** and **83** were converted into corresponding aza-(dibenzo) BODIPYs in the presence of $BF_3.OEt_2$ as boron source, and TEA as a base in dry DCM, producing the desired corresponding boron complexes **84** and **85** in moderate yield as mentioned previously (Scheme 2.40).[41]

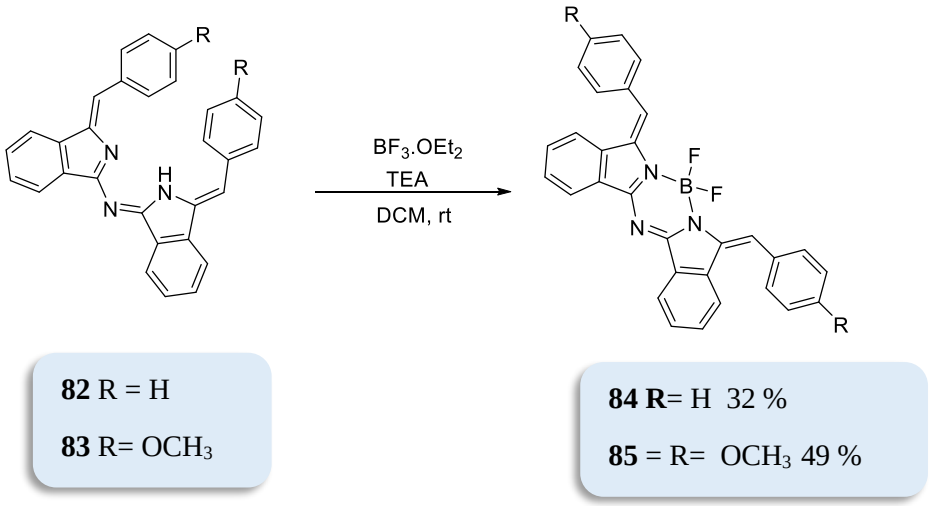

82 R = H

83 R= OCH_3

84 R= H 32 %

85 = R= OCH_3 49 %

Scheme 2.40: Synthesis of aza (dibenzo) BODIPYs **84** and **85**.[41]

Aza (dibenzo) BODIPYs **84** and **85** were isolated as single products displaying *E*, *E* configuration in the solid state. However, they are prone to isomerisation in solution producing a mixture of stereoisomers in the equilibrium reaction as mentioned in the introduction chapter.[41] Accordingly, to start the investigation to improve the resulting yield and expand in the formation of different derivatives of aza BODIPYs, the reaction was repeated with 3-methoxy phenyl methylene ADBDP **155** as the starting material. Compound **155** was stirred in dry DCM in the presence of DBU or TEA as a base, followed by the dropwise addition of $BF_3.OEt_2$. The reaction was kept stirring under N_2 for 24 h. The product formed was clearly observed on the TLC after adding excess of $BF_3.OEt_2$ along with a major quantity of starting material. After the work up compound **172** was isolated in 40 % yield. Leaving the reaction for more than 24 h and increasing the temperature up to 50 ℃ did not help to improve of conversion of the starting material to the target product, which in turn caused a challenging isolation and resulted in low yield. The suggestion is that there is an equilibrium between the starting material **155** and the resulting boron complex compound **172**. To investigate the equilibrium, tetrabutylammonium fluoride hydrate as the fluoride ion source was added to the pure sample of the compound **172**, it was observed that the aza BODIPY **172** was destroyed very quickly, and TLC shows mixture of multiple red spots with none of them matching compound **172**. However, the ^{1}HNMR spectrum indicates a complex mixture, possibly of stereoisomers that might be formed as a result of removing of BF_2 from compound **172**. Thus, this did not investigate further, because the key result (ion fluoride F^- reacts with the aza BODIPY) was conclusive. However, adding excess of BF_3 had negligible effects, so a strategy to remove the formed fluoride ion from the reaction to drive the

equilibrium towards the desired aza BODIPYs was required. It was suggested that replacing boron fluorine B-F with silicone fluorine Si-F which has greater bond energy than B-F (Si-F > B-F), the difference in these energies might shift the equilibrium towards the desired product i.e., fluoride ion could be remove from the equilibrium. Therefore, it was decided to investigate the treatment of fluoride ion with a suitable silane reagent, trimethylsilyl chloride (TMS-Cl) was chosen due to its availability and its ability to remove the fluoride ion, producing trimethylsilyl fluoride as described in Scheme 2.41. To examine this strategy, the synthesis of compound **172** was repeated following the standard procedure, and after 24 h the orange spot had appeared on the TLC along with a major red spot corresponding to the starting material. Then TMS-Cl was added to the reaction mixture. TLC was monitored and after 8 h and no dimer was observed. As we expected, adding of TMS-Cl helped to shift the equilibrium towards the target product giving the single orange spot with improved outcome. Compound **172** was isolated as orange crystals in 73 % yield. Warming the reaction mixture up to 50 °C successfully assisted to reduce the conversion period time, producing the desired product after 3 h. This procedure was adopted for all subsequent BF_2 complexations.

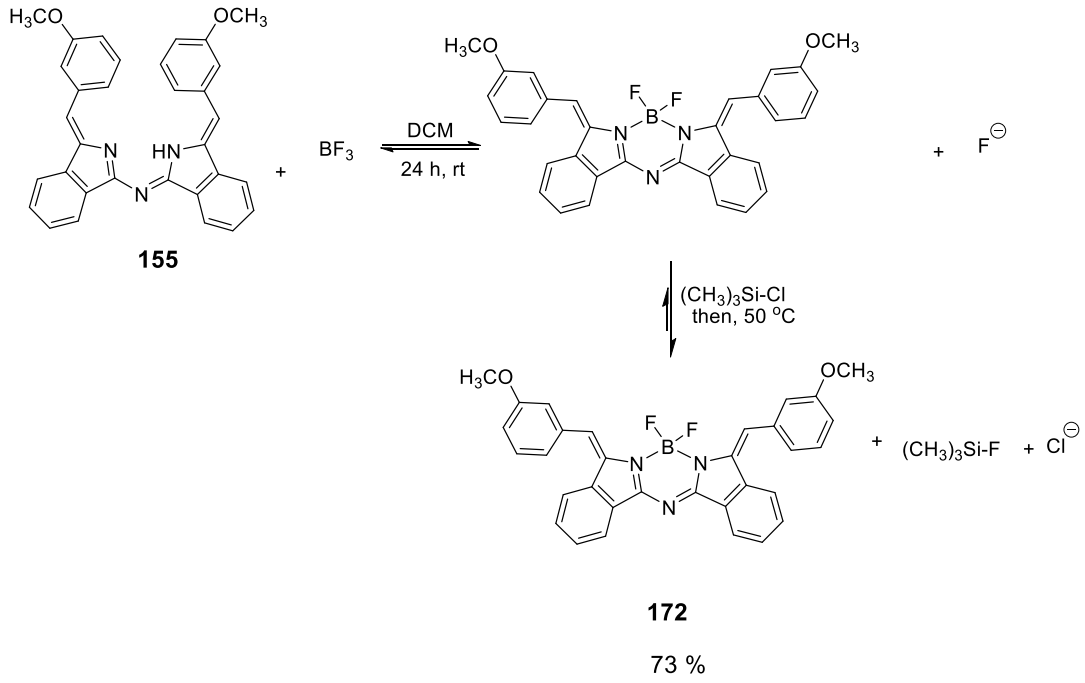

Scheme 2.41: Optimized synthesis strategy towards aza BODIPYs.

Isolation and characterization of aza (dibenzo) BODIPYs analogues proved more complicated than their precursors. Nonetheless their crystals were finally grown from 1:1 DCM:PE as orange crystals in good yield (73 %). This issue might be because these compounds were prone to isomerisation in solution at room temperature which led to

the observation of a mixture of *E* and *Z* isomers. The ^{1}H-NMR spectrum proved initially one molecular type corresponding to the *E, E* configuration. However, when these compounds remain in solution, isomerisation occurs at room temperature leading to the formation of a mixture of *E* and *Z* isomers after a few hours. This suggests that the *E, E* configuration is favoured solely by the crystal packing and solid-state interactions.[41] Figure 2.30 illustrates the ^{1}H-NMR and ^{19}F-NMR spectrum of compound **172**, and it shows a singlet corresponding to the alkene proton at 7.8 ppm which confirmed the *E, E* configuration, the other singlet corresponding to the proton on the phenyl ring at 7.14 ppm is labelled *. Protons on the phenyl and benzene rings appeared as expected at the range from 8.21 ppm - 6.97 ppm. The methoxy group protons appeared as a singlet peak at 3.8 ppm. ^{19}F-NMR spectrum strongly supported the presence of the fluorine linked with boron compound in the structure, the ^{19}F-NMR signal appeared around -139 ppm.

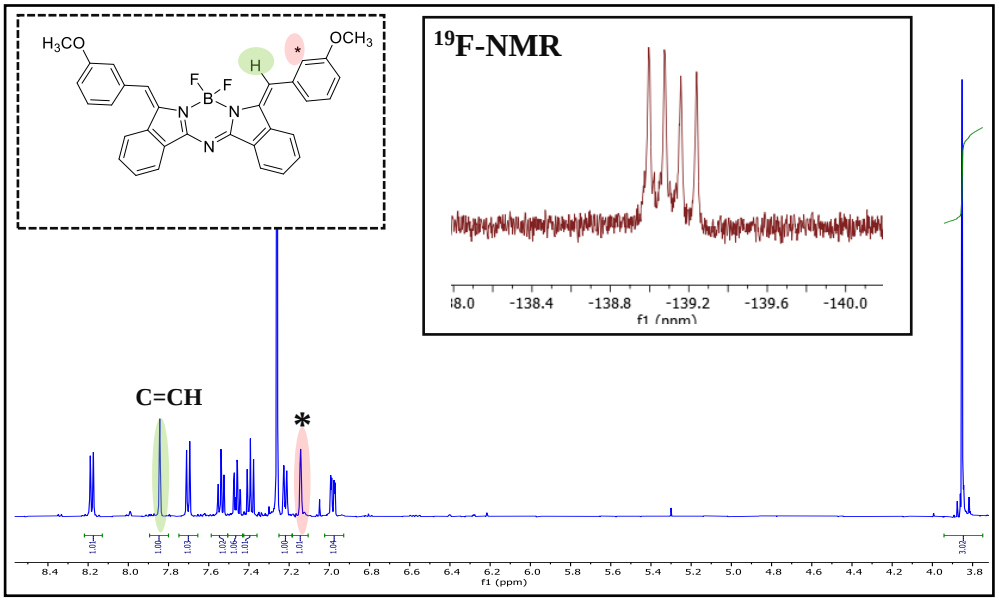

Figure 2.30: ^{1}H-NMR and ^{19}F-NMR spectrum of compound **172**.

Aza (dibenzo) BODIPYs derivatives **173, 174, 175, 176** and **177** were synthesised following the same synthetic procedure, and were fully characterised by ^{1}H-NMR,^{13}C-NMR, ^{19}F-NMR spectroscopy and MALDI-TOF mass spectrometry to confirm the structures. Table 2.5 outlines the aza BODIPY compounds obtained and the resulting yield.

aza BODIPY compounds	Yield %
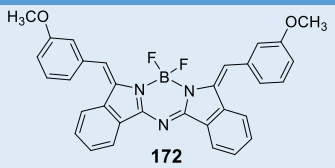 **172**	73 %
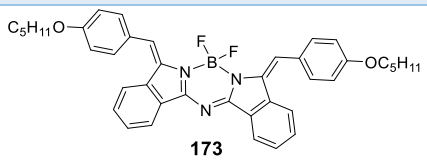 **173**	74 %
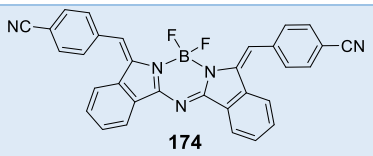 **174**	73 %
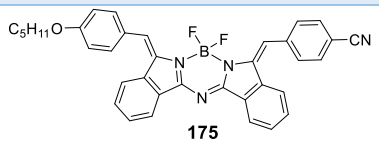 **175**	70 %
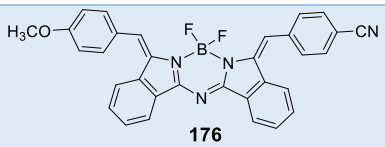 **176**	71 %
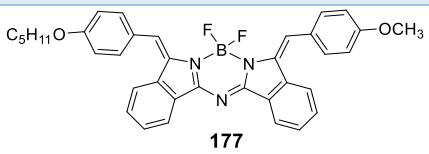 **177**	72 %

Table 2.5: Summary for synthesis of aza-BODIPY derivatives.

As mentioned previously, X-ray crystallography confirmed that the *Z, Z* configuration existed in the starting material (ADBDPs). Whilst the corresponding aza (dibenzo) BODIPYs obviously demonstrated the *E, E* configuration which is the opposite configuration.[41] This was supported by ^{1}HNMR spectroscopy with a singlet peak corresponding to the alkene protons around 8.00 ppm as a result of the steric clashes between the aryl groups and the BF_2 in the aza (dibenzo) BODIPYs structures. Both compounds **172** and **174** gave a single crystal suitable for X-ray diffraction analysis and their structures were confirmed to contain the *E, E* configuration as shown in Figure 2.31. These crystals were grown from a mixture of 1:1 DCM:PE. Crystal data and brief description are included in the appendix.

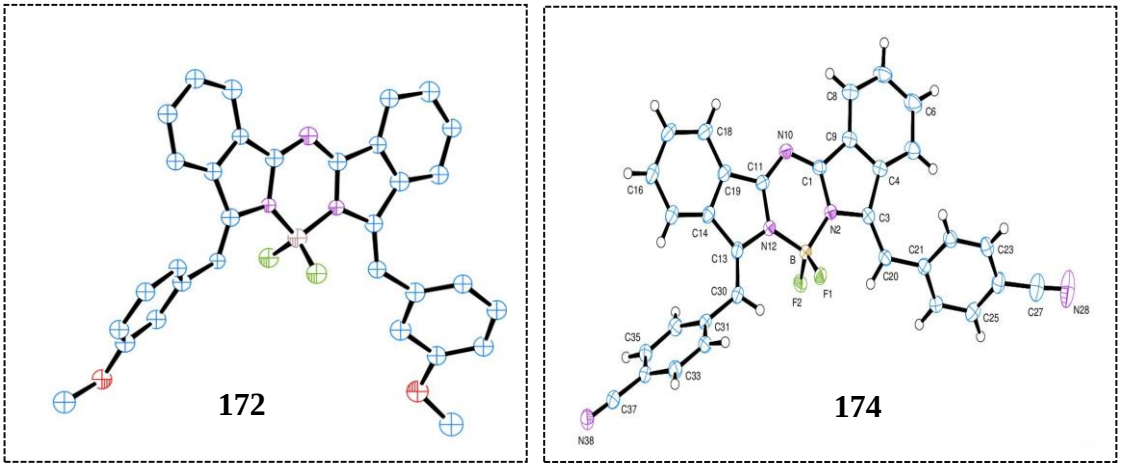

Figure 2.31: X-ray structure for compound **172** and compound **174**.

To clarify the equilibrium reaction between these isomers they were studied by TLC. The freshly obtained TLC of aza (dibenzo) BODIPYs compounds showed a single orange spot corresponding to the *E*, *E* BF_2 complexes, then two new spots were observed after a few hours. The isomerisation was clearly ongoing when 2D TLC was performed. To investigate this, some analyses were carried out on the new major compound formed from **173**. It was separated and analysed by MALDI- TOF mass spectrometry, UV-Visible spectroscopy, ^{1}HNMR and ^{19}FNMR spectrum. All this analysis indicated the presence of BF_2 in the compound. UV-vis spectra showed a similar absorption pattern to the aza (dibenzo) BODIPYs, they displayed two absorption bands at 478 nm and 335 nm (Figure 2.32).

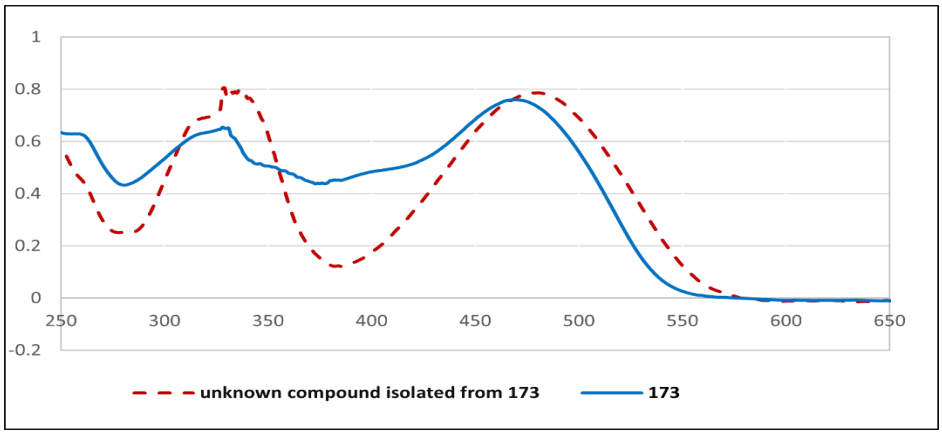

Figure 2.32: UV-Visible spectra for compound **173** and the new compound formed from compound **173.**

Furthermore, ^{19}F-NMR spectrum of this compound showed the fluoride signals as overlapping multiple peaks, indicating formation of isomers of compound **173**. Furthermore, the ^{1}H-NMR spectra for the isolated fraction from compound **173** supported presence of the unsymmetrical *E*, *Z* configuration compound. Figure 2.33

shows two singlets corresponding to the alkene protons at 8.09 ppm, and 7.78 ppm respectively in addition to signals for sixteen aromatic protons at the range from 8.24 ppm - 7.01 ppm. The protons of the methylene group on the pentaloxy chains were found at 4.06 ppm as two overlapping triplets, followed by the set of peaks that appeared at 1.83 ppm, 1.41 ppm and 0.95 ppm with the integration for two pentaloxy chains. After we had evidence that BF_2 is still coupled in these compounds, it underwent recrystallisation again to yield crystals that displayed the *E*, *E* configuration which confirms that there is a reversible isomerisation between these isomers.

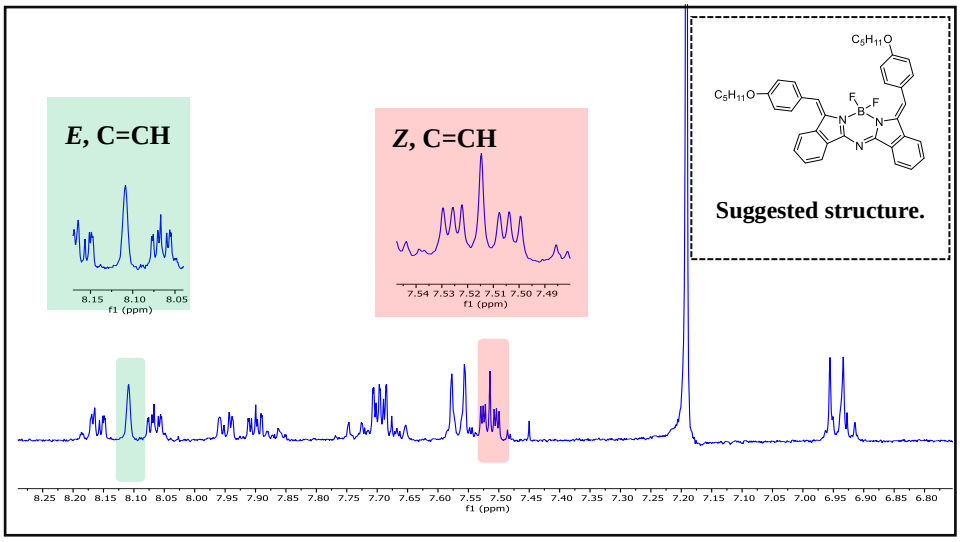

Figure 2. 33: ^{1}HNMR spectrum of the new compound formed from compound **173.**

2.8 Optical properties of symmetrical and unsymmetrical aza BODIPYs and their precursor aza (dibenzo) dipyrromethenes (ADBDPs).

Figure 2.34 shows the UV-Vis spectra of symmetrical and unsymmetrical aza (dibenzo) dipyrromethene compounds in dichloromethane. All aza (dibenzo) dipyrromethenes are red in colour, they displayed three absorption bands in the visible region. Depending on the substitution pattern, the absorption ranged from 477 nm for compound **155** to 508 nm for compound **162**. There was slight difference (around 14 nm) in the absorption of compounds 1**55** when the methoxy group is located on the *meta* position compared with compound **83** with methoxy group on the *para* position, they displayed 477 nm and 491 nm respectively. However, introduction of electron withdrawing substituent (nitrile group) on the *para* position **157** exhibits absorption at 492 nm which is identical

absorption to compound **83**. Further conjugation applied by entering of 4-pentaloxy substituents on the *para* position compound **156** red shifts the absorption by around 14 nm compared to compound **83**. On the other hand, unsymmetrical aza (dibenzo) dipyrromethene compounds **160**, **161** and **162** show absorption maxima at 500 nm, 495 nm and 508 nm, respectively and this indicates that electronic properties of the substituent groups (electron withdrawing or electron donating) on the aza dipyrromethene units have similar effect on the absorption as seen in Figure 2.34.

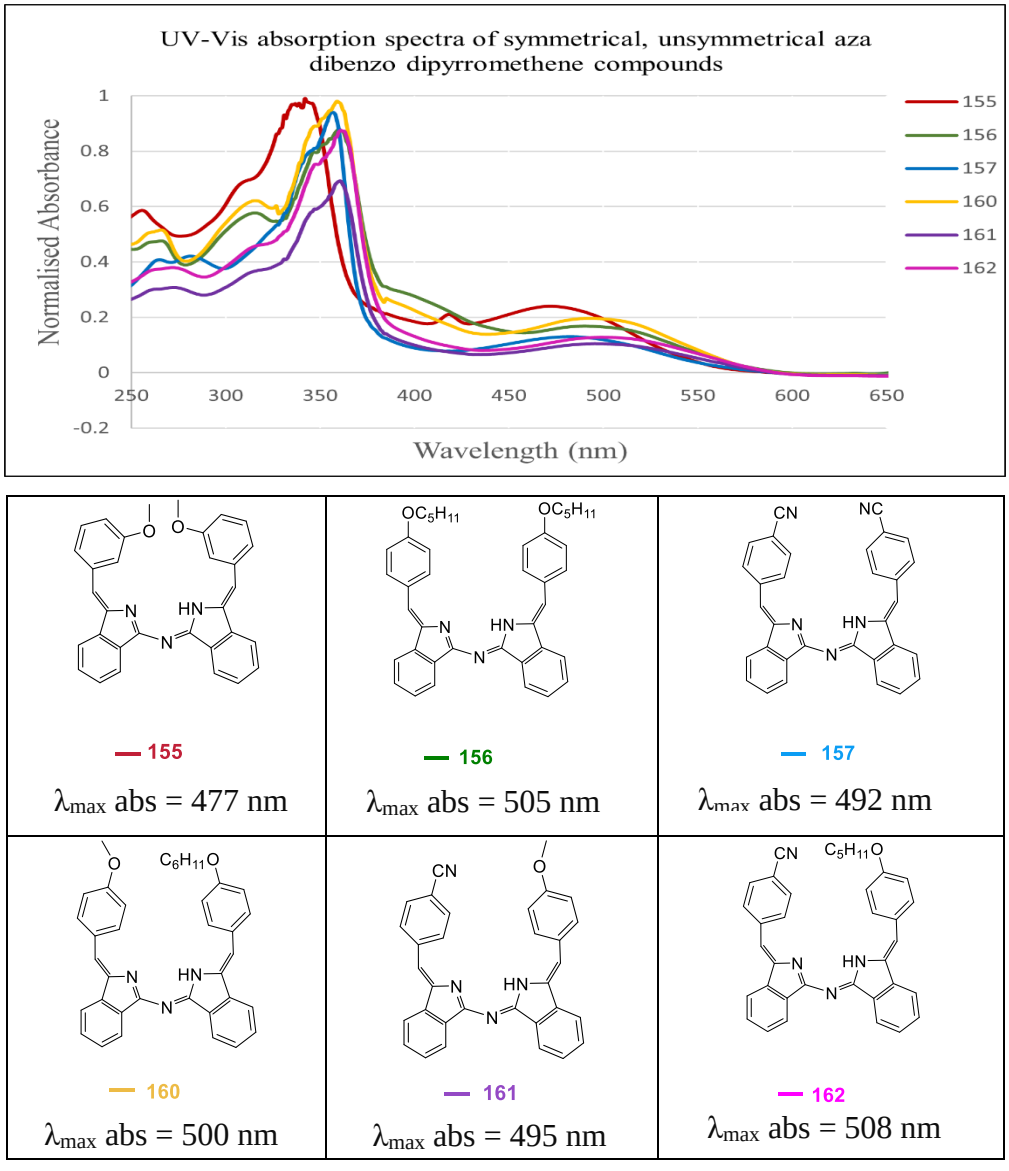

Figure 2. 34: UV-vis spectra of symmetrical, unsymmetrical aza (dibenzo) dipyrromethene compounds.

Boron difluoride complexes are orange in colour, they showed two absorption bands in the visible region at 321 nm - 330 nm and 441 nm - 475 nm. Figure 2.35 demonstrated the absorption, emission and excitation spectra of aza (dibenzo) BODIPYs compound

172, the emission band in this molecule shown at 523 nm after excitation at 445 nm, these features give significant Stokes Shift of around 78 nm.

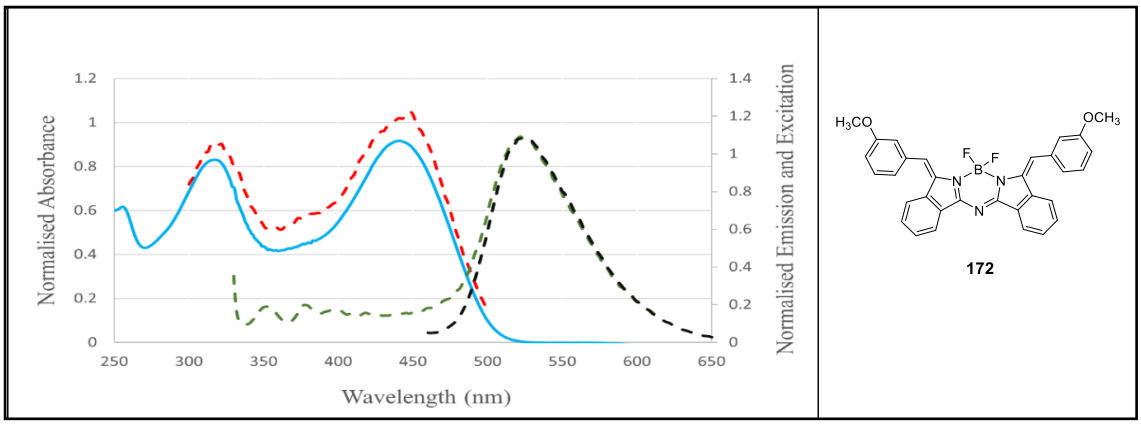

Figure 2. 35: Normalized UV−Vis absorption (blue solid line) and fluorescence emission (black and green dotted line) and the excitation spectrum spectra (red dotted line) of **172** in DCM.

Figure 2.36 shows a comparison between the symmetrical aza (dibenzo) BODIPYs **173**, **174** and unsymmetrical aza (dibenzo) BODIPYs **175**. Compound **173** and **174** display absorption maxima at 475 nm, 441 nm respectively and fluorescence with Stokes shifts of 86 nm. This indicates that in case of introduction of further conjugation of electron donating substituents (4- pentaloxy group) **173**, red shift the absorption to around 35 nm compared with the molecule with electron withdrawing substituents (4- nitrile group) **174**. While unsymmetrical compound **175** exhibits emission at 567 nm upon excitation at 465 nm, and Stokes Shift of 102 nm which demonstrated the electronic effects donor and acceptor substituents on the absorption. In general, the observed Stokes shift in the series are larger than typically found for the BODIPYs (10-30 nm).[111]

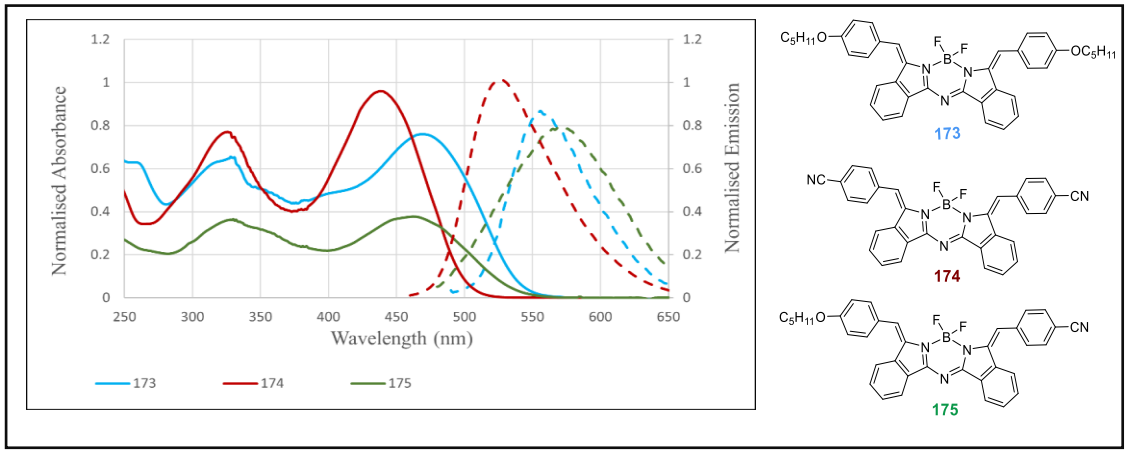

Figure 2.36: Normalized UV−Vis absorption (solid line) and fluorescence emission (dotted line) of compound **173**, **174**, and **175** in DCM.

2.9 Oxidative cyclisations to give fused and/or macrocyclic aza (dibenzo) dipyrromethenes system

Two strategies were investegated to modify the properties of aza (dibenzo) dipyrromethene (ADBDP) materials. The first strategy is π extension (fusion) that is expected to shift the absorption/emmission to longer wavelength. The second strateg is oxidative coupling leading to rigid macrocycles (Scheme 2.42)

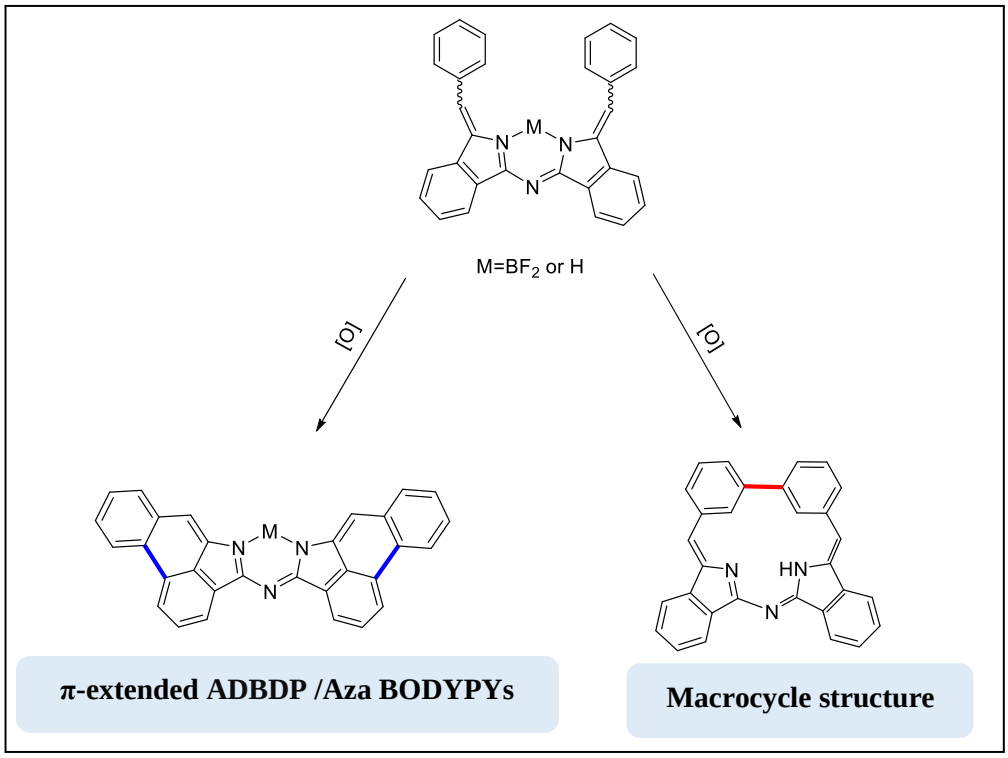

Scheme 2.42: Proposed strategies to extentd π conjugation in the aza (dibenzo) dipyrromethens (ADBDP) and aza BODIPYs unit.

As mentioned in the introductory chapter, there have been examples published recently in the literature of ring fused aza-BODIPYs that are synthesised by oxidative aromatic coupling. One example is shown in Scheme 2.43, 10 equivalents of iron(III) chloride with nitromethane (CH_3NO_2) in dry DCM were reacted with aza BODIPY **95a**, and this straightforward reaction was regioselective, producing [b] fused aza BODIPY **96a** in excellent yield, and no [c] fused aza BODIPYs was observed. The modified structure leads to more than 100 nm red-shift in both absorption and emission.[78]

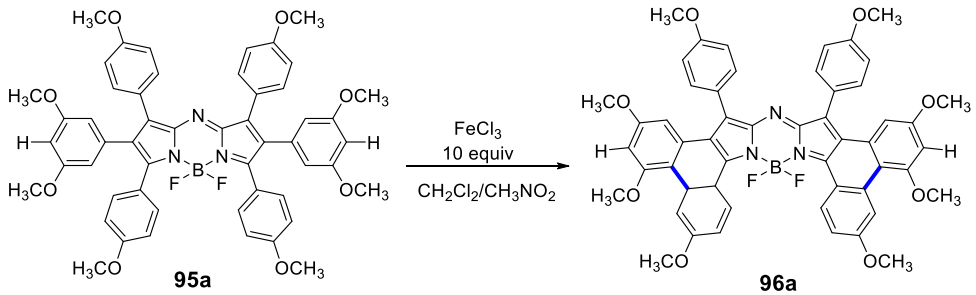

λ_{max} abs = 683 nm

λ_{max} em = 716 nm

λ_{max} abs = 804 nm

λ_{max} em = 816 nm

Scheme 2.43: Synthesis of benzo fused aza BODIPY **96a**.[78]

Accordingly, investigation of the ring fused aza (dibenzo) BODIPYs by oxidation reaction was carry out using aza (dibenzo) BODIPY **172** that was available from previous synthesis. Compound **172** was selected, due to presence of the methoxy group on the *meta* position in the phenyl ring that is expected to dierct the coupling to produce the desired fused aza BODIPY compound **178**. Compound **172** was treated with 10 equivalents of $FeCl_3$ in dry DCM. The mixture was stirred at room temperature and monitored by TLC over 24 h. Since no reaction occurred an excess of $FeCl_3$ (more 10 equivalents) with CH_3NO_2 in DCM were added. Unfortunately, this did not produce the corresponding fused ring system, and then starting material started to isomerise in the solution. Then a photocyclisation reaction was performed in the presence of iodine as an oxidant, but no effect was seen through TLC or in the ^{1}HNMR spectroscopy even after a powerful UV light was applied to compound **172** (Scheme 2.44). The main suggested reason that prevents the oxidative coupling to occur is the BODIPY unit might be behaving as an electron poor group.

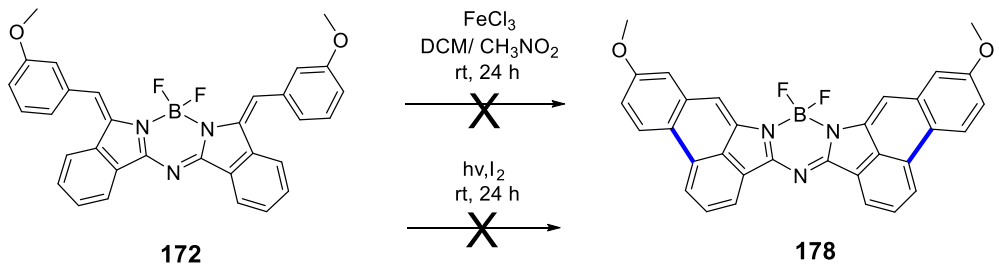

Scheme 2.44: Synthesis attempts for compound **178**.

2.9.1 Macrocycle formation attempts from aza dipyrromethene derivatives.

2.9.1.1 From 4-methoxy phenyl methylene aza dipyrromethene compound 83

The first attempt towards formation of the macrocycle structure **179** was by treating of 4-methoxy phenyl methylene aza dipyrromethene **83** with iron(III) chloride in dry DCM. Compound **83** was selected due to presence of the methoxy group on the *para* position that is expected to direct the coupling to the right position producing the closed structure **179**. Unfortunately this was unsuccessful to produce the target compound, the starting material appeared to remain unreacted.

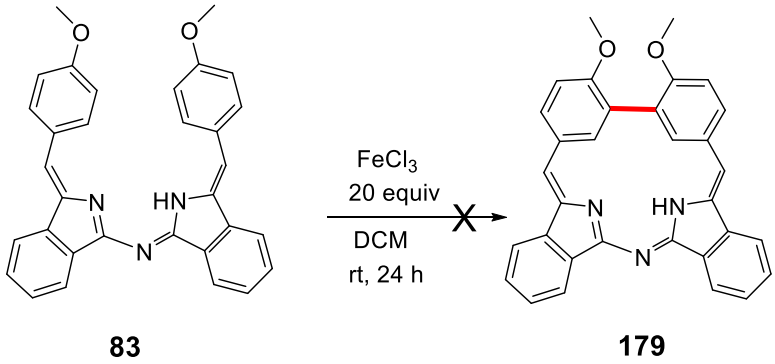

83 **179**

Scheme 2.45: Synthesis attempts for compound **179**.

2.9.1.2 From 3-methoxy phenyl methylene aza dipyrromethene compound 155

Formation of the macrocycle compound **182** from the precursor 3-methoxy phenyl methylene aza (dibenzo) dipyrromethene compound **155**, was one of the targets. Compound **155** was chosen due to the possibilities of direct coupling of the phenyl rings to produce the closed structure **182**. It was reasoned this could be achieved following three steps, starting with demethylation of the compound **155**, followed by converting the hydroxy group into the triflate producing the corresponding compound **181**. Homocoupling in the last step (macrocyclisation step) would lead to the desired macrocycle structure **182**. Scheme 2.46 outlines the proposed plan toward the desired macrocycle **182**.

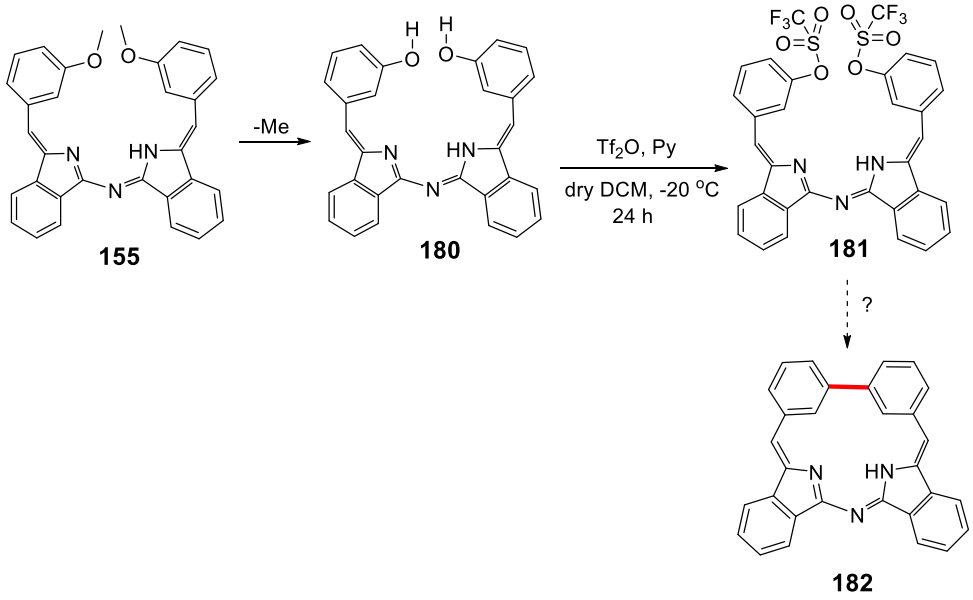

Scheme 2.46: Proposed plan to synthesis of the macrocycle **182**.

To achieve our target, we started with demethylation of the 3-methoxy phenyl aza dipyrromethene compound **155** following the procedure reported by Chakraborti et al.[112] Compound **155** was treated with three equivalents of thiophenol and potassium carbonate in dry DMF at 150 °C for 6 h (Scheme 2.47).

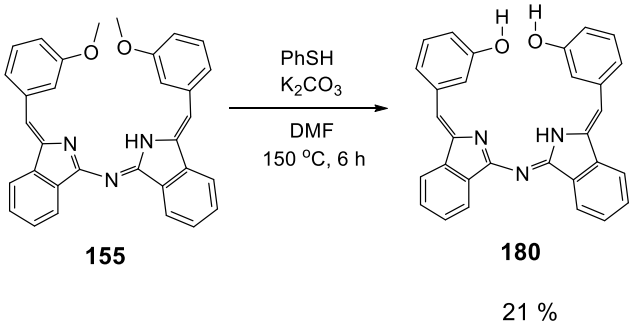

Scheme 2.47: Demethylation of compound **155**.

The reaction was monitored by the ^{1}HNMR until the singlet peak of the methoxy group had disappeared, then it was quenched by washing the mixture with water and extracted with ethyl acetate. The resulting mixture was analysed by MALDI-TOF mass spectrometry, which showed three ion peaks (Figure 2.37). The peak at *m/z* 457 indicates formation of the desired product compound **180**, while the other peak at *m/z* 471 we expected this an indication of partial demethylation occurring at one methoxy

group producing the unsymmetrical dipyrromethene **183**. The third peak observed appears at *m/z* 699 and it was suggested this could be correspond to the formation of TBDAP-OH molecule, this was noticed as well during the separation of aza dipyrromethene derivatives as mentioned before (Figure 2.37 **A**). The crude mixture was separated by column chromatography. The desired product **180** was isolated in low yield, in addition to trace amounts of a green fraction with *m/z* 699. No further analyses were performed for this fraction due to the poor isolated yield < 3 % (Figure 2.37 **B**).

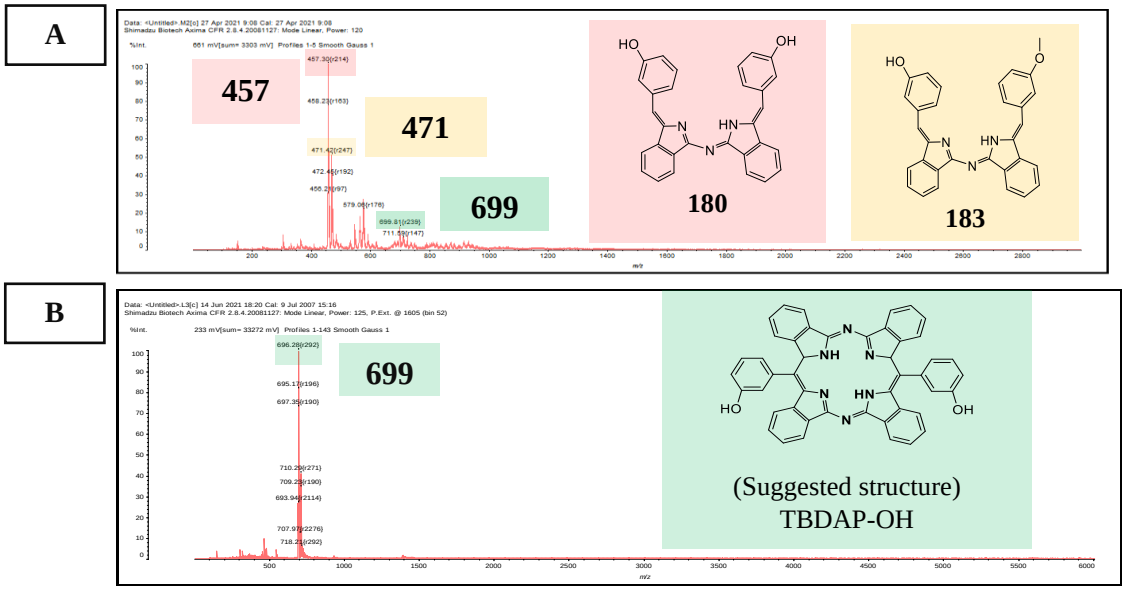

Figure 2. 37: MALDI-TOF obtained from demethylation of compound **155** following Chakraborti precedure.

This was studied further to clarify what was occurring in this reaction. The starting material **155** was refluxed in DMF at 150 °C and after 2 h the TLC was checked and revealed just the starting material. Then 1.2 eq of $MgBr_2$ was added to the reaction mixture to investigate if there was a possibility for the formation of any macrocycle compounds. The reaction was monitored by TLC, but no macrocycle was observed even after adding excess $MgBr_2$ and leaving the reaction longer. This was not surprising as our group had investigated before that the aza (dibenzo) dipyrromethenes do not lead to significant formation of any macrocycle when they were re-subjected to the macrocycle reaction conditions (TBTAPs and Sub TBDAPs) as shown in scheme 2.48.[106, 109]

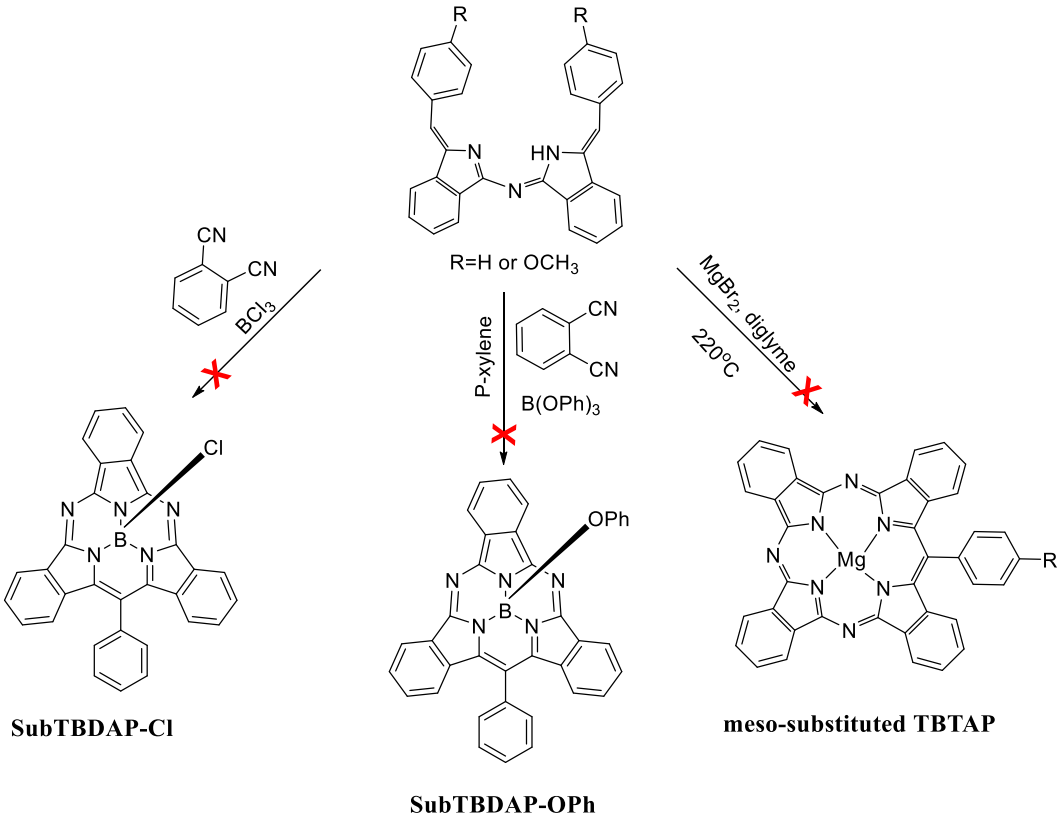

Scheme 2.48: Reaction attempts performed by our group towards the formation of the macrocycle structures.[106, 109]

To control the reaction, and to obtain a better yield of compound **180**, the reaction was repeated starting with 3-methoxy phenyl methylene aminoisoindoline **137**. Compound **137** was reflux in DMF at 150 ℃, once the dimer **155** formed (as observed by TLC) two drops of thiophenol, and K_2CO_3 were added to the reaction mixture, then we continued to heat under reflux at 150 ℃ until the reaction had ceased, as observed by TLC. A large amount of the intermediate dimer **155** was not consumed. The ^{1}HNMR spectrum confirmed formation of the target product **180**. Unfortunately, the yield was very low by using this procedure.

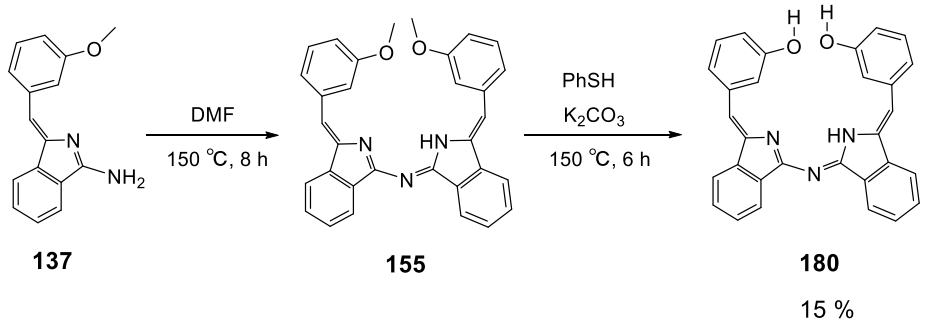

Scheme 2.49: Demethylation of compound **188** starting with compound **137**.

Since this procedure did not give reasonable yield of compound **180**, another demethylation reaction was explored, using boron tribromide in DCM.[113] Due to its availability from previous synthesis, the 4-methoxy phenyl methylene aza (dibenzo) dipyrromethene **83** was used to test the effectiveness of using BBr_3 to deprotect the methyl groups in compound **83**. Unfortunately, most of the starting material remained unreacted, however a new product was formed in this reaction, it was isolated by column chromatography in the trace amount. The characterisation of the isolating compound did not identify compound **184** as expected. It was speculated that the boron might reacted to form the aza BODIPY (the potential structure **185**). This indication was because of the ^{1}HNMR spectra as shown in Figure 2.38. A singlet peak appears at 8.10 ppm corresponding to the alkene protons, this chemical shift indicates the linkage of the boron with the nitrogen atoms in the dimer. A doublet peak at 6.81 ppm (J = 7.2 Hz) integrating to two proton corresponds to protons in the phenyl group labelled **a**, and the further six aromatic protons appeared as a multiplet in the range 7.76 ppm - 7.66 ppm. No methoxy groups were present in the NMR spectrum that indicates that starting material **83** has been successfully demethylated, and also that there is no methoxy group on boron. However, MALDI-TOF mass spectra did not gives any peaks that recognised. At this stage we choice different way to make it.

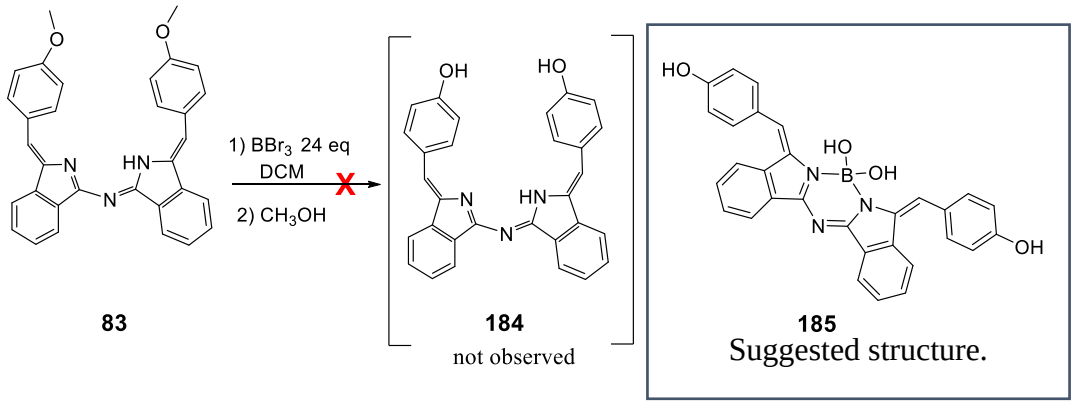

Scheme 2.50: Demethylation of compound **83** using tribromide boron.

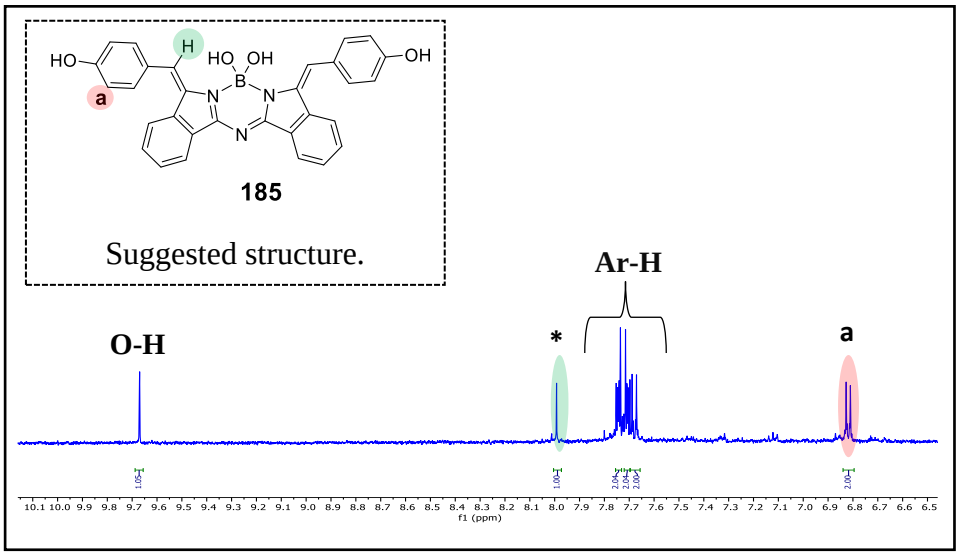

Figure 2. 38: ^{1}H-NMR spectrum of the resulting from demethylation of compound **83** using tribromide boron.

We therefore, turned to synthesis of compound **180** from its precursor 3-hydroxy phenyl aminoisoindoline **187**, following the procedure published by Hellal et al., as explained previously.[75] Using this method compound **187** was synthesised in good yield, followed by a self-condensation reaction in p-xylene at 140 ℃ to produce the desired dimer product **180** in moderate yield.

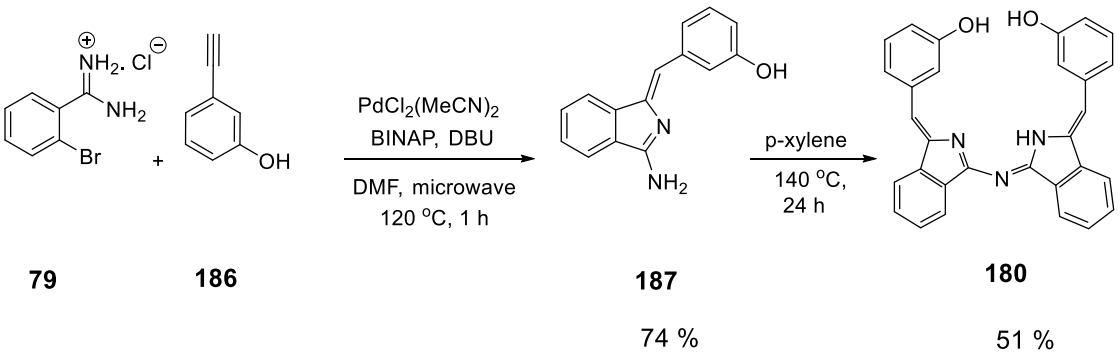

Scheme 2.51: Synthetic routes toward compound **180**.

Figure 2.39 illustrates the ^{1}HNMR spectrum of compound **180**, showing a singlet corresponding to the alkene proton at 7.04 ppm, and a signal corresponding to the proton on the phenyl ring at 7.43 ppm is labelled **a**. Protons on the phenyl and benzene rings appeared as expected at the range from 8.08 ppm - 6.66 ppm.

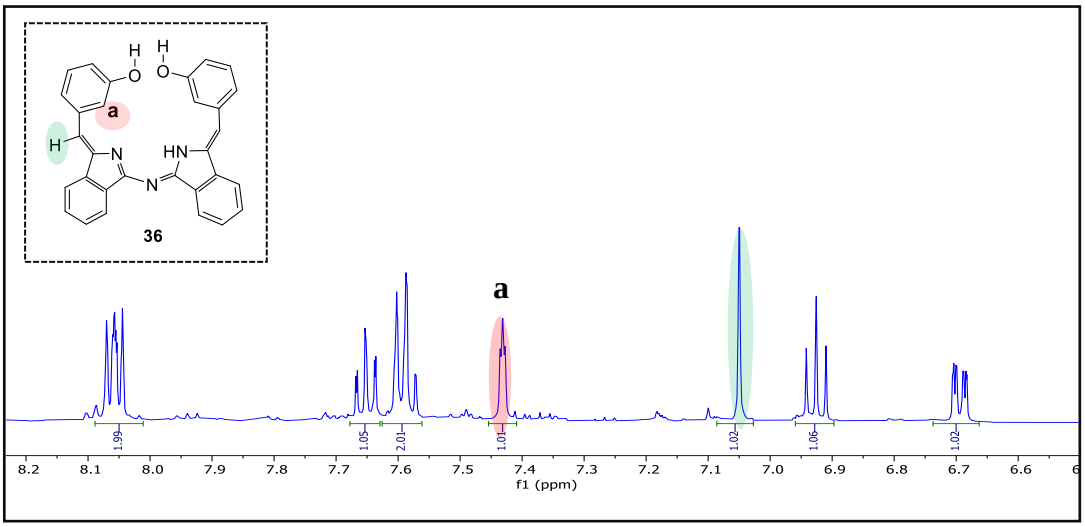

Figure 2. 39: ^{1}H-NMR spectrum of compound **180**.

After successfully producing of compound **180** it was converted to its corresponding triflate by treating with trifluoromethanesulfonic anhydride with pyridine as a base in dry DCM under nitrogen at -20 ºC. Workup was by washing the mixture with water then extracted with DCM. The crude was purified by column chromatography using 1:3 DCM:PE to give the desired product **181** in 24 % yield.

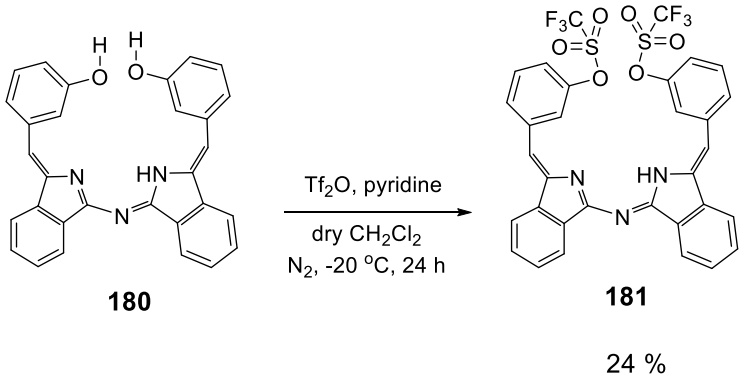

Scheme 2.52: Synthesis of compound **181**.

Figure 2.39 shows the ^{1}HNMR spectrum of compound **181**, it shows a singlet peak at 7.82 ppm for the alkene proton, multiplet peaks appeared at 7.03ppm - 6.94 ppm refer to the phenyl ring protons labelled **a** & **b**. Also, the hydroxyl proton peak in the precursor **180** disappeared from 5.6 ppm. The resulting peak from the MALDI-TOF

mass spectrometry showed peak at *m/z* 717 which corresponds to the product (Figure 2.40 inset).

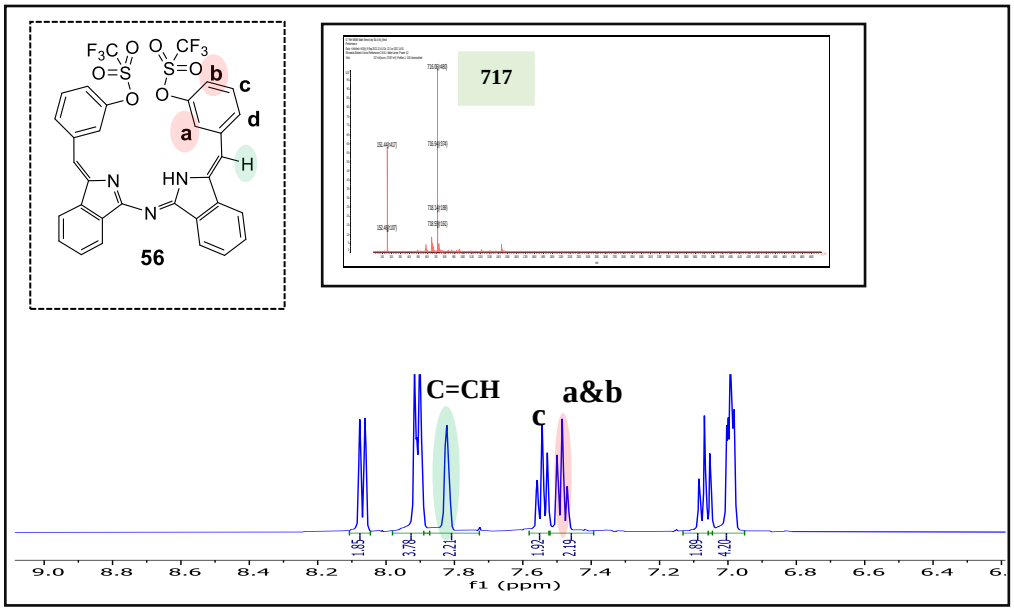

Figure 2.40: ^{1}HNMR spectrum and MALDI-TOF mass spectrum of compound **181**.

According to the literature, conversion of Ar-OTF into Ar-Ar can be achieved by treating of Ar-OTF with catalytic amount of $NiCl_2$.[114] However, at this stage of the project an extended work on these aza (dibenzo) dipyrromethenes revealed a general flaw to our strategy (discussed next). We realised that isomerisation of the alkene occurred in the presence of any metal, and this would prevent homocoupling (macrocyclisation). The reaction was therefore not attempted.

2.9.1.3 From thiophene methylene aza dipyrromethene compound 201

The macrocycle formation from compounds **83** and **155** was not possible, due to the poor yield resulting from the triflation of compound **180,** but mostly the probability of isomerisation by the metal in the last step (macrocyclisation step). An alternative derivative of aza (dibenzo) dipyrromethene was investigated at the same time that could be coupled to give an interesting macrocycle structure. In compound **201** the aryl units are thiophenes and it gives different opportunities for closing the structure, giving fully conjugated macrocycles. Direct oxidative coupling might give a "corrole" type ring system **188**, as shown in Figure 2.41.

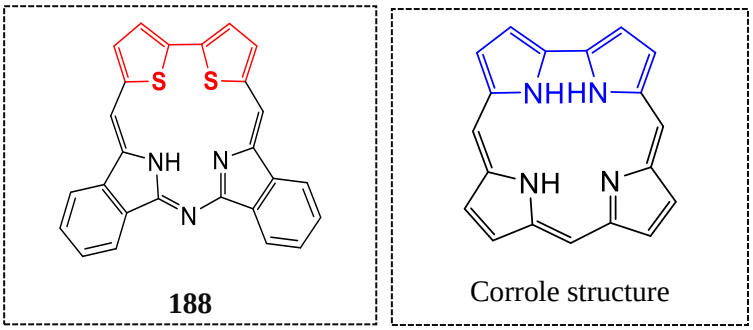

Figure 2.41: Corrole structure and the possible macrocycle structure **188**.

Therefore, it was turned to synthesis of thiophene methylene aza (dibenzo) dipyrromethene **201** from its precursor thiophene methylene aminoisoindoline **200** which was synthesised by following a procedure published by Hellal et al., as explained previously[75] and modified by other members of our group. Here, TMS protected thiophene acetylene is employed in the reaction. Following this procedure, compound **200** was isolated in 76 % yield. Then compound **200** underwent self-condensation reaction in toluene at 120 ℃. After 24 h reflux the solvent was evaporated, and purification achieved by using column chromatography with DCM, to give the desired dimer product **201** in 77 % yield.

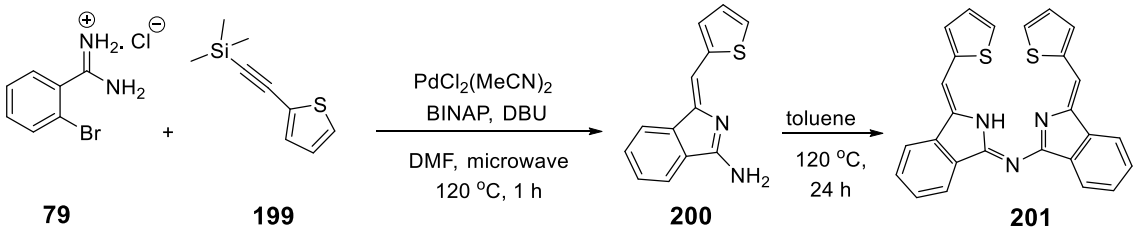

Scheme 2.53: Synthesis of compound **201**.

The ^{1}HNMR spectrum was run in deuterated acetone, and the spectrum obtained proves that compound **201** has successfully formed. A doublet of doublet appeared at 7.05 ppm integrating to one proton (labelled **a**) , in addition to a multiplet appeared at 7.56 ppm integrating to two protons (labelled **b** & **c**) indicating presence of the thiophene ring. The alkene proton appeared as a singlet at 7.32 ppm as expected, the integration of the other peaks matches the benzene and thiophene rings protons as expected (Figure 2.42).

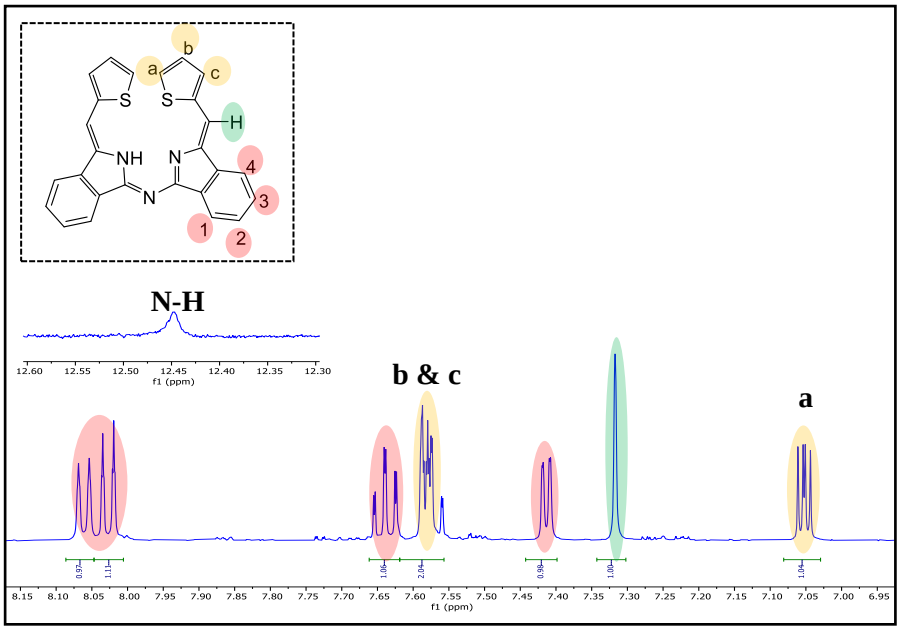

Figure 2.42: ^{1}H-NMR spectrum of compound **201**.

Starting with thiophene methylene aza (dibenzo) dipyrromethene **201**, two strategies have been attempted to close the macrocycle structure that might present interesting properties. The first strategy was performed using direct oxidative coupling starting with compound **201,** this might allow to close the macrocycle giving a fully conjugated π system, inspired by a "corrole" type ring system. However, oxidative cross coupling reaction using iron(III) chloride was unsuccessful to produce the desired macrocycle **188**, starting material remained unreacted. Another attempt was performed using iodine under the UV lamp. Unfortunately, this procedure failed to give the target macrocycle compound **188**, and starting material remained unreacted.

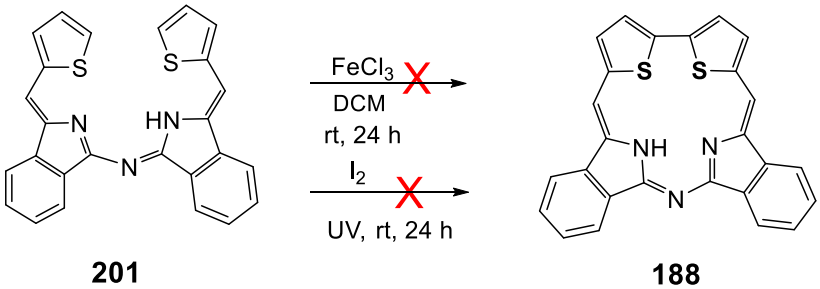

Scheme 2.54: Direct oxidative coupling attempts to formation the macrocycle **188**.

The second strategy has been attempted followed the procedure published by Li, Zhang et al., which is a direct catalytic C-H activation homocoupling of thiophene using

palladium(II) as a catalyst and oxygen as an oxidant in the presence of TFA to complete the catalytic cycle. This proceeds with complete C5 position regioselectivity (Scheme 2.55 inset).[115] To investigate the direct catalytic C-H activation homocoupling of compound **201**, it was catalysed by Pd(II) acetate in the presence of TFA, oxygen, and dimethyl sulfoxide at room temperature (Scheme 2.55). TLC was monitored, and after 24 h formation of a new red spot was observed. This spot became clearer after warming the mixture up to 50 ℃, but most of the starting material also remained unreacted. The work up was done by adding water then extracting with DCM. The mixture was purified by column chromatography using 1:3 DCM:PE.

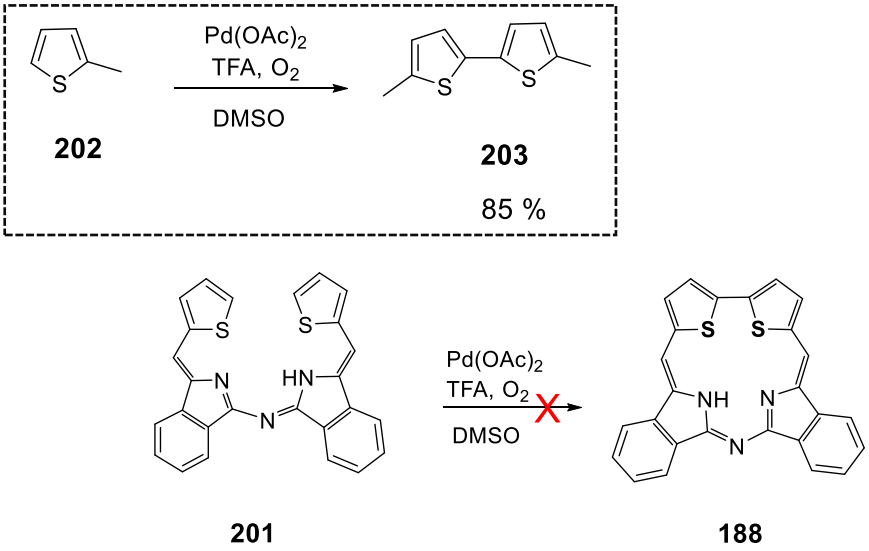

Scheme 2.55: Metal activation attempt to form the macrocycle **188**.

The ^{1}HNMR spectrum for the resulting product illustrated that the alkene singlet peak was shifted from 7.30 ppm in the starting material spectrum to the 6.94 ppm in the resulting product spectrum, all thiophene signals were intact, a doublet of doublet integrating one proton appeared at 7.15 ppm and a multiplet with two protons at 7.55 ppm, which confirmed no thiophene coupling occurred, and the isolated product might be symmetrical isomer of compound **201** (Figure 2.43). MALDI-TOF mass spectrum showed starting material peak at *m/z* 433 and other peak at *m/z* 539 which indicates that the isomerisation had taken place due to the palladium effect (Figure 2.44).

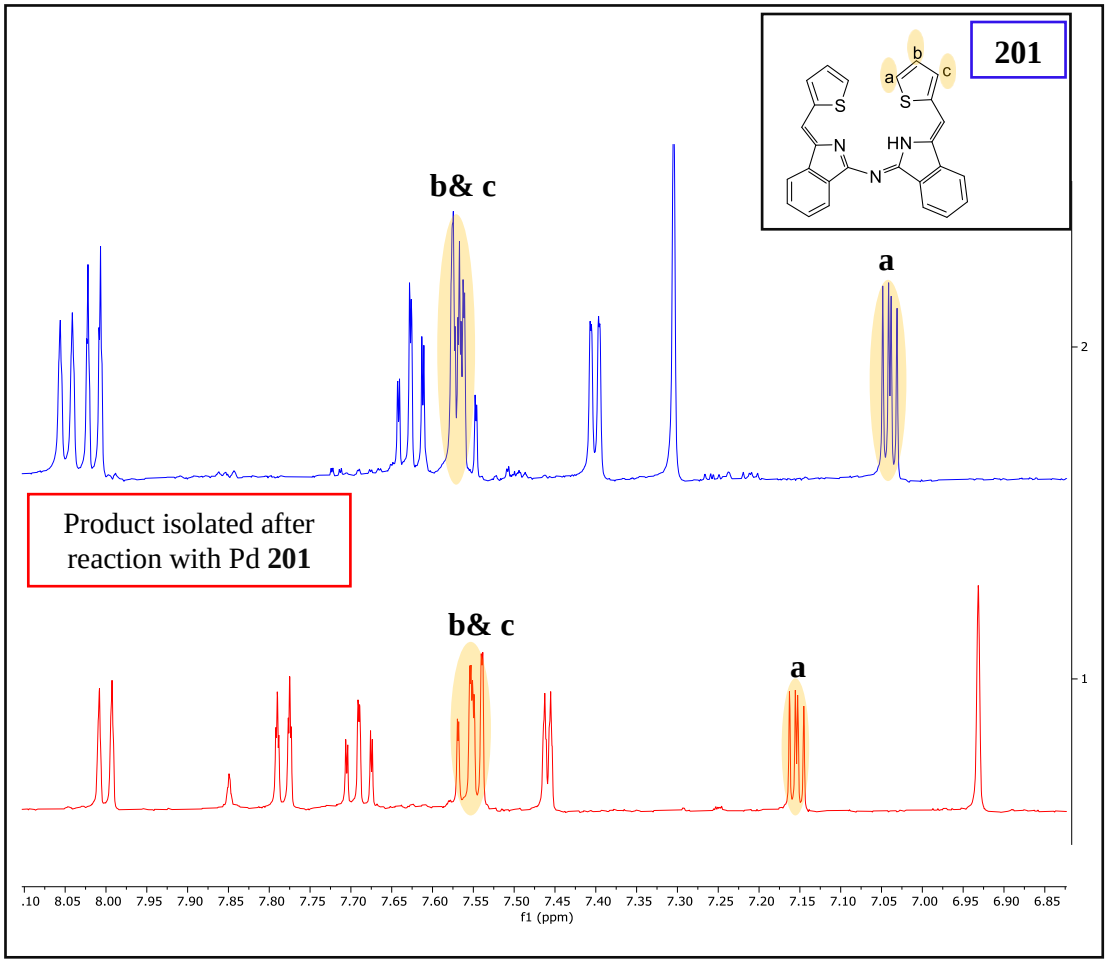

Figure 2.43: Comparison between ^{1}HNMR spectrum of compound **201** and the isolating compound after reaction with Pd.

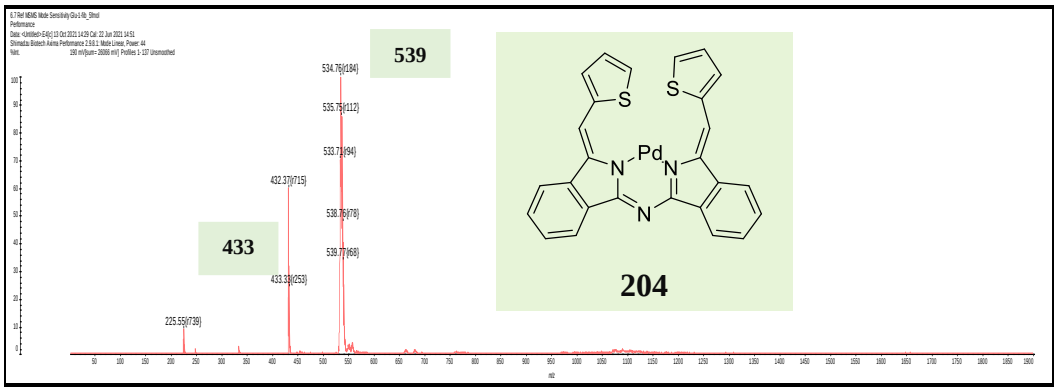

Figure 2. 44: MALDI-TOF mass spectrum of the isolated product after reaction with Pd and the suggested structure **204**.

Direct reaction was also attempted starting from the precursors thiophene methylene aminoisoindoline **200** as shown in the Scheme 2.56. However, treating with Pd(II) acetate and TFA resulted no reaction, probably due to the protonation of the starting material **200** in the presence of TFA, and no further reaction. This proved by neutralising the sample which recovered the original NMR spectrum of compound **200**.

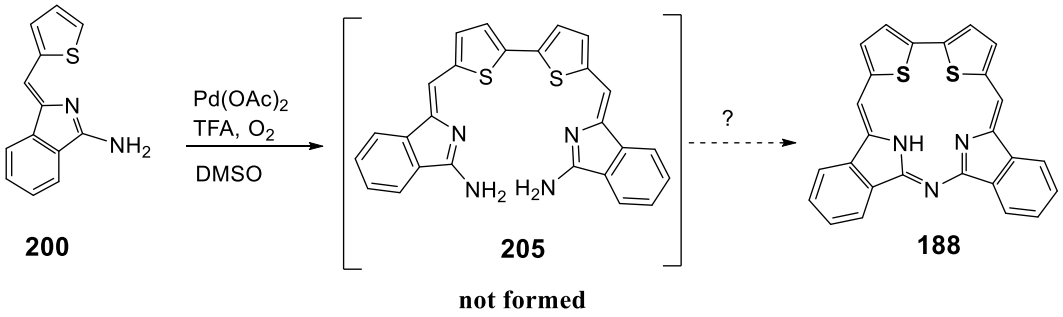

Scheme 2.56: Metal activation attempt to form the macrocycle **188** from compound **200**.

Similar procedure was also performed using 4-methoxy phenyl methylene aza (dibenzo) dipyrromethene **83** and 3-methoxy phenyl methylene aza (dibenzo) dipyrromethene **155** to investigate whether there is a possibility of cyclisation occurring due to presence of palladium catalyst and TFA. This might be activating the C-H homocoupling to give the desired compound (Scheme 2.57). Unfortunately, this was unsuccessful to produce the closed structure.

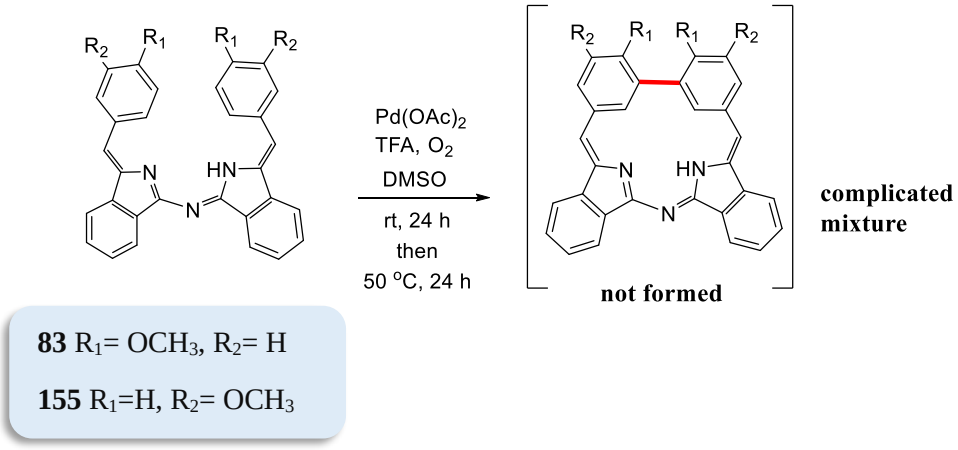

Scheme 2.57: Metal activation attempt to form the macrocycle structures from the aza (dibenzo) dipyrromethene **83** and **155**.

The ^{1}HNMR spectra for reaction with **155** are shown in Figure 2.45. It is immediately clear that the spectrum becomes more complex over time. At this stage the complexity of this spectrum gives clear evidence that cyclisation has not occurred. This was unsurprising because there was no clear change in the sample. Although the spectrum cannot be analysed completely, signals are present which indicate that we are likely to be observing isomerisation and formation of an unsymmetrical compound as major product in the mixture.

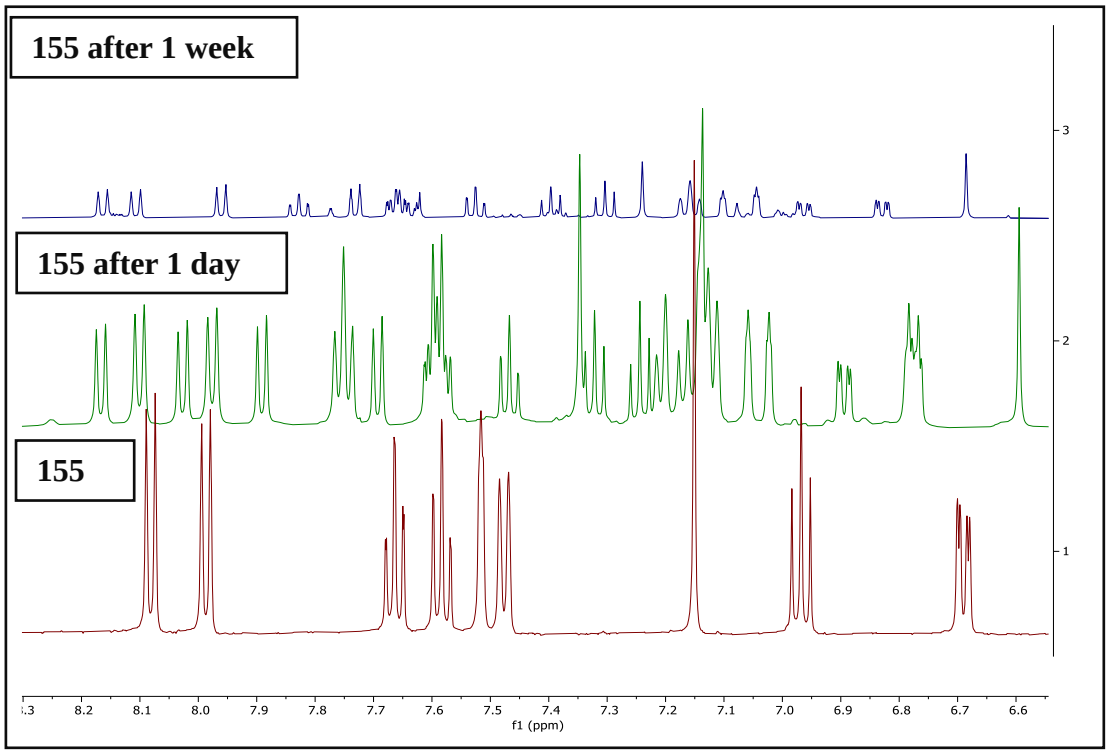

Figure 2.45: ^{1}HNMR spectra of compound **155** in deuterated DMSO (red spectra), and the resulting mixture after adding Pd and TFA (green spectra after 1day), and (blue spectra after one week).

2.9.1.4 Macrocycle formation attempt using aldehyde methine linkage

Modification of the porphyrin core by replacing of pyrrole units by other heterocycle units such as thiophene are relatively rare but known to show interesting properties by changing the electronic environment of the macrocycle core π system.[116]

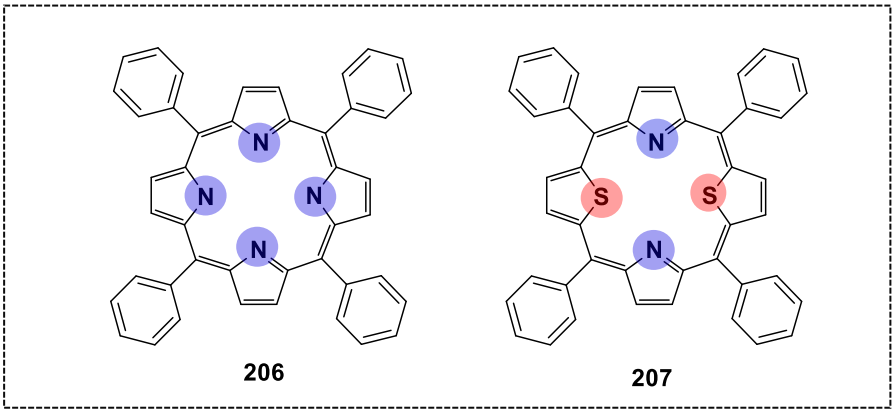

Figure 2.46: Structures of tetra phenyl porphyrin **206** and thiophene substituted tetra phenyl porphyrin **207**.

The closed structure **188** (Scheme 2.55) was not formed, probably due to combination of strain and isomerisation discussed above. It was reasoned that the problem could be solved by shifting to more porphyrin-like structures (as opposed corrole-like). Reactions between thiophene and aldehyde are well known. This strategy was therefore investigated, selecting benzaldehyde due to its wide use in porphyrin chemistry, but also because it might break the planarity leading to formation of the macrocycle structure **209**, and its likely contribution to aiding solubility in any product. A literature search revealed that commonly used mild conditions for reacting thiophenes with aldehydes employed iodine-catalysed Fridel-Crafts reaction in toluene open to the air. This synthetic pathway successfully produced the product **208** with high selectively in 71 % yield (Scheme 2.58 inset).[117] Consequently, di thiophene aza (dibenzo) dipyrromethene **201** was mixed with benzaldehyde in presence of iodine, toluene, and air at room temperature. The reaction was monitored by TLC showing no reaction occurred after 48 h. TLCs revealed no change even with raised temperature up to 60 ℃ or refluxing the mixture at 120 ℃. Continuing to monitor the reaction showed no change or consumption of the starting material. Using excess of iodine and benzaldehyde were not assisting to convert the starting material to the macrocycle structure **209**, see Scheme 2.58 (Reaction condition **A**).

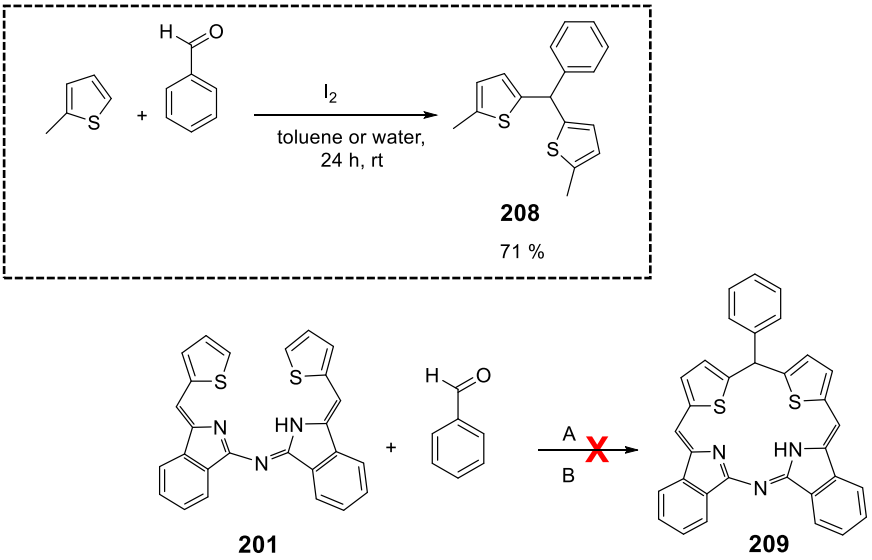

Reaction condition **A**: I_2, toluene, rt then 60 °C, then 120 °C.

Reaction condition **B**: propionic acid, 140 °C.

Scheme 2.58: Synthesis attempt to the formation of macrocycle **209**.

Therefore, it was looked to mimic classic porphyrin formation reaction conditions and attempted the cyclisation using propionic acid at reflux (Scheme 2.58, reaction condition **B**). TLCs from propionic acid solution were unclear. Instead the reaction was followed by removal of aliquots at intervals, simple workup, ^{1}HNMR and MALDI-TOF mass spectrometry analysis. MALDI-TOF mass spectrum for the crude mixture displayed presence of a peak close to the desired macrocycle **209** at *m/z* 520, and the starting material peak at *m/z* 434 (Figure 2.47).

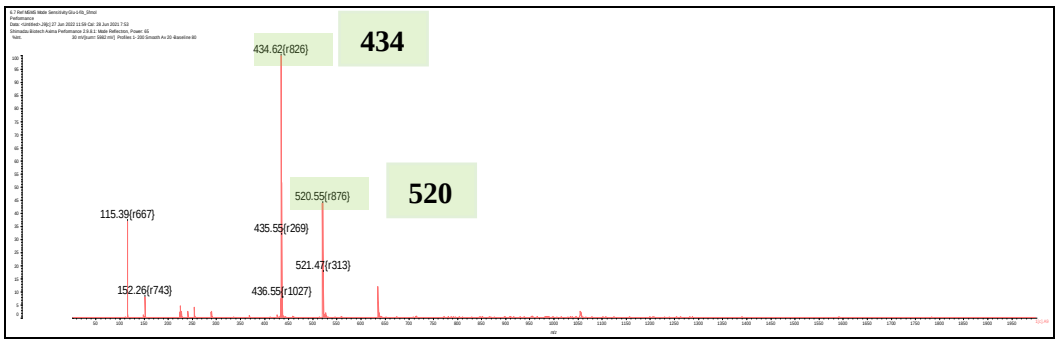

Figure 2.47: MALDI-TOF mass spectrum of the reaction crude.

However, the ^{1}HNMR spectra showed evidence that no cyclisation was occurring, as thiophene protons were present as a doublet of doublet with one proton appeared at 7.12 ppm and a multiplet integrating two protos at 7.49 ppm. Sets of peaks referring to the benzene ring protons in the isoindoline unit appeared in the aromatic region as expected. In the resulting product the singlet alkene proton was shift to 6.72 ppm, compared with the chemical shift of the alkene singlet in starting material which was at 6.96 ppm **201** (Figure 2.48). It became clear that no cyclisation was occurring, but rather once again isomerisation (to a likely unreactive configuration) was evident.

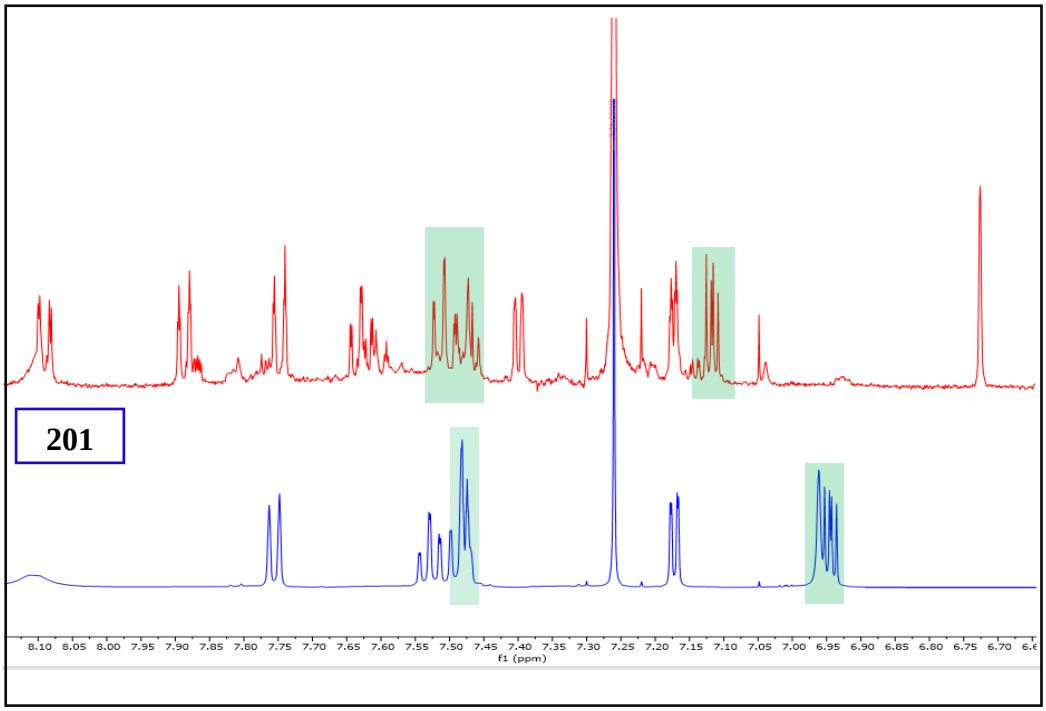

Figure 2.48: ^{1}HNMR spectrum of compound **201** in deuterium $CDCl_3$ (blue colour) and the resulting mixture after refluxing compound **201** with benzaldehyde and propionic acid (red colour).

Therefore, to force the reaction to occur, concentrated H_2SO_4 was added to the small sample of the reaction mixture, but this led to hydrolysis the mixture. Then the reaction was repeated using acetone instead of the benzaldehyde in presence of iodine, and toluene, then it left stirring at room temperature overnight, but no effect of acetone was observed through the ^{1}HNMR spectra. Consequently, after removing of propionic acid, TLC showed three spots, the top major spot was red colour, the second spot was trace of the starting material **201,** and some hydrolysis was seen in the baseline. The mixture

was precipitated by adding petroleum ether to remove the benzaldehyde, then crystallised by DCM: MeOH. ^{1}HNMR spectra indicated presence of mixture of 7 % of starting material **201** and another isomer formed in 70 % yield (blue spectra, Figure 2.49). Subsequently the reaction was repeated by refluxing of compound **201** in propionic acid in the absence of benzaldehyde. After 4 h reflux, simple work up, and TLC revealed presence of the starting material and the other red spot. The ^{1}HNMR spectra showed that the isomerisation occurred under refluxing of compound **201** in the propionic acid (green spectra, Figure 2.49), producing similar ^{1}HNMR spectra for that was isolated from the previous reaction. Figure 2.49 illustrates stacked ^{1}HNMR spectra of starting material **201** shown in the red colour, and the resulting isomers. It is clear that the alkene singlet peak in the starting material was shifted from 7.29 ppm to 6,94 ppm in the resulting isomer.

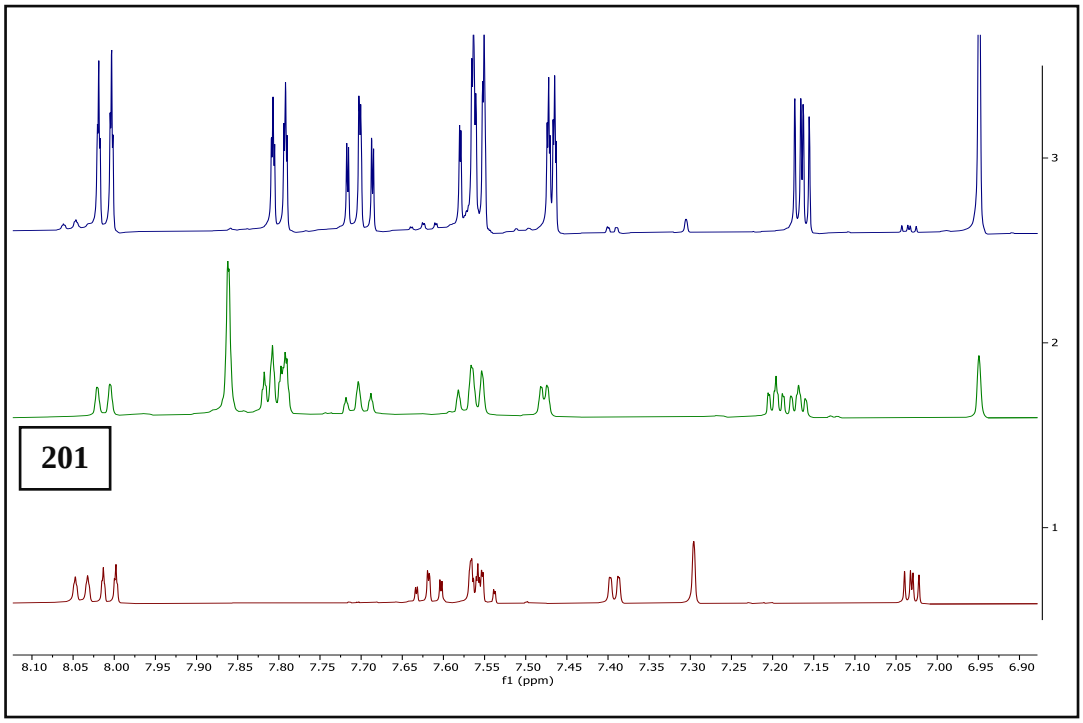

Figure 2.49: Stacked ^{1}HNMR spectrum of compound **201,** and the resulting compound after refluxing of **201** with propionic acid (green spectra), and the resulting compound after refluxing of **201** with benzaldehyde in toluene (blue spectra).

The explanation for no reaction occurring under the conditions described above, although these strategies performed were effective when applied using normal thiophene, might be because of the substituent at the position 2 on the thiophene ring in the aza (dibenzo) dipyrromethene **201** behaves as deactivating group. This leads to

decrease the reactivity of thiophene ring, which make it impossible for any reaction to occur. This is reasonable assumption because we see no clear evidence for intermolecular reaction either indicating that the problems stem from low reactivity.

2.10 Conclusion

A detailed investigation of the formation of aminoisoindolines using reaction of alkyl and benzyl acetylenes with bromo benzamidine under microwave conditions has been performed. Treating the amidine with 1-hexyne under Sonogashira copper-free cross coupling reaction conditions led to unexpected formation of the six-membered ring compound, 3-butyl isoquinoline -1-amine in 31% yield. However, using aryl acetylene in the synthesis of the precursor aminoisoindolines successfully produced the required 5-member ring compounds (aminoisoindolines) in good yield. It was concluded that only aryl acetylenes can be used in this method for aminoisoindoline synthesis.

A variety of new symmetrical and unsymmetrical aza BODIPYs and their precursors aza (dibenzo) dipyrromethenes bearing electron withdrawing or electron donating substituents have been smoothly synthesised and isolated in good yield. The synthesis of unsymmetrical analogues was achieved using simple mixed condensation reactions. Approximately statistical mixtures were produced when the precursor aminoisoindolenes were electronically similar. However, when they were different, the reaction favoured the formation of the two symmetrical derivatives, presumably because of favourable homo-condensation of the more reactive component. Consequently, a new synthetic procedure has been developed to control synthesis of unsymmetrical analogues by converting of the amino group of one aminoisoindoline into good leaving group such as triflate or tosylate. X-ray crystallography proved that tosylation (reaction) occurs on the amino nitrogen. Reactions employing the tosylates and triflates successfully led to preferred formation of the unsymmetrical aza (dibenzo) dipyrromethene with remarkable improvement of the reaction yields to those obtained via the mixed condensation synthetic method.

Complexation of the symmetrical and unsymmetrical aza dipyrromethenes has been successfully achieved following the procedure published by our group with the optimization in the reaction conditions. The new optimized synthetic method involves treating the reaction mixture of dipyrromethene, BF_3 with TMS-Cl to remove the fluoride ion to drive the equilibrium towards the target aza BODIPYs with remarkable improvement in the outcome. All symmetrical and unsymmetrical aza BODIPYs and

their precursors aza dipyrromethene were successfully characterised by MALDI-TOF, ^{1}HNMR, ^{13}CNMR, UV-Vis spectroscopy.

Extention of π conjugation system on the aza BODIPYs and their precusrsor aza dipyrromethenes via oxidative ring fusion reactions or macrocyclisation reactions were unfortunately unsuccessful. In oxidative ring fusion reactions of aza (dibenzo) BODIPYs like **172**, the main suggested reason that prevents the oxidative coupling to occur is that the BODIPY unit behaves as strong electron withdrawing group (preventing the oxidation first step). Compounds **83**, **155** and **201** were not good choice to formation of the macrocycle structures due to the isomerisation that occurred in the presence of the metal reagent/catalyst. Switching to more porphyrin-like structures (as opposed corrole-like), by treating of compound **201** with benzaldehyde did not lead to any reaction, and again this is likely because of the substituent at the position 2 on the thiophene ring in the aza dibenzo dipyrromethene **201** behaving as a deactivating group leading to decrease the reactivity of thiophene ring.

2.11 Future work

Following the successes and failures of this work there are two areas that are now primed for further investigation and likely to yield promising results.

- Expand the range of unsymmetrical systems, now that this triflate/tosylate strategy is demonstrated, this could include stronger donor/acceptor systems, or introduction of further conjugated aryl groups to give red shifted absorption and fluorescence.
- Change the synthetic strategy to build macrocyclic analogues by first synthesising diaryl-diacetylene as shown in Scheme 2.58.

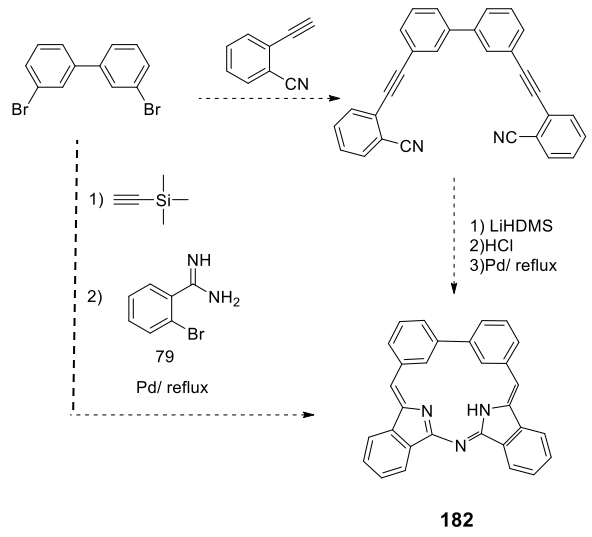

Scheme 2.58: Proposed synthesis of structure **182**.

Chapter 3: Experimental

3.1 General Methods

All reagents and solvents were bought from commercial suppliers unless otherwise stated and no additional purification was used. Dichloromethane was dried over calcium hydride and distilled under nitrogen, triethylamine (TEA) dried using molecular sieves under nitrogen, and THF was freshly distilled from sodium and benzophenone. Rotary Evaporator Buchi was used to evaporate the solvents under reduced pressure.

Thin layer chromatography (TLC) was run using Merck Silica Gel 60 F254 aluminium backed sheets and was monitored under UV light. Column chromatography was run using Silica gel 60A 40-63 micron at ambient temperature. Melting points were measured by using Reichert Thermovar microscope with Thermopar based temperature control. Reactions carried out under microwave irradiation were irradiated in Biotage Initiator Microwave system.

^{1}H NMR (500 MHz), ^{13}C NMR (126 MHz) and ^{19}FNMR spectra were recorded with a Bruker Avance 500 MHz spectrometer or at 400 MHz on a Varian 400 spectrometer using deuterated chloroform, acetone, dimethyl sulfoxide, methanol and methylene chloride as the solvents. Signals for both ^{1}HNMR and ^{13}CNMR were recorded in ppm and the coupling constant (*J* values) are reported in Hz. The spectra were obtained at room temperature unless otherwise stated.

A Perkin-Elmer Spectrum BX FT-IR spectrometer was used to record Infrared spectra. Ultraviolet-Visible absorption spectra were taken on a Perkin-Elmer Lambda 35 UV/Vis Spectrophotometer in solvent as stated, and emission spectra were recorded using Hitachi F-4500 fluorescence spectrophotometer. MALDI-TOF mass spectra were carried out on a Shimadzu Biotech Axima instrument.

3.2 Synthesis of 2-bromobenzamidine Hydrochloride 79 [86]

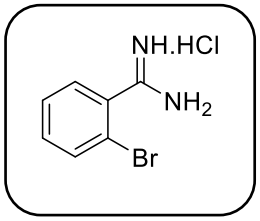

2-Bromobenzonitrile (4.20 g, 23.0 mmol) was dissolved in dry THF (3 ml). Lithium bis(trimethylsilyl)amide (1 M in THF), (25 ml, 1.1eq) was added. The reaction mixture stirred at room temperature for 4 h. Then the reaction was cooled down on an ice bath and quenched by adding dropwise of 15 ml of a 1:1 mixture of HCl (5N) and isopropanol, and then it was left to stir overnight. The colourless precipitate was filtered (cold) and washed twice with diethyl ether (10 ml) to give 2-bromobenzamidine hydrochloride (5.07 g, 94 %).

^{1}H NMR (500 MHz, DMSO-d_6) δ 9.46 (s, 2H), 9.22 (s, 1H), 7.83 – 7.79 (m, 1H), 7.62 (dd, J = 7.3, 2.1 Hz, 1H), 7.60 – 7.52 (m, 2H).
^{13}C NMR (126 MHz, DMSO-d_6) δ 166.09, 133.57, 133.50, 132.43, 130.31, 128.45, 119.99.

3.3 Synthesis of 3-butyl isoquinoline -1-amine 112.

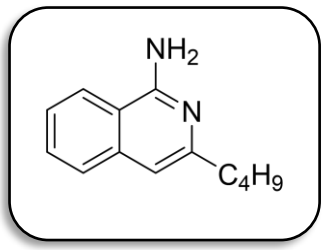

A mixture of 2-bromobenzamidine hydrochloride **79** (0.353 g, 1.498 mmol), BINAP (0.051 g, 0.082 mmol, 0.027 eq) and $PdCl_2(MeCN)_2$ (0.019 g, 0.073 mmol, 0.025 eq) was sealed in a microwave vessel with magnetic bar. It was purged and refilled with nitrogen for 5 min. Then a solution of 1-hexyne (0.492 g, 5.998 mmol, 4 eq), DBU (0.560 ml, 3.740 mmol, 2.5 eq) in dry DMF (6 ml) was added. The reaction was kept stirring under N_2 for a further 5 min. Then the mixture was irradiated by microwave at 120 °C for 1 h. The solution was allowed to cool down. The reaction was stopped by adding AcOEt (25 ml) then it was washed with a saturated solution of $NaHCO_3$ (3x10 ml). The organic layer was dried over $MgSO_4$, filtered and the solvents evaporated. The

crude mixture was purified by column chromatography eluting with DCM then AcOEt: PE 1:1. Finally the product was recrystallised using 1:1 DCM:PE to give 3-butyl isoquinoline -1-amine (0.1 g, 33 %).

Rf = 0.26 (AcOEt: pet ether 1:1).

IR (thin film cm $^{-1}$) 3398 (N-H), 2998 (C-H), 1274 (C=C).

MP = 90-92 °C.

^{1}H NMR (500 MHz, Chloroform-*d*) δ 7.84 (d, *J* = 8.5 Hz, 1H), 7.67 – 7.57 (m, 2H), 7.43 (m, 1H), 6.84 (s, 1H), 5.73 (s, 2H-NH_2), 2.72 (t, *J* = 7.8 Hz, 2H), 1.82 – 1.63 (m, 2H), 1.41 (h, *J* = 8.0 Hz, 2H), 0.95 (t, *J* = 8.0 Hz, 3H).

^{13}C NMR (126 MHz, Chloroform-*d*) δ 167.87, 132.51, 132.24, 130,91,128.78, 127.99, 127.54, 117.83, 115.32, 30.46, 21.99, 19.28, 13.61.

MS (MALDI-TOF): *m/z* = 200 [M, 100 %].

3.4 Synthesis of 2-hexynylbenzonitrile 117 [103]

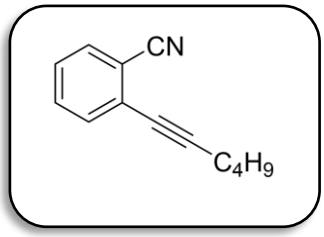

A mixture of 2-bromobenzonitrile (1.820 g, 9.998 mmol, 1 eq), 1-hexyne (0.985 g, 11.99 mmol, 1.2 eq), $Pd(PPh_3)_2Cl_2$ (0.160 g, 0.227 mmol, 0.022 eq), CuI (0.080 g, 0.42 mmol, 0.042 eq), and NEt_3 (4 ml) was heated in a sealed tube at 120 °C for 24 h. The reaction mixture was diluted with H_2O, extracted with PE, dried and purified by column chromatography using 1:9 AcOEt and PE to give a pure 2-hexynylbenzonitrile as an oil (1.5 g, 82 %).

Rf = 0.7 (AcOEt: pet ether 1:9).

IR (thin film cm $^{-1}$) 3067, 2230 (CN).

^{1}H NMR (500 MHz, Chloroform-*d*) δ 7.60 (dt, *J* = 7.9, 1.0 Hz, 1H), 7.52 – 7.48 (m, 2H), 7.39 – 7.30 (m, 1H), 2.49 (t, *J* = 7.1 Hz, 2H), 1.66 – 1.60 (m, 2H), 1.55 – 1.47 (m, 2H), 0.96 (t, *J* = 7.3 Hz, 3H).

^{13}C NMR (126 MHz, Chloroform-*d*) δ 132.37, 132.25, 132.21, 127.93, 127.60, 117.67, 115.14, 97.78, 30.40, 21.90, 19.17, 13.52.

MS (MALDI-TOF): *m/z* = 183 [M, 100 %].

3.5 Synthesis of 2-[2-(4-methoxyphenyl)ethynyl] benzonitrile 118.[99]

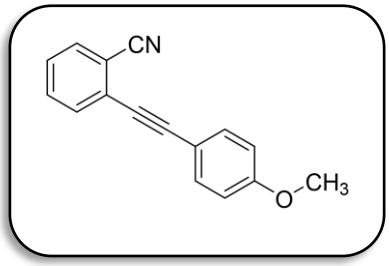

A mixture of 2-bromobenzonitrile (1.820 g, 9.998 mmol, 1 eq), 4-methoxyphenyl acetylene (1.585 g, 11.99 mmol, 1.2 eq), $Pd(PPh_3)_2Cl_2$ (0.160 g, 0.227 mmol, 0.022 eq), CuI (0.080 g, 0.42 mmol, 0.042 eq), and NEt_3 (5 ml) was heated in a sealed tube at 120 °C for 24 h. The reaction was quenched with saturated solution of NH_4Cl, extracted with ethyl acetate, dried and purified by column chromatography using 1:20 AcOEt and hexane to give colourless crystals (1.6 g, 68 %).

MP = 78–79 °C (Lit MP).[99]

Rf = 0.43 (AcOEt: hexane 1:20).

IR (thin film cm $^{-1}$) 3434, 2215 (CN).

^{1}H NMR (500 MHz, Chloroform-*d*) δ 7.66 (d, *J* = 7.7 Hz, 1H), 7.62 – 7.58 (m, 1H), 7.58 – 7.53 (m, 3H), 7.38 (td, *J* = 7.6, 1.4 Hz, 1H), 6.90 (d, *J* = 9.0 Hz, 2H), 3.84 (s, 3H).

^{13}C NMR (126 MHz, Chloroform-*d*) δ 160.42, 133.62, 132.63, 132.34, 131.84, 127.80, 127.70, 117.73, 115.05, 114.15, 114.12, 96.38, 84.65, 55.37.

3.6 Synthesis of 1,6-diethyl 2,4-hexadienedioate 132.

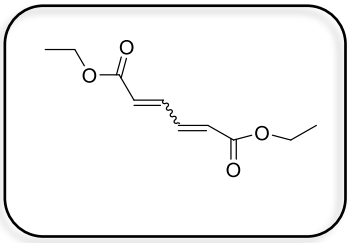

A mixture of 2-bromobenzonitrile (3.00 g, 16.5 mmol, 1 eq), $Pd(PPh_3)_2Cl_2$ (0.34 g, 0.48 mmol, 0.03 eq), CuI (0.16 g, 0.84 mmol, 0.05 eq) was stirred in NEt_3 (50 ml). Then ethyl propiolate (3.18 g, 32.5 mmol, 2 eq) was dissolved in NEt_3 (25 ml) and slowly added to the mixture during (6 h). After the completion of the addition the mixture was refluxed overnight. The reaction was worked up by adding water and extracted with DCM, dried and purified by column chromatography using 1:20 AcOEt and PE to give yellow oil (1 g, 33 %) that was presumed to be the product of alkyne homocoupling and reduction.

^{1}H NMR (500 MHz, Chloroform-*d*) δ 7.57 (d, *J* = 12.1 Hz, 1H), 5.65 (d, *J* = 12.1 Hz, 1H), 4.20 (q, *J* = 7.1 Hz, 2H), 1.29 (t, *J* = 7.1 Hz, 3H).

3.7 Synthesis of 2-(2-bromophenyl)-4(3H)-pyrimidinone.

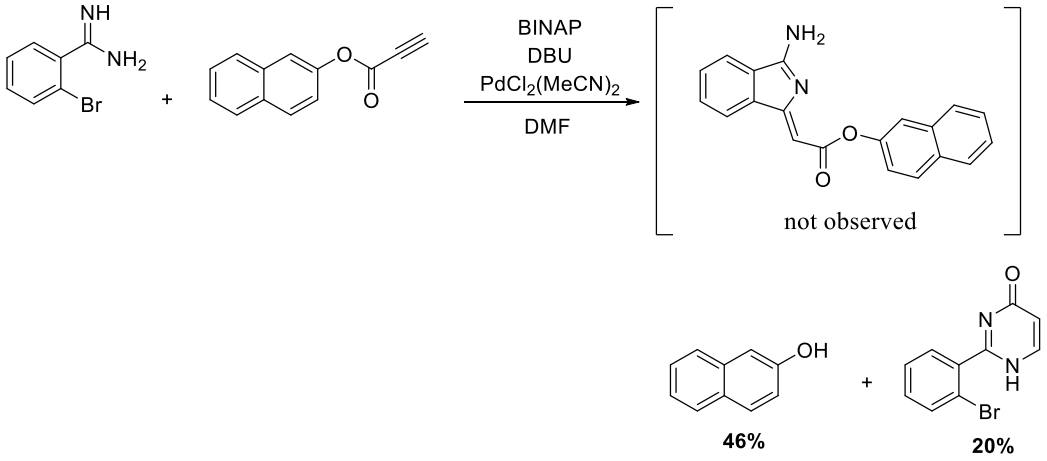

A mixture of 2-bromobenzamidine hydrochloride **79** (0.706 g, 2.997 mmol, 1 eq), BINAP (0.102 g, 0.165 mmol, 0.055 eq) and $PdCl_2(MeCN)_2$ (0.039 g, 0.150 mmol, 0.05

eq) was sealed in a microwave vessel with magnetic bar. It was purged and refilled with nitrogen for 5 min. Then naphthyl propiolate (0.705 g, 3.596 mmol, 1.2 eq), DBU (1.120 ml) in dry DMF (12 ml) was added. The reaction was kept stirring under N_2 for a further 5 min. Then the mixture irradiated by microwave at 120 °C for 1 h. The solution was allowed to cool down. The reaction was stopped by adding AcOEt (50 ml) then washed with a saturated solution of $NaHCO_3$ (3x25 ml). The organic layer was extracted and dried over $MgSO_4$, filtered then the solvents removed. Finally, the crude was purified by column chromatography eluting with DCM then 1:3 AcOEt: PE then AcOEt to give 2-naphthol (0.2 g, 46 %), and (2-bromophenyl)-4(3H)-pyrimidinone (0.15 g, 20 %).

- **3.7.1: 2-naphthalenol 135.[118]**

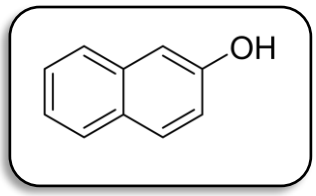

^{1}H NMR (500 MHz, Chloroform-*d*) δ 7.80 – 7.73 (t, *J* = 8.7 Hz, 2H), 7.68 (d, *J* =8.7 Hz, 1H), 7.43 (ddd, *J* = 8.3, 6.9, 1.3 Hz, 1H), 7.33 (ddd, *J* = 8.1, 6.9, 1.2 Hz, 1H), 7.16 (dd, *J* = 2.5, 0.6 Hz, 1H), 7.11 (dd, *J* = 8.8, 2.5 Hz, 1H), 5.48 (s, 1H).

- **3.7.2: 2-(2-bromophenyl)-4(3H)-pyrimidinone 136.**

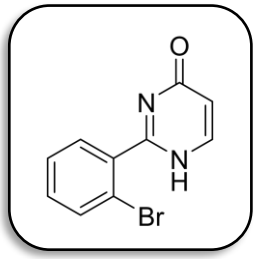

MP = 164-165 °C.

IR (thin film cm $^{-1}$) 3311, 1633, 1596.

^{1}H NMR (500 MHz, Chloroform-*d*) δ 8.08 (d, *J* = 7 Hz, 1H), 7.69 (ddd, *J* = 16.7, 7.8, 1.5 Hz, 2H), 7.50 – 7.46 (m, 1H), 7.40 (td, *J* = 7.7, 1.8 Hz, 1H), 6.45 (d, *J* = 7 Hz, 1H).

^{13}C NMR (126 MHz, Chloroform-*d*) δ 162.89, 157.68, 154.98, 134.03, 133.93, 132.37, 131.17, 127.94, 120.74, 114.70.

3.8 Synthesis of 2-[2-(4-methoxyphenyl)ethynyl]-benzamidine hydrochloride 120.

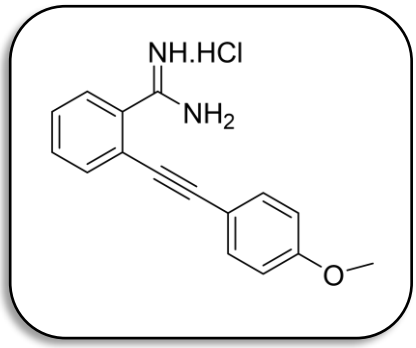

A solution of 2-[2-(4-methoxyphenyl)ethynyl] benzonitrile **118** (0.50 g, 2.14 mmol, 2 eq) in dry THF (3 ml) was stirred at room temperature. Lithium bis(trimethylsilyl) amide (1M in THF), (4.3 ml, 4.3 mmol, 2 eq) was added and stirring continued at room temperature overnight. Then the reaction was cooled down on an ice bath and quenched by adding dropwise of 8 ml of a 1:1 mixture of HCl (5N) and isopropanol, and then it was left to stir overnight. The resulting precipitate was filtered off and washed twice with diethyl ether to give the product as yellow crystals (0.4 g, 80 %).

^{1}H NMR (500 MHz, Methanol-d_4) δ 7.75 (dd, *J* = 7.8, 1.4 Hz, 1H), 7.72 – 7.65 (m, 2H), 7.58 (td, *J* = 7.6, 1.3 Hz, 1H), 7.51 (d, *J* = 8.8 Hz, 2H), 7.00 (d, *J* = 8.8 Hz, 2H), 3.87 (s, 3H).
^{13}C NMR (126 MHz, Methanol-d_4) δ 167.12, 160.64, 132.84, 132.55, 131.95, 131.31, 128.16, 127.93, 122.10, 114.01, 113.96, 94.70, 82.90, 54.41.

3.9 Synthesis of 2-(3-hydroxy-3-methyl-1-butynyl) benzonitrile 148.[103]

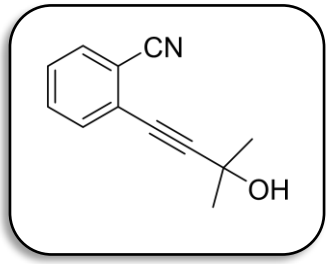

A mixture of 2-bromobenzonitrile (3.00 g, 16.5 mmol, 1 eq), $Pd(PPh_3)_2Cl_2$ (0.34 g, 0.49 mmol, 0.03 eq), CuI (0.22 g, 1.15 mmol, 0.07 eq), and PPh_3 (0.51 g, 1.97 mmol, 0.12 eq) were dissolved in NEt_3 (50 ml). Then 2-methyl-but-3n-2-ol (2.77 g, 32.5 mmol, 2 eq) was dissolved in (25 ml) TEA and added slowly using the syringe pump to the reaction mixture (4 ml per h). After completion of the addition the reaction mixture was refluxed overnight. Then the reaction mixture was diluted with H_2O, extracted with DCM, dried and purified by column chromatography using 1:8 AcOEt: PE to give the target product as yellow oil (3 g, 98 %).

^{1}H NMR (500 MHz, $CDCl_3$) δ 7.65 – 7.62 (m, 1H), 7.56 – 7.50 (m, 2H), 7.44 – 7.37 (m, 1H), 1.66 (s, 6H).

^{13}C NMR (126 MHz, Chloroform-*d*) δ 132.53, 132.35, 132.14, 128.39, 126.72, 117.45, 115.62, 100.54, 65.70, 31.20, 22.63.

3.10 synthesis of 2-[2-(4-nitrophenyl)ethynyl] benzonitrile 150.[105]

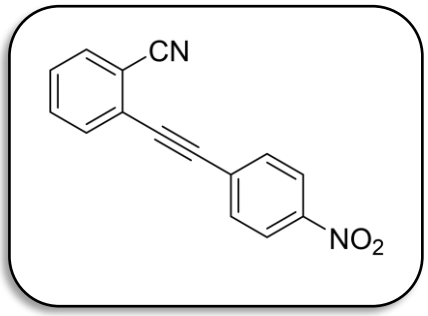

A mixture of 2-(3-hydroxy-3-methyl-1-butynyl) benzonitrile **148** (0.55 g, 2.96 mmol, 1 eq), 1-Iodo-4-nitrobenzene (0.49 g, 1.98 mmol, 0.67 eq), $Pd(PPh_3)_2Cl_2$ (0.04 g, 0.05 mmol, 0.02 eq), CuI (0.06 g, 0.3 mmol, 0.1 eq), BU_4NI (0.11 g, 0.03 mmol, 0.01 eq), NaOH (5 M) and toluene (5 ml) was heated in a sealed tube at 60 °C under N_2 for 1 h. Then it was filtered over a silica pad and washed with AcOEt. The product was purified by column chromatography using 1:20 AcOEt and PE and recrystalised from DCM:PE to give colourless crystals (0.5 g, 67 %).

MP = 143–144 °C (Lit MP).[103]

IR (thin film cm $^{-1}$) 3070 (C-H), 2223 (CN), 1592, 1513 (N=O).

^{1}H NMR (500 MHz, Chloroform-*d*) δ 8.25 (d, *J* = 7.7 Hz, 2H), 7.77 (d, *J* = 8.8 Hz, 2H), 7.75 – 7.71 (m, 1H), 7.71 – 7.66 (m, 1H), 7.66 – 7.60 (m, 1H), 7.53 – 7.48 (m, 1H).

^{13}C NMR (126 MHz, Chloroform-*d*) δ 147.66, 132.84, 132.78, 132.60, 132.39, 129.32, 128.80, 126.01, 123.73, 117.27, 115.77, 93.48, 90.14.

3.11 Synthesis of 2-[2-(4-nitrophenyl)ethynyl]-benzamidine hydrochloride 151.

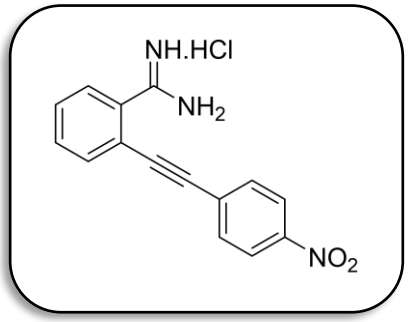

A solution of 2-[2-(4-nitrophenyl)ethynyl] benzonitrile **150** (0.165 g, 0.664 mmol, 1 eq) was stirred in dry THF (2 ml). Lithium bis(trimethylsilyl)amide (1M in THF), (1.32 ml, 1.32 mmol, 2 eq) was added and stirring continued at room temperature overnight. Then the reaction was cooled down on an ice bath and quenched by adding dropwise of 6 ml of a 1:1 mixture of HCl (5N) and isopropanol, and then it was left to stir overnight. The resulting precipitate was filtered in cold and washed twice with diethyl ether (5 ml) to give yellow crystals (50 mg, 28 %).

^{1}H NMR (500 MHz, Methanol-d_4) δ 8.22 (d, J = 9.0 Hz, 2H), 7.76 – 7.74 (m, 3H), 7.70 (ddd, J = 7.9, 1.4, 0.7 Hz, 1H), 7.67 – 7.64 (m, 1H), 7.52 (td, J = 7.7, 1.4 Hz, 1H).
^{13}C NMR (126 MHz, Methanol-d_4) δ 166.88, 160.43, 145.86, 140.14, 139.79, 132.82, 132.45, 131.80, 128.12, 127.84, 113.90, 96.35, 94.81.

3.12 Synthesis of aminoisoindoline derivatives.

3.12.1 General procedure [75]

A mixture of 2-bromobenzamidine hydrochloride **79** (0.706 g, 2.997 mmol, 1 eq), BINAP (0.102 g, 0.165 mmol, 0.055 eq) and $PdCl_2(MeCN)_2$ (0.039 g, 0.15 mmol, 0.05 eq) was sealed in a microwave vessel with magnetic bar. It was purged and refilled with N_2 for 5 min. Then a solution of acetylene derivatives (1.2 eq), DBU (1.120 ml, 7.492 mmol, 2.5 eq) in dry DMF (12 ml) was added. The reaction was kept stirring under N_2 for a further 5 min to yield a clear yellow solution with a white solid. Then the mixture was irradiated by microwave at 120 °C for 1 h. The solution was allowed to cool down. The reaction was stopped by adding AcOEt (50 ml) then it was washed with a saturated solution of $NaHCO_3$ (3x25 ml). The organic layer was extracted and dried over $MgSO_4$, filtered then the solvents removed. Finally, the crude was purified by crystallisation using DCM:PE to give the desired compound in good yield.

3.12.2 Synthesis of (Z)-1-(4-methoxyphenylmethylene) -1H-isoindol-3-amine 81 [41]

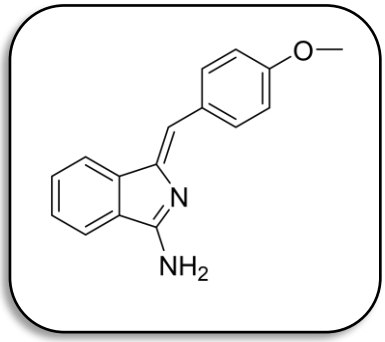

This compound was isolated as yellow needles; yield (560 mg, 74 %).

^{1}H NMR (500 MHz, Chloroform-*d*) δ 8.08 (d, *J* = 8.7 Hz, 2H), 7.78 (d, *J* = 7.9 Hz, 1H), 7.49 – 7.43 (m, 2H), 7.36 (td, *J* = 7.4, 0.9 Hz, 1H), 6.94 (d, *J* = 8.8 Hz, 2H), 6.75 (s, 1H), 3.85 (s, 3H).

^{13}C NMR (126 MHz, Chloroform-*d*) δ 164.49, 159.10, 145.81, 143.20, 132.00, 130.71, 129.60, 128.90, 126.76, 119.57, 118.74, 115.63, 114.00, 55.31.

3.12.3 Synthesis of (Z)-1-(3-methoxyphenylmethylene)-1H-isoindol-3-amin 137.

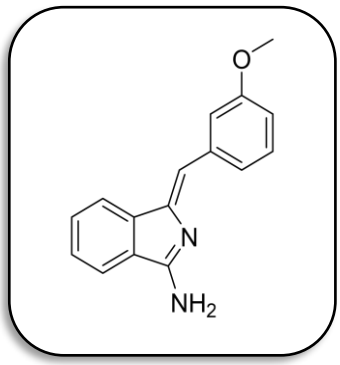

This compound was isolated as yellow crystals; yield (540 mg, 72 %).

MP = 183 – 184 °C.

Rf = 0.63 (AcOEt)

IR (thin film cm $^{-1}$) 3440 (C-H), 1665 (C=C), 1571 (C=N).

^{1}H NMR (500 MHz, $CDCl_3$) δ 7.84 (s, 1H), 7.79 (dt, *J* = 7.7, 1.0 Hz, 1H), 7.57 (d, *J* = 7.5 Hz, 1H), 7.50 – 7.44 (m, 2H), 7.38 (td, *J* = 7.4, 1.0 Hz, 1H), 7.31 (t, *J* = 8.0 Hz, 1H), 6.83 (ddd, *J* = 8.1, 2.7, 0.9 Hz, 1H), 6.73 (s, 1H), 3.89 (s, 3H).

^{13}C NMR (126 MHz, Chloroform-*d*) δ 165.21, 159.61, 147.62, 142.95, 141.68,138.07, 131.11, 129.23, 127.27, 123.25, 119.82, 118.89, 115.54, 114.85, 113.31, 55.35.

MS (MALDI-TOF): *m/z* = 250 [M, 100 %].

UV−Vis (CH_2Cl_2) λmax/nm (ε/$dm^3.mol^{-1}.cm^{-1}$): 389 (2.6 x 10^4), 360 (5.5x10^4), 315 (2.7x10^4), 230 (6.7x10^4), 277 (2.9x10^4), 229 (6.8x10^4).

3.12.4 Synthesis of (Z)-1-(4-pentyloxyphenylmethylene)-1H-isoindol-3-amine 138.

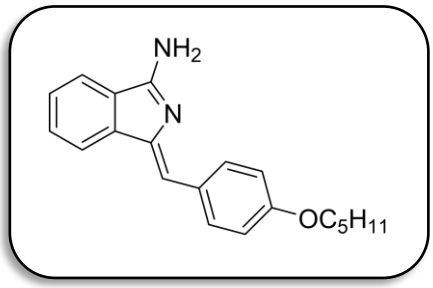

This compound was isolated as yellow crystals; yield (670 mg, 73 %).

MP =120-122 °C.

Rf = 0.66 (AcOEt)

IR (thin film cm^{-1}) 3358 (C-H), 1602 (C=C), 1505 (C=N).

^{1}H NMR (500 MHz, Chloroform-*d*) δ 8.07 (d, *J* = 8.6 Hz, 2H), 7.77 (d, *J* = 7.1 Hz, 1H), 7.45 (dd, *J* = 8.3, 7.2 Hz, 2H), 7.35 (td, *J* = 7.2, 1.0 Hz, 1H), 6.93 (d, *J* = 8.8 Hz, 2H), 6.74 (s, 1H), 4.00 (t, *J* = 6.6 Hz, 2H), 1.83 – 1.77 (m, 2H), 1.48 – 1.36 (m, 4H), 0.94 (t, *J* = 7.1 Hz, 3H).

^{13}C NMR (126 MHz, Methylene Chloride-d_2) δ 165.42, 158.98, 139.86, 139.83, 139.77, 131.15, 130.00, 128.10, 127.90, 122.02, 121.91, 119.24, 115.05, 67.88, 28.97, 28.17, 22.52, 13.80.

MS (MALDI-TOF): *m/z* = 306 [M, 100 %].

UV−Vis (CH_2Cl_2) λmax/nm (ε/$dm^3.mol^{-1}.cm^{-1}$): 397 (5.6x10^4), 377 (8.2x10^4), 288 (2.4x10^4), 230 (6.7x10^4).

3.12.5 Synthesis of (Z)-1-(4-cyanophenylmethylene)-1H-isoindol-3-amine 154.

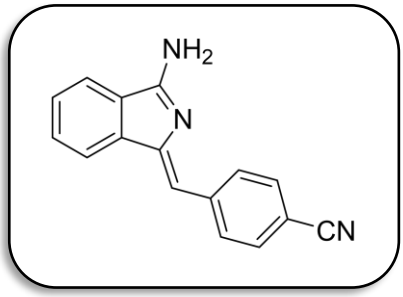

This compound was isolated as yellow powder; yield (480 mg, 65 %).

MP = 226– 228 °C.

Rf = 0.86 (AcOEt).

IR (thin film cm $^{-1}$) 3428 (C-H), 2220 (CN), 1671 (C=C), 1530 (C=N).

^{1}H NMR (500 MHz, Acetone-d_6) δ 8.50 (d, *J* = 9.0 Hz, 2H), 7.91 (dt, *J* = 7.6, 0.9 Hz, 1H), 7.86 (dt, *J* = 7.5, 0.9 Hz, 1H), 7.76 (d, *J* = 8.0 Hz, 2H), 7.52 (td, *J* = 7.4, 1.1 Hz, 1H), 7.46 (td, *J* = 7.4, 1.0 Hz, 1H), 7.28 (s, 2H-NH_2), 6.79 (s, 1H).

^{13}C NMR (126 MHz, Acetone-d_6) δ 167.09, 152.60, 143.31, 142.63, 132.43, 131.62, 130.62, 129.23, 127.83, 119.98, 119.79, 119.06, 110.45, 108.75.

MS (MALDI-TOF): *m/z* = 245 [M, 100 %].

UV−Vis (CH_2Cl_2) λmax/nm (ε/$dm^3.mol^{-1}.cm^{-1}$): 406 ($3.8x10^4$), 379 ($7.6x10^4$), 327 ($3.6x10^4$), 291 ($3.4x10^4$), 232 ($7.6x10^4$).

3.12.6 Synthesis of (Z)-1-(4-hydroxyphenylmethylene)-1H-isoindol-3-amine 187.

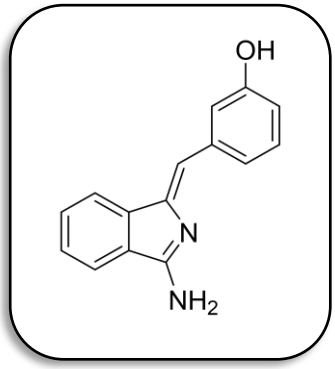

This compound was isolated as yellow powder; yield (530 mg, 74 %).

MP = 123-125 °C.

Rf = 0.33 (AcOEt).

IR (thin film cm $^{-1}$) 3450 (C-H), 2985 (O-H), 1647 (C=C), 1528 (C=N).

^{1}H NMR (500 MHz, Acetone-d_6) δ 7.92 (dd, *J* = 2.6, 0.53 Hz, 1H), 7.86 (dt, *J* = 7.7, 1.0 Hz, 1H), 7.79 (dt, *J* = 7.5, 0.9 Hz, 1H), 7.65 (dt, *J* = 1.6, 0.8 Hz, 1H), 7.46 (dd, *J* = 7.4, 1.1 Hz, 1H), 7.40 – 7.37 (m, 1H), 7.15 (t, *J* = 7.8 Hz, 1H), 6.71 (ddd, *J* = 8.0, 2.5, 1.0 Hz, 1H), 6.69 (s, 1H).

^{13}C NMR (126 MHz, Acetone-d_6) δ 165.65, 157.12, 149.04, 143.72, 138.96, 132.10, 128.73, 128.59, 126.94, 122.28, 119.59, 119.33, 117.19, 113.94, 113.45.

MS (MALDI-TOF): *m/z* = 236 [M, 100 %].

UV−Vis (CH_2Cl_2) λmax/nm (ε/$dm^3.mol^{-1}.cm^{-1}$): 390 ($2.9x10^4$), 370 ($4.8x10^4$), 334 ($2.8x10^4$), 282 ($4.4x10^4$), 229 ($5.0x10^4$).

3.12.7 Synthesis of (Z)-1-(2-thiophenylmethylene)-1H-isoindol-3-amine 200.

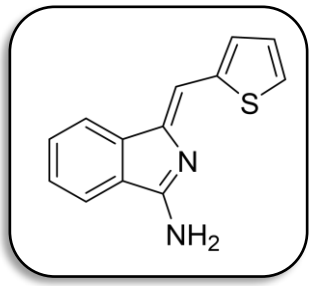

This compound was isolated as yellow powder; yield (520 mg, 76 %).

MP = 133-135 °C.

Rf = 0.8 (AcOEt).

^{1}H NMR (500 MHz, Acetone-d_6) δ 7.82 (dt, *J* = 7.5, 1.0 Hz, 1H), 7.77 (dt, *J* = 7.5, 1.0 Hz, 1H), 7.45 – 7.40 (m, 2H), 7.35 (td, *J* = 7.4, 1.0 Hz, 1H), 7.31 (m, 1H), 7.05 (s, 1H), 7.00 (dd, *J* = 5.2, 3.6 Hz, 1H) 6.88 (brs, 1H, NH_2).

^{13}C NMR (126 MHz, Acetone-d_6) δ 164.92, 147.50, 142.82, 141.50, 133.21, 128.97, 128.60, 128.42, 127.18, 126.68, 120.21, 119.67, 108.27.

MS (MALDI-TOF): *m/z* = 227 [M+1].

UV−Vis (CH_2Cl_2) λmax/nm (ε/$dm^3.mol^{-1}.cm^{-1}$): 403 ($4.5x10^4$), 385 ($6.3x10^4$), 354 ($4.2x10^4$), 281 ($4.8x10^4$), 230 ($6.5x10^4$).

3.13 Synthesis of aza (dibenzo) dipyrromethene derivatives.

3.13.1 General procedure [41]

Aminoisoindolene derivatives (500 mg) were refluxed in toluene at 120 ℃ (10 ml), in diglyme (6 ml) at 200 ℃ (in the synthesis of compound **157**), or p-xylene (6 ml) at 140 ℃ (in the synthesis of compound **180**), for 24 h. After evaporation of the solvents, the crude mixture was purified by column chromatography eluting with DCM. The resulting red solid was recrystallised from 1:1 DCM and methanol.

3.13.1 Synthesis of aza (dibenzo) dipyrromethene 83 [41]

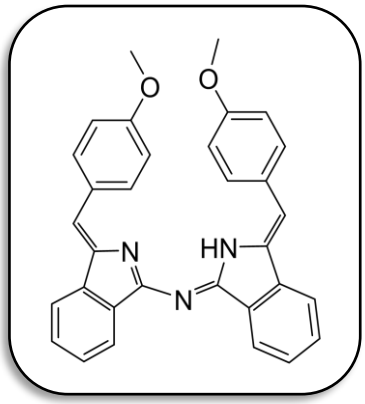

This compound was isolated as red crystals (400 mg, 82%).

MP = 204°C. (Lit MP).[41]

^{1}H NMR (500 MHz, Chloroform-*d*) δ 13.09 (s, 1H), 8.09 (dt, *J* = 7.5, 1.0 Hz, 1H), 7.86 (d, *J* = 8.7 Hz, 2H), 7.80 (dt, *J* = 7.7, 1.0 Hz, 1H), 7.54 (td, *J* = 7.4, 1.2 Hz, 1H), 7.49 (td, *J* = 7.4, 1.1 Hz, 1H), 6.78 (s, 1H), 6.62 (d, *J* = 8.7 Hz, 2H), 3.70 (s, 3H).
^{13}C NMR (126 MHz, Chloroform-*d*) δ 159.91, 150.42, 148.07, 141.82, 139.52, 135.88, 130.33, 130.10, 128.45, 123.11, 122.96, 122.07, 119.46, 115.22, 113.94, 55.03.

3.13.2 Synthesis of aza (dibenzo) dipyrromethene 155

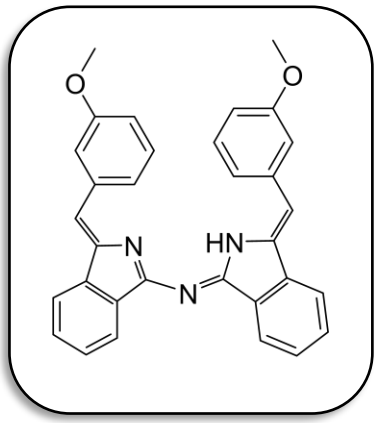

This compound was isolated as red crystals (410 mg, 84 %).

MP = 140– 142 °C.

Rf = 0.55 (DCM).

IR (thin film cm $^{-1}$) 2930 (N-H), 1577 (C=C).

^{1}H NMR (500 MHz, Chloroform-*d*) δ 13.37 (s, 1H), 8.11 (d, *J* = 7.1 Hz, 1H), 7.83 (d, *J* = 7.4 Hz, 1H), 7.60 – 7.55 (m, 2H), 7.53 (s, 1H), 7.48 (d, *J* = 7.4 Hz, 1H), 7.02 (t, *J* = 7.9 Hz, 1H), 6.79 (s, 1H), 6.62 (dd, *J* = 8.3, 2.6 Hz, 1H), 3.65 (s, 3H).

^{13}C NMR (126 MHz, Chloroform-*d*) δ 164.49, 159.10, 145.81, 143.20, 132.00, 130.71, 129.60, 128.90, 126.76, 119.57, 118.74, 115.63, 114.00, 55.31.

MS (MALDI-TOF): *m/z* = 483 [M, 100 %].

UV−Vis (CH_2Cl_2) λmax/nm (ε/$dm^3.mol^{-1}.cm^{-1}$): 341 ($9.5x10^4$), 421 ($2.0x10^4$), 477 ($2.3x10^4$).

3.13.3 Synthesis of aza (dibenzo) dipyrromethene 156

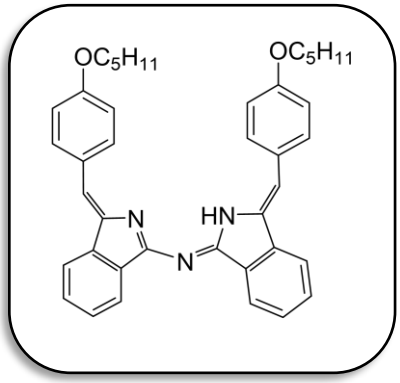

This compound was isolated as red crystals (390 mg, 80 %).

MP = 150-152 °C.

Rf = 0.7(DCM).

IR (thin film cm $^{-1}$) 2934 (N-H), 1577, 1508.

^{1}H NMR (400 MHz, Methylene Chloride-d_2) δ 12.79 (brs, 1H), 8.06 (d, *J* = 7.5 Hz, 1H), 7.87 – 7.80 (m, 3H), 7.61 – 7.44 (m, 2H), 6.82 (s, 1H), 6.62 (d, *J* = 8.6 Hz, 2H), 3.79 (t, *J* = 6.7 Hz, 2H), 1.81 – 1.69 (m, 2H), 1.48 – 1.37 (m, 4H), 0.95 (t, *J* = 6.9 Hz, 3H).

^{13}C NMR (126 MHz, Chloroform-*d*) δ 164.37, 158.73, 145.49, 143.18, 131.98, 130.62, 129.31, 128.90, 126.72, 119.56, 118.75, 115.79, 114.60, 68.02, 28.98, 28.22, 22.50, 14.04.

MS (MALDI-TOF): *m/z* = 596 [M+1].

UV−Vis (CH_2Cl_2) λmax/nm (ε/$dm^3.mol^{-1}.cm^{-1}$): 363 ($8.9x10^4$), 416 ($2.2x10^4$), 505 ($1.6x10^4$).

3.13.4 Synthesis of aza (dibenzo) dipyrromethene 157

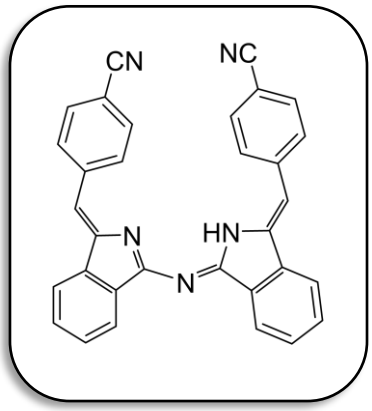

This compound was isolated as red crystals (290 mg, 60 %).

MP= 290-292 °C.

Rf = 0.36 (DCM).

IR (thin film cm $^{-1}$) 2935(N-H), 2218 (CN), 1575, 1500.

^{1}H NMR (500 MHz, Acetone-d_6) δ 13.56 (brs, 1H), 8.18 (d, *J*=8.3 Hz, 2H), 7.93 (m, 2H), 7.56 (td, *J* = 7.5, 1.2 Hz, 1H), 7.51 (td, *J* = 7.4, 1.0 Hz, 1H), 7.34 (d, *J*=8.4 Hz, 2H), 7.01 (s, 1H).

^{13}C NMR (126 MHz, Chloroform-*d*) δ 140.48, 132.43, 131.11, 130.77, 130.45, 130.05, 128.98, 122.17, 121.98, 120.19, 119.79, 114.68, 114.49, 110.24.

MS (MALDI-TOF): *m/z* = 473 [M, 100 %].

UV−Vis (CH_2Cl_2) λmax/nm (ε/$dm^3.mol^{-1}.cm^{-1}$): 358 ($9.3x10^4$), 492 ($1.2x10^4$).

3.13.5 Synthesis of aza (dibenzo) dipyrromethene 180

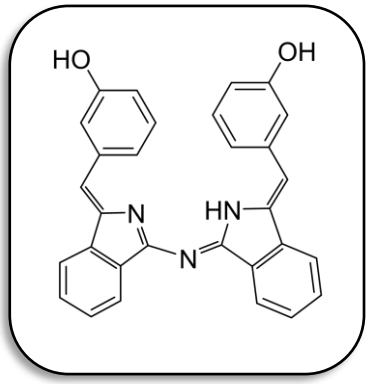

This compound was isolated as brown powder (250 mg, 51 %).

MP = 168-170 °C.

Rf = 0.1 (DCM).

IR (thin film cm $^{-1}$) 3300 (O-H), 2980 (N-H), 1572 (C=C).

^{1}H NMR 500 MHz, Acetone-d_6) δ 8.06 (m, 2H), 7.68 – 7.63 (m, 1H), 7.63 – 7.56 (m, 2H), 7.43 (t, *J* = 2.1 Hz, 1H), 7.05 (s, 1H), 6.93 (t, *J* = 7.9 Hz, 1H), 6.69 (ddd, *J* = 8.1, 2.5, 0.9 Hz, 1H).

^{13}C NMR (126 MHz, Acetone-d_6) δ 146.56, 137.24, 133.42, 130.23, 129.64, 129.47, 128.76, 127.98, 123.65, 123.10, 121.39, 121.16, 119.77, 116.60, 115.33.

MS (MALDI-TOF): *m/z* = 455 [M, 100 %].

UV−Vis (CH_2Cl_2) λmax/nm (ε/$dm^3.mol^{-1}.cm^{-1}$): 349 ($8.73x10^4$), 469 ($2.3x10^4$).

3.13.6 Synthesis of aza (dibenzo) dipyrromethene 201

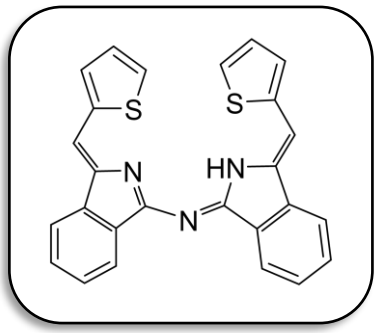

This compound was isolated as red crystals (370 mg, 77 %).

MP = 192-195 °C.

Rf = 0.73 (DCM).

IR (thin film cm $^{-1}$) 3330, 2970 (N-H), 1584 (C=C).

^{1}H NMR (500 MHz, Acetone-d_6) δ 12.45 (s, 1H), 8.06 (dt, *J* = 7.5, 1.0 Hz, 1H), 8.03 (dt, *J* = 7.7, 0.9 Hz, 1H), 7.64 (td, *J* = 7.4, 1.2 Hz, 1H), 7.62 – 7.56 (m, 2H), 7.41 (dd, *J* = 5.2, 1.1 Hz, 1H), 7.32 (s, 1H), 7.05 (dd, *J* = 5.1, 3.6 Hz, 1H).

^{13}C NMR (126 MHz, Acetone-d_6) δ 139.07, 138.71, 136.87, 135.01, 130.42, 129.41, 129.05, 128.30, 127.99, 123.67, 122.12, 119.77, 108.17.

MS (MALDI-TOF): *m/z* = 435 [M, 100 %].

UV−Vis (CH_2Cl_2) λmax/nm (ε/$dm^3.mol^{-1}.cm^{-1}$): 315 ($5.1x10^4$), 360 ($8.6x10^4$), 505 ($1.9x10^4$).

3.14 Synthesis of triflate aza (dibenzo) dipyrromethene 181.

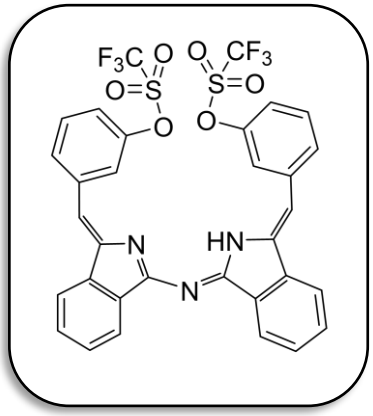

According to the procedure of Henach et al.,[108] to a stirred solution of compound 1-(3-hydroxyphenylmethylene)-1H-isoindol-3-amine **180** (0.250 g, 0.549 mmol), and pyridine (0.1 ml, 0.823 mmol, 1.5 eq) in dry DCM (30 ml) was dropwise added trifluoromethanesulfonic acid anhydride (0.24 ml, 0.823 mmol, 1.5 eq) at -20 °C over 30 min under nitrogen. The resulting mixture was left overnight at room temperature. After dilution with H_2O (60 ml), the mixture was extracted with DCM (3x15 ml). The solvent was evaporated in vacuo and the obtained product was purified by column chromatography (eluting with 1:3 DCM:PE) and recrystallized from DCM and MeOH to give the desired compound (98 mg, 24 %)

^{1}H NMR (500 MHz, Acetone-d_6) δ 13.38 (s, 1H), 8.07 (dd, *J* = 7.5, 1.2 Hz, 1H), 7.91 (dd, *J* = 7.8, 3.0 Hz, 2H), 7.82 (s, 1H), 7.59 – 7.52 (m, 1H), 7.52 – 7.45 (m, 1H), 7.07 (td, *J* = 8.1, 2.5 Hz, 1H), 7.03 – 6.94 (m, 2H).
^{13}C NMR (126 MHz, Acetone-d_6) δ 168.48, 162.77, 159.52, 150.02, 131.64, 130.66, 129.37, 128.72, 125.54, 125.31, 123.43, 122.21, 119.97, 119.78, 108.90.
MS (MALDI-TOF): *m/z* = 719 [M,100 %].

3.15 Tosylation of aminoisoindoline derivatives

3.15.1 Tosylation of (Z)-1-(4-methoxyphenylmethylene)-1H-isoindol-3-amine 163

Following the general procedure,[107] aminoisoindoline **81** (0.250 g, 0.998 mmol, 1 eq) was stirred with p-toluene sulfonyl chloride (0.209 g, 1.098 mmol, 1.1 eq) in the presence of triethylamine (0.3 ml, 2.994 mmol, 3 eq) in dry DCM (6 ml) at room temperature. The reaction was monitored by TLC until the completion then diluted with H_2O and extracted by DCM, dried over $MgSO_4$ and filtered. Finally, recrystallisation using 1:1 DCM:PE yielded the target product as yellow crystals (380 mg, 94 %).

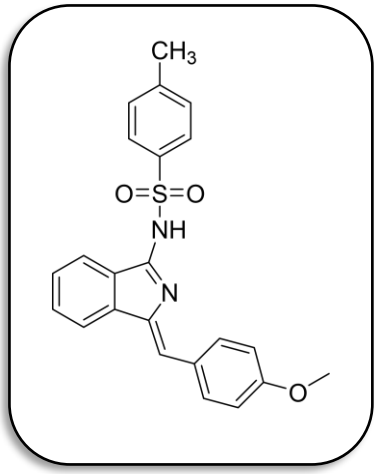

MP = 196-197 °C.

IR (thin film cm $^{-1}$) 3392,1596, 1577.

^{1}H NMR (500 MHz, Chloroform-*d*) δ 10.58 (s, 1H), 7.91 (dd, *J* = 8.2, 2.8 Hz, 3H), 7.77 (d, *J* = 7.8 Hz, 1H), 7.63 (t, *J* = 7.6 Hz, 1H), 7.47 (dd, *J* = 8.2, 6.0 Hz, 3H), 7.29 (d, *J* = 8.0 Hz, 2H), 7.05 (d, *J* = 8.3 Hz, 2H), 6.69 (s, 1H), 3.88 (s, 3H), 2.40 (s, 3H).

^{13}C NMR (126 MHz, Chloroform-*d*) δ 159.87, 159.25, 143.17, 139.15, 136.43, 132.68, 132.65, 130.73, 130.14, 129.44, 128.92, 126.76, 126.60, 124.05, 119.58, 115.18, 109.95, 55.45, 21.56.

MS (MALDI-TOF): *m/z* = 404 [M,100 %].

3.15.2 Tosylation of (Z)-1-(4-pentyloxyphenylmethylene)-1H-isoindol-3-amine 164

Following the general procedure,[107] aminoisoindoline **138** (0.250 g, 0.816 mmol, 1 eq) was stirred with p-toluene sulfonyl chloride (0.171 g, 0.898 mmol, 1.1 eq) in the presence of triethylamine (0.3 ml, 2.448 mmol, 3 eq) in dry DCM (6 ml) at room temperature. The reaction was monitored by TLC until the completion then diluted with H_2O and extracted by DCM, dried over $MgSO_4$ and filtered. Finally, recrystallisation using 1:1 DCM:PE yielded the target product as yellow crystals (345 mg, 92 %).

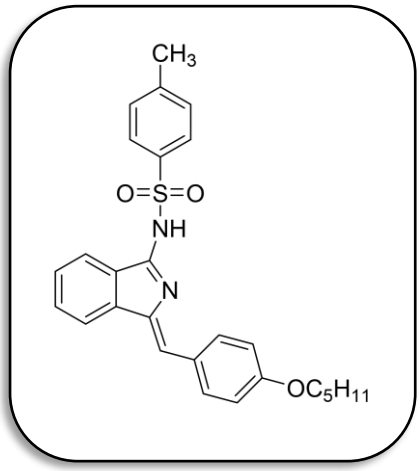

MP =. 105-106 °C.

IR (thin film cm $^{-1}$) 3374, 1593, 1511.

^{1}H NMR (500 MHz, Chloroform-*d*) δ 10.58 (s, 1H), 7.91 (dd, *J* = 7.5, 5.5 Hz, 3H), 7.76 (d, *J* = 8.0 Hz, 1H), 7.63 (td, *J* = 7.6, 1.1 Hz, 1H), 7.46 (dd, *J* = 8.2, 5.5 Hz, 3H), 7.29 (d, *J* = 8.1 Hz, 2H), 7.03 (d, *J* = 8.0 Hz, 2H), 6.68 (s, 1H), 4.02 (t, *J* = 6.6 Hz, 2H), 2.40 (S, 1H), 1.89-1.79 (m, 2H), 1.49 – 1.38 (m, 4H), 0.95 (t, *J* = 7.1 Hz, 3H).

^{13}C NMR (126 MHz, Chloroform-*d*) δ 159.50, 159.24, 143.16, 139.17, 136.46, 132.67, 132.48, 130.67, 130.14, 129.44, 128.86, 126.60, 126.49, 124.03, 119.57, 115.68, 110.15, 68.23, 28.90, 28.19, 22.47, 21.55, 14.04.

MS (MALDI-TOF): *m/z* = 460 [M, 100 %].

3.16 Triflation of (Z)-1-(4-methoxyphenylmethylene)-1H-isoindol-3-amine 165.

According to the published procedure,[108] a solution of 4-methoxy phenyl methylene aminoisoindoline **81** (0.250 g, 0.998 mmol, 1 eq), and pyridine (0.039 g, 0.495 mmol, 1.5 eq) in dry CH_2Cl_2 (30 ml) was stirred at -20 °C, then trifluoromethanesulfonic acid anhydride (0.330 g, 1.188 mmol, 1.2 eq) was added dropwise to the solution mixture over 30 min under nitrogen. The resulting mixture was left stirring overnight at room temperature. After complication of the reaction (TLCs monitored), the mixture was diluted with H_2O (60 ml) and extracted with DCM (3x15 ml). The solvent was evaporated, and the crude was purified by column chromatography (eluting with DCM) and recrystallized from DCM and petroleum ether to give the desired compound (280 mg, 74 %).

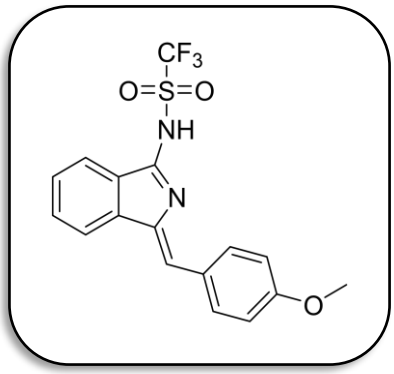

MP = 150 °C.

^{1}H NMR (400 MHz, Chloroform-*d*) δ 10.41 (s, 1H), 7.93 (dt, *J* = 7.8, 1.0 Hz, 1H), 7.77 (dt, *J* = 7.9, 0.9 Hz, 1H), 7.73 – 7.63 (m, 1H), 7.49 (ddd, *J* = 8.1, 7.3, 1.0 Hz, 1H), 7.37 (d, *J* = 8.0 Hz, 2H), 6.97 (d, *J* = 8.0 Hz, 2H), 6.86 (s, 1H), 3.82 (s, 3H).

^{13}C NMR (101 MHz, Chloroform-*d*) δ 163.10, 160.70, 136.37, 133.92, 131.68, 130.60, 129.56, 129.44, 125.77, 124.58, 119.85, 115.45, 114.66, 55.50, 53.44.

MS (MALDI-TOF): m/z 382 [M, 100 %].

3.17 Synthesis of unsymmetrical aza (dibenzo) dipyrromethene derivatives.

3.17.1 Dimerization of (Z)-1-(4-methoxyphenylmethylene)-1H-isoindol-3-amine 81 and (Z)-1-(4-pentaloxyphenylmethylene)-1H-isoindol-3-amine 138

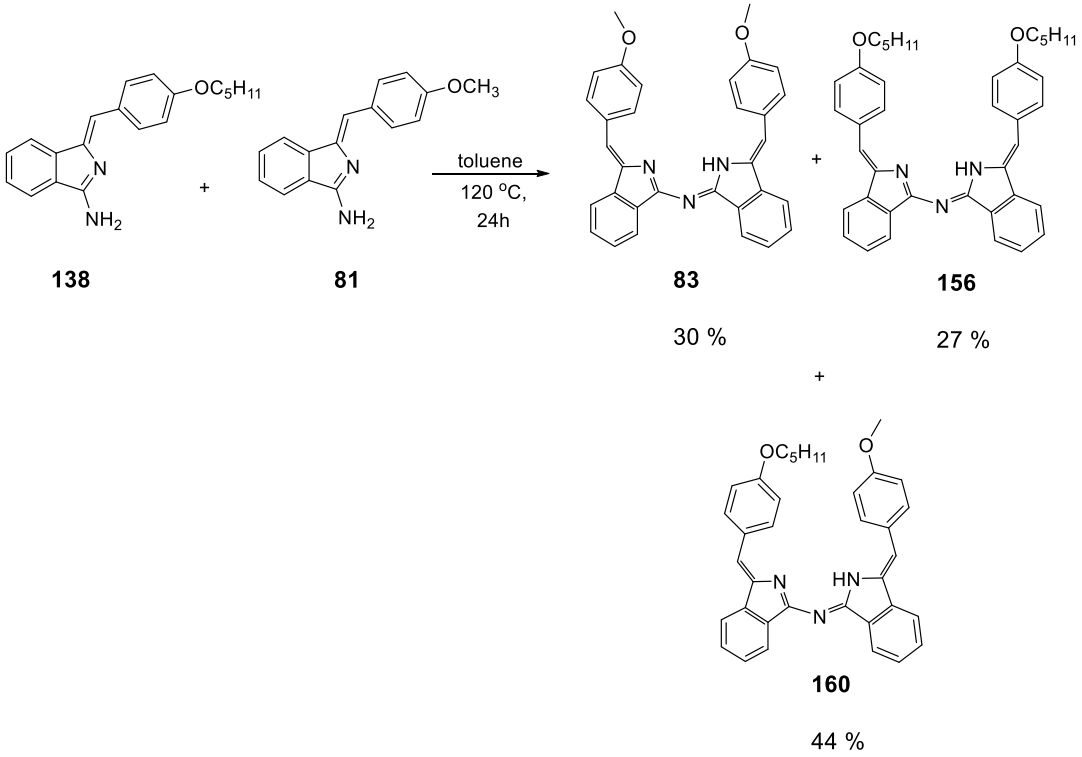

A mixture of aminoisoindoline **138** (0.200 g, 0.652 mmol, 1 eq) and compound **81** (0.195 g, 0.783 mmol, 1.2 eq) was dissolved in (12 ml) toluene. The mixture was refluxed overnight. After evaporating the solvents, the crude mixture was purified by column chromatography using DCM and petroleum ether 3:1. The isolated compounds were recrystallised from 1:1 DCM and methanol to produce compound **83** (55 mg, 30 %), compound **156** (53 mg, 27 %), and the desired unsymmetrical dimer **160** (155 mg, 44 %).

- **Compound 160**

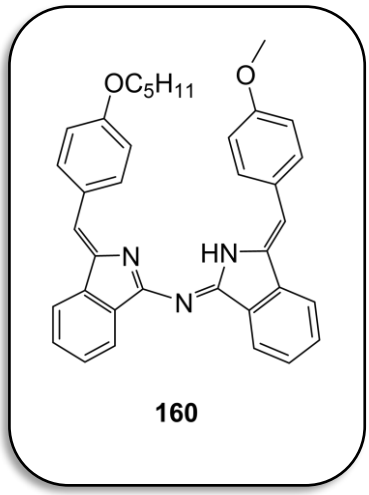

160

MP = 151-152 °C.

Rf = 0.56 (DCM).

IR (thin film cm $^{-1}$) 2933 (N-H), 1580, 1509.

^{1}H NMR (500 MHz, Chloroform-*d*) δ 8.10 (d, *J* = 7.5 Hz, 2H), 7.88 – 7.83 (m, 4H), 7.80 (dd, *J* = 7.5, 1.1 Hz, 2H), 7.53 (td, *J* = 7.4, 1.2 Hz, 2H), 7.50 – 7.46 (m, 2H), 6.78 (s, 2H), 6.62 (dd, *J* = 8.8, 2.8 Hz, 4H), 3.79 (t, *J* = 6.7 Hz, 2H), 3.69 (s, 3H), 1.80 – 1.71 (m, 2H), 1.50 – 1.36 (m, 4H), 0.95 (t, *J* = 7.1 Hz, 3H).

^{13}C NMR (126 MHz, Chloroform-*d*) δ 165.45, 159.14, 158.81, 140.10, 139.86, 139.73, 139.67, 131.19, 130.00, 129.98, 128.34, 128.11, 127.97, 122.48, 119.17, 115.13, 114.62, 67.88, 55.00, 28.94, 28.16, 22.50, 13.80.

MS (MALDI-TOF): *m/z* = 539 [M,100 %].

UV−Vis (CH_2Cl_2) λmax/nm (ε/$dm^3.mol^{-1}.cm^{-1}$): 360 ($9.7x10^4$), 500 ($1.9x10^4$).

3.17.2 Synthesis of unsymmetrical aza (dibenzo) dipyrromethene 160 by reacting of (Z)-1-(4-pentyloxyphenylmethylene)-1H-isoindol-3-amine tosylate 164, and compound 81

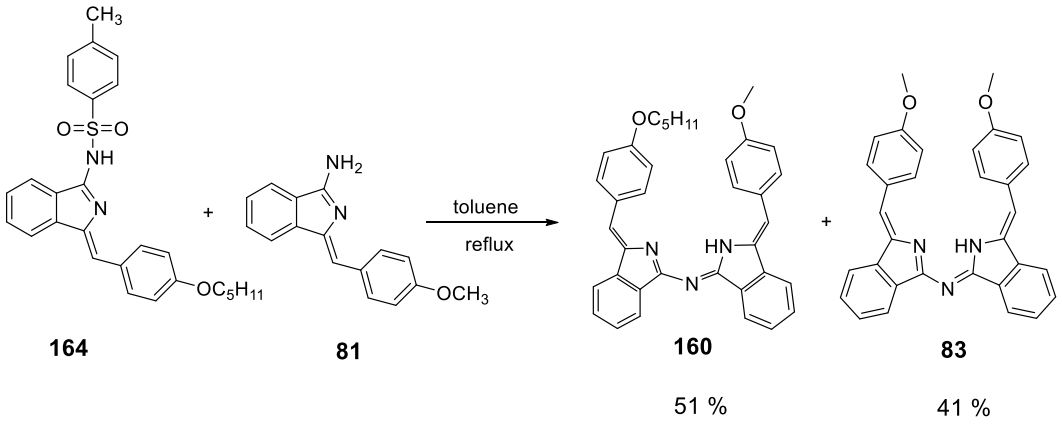

A mixture of compound **164** (0.050 g, 0.108 mmol, 1 eq) and compound **81** (0.049 g, 0.196 mmol, 1.8 eq) was dissolved in (4 ml) toluene. The mixture was refluxed overnight. After evaporating the solvents, the crude mixture was purified by column chromatography using DCM and petroleum ether 3:1. The isolated compounds were recrystallised from 1:1 DCM and methanol to produce compound **83** (20 mg, 41 %), and the desired unsymmetrical compound **160** (30 mg, 51 %).

3.17.3 Synthesis of unsymmetrical aza (dibenzo) dipyrromethene 160 by reacting of (Z)-1-(4-pentyloxyphenylmethylene)-1H-isoindol-3-amine 138, and 4-methoxy phenyl methylene aminoisoindoline triflate 165

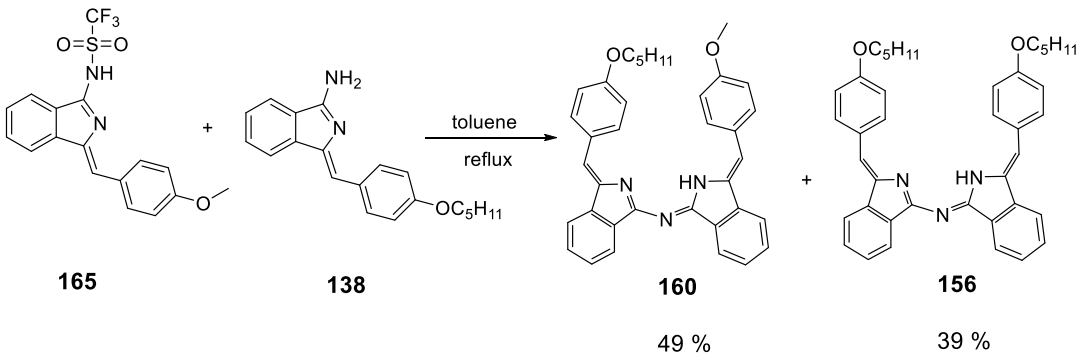

A mixture of compound **165** (0.060 g, 0.156 mmol, 1 eq) and compound **138** (0.062 g, 0.202 mmol, 1.3 eq) was dissolved in (4 ml) toluene. The mixture was refluxed overnight. After evaporating the solvents, the crude mixture was purified by column chromatography using DCM and petroleum ether 3:1. The isolated compounds were recrystallised from 1:1 DCM and methanol to produce compound **156** (23 mg, 39 %), and the desired unsymmetrical compound **160** (42 mg, 49 %).

3.17.4 Synthesis of unsymmetrical aza (dibenzo) dipyrromethene 161 by reacting of (Z)-1-(4-methoxyphenylmethylene)-1H-isoindol-3-amine tosylate 163, and 4-cyano phenyl methylene aminoisoindoline 154

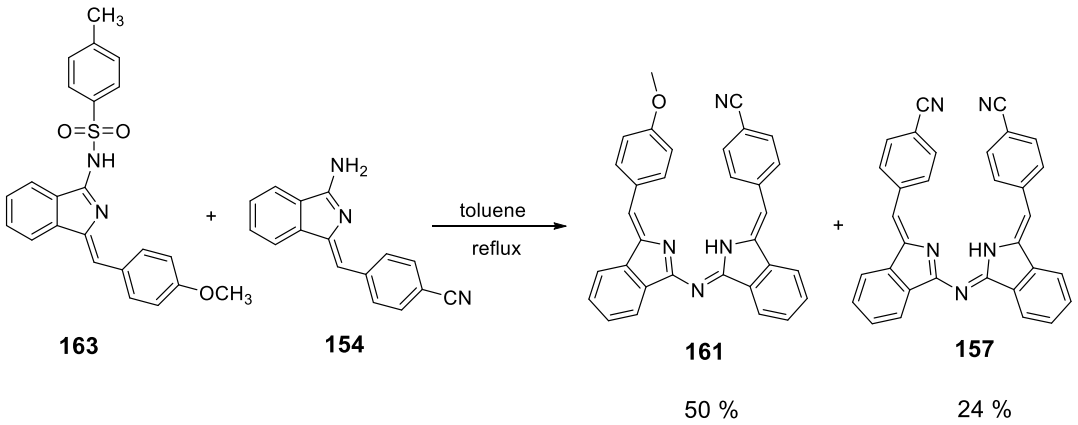

163 **154** **161** **157**

50 % 24 %

A mixture of compound **163** (0.082 g, 0.203 mmol, 1 eq) and compound **154** (0.050 g, 0.203 mmol, 1 eq) was dissolved in (4 ml) toluene. The mixture was refluxed overnight. After evaporating the solvents, the crude mixture purified was by column chromatography using DCM and petroleum ether 3:1. The isolated compounds were recrystallised from 1:1 DCM and methanol to produce compound **157** (12 mg, 24 %), and the desired unsymmetrical compound **161** (49 mg, 50 %).

- **Compound 161**

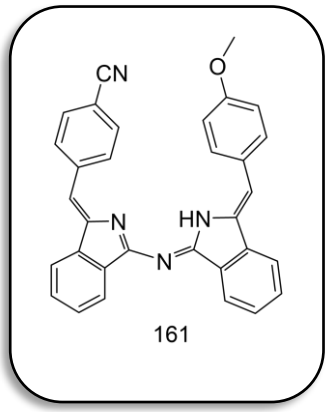

161

MP = 219-220 °C.

Rf = 0.5 (DCM).

IR (thin film cm $^{-1}$) 2225, 1571.

^{1}H NMR (500 MHz, Acetone-d_6) δ 13.08 (s, 2H), 8.01 (d, *J* = 8.1 Hz, 2H), 7.97 – 7.88 (m, 4H), 7.74 (d, *J* = 8.3 Hz, 2H), 7.56 – 7.44 (m, 4H), 7.25 (d, *J* = 8.3 Hz, 2H), 7.00 (s, 1H), 6.97 (s, 1H), 6.56 (d, *J* = 8.7 Hz, 2H), 3.67 (s, 3H).

^{13}C NMR (126 MHz, Acetone-d_6) 159.90, 140.85, 132.44, 133.18, 130.80, 130.46, 130.08, 129.00, 128.32, 122.14, 121.95, 120.24, 119.89, 118.45, 114.80, 114.62, 112.53, 110.26, 54.76.

MS (MALDI-TOF): *m/z* = 478 [M, 100 %].

UV−Vis (CH_2Cl_2) λmax/nm (ε/$dm^3.mol^{-1}.cm^{-1}$): 362 ($6.8x10^4$), 495 ($1.0x10^4$).

3.17.5 Synthesis of unsymmetrical aza (dibenzo) dipyrromethene 161 by reacting of (Z)-1-(4-methoxyphenylmethylene)-1H-isoindol-3-amine triflate 165, and 4-cyano phenyl methylene aminoisoindoline 154

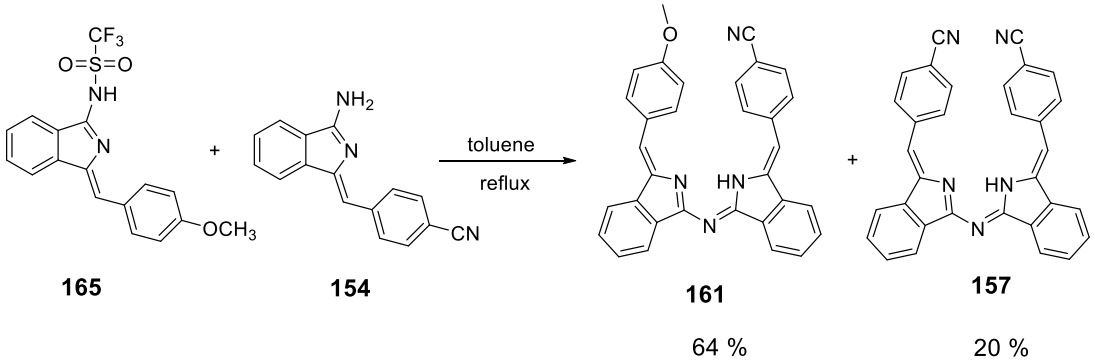

165 **154** **161** 64 % **157** 20 %

A mixture of compound **165** (0.077 g, 0.203 mmol, 1 eq) and compound **154** (0.050 g, 0.203 mmol, 1eq) was dissolved in (4 ml) toluene. The mixture was refluxed overnight. After evaporating the solvents, the crude mixture was purified by column chromatography using DCM and petroleum ether 3:1. The isolated compounds were recrystallised from 1:1 DCM and methanol to produce compound **157** (10 mg, 20 %), and the desired unsymmetrical compound **161** (63 mg, 64 %).

3.17.6 Dimerization of (Z)-1-(4-pentaloxyphenylmethylene)-1H-isoindol-3-amine tosylate 164, and (Z)-1-(4-benzonitlile methylene)-1H-isoindol-3-amine 154

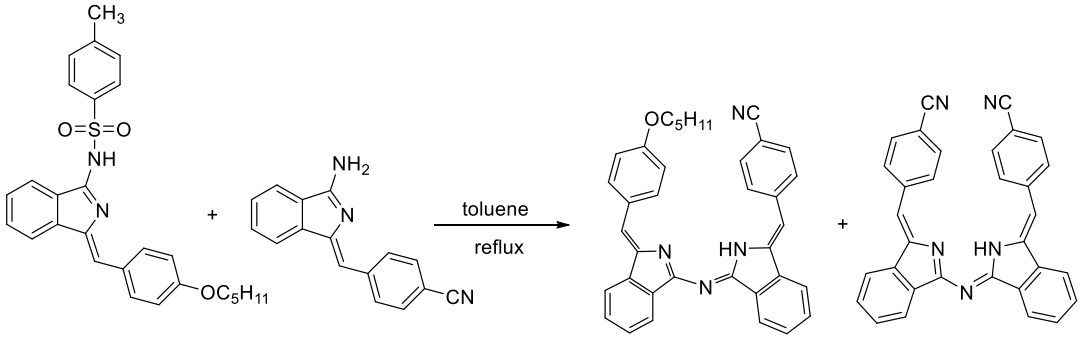

164 **154** **162** 49 % **157** 23 %

A mixture of compound **164** (0.093 g, 0.203 mmol, 1 eq) and compound **154** (0.050 g, 0.203 mmol, 1 eq) was dissolved in (4 ml) toluene. The mixture was refluxed overnight. After evaporating the solvents, the crude mixture was purified by column chromatography using DCM and petroleum ether 3:1. The isolated compounds were recrystallised from 1:1 DCM and methanol to produce compound **157** (11 mg, 23 %), and the desired unsymmetrical compound **162** (54 mg, 49 %).

- **Compound 162**

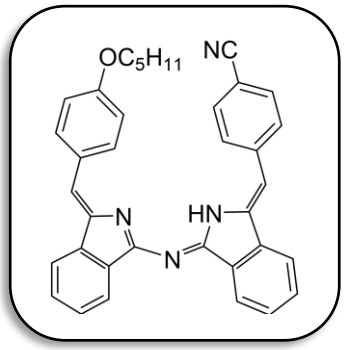

MP =197-198 °C.

Rf = 0.63 (DCM).

IR (thin film cm $^{-1}$) 2993, 2220, 1573.

^{1}H NMR (500 MHz, Acetone-d_6) δ 13.08 (s, 1H), 8.02 (d, *J* = 8.4 Hz, 2H), 7.98 – 7.89 (m, 4H), 7.73 (d, *J* = 8.1 Hz, 2H), 7.56 – 7.44 (m, 4H), 7.24 (d, *J* = 8.2 Hz, 2H), 7.00 (s, 1H), 6.97 (s, 1H), 6.56 (d, *J* = 8.2 Hz, 2H), 3.81 (t, *J* = 6.6 Hz, 2H), 1.72 – 1.65 (m, 2H), 1.38 – 1.26 (m, 4H), 0.83 (t, *J* = 7.3 Hz, 3H).

^{13}C NMR (126 MHz, Acetone-d_6) 156.33, 151.24, 143.41, 138.19, 132.40, 131.19, 130.81, 130.46, 130.08, 129.00, 128.30, 127.80, 122.14, 121.94, 120.24, 119.87, 115.05, 112.51, 67.78, 54.06, 28.04, 22.31, 13.44.

MS (MALDI-TOF): *m/z* = 534 [M, 100 %].

UV−Vis (CH_2Cl_2) λmax/nm (ε/dm^3.mol^{-1}.cm^{-1}): 363 (8.7x10^4), 508 (1.2x10^4).

3.18 Synthesis of aza (dibenzo) BODIPYs derivatives.

3.18.1 Aza (dibenzo) BODIPY compound 172.

A solution of aza (dibenzo) dipyrromethene **155** (0.100 g, 0.206 mmol, 1 eq) was stirred in dry DCM (20 ml), then DBU (0.30 ml, 2.06 mmol, 10 eq) and $BF_3.Et_2O$ (1.50 g, 10.30 mmol, 50 eq) were added to the reaction mixture. The mixture was left stirring overnight at room temperature. After 24 h yellow spot appeared on the TLC, trimethylsilyl chloride (1.5 ml) was added to the reaction mixture, then the mixture was refluxed for 3 h. After completion of the reaction (TLCs followed), the mixture was cooled down at room temperature, diluted by DCM (50 ml), and washed by HCl (1 M, 50 ml). The orange crystals were isolated from recrystallisation from 1:1 DCM:PE to yield the desired product **172** in (80 mg, 73 %).

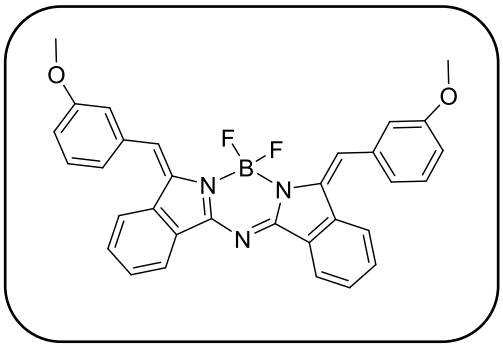

MP = 190-192 °C.

Rf = 0.66 (DCM).

IR (thin film cm^{-1}) 2995, 2830, 1574.

^{1}H NMR (500 MHz, Chloroform-*d*) δ 8.18 (dd, *J* = 7.7, 1.1 Hz, 1H), 7.84 (s, 1H), 7.70 (d, *J* = 7.9 Hz, 1H), 7.54 (td, *J* = 7.5, 1.0 Hz, 1H), 7.46 (ddd, *J* = 8.3, 7.4, 1.2 Hz, 1H), 7.40 (t, *J* = 7.8 Hz, 1H), 7.22 (d, *J* = 7.4 Hz, 1H), 7.15 (s, 1H), 6.98 (dd, *J* = 8.3, 2.6 Hz, 1H), 3.85 (s, 3H).

^{13}C NMR (126 MHz, Chloroform-*d*) δ 163.79, 159.75, 138.71, 136.26, 133.20, 132.50, 129.72, 129.31, 125.39, 123.72, 123.66, 122.06, 119.71, 114.91, 114.44, 55.40.

^{19}F NMR (376 MHz, Chloroform-*d*) δ -139.12 (dd, *J* = 61.1, 30.5 Hz).

MS (MALDI-TOF): *m/z* = 530 [M-1].

UV−Vis (CH_2Cl_2) λmax/nm (ε/$dm^3.mol^{-1}.cm^{-1}$): 321 ($8.2x10^4$), 449 ($9.0x10^4$).

Fluorescence (DCM, Excitation at 445 nm): 523 nm.

3.18.2 Aza (dibenzo) BODIPY compound 173.

A solution of aza (dibenzo) dipyrromethene **156** (0.100 g, 0.168 mmol, 1 eq) was stirred in dry DCM (20 ml), then DBU (0.251 ml, 1.680 mmol, 10 eq) and $BF_3.Et_2O$ (1.20 g, 8.40 mmol, 50 eq) were added to the reaction mixture. The mixture was left stirring overnight at room temperature. After 24 h yellow spot appeared on the TLC, trimethylsilyl chloride (1.5 ml) was added to the reaction mixture, then the mixture was refluxed for 3 h. after completion of the reaction (TLCs followed), the mixture was cooled down at room temperature, diluted by DCM (50 ml), and washed by HCl (1 M, 50 ml). The orange crystals were isolated from recrystallisation from DCM:PE to yield the desired product **173** in (80 mg, 74 %).

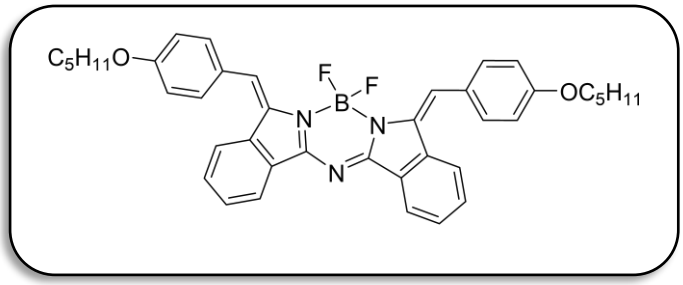

MP = 170-171 °C.

Rf = 0.83 (DCM).

IR (thin film cm $^{-1}$) 2929, 1648.

^{1}H NMR (500 MHz, Methylene Chloride-d_2) δ 8.28 (d, *J* = 7.5 Hz, 1H), 7.89 (dt, *J* = 7.9, 0.9 Hz, 1H), 7.82 (s, 1H), 7.62 (d, *J* = 8.0 Hz, 2H), 7.60 – 7.52 (m, 2H), 7.05 (d, *J* = 8.0 Hz, 2H), 4.10 (t, *J* = 6.6 Hz, 2H), 1.91 – 1.85 (m, 2H), 1.54 – 1.45 (m, 4H), 1.00 (t, *J* = 7.2 Hz, 3H).

^{13}C NMR (126 MHz, Methylene Chloride-d_2) 159.97, 140.05, 132.22, 132.17, 131.35, 130.91, 129.15, 126.86, 125.73, 123.48, 123.24, 114.60, 113.57, 68.22, 48.82, 28.94, 22.48, 13.80.

^{19}F NMR (376 MHz, Methylene Chloride-d_2) δ -138.48 (dd, *J* = 63.53, 33.73 Hz).

MS (MALDI-TOF): *m/z* = 643 [M,100 %].

UV−Vis (CH_2Cl_2) λmax/nm (ε/$dm^3.mol^{-1}.cm^{-1}$): 324 ($6.5x10^4$), 475 ($7.5x10^4$).

Fluorescence (DCM, Excitation at 475 nm): 561 nm.

3.18.3 Aza (dibenzo) BODIPY compound 174.

A solution of aza (dibenzo) dipyrromethene **157** (0.100 g, 0.211 mmol, 1 eq) was stirred in dry DCM (20 ml), then DBU (0.31 ml, 2.11 mmol, 10 eq) and $BF_3.Et_2O$ (1.50 g, 10.55 mmol, 50 eq) were added to the reaction mixture. The mixture was left stirring overnight at room temperature. After 24 h yellow spot appeared on the TLC, trimethylsilyl chloride (1.5 ml) was added to the reaction mixture, then the mixture was refluxed for 3 h. after completion of the reaction (TLCs followed), the mixture was cooled down at room temperature, diluted by DCM (50 ml), and washed by HCl (1 M, 50 ml). The orange crystals were isolated from recrystallisation from DCM:PE to yield the desired product **174** in (80 mg, 73 %).

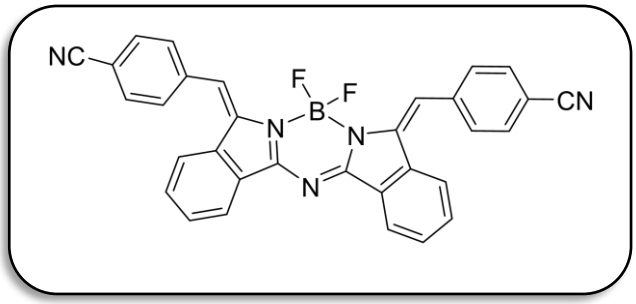

MP = 329-330 °C.

Rf = 0.4 (DCM).

IR (thin film cm^{-1}) 2227, 1499.

^{1}H NMR (400 MHz, Chloroform-*d*) δ 8.21 (d, *J* = 7.7 Hz, 1H), 7.82 – 7.72 (m, 5H), 7.60 (ddd, *J* = 7.7, 6.8, 1.4 Hz, 1H), 7.56 – 7.47 (m, 2H).

^{13}C NMR (126 MHz, Chloroform-*d*) 164.44, 139.95, 139.70, 132.92, 132.87, 132.62, 132.49, 130.41, 130.16, 124.25, 123.32, 122.87, 118.53, 112.31.

^{19}F NMR (376 MHz, Chloroform-*d*) δ -139.16 (dd, *J* = 62.44, 30.25 Hz).

MS (MALDI-TOF): *m/z* = 521 [M, 100 %].

UV−Vis (CH_2Cl_2) λmax/nm (ε/$dm^3.mol^{-1}.cm^{-1}$): 328 ($7.6x10^4$), 441 ($9.2x10^4$).

Fluorescence (DCM, Excitation at 441 nm): 527 nm.

3.18.4 Aza (dibenzo) BODIPY compound 175.

A solution of aza (dibenzo) dipyrromethene **162** (0.100 g, 0.187 mmol, 1 eq) was stirred in dry DCM (20 ml), then DBU (0.28 ml, 1.87 mmol, 10 eq) and $BF_3.Et_2O$ (1.32 g, 9.35 mmol, 50 eq) were added to the reaction mixture. The mixture was left stirring overnight at room temperature. After 24 h yellow spot appeared on the TLC, trimethylsilyl chloride (1.5 ml) was added to the reaction mixture, then the mixture was refluxed for 3 h. after completion of the reaction (TLCs followed), the mixture was cooled down at room temperature, diluted by DCM (50 ml), and washed by HCl (1 M, 50 ml). The orange crystals were isolated from recrystallisation from DCM:PE to yield the desired product **175** in (77 mg, 70 %).

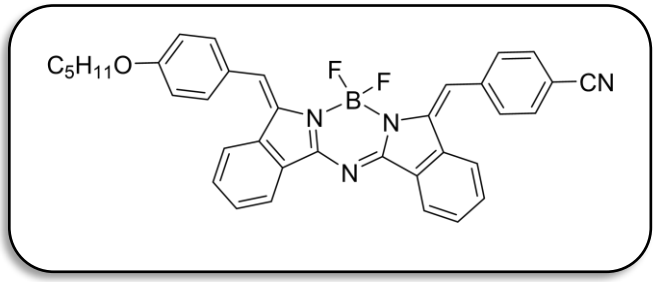

MP = 234-235 ℃.

Rf = 0.71 (DCM).

IR (thin film cm $^{-1}$) 2997, 2223.

^{1}H NMR (500 MHz, Methylene Chloride-d_2) δ 8.25 (dt, *J* = 7.7, 1.1 Hz, 2H), 7.92 (dt, *J* = 7.8, 0.9 Hz, 1H), 7.86 (s, 1H), 7.85 – 7.81 (m, 2H), 7.80 – 7.77 (m, 2H), 7.75 (s, 1H), 7.66 – 7.51 (m, 7H), 7.06 (d, *J* = 8.6 Hz, 2H), 4.10 (t, *J* = 6.6 Hz, 2H), 1.93 – 1.84 (m, 2H), 1.55 – 1.44 (m, 4H), 1.00 (t, *J* = 7.2 Hz, 3H).

^{13}C NMR (126 MHz, Methylene Chloride-d_2) δ 163.11, 160.15, 139.93, 137.47, 136.00, 133.45, 132.47, 132.43, 131.43, 130.35, 130.00, 129.25, 126.86, 126.67, 123.75, 123.53, 123.37, 123.25, 121.61, 118.61, 114.64, 112.01, 68.24, 28.93, 28.19, 22.47, 13.80.

^{19}F NMR (376 MHz, Methylene Chloride-d_2) δ -138.99 (dd, *J* = 62.05, 30.03 Hz).

MS (MALDI-TOF): *m/z* = 582 [M, 100 %].

UV−Vis (CH_2Cl_2) λmax/nm (ε/$dm^3.mol^{-1}.cm^{-1}$): 326 ($7.5x10^4$), 465 ($5.8x10^4$).

Fluorescence (DCM, Excitation at 465 nm): 567 nm.

3.18.5 Aza (dibenzo) BODIPY compound 176.

A solution of aza (dibenzo) dipyrromethene **161** (0.100 g, 0.208 mmol, 1 eq) was stirred in dry DCM (20 ml), then DBU (0.3 ml, 2.08 mmol, 10 eq) and $BF_3.Et_2O$ (1.50 g, 10.40 mmol, 50 eq) were added to the reaction mixture. The mixture was left stirring overnight at room temperature. After 24 h yellow spot appeared on the TLC, trimethylsilyl chloride (1.5 ml) was added to the reaction mixture, then the mixture was refluxed for 3 h. after completion of the reaction (TLCs followed), the mixture was cooled down at room temperature, diluted by DCM (50 ml), and washed by HCl (1 M, 50 ml). The orange crystals were isolated from recrystallisation from DCM:PE to yield the desired product **176** in (78 mg, 71 %).

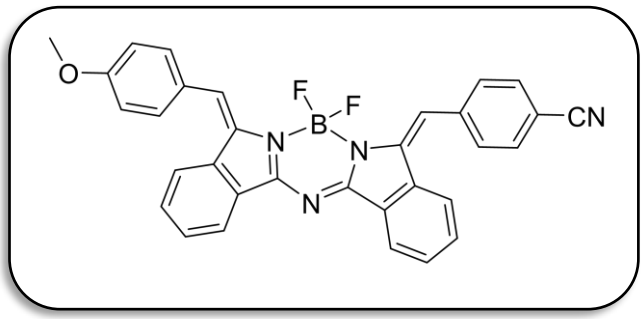

MP = 252-253 ^{o}C.

Rf = 0.63 (DCM).

IR (thin film cm $^{-1}$) 2223, 1583.

^{1}H NMR (400 MHz, Acetone-d_6) δ 8.10 – 8.06 (m, 3H), 7.84 (d, *J* = 8.4 Hz, 2H), 7.81 – 7.77 (m, 3H), 7.71 (s, 1H), 7.68 (d, *J* = 7.8 Hz, 1H), 7.61 (s, 1H), 7.56 – 7.53 (m, 5H), 7.01 (d, *J* = 8.0 Hz, 2H), 3.80 (s, 3H).

^{13}C NMR (126 MHz, Acetone-d_6) δ 164.75, 161.67, 158.81, 154.30, 137.99, 133.93, 133.03, 132.58, 131.38, 130.40, 129.56, 126.64, 123.56, 122.81, 114.32, 113.41, 112.89,54.71.

^{19}F NMR (376 MHz, Acetone-d_6) δ -138.54 (dd, *J* = 61.25, 30.00 Hz).

MS (MALDI-TOF): *m/z* = 526 [M,100 %].

UV−Vis (CH_2Cl_2) λmax/nm (ε/$dm^3.mol^{-1}.cm^{-1}$): 332 ($5.4x10^4$), 453 ($4.5x10^4$).

Fluorescence (DCM, Excitation at 453 nm): 531 nm.

3.18.6 Aza-(dibenzo) BODIPY compound 177

A solution of aza (dibenzo) dipyrromethene **160** (0.100 g, 0.185 mmol, 1 eq) was stirred in dry DCM (20 ml), then DBU (0.280 ml, 1.855 mmol, 10 eq) and $BF_3.Et_2O$ (1.30 g, 9.25 mmol, 50 eq) were added to the reaction mixture. The mixture was left stirring overnight at room temperature. After 24 h yellow spot appeared on the TLC, trimethylsilyl chloride (1.5 ml) was added to the reaction mixture, then the mixture was refluxed for 3 h. after completion of the reaction (TLCs followed), the mixture was cooled down at room temperature, diluted by DCM (50 ml), and washed by HCl (1 M, 50 ml). The orange crystals were isolated from recrystallisation from DCM:PE to yield the desired product **177** in (78 mg, 71 %).

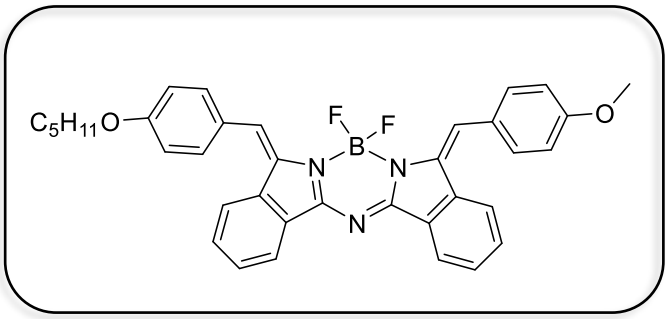

MP = 184-185 °C.

Rf = 0.67 (DCM).

IR (thin film cm $^{-1}$) 2927, 1585.

^{1}H NMR (400 MHz, Acetone-d_6) δ 8.22 (d, *J* = 7.4 Hz, 2H), 7.92 (t, *J* = 8.0 Hz, 2H), 7.82 (s, 2H), 7.74 – 7.60 (m, 8H), 7.14 (dd, *J* = 8.8, 3.3 Hz, 4H), 4.14 (t, *J* = 6.5 Hz, 2H), 3.94 (s, 3H), 1.90 – 1.83 (m, 2H), 1.57 – 1.43 (m, 4H), 0.98 (t, *J* = 7.2 Hz, 3H).

^{13}C NMR (126 MHz, Acetone-d_6) δ 162.83, 160.55, 160.14, 137.41, 135.68, 132.56, 131.34, 129.47, 126.78, 126.60, 125.53, 125.33, 123.31, 123.18, 114.82, 114.34, 113.03, 67.71, 54.82, 22.23, 22.07, 21.94, 13.42.

^{19}F NMR (376 MHz, Acetone-d_6) δ -138.15 (dd, *J* = 62.08, 30.06 Hz).

MS (MALDI-TOF): *m/z* = 587 [M, 100 %].

UV−Vis (CH_2Cl_2) λmax/nm (ε/$dm^3.mol^{-1}.cm^{-1}$): 330 ($5.6x10^4$), 474 ($7.0x10^4$).

Fluorescence (DCM, Excitation at 474 nm): 552 nm.

References

(1) Treibs, A.; Kreuzer, F. H. *European Journal of Organic Chemistry* **1968**, *718* (1), 208-223.

(2) Heisig, F.; Gollos, S.; Freudenthal, S. J.; El-Tayeb, A.; Iqbal, J.; Müller, C. E. Synthesis of BODIPY derivatives substituted with various bioconjugatable linker groups: a construction kit for fluorescent labeling of receptor ligands. *Journal of Fluorescence* **2014**, *24* (1), 213-230.

(3) Boens, N.; Leen, V.; Dehaen, W. Fluorescent indicators based on BODIPY. *Chemical Society Reviews* **2012**, *41* (3), 1130-1172.

(4) Ulrich, G.; Ziessel, R.; Harriman, A. Minireviews fluorescent molecular devices the chemistry of fluorescent BODIPY dyes. *Versatility Unsurpassed. Angewandte Chemie International Edition* **2008**, *47*, 1184-1201.

(5) Shah, M.; Thangaraj, K.; Soong, M.-L.; Wolford, L. T.; Boyer, J. H.; Politzer, I. R.; Pavlopoulos, T. G. Pyrromethene–BF2 complexes as laser dyes:1. *Heteroatom Chemistry* **1990**, *1* (5), 389-399.

(6) Chu, G. M.; Guerrero-Martínez, A.; Fernández, I.; Sierra, M. Á. Tuning the Photophysical Properties of BODIPY Molecules by π-Conjugation with Fischer Carbene Complexes. *Chemistry – A European Journal* **2014**, *20* (5), 1367-1375.

(7) Vos, d. W. E.; Pardoen, JA; Van, Koeveringe, JA; Lugtenburg. *Recl. Trav. Chim. Pays-Bas* **1977**, *96*, 306.

(8) Bañuelos, J. BODIPY Dye, the Most Versatile Fluorophore Ever? *The Chemical Record* **2016**, *16* (1), 335-348.

(9) Ziessel, R.; Ulrich, G.; Harriman, A. The chemistry of Bodipy: A new El Dorado for fluorescence tools. *New Journal of Chemistry* **2007**, *31* (4), 496-501.

(10) Boens, N.; Verbelen, B.; Dehaen, W. Postfunctionalization of the BODIPY core: synthesis and spectroscopy. *European Journal of Organic Chemistry* **2015**, *2015* (30), 6577-6595.

(11) Loudet, A.; Burgess, K. BODIPY Dyes and Their Derivatives: Syntheses and Spectroscopic Properties. *Chemical Reviews* **2007**, *107* (11), 4891-4932.

(12) Ziessel, R.; Ulrich, G.; Elliott, K. J.; Harriman, A. Electronic Energy Transfer in Molecular Dyads Built Around Boron–Ethyne-Substituted Subphthalocyanines. *Chemistry A European Joural* **2009**, *15* (20), 4980-4984.

(13) Wood, T. E.; Thompson, A. Advances in the chemistry of dipyrrins and their complexes. *Chemical Reviews* **2007**, *107* (5), 1831-1861.

(14) Boens, N.; Verbelen, B.; Ortiz, M. J.; Jiao, L.; Dehaen, W. Synthesis of BODIPY dyes through postfunctionalization of the boron dipyrromethene core. *Coordination Chemistry Reviews* **2019**, *399*, 213024.

(15) Cammidge, A. N.; Chambrier, I.; Cook, M. J.; Sosa-Vargas, L. 75 Synthesis and Properties of the Hybrid Phthalocyanine-Tetrabenzoporphyrin Macrocycles. In *Handbook of Porphyrin Science: With Applications to Chemistry, Physics, Materials Science, Engineering, Biology and Medicine—Volume 16: Synthetic Developments (Part I)*, World Scientific, 2012; pp 331-404.

(16) Burghart, A.; Thoresen, L. H.; Chen, J.; Burgess, K.; Bergström, F.; Johansson, L. B.-Å. Energy transfer cassettes based on BODIPY® dyesElectronic supplementary information (ESI) available: absorption and emission spectra of donor and acceptor A and of 1 and experimental details for the spectroscopic measurements. *Chemical Communications* **2000**, (22), 2203-2204.

(17) Killoran, J.; Allen, L.; Gallagher, J. F.; Gallagher, W. M.; Donal, F. Synthesis of BF 2 chelates of tetraarylazadipyrromethenes and evidence for their photodynamic therapeutic behaviour. *Chemical Communications* **2002**, (17), 1862-1863.

(18) Wada, M.; Ito, S.; Uno, H.; Murashima, T.; Ono, N.; Urano, T.; Urano, Y. Synthesis and optical properties of a new class of pyrromethene–BF2 complexes fused with rigid bicyclo rings and benzo derivatives. *Tetrahedron Letters* **2001**, *42* (38), 6711-6713.

(19) Burghart, A.; Kim, H.; Welch, M. B.; Thoresen, L. H.; Reibenspies, J.; Burgess, K.; Bergström, F.; Johansson, L. B.-Å. 3, 5-Diaryl-4, 4-difluoro-4-bora-3a, 4a-diaza-s-indacene (BODIPY) dyes: synthesis, spectroscopic, electrochemical, and structural properties. *The Journal of Organic Chemistry* **1999**, *64* (21), 7813-7819.

(20) Jean-Gérard, L.; Vasseur, W.; Scherninski, F.; Andrioletti, B. Recent advances in the synthesis of [a]-benzo-fused BODIPY fluorophores. *Chemical Communications* **2018**, *54* (92), 12914-12929.

(21) Chen, J.; Burghart, A.; Derecskei-Kovacs, A.; Burgess, K. 4, 4-Difluoro-4-bora-3a, 4a-diaza-s-indacene (BODIPY) dyes modified for extended conjugation and restricted bond rotations. *The Journal of Organic Chemistry* **2000**, *65* (10), 2900-2906.

(22) Xuan, S.; Zhao, N.; Ke, X.; Zhou, Z.; Fronczek, F. R.; Kadish, K. M.; Smith, K. M.; Vicente, M. G. H. Synthesis and spectroscopic investigation of a series of push–pull boron dipyrromethenes (BODIPYs). *The Journal of Organic Chemistry* **2017**, *82* (5), 2545-2557.

(23) Wang, Y. W.; Descalzo, A. B.; Shen, Z.; You, X. Z.; Rurack, K. Dihydronaphthalene-Fused Boron–Dipyrromethene (BODIPY) Dyes: Insight into the Electronic and Conformational Tuning Modes of BODIPY Fluorophores. *Chemistry–A European Journal* **2010**, *16* (9), 2887-2903.

(24) Lee, C.-H.; Lindsey, J. S. One-flask synthesis of meso-substituted dipyrromethanes and their application in the synthesis of trans-substituted porphyrin building blocks. *Tetrahedron* **1994**, *50* (39), 11427-11440.

(25) Boyle, R. W.; Bruckner, C.; Posakony, J.; James, B. R.; Dolphin, D. 5-Phenyldipyrromethane and 5, 15-Diphenylporphyrin. *Organic Syntheses* **2003**, *76*, 287-287.

(26) Dolušić, E.; Ngo, H. T.; Maes, W.; Dehaen, W. Efficient synthesis of aryldipyrromethanes in water and their application in the synthesis of corroles and dipyrromethenes. *Arkivoc* **2007**, *10*, 307-324.

(27) Brückner, C.; Karunaratne, V.; Rettig, S. J.; Dolphin, D. Synthesis of meso-phenyl-4, 6-dipyrrins, preparation of their Cu (II), Ni (II), and Zn (II) chelates, and structural characterization of bis [meso-phenyl-4, 6-dipyrrinato] Ni (II). *Canadian Journal of Chemistry* **1996**, *74* (11), 2182-2193.

(28) Yu, L.; Muthukumaran, K.; Sazanovich, I. V.; Kirmaier, C.; Hindin, E.; Diers, J. R.; Boyle, P. D.; Bocian, D. F.; Holten, D.; Lindsey, J. S. Excited-state energy-transfer dynamics in self-assembled triads composed of two porphyrins and an intervening bis (dipyrrinato) metal complex. *Inorganic Chemistry* **2003**, *42* (21), 6629-6647.

(29) Wories, H.; Koek, J.; Lodder, G.; Lugtenburg, J.; Fokkens, R.; Driessen, O.; Mohn, G. A novel water-soluble fluorescent probe: Synthesis, luminescence and biological properties of the sodium salt of the 4-sulfonato-3, 3′, 5, 5′-tetramethyl-2, 2′-pyrromethen-1, 1′-BF2 complex. *Collection of Chemical Works of the Netherlands* **1985**, *104* (11), 288-291.

(30) Zhao, C.; An, J.; Zhou, L.; Fei, Q.; Wang, F.; Tan, J.; Shi, B.; Wang, R.; Guo, Z.; Zhu, W.-H. Transforming the recognition site of 4-hydroxyaniline into 4-methoxyaniline grafted onto a BODIPY core switches the selective detection of peroxynitrite to hypochlorous acid. *Chemical Communications* **2016**, *52* (10), 2075-2078.

(31) Boyer, J. H.; Haag, A. M.; Sathyamoorthi, G.; Soong, M. L.; Thangaraj, K.; Pavlopoulos, T. G. Pyrromethene–BF2 complexes as laser dyes: 2. *Heteroatom Chemistry* **1993**, *4* (1), 39-49.

(32) Li, T.; Gu, W.; Yu, C.; Lv, X.; Wang, H.; Hao, E.; Jiao, L. Syntheses and Photophysical Properties of meso-Phenylene ridged Boron Dipyrromethene Monomers, Dimers and Trimer. *Chinese Journal of Chemistry* **2016**, *34* (10), 989-996.

(33) Xie, R.; Yi, Y.; He, Y.; Liu, X.; Liu, Z.-X.; Upadhyaya, K.; Ajay, A.; Mahar, R.; Pandey, R.; Kumar, B. A simple BODIPYeimidazole-based probe for the colorimetric and fluorescent sensing of Cu (II) and Hg (II) pp 8541e8546. *Tetrahedron* **2013**, *69* (40), 8535e8539.

(34) Li, Z.; Mintzer, E.; Bittman, R. First synthesis of free cholesterol− BODIPY conjugates. *The Journal of Organic Chemistry* **2006**, *71* (4), 1718-1721.

(35) Yakubovskyi, V. P.; Shandura, M. P.; Kovtun, Y. P. Boradipyrromethenecyanines. *European Journal of Organic Chemistry*: 2009; pp 3237-3243.

(36) Wu, L.; Burgess, K. A new synthesis of symmetric boraindacene (BODIPY) dyes. *Chemical Communications* **2008**, (40), 4933-4935.

(37) Deng, Y.; Bennink, J. R.; Kang, H.; Haugland, R. P.; Yewdell, J. Fluorescent conjugates of brefeldin A selectively stain the endoplasmic reticulum and Golgi complex of living cells. *Journal of Histochemistry & Cytochemistry* **1995**, *43* (9), 907-915.

(38) Handy, S.; Lavender, K. Organic synthesis in deep eutectic solvents: Paal–Knorr reactions. *Tetrahedron Letters* **2013**, *54* (33), 4377-4379.

(39) Kotali, A.; Tsoungas, P. G. Oxidation of N-Aroylhydrazones of o-hydroxyaryl ketones withlead (IV) acetate: A facile route to aromatic o-diketones. *Tetrahedron Letters* **1987**, *28* (37), 4321-4322.

(40) Ito, S.; Murashima, T.; Ono, N. A new synthesis of pyrroles fused with polycyclic skeletons. *Journal of the Chemical Society, Perkin Transactions 1* **1997**, (21), 3161-3166.

(41) Díaz-Moscoso, A.; Emond, E.; Hughes, D. L.; Tizzard, G. J.; Coles, S. J.; Cammidge, A. N. Synthesis of a class of core-modified aza-BODIPY derivatives. *The Journal of Organic Chemistry* **2014**, *79* (18), 8932-8936.

(42) Li, W.; Gong, Q.; Guo, X.; Wu, Q.; Chang, F.; Wang, H.; Zhang, F.; Hao, E.; Jiao, L. Synthesis, Reactivity, and Properties of a Class of π-Extended BODIPY Derivatives. *The Journal of Organic Chemistry* **2021**, *86* (23), 17110-17118.

(43) Killoran, J.; Allen, L.; Gallagher, J. F.; Gallagher, W. M.; O′Shea, D. F. Synthesis of BF2 chelates of tetraarylazadipyrromethenes and evidence for their photodynamic therapeutic behaviour. *Chemical Communications* **2002**, (17), 1862-1863.

(44) Donyagina, V. F.; Shimizu, S.; Kobayashi, N.; Lukyanets, E. A. Synthesis of N, N-difluoroboryl complexes of 3, 3′-diarylazadiisoindolylmethenes. *Tetrahedron Letters* **2008**, *49* (42), 6152-6154.

(45) Lu, H.; Shimizu, S.; Mack, J.; Shen, Z.; Kobayashi, N. Synthesis and Spectroscopic Properties of Fused-Ring-Expanded Aza-Boradiazaindacenes. *Chemistry–An Asian Journal* **2011**, *6* (4), 1026-1037.

(46) Gorman, A.; Killoran, J.; O'Shea, C.; Kenna, T.; Gallagher, W. M.; O'Shea, D. F. In Vitro Demonstration of the Heavy-Atom Effect for Photodynamic Therapy. *Journal of the American Chemical Society* **2004**, *126* (34), 10619-10631. DOI: 10.1021/ja047649e.

(47) Zhao, W.; Carreira, E. M. Conformationally Restricted Aza-Bodipy: A Highly Fluorescent, Stable, Near-Infrared-Absorbing Dye. *A Journal of the German Chemical society* **2005**, *117* (11), 1705-1707.

(48) Jiang, X.-J.; Lo, P.-C.; Tsang, Y.-M.; Yeung, S.-L.; Fong, W.-P.; Ng, D. K. P. Phthalocyanine–Polyamine Conjugates as pH-Controlled Photosensitizers for Photodynamic Therapy. *Chemistry A European Joural* **2010**, *16* (16), 4777-4783.

(49) Adarsh, N.; Shanmugasundaram, M.; Avirah, R. R.; Ramaiah, D. Aza-BODIPY Derivatives: Enhanced Quantum Yields of Triplet Excited States and the Generation of Singlet Oxygen and their Role as Facile Sustainable Photooxygenation Catalysts. *Chemistry A European Joural* **2012**, *18* (40), 12655-12662.

(50) Rogers, M. A. T. 156. 2: 4-Diarylpyrroles. Part I. Synthesis of 2: 4-diarylpyrroles and 2: 2′: 4: 4′-tetra-arylazadipyrromethines. *Journal of the Chemical Society (Resumed)* **1943**, 590-596.

(51) Davies, W.; Rogers, M. A. 46. 2: 4-Diarylpyrroles. Part IV. The formation of acylated 5-amino-2: 4-diphenylpyrroles from β-benzoly-α-phenylpropionitrile and some notes on the Leuckart reaction. *Journal of the Chemical Society (Resumed)* **1944**, 126-131.

(52) Ge, Y.; O'Shea, D. F. Azadipyrromethenes: from traditional dye chemistry to leading edge applications. *Chemical Society Reviews* **2016**, *45* (14), 3846-3864.

(53) Allik, T. H.; Hermes, R. E.; Sathyamoorthi, G.; Boyer, J. H. Spectroscopy and laser performance of new BF2-complex dyes in solution. 1994; *International Society for Optics and Photonics*: Vol. 2115, pp 240-248.

(54) Sathyamoorthi, G.; Soong, M. L.; Ross, T. W.; Boyer, J. H. Fluorescent tricyclic β-azavinamidine–BF2 complexes. *Heteroatom Chemistry* **1993**, *4* (6), 603-608.

(55) Hall, M. J.; McDonnell, S. O.; Killoran, J.; O'Shea, D. F. A modular synthesis of unsymmetrical tetraarylazadipyrromethenes. *The Journal of Organic Chemistry* **2005**, *70* (14), 5571-5578.

(56) McDonnell, S. O.; O'Shea, D. F. Near-infrared sensing properties of dimethlyamino-substituted BF2− azadipyrromethenes. *Organic Letters* **2006**, *8* (16), 3493-3496.

(57) Antina, E. V.; Bumagina, N. A. Tetraaryl-substituted aza-BODIPY: synthesis, spectral properties, and possible applications (microreview). *Chemistry of Heterocyclic Compounds* **2017**, *53*, 39-41.

(58) Jiao, L.; Wu, Y.; Wang, S.; Hu, X.; Zhang, P.; Yu, C.; Cong, K.; Meng, Q.; Hao, E.; Vicente, M. G. H. Accessing near-infrared-absorbing BF2-azadipyrromethenes via a push–pull effect. *The Journal of Organic Chemistry* **2014**, *79* (4), 1830-1835.

(59) Le Guennic, B.; Maury, O.; Jacquemin, D. Aza-boron-dipyrromethene dyes: TD-DFT benchmarks, spectral analysis and design of original near-IR structures. *Physical Chemistry Chemical Physics* **2012**, *14* (1), 157-164.

(60) Bredereck, H.; Vollmann, H. W. Synthesen in der heterocyclischen Reihe, XV. Über 1-[3-Aryl-isoindolyl-(1)-imino]-3-aryl-1H-isoindole. *European Journal of Organic Chemistry* **1972**, *105* (7), 2271-2283.

(61) Wang, J.; Yu, C.; Hao, E.; Jiao, L. Conformationally restricted and ring-fused aza-BODIPYs as promising near infrared absorbing and emitting dyes. *Coordination Chemistry Reviews* **2022**, *470*, 214709.

(62) Rurack, K.; Kollmannsberger, M.; Daub, J. A highly efficient sensor molecule emitting in the near infrared (NIR): 3, 5-distyryl-8-(p-dimethylaminophenyl) difluoroboradiaza-s-indacene. *New Journal of Chemistry* **2001**, *25* (2), 289-292.

(63) Killoran, J.; McDonnell, S. O.; Gallagher, J. F.; O'Shea, D. F. A substituted BF 2-chelated tetraarylazadipyrromethene as an intrinsic dual chemosensor in the 650–850 nm spectral range. *New Journal of Chemistry* **2008**, *32* (3), 483-489.

(64) Mueller, T.; Gresser, R.; Leo, K.; Riede, M. Organic solar cells based on a novel infrared absorbing aza-bodipy dye. *Solar energy materials and solar cells* **2012**, *99*, 176-181.

(65) Gresser, R.; Hummert, M.; Hartmann, H.; Leo, K.; Riede, M. Synthesis and characterization of near-infrared absorbing benzannulated aza-BODIPY dyes. *Chemistry–A European Journal* **2011**, *17* (10), 2939-2947.

(66) Shamova, L. I.; Zatsikha, Y. V.; Nemykin, V. N. Synthesis pathways for the preparation of the BODIPY analogues: aza-BODIPYs, BOPHYs and some other pyrrole-based acyclic chromophores. *Dalton Transactions* **2021**, *50* (5), 1569-1593.

(67) Majumdar, P.; Mack, J.; Nyokong, T. Synthesis, characterization and photophysical properties of an acenaphthalene fused-ring-expanded NIR absorbing aza-BODIPY dye. *RSC Advances* **2015**, *5* (95), 78253-78258.

(68) Herold, D. A.; Rieke, R. D. Synthesis of 1, 2-disubstituted acenaphthylenes. *The Journal of Organic Chemistry* **1979**, *44* (8), 1359-1361.

(69) Zhang, L.; Zhao, L.; Wang, K.; Jiang, J. Chiral benzo-fused Aza-BODIPYs with optical activity extending into the NIR range. *Dyes and Pigments* **2016**, *134*, 427-433.

(70) Zou, B.; Liu, H.; Mack, J.; Wang, S.; Tian, J.; Lu, H.; Li, Z.; Shen, Z. A new aza-BODIPY based NIR region colorimetric and fluorescent chemodosimeter for fluoride. *RSC Advances* **2014**, *4* (96), 53864-53869.

(71) Zheng, W.; Wang, B. B.; Li, C. H.; Zhang, J. X.; Wan, C. Z.; Huang, J. H.; Liu, J.; Shen, Z.; You, X. Z. Asymmetric Donor–π-Acceptor-Type Benzo-Fused Aza-BODIPYs: Facile Synthesis and Colorimetric Properties. *Angewandte Chemie* **2015**, *127* (31), 9198-9202.

(72) Xiang, S.-K.; Tan, W.; Zhang, D.-X.; Tian, X.-L.; Feng, C.; Wang, B.-Q.; Zhao, K.-Q.; Hu, P.; Yang, H. Synthesis of benzimidazoles by potassium tert-butoxide-promoted intermolecular cyclization reaction of 2-iodoanilines with nitriles. *Organic & Biomolecular Chemistry* **2013**, *11* (42), 7271-7275.

(73) Mckeown, G. R.; Manion, J. G.; Lough, A. J.; Seferos, D. S. Synthesis of fused-ring aza-dipyrromethenes from aromatic nitriles. *Chemical Communications* **2018**, *54* (64), 8893-8896.

(74) Krizan, T. D.; Martin, J. Directed ortho lithiation of isophthalonitrile. New methodology for the synthesis of 1, 2, 3-trisubstituted benzenes. *The Journal of Organic Chemistry* **1982**, *47* (13), 2681-2682.

(75) Hellal, M.; Cuny, G. D. Microwave assisted copper-free Sonogashira coupling/5-exo-dig cycloisomerization domino reaction: access to 3-(phenylmethylene)isoindolin-1-ones and related heterocycles. *Tetrahedron Letters* **2011**, *52* (42), 5508-5511.

(76) Shimizu, S.; Murayama, A.; Haruyama, T.; Iino, T.; Mori, S.; Furuta, H.; Kobayashi, N. Benzo [c, d] indole-Containing Aza-BODIPY Dyes: Asymmetrization-Induced Solid-State Emission and Aggregation-Induced Emission Enhancement as New Properties of a Well-Known Chromophore. *Chemistry–A European Journal* **2015**, *21* (37), 12996-13003.

(77) Shimizu, S.; Iino, T.; Saeki, A.; Seki, S.; Kobayashi, N. Rational Molecular Design towards Vis/NIR Absorption and Fluorescence by using Pyrrolopyrrole aza-BODIPY and its Highly Conjugated Structures for Organic Photovoltaics. *Chemistry–A European Journal* **2015**, *21* (7), 2893-2904.

(78) Sheng, W.; Zheng, Y.-Q.; Wu, Q.; Wu, Y.; Yu, C.; Jiao, L.; Hao, E.; Wang, J.-Y.; Pei, J. Synthesis, properties, and semiconducting characteristics of BF2 complexes of β, β-bisphenanthrene-fused azadipyrromethenes. *Organic Letters* **2017**, *19* (11), 2893-2896.

(79) Sheng, W.; Cui, J.; Ruan, Z.; Yan, L.; Wu, Q.; Yu, C.; Wei, Y.; Hao, E.; Jiao, L. [a]-Phenanthrene-Fused BF2 Azadipyrromethene (AzaBODIPY) Dyes as Bright Near-Infrared Fluorophores. *The Journal of Organic Chemistry* **2017**, *82* (19), 10341-10349.

(80) Sheng, W.; Wu, Y.; Yu, C.; Bobadova-Parvanova, P.; Hao, E.; Jiao, L. Synthesis, crystal structure, and the deep near-infrared absorption/emission of bright AzaBODIPY-based organic fluorophores. *Organic letters* **2018**, *20* (9), 2620-2623.

(81) Fukui, N.; Cha, W. Y.; Lee, S.; Tokuji, S.; Kim, D.; Yorimitsu, H.; Osuka, A. Oxidative Fusion Reactions of meso-(Diarylamino) porphyrins. *Angewandte Chemie* **2013**, *125* (37), 9910-9914.

(82) Nowak-Krol, A.; Gryko, D. T. Oxidative aromatic coupling of meso-arylamino-porphyrins. *Organic Letters* **2013**, *15* (22), 5618-5621.

(83) Alberico, D.; Scott, M. E.; Lautens, M. Aryl− aryl bond formation by transition-metal-catalyzed direct arylation. *Chemical Reviews* **2007**, *107* (1), 174-238.

(84) Loudet, A.; Bandichhor, R.; Wu, L.; Burgess, K. Functionalized BF2 chelated azadipyrromethene dyes. *Tetrahedron* **2008**, *64* (17), 3642-3654.

(85) Loudet, A.; Bandichhor, R.; Burgess, K.; Palma, A.; McDonnell, S. O.; Hall, M. J.; O'Shea, D. F. B, O-chelated azadipyrromethenes as near-IR probes. *Organic letters* **2008**, *10* (21), 4771.

(86) Dalai, S.; Belov, V. N.; Nizamov, S.; Rauch, K.; Finsinger, D.; de Meijere, A. Access to Variously Substituted 5,6,7,8-Tetrahydro-3H-quinazolin-4-ones via Diels–Alder Adducts of Phenyl Vinyl Sulfone to Cyclobutene-Annelated Pyrimidinones. *European Journal of Organic Chemistry* **2006**, *2006* (12), 2753-2765.

(87) Chinchilla, R.; Nájera, C. Recent advances in Sonogashira reactions. *Chemical Society Reviews* **2011**, *40* (10), 5084-5121.

(88) Shirai, H.; Amano, N.; Hashimoto, Y.; Fukui, E.; Ishii, Y.; Ogawa, M. Trisannelated benzene synthesis by zirconium halide catalyzed cyclodehydration of cycloalkanones. *The Journal of Organic Chemistry* **1991**, *56* (6), 2253-2256.

(89) Niu, Y.-N.; Yan, Z.-Y.; Gao, G.-L.; Wang, H.-L.; Shu, X.-Z.; Ji, K.-G.; Liang, Y.-M. Synthesis of isoquinoline derivatives via Ag-catalyzed cyclization of 2-alkynyl benzyl azides. *The Journal of Organic Chemistry* **2009**, *74* (7), 2893-2896.

(90) Kmieciak, A.; Ćwiklińska, M.; Jeżak, K.; Shili, A.; Krzemiński, M. P. Searching for new biologically active compounds derived from isoquinoline alkaloids. *Chemistry Proceedings* **2020**, *3* (1), 97.

(91) Dyke, S.; Kinsman, R. Properties and Reactions of Isoquinolines and their Hydrogenated Derivatives. *Chemistry of Heterocyclic Compounds: Isoquinolines, Part 1* **1981**, *38*, 1-137.

(92) Guimond, N.; Fagnou, K. Isoquinoline synthesis via rhodium-catalyzed oxidative cross-coupling/cyclization of aryl aldimines and alkynes. *Journal of the American Chemical Society* **2009**, *131* (34), 12050-12051.

(93) Roesch, K. R.; Larock, R. C. Synthesis of isoquinolines and pyridines via palladium-catalyzed iminoannulation of internal acetylenes. *The Journal of Organic Chemistry* **1998**, *63* (16), 5306-5307.

(94) Whaley, W.; Govindachari, T. Organic Reactions, ed R Adams. Wiley, New York: 1951; pp 151-190.

(95) Negishi, E.-i.; Anastasia, L. Palladium-catalyzed alkynylation. *Chemical Reviews* **2003**, *103* (5), 1979-2018.

(96) Zeni, G.; Larock, R. C. Synthesis of heterocycles via palladium-catalyzed oxidative addition. *Chemical Reviews* **2006**, *106* (11), 4644-4680.

(97) Reddy, V.; Jadhav, A. S.; Anand, R. V. Catalyst-Controlled Regioselective Approach to 1-Aminoisoquinolines and/or 1-Aminoisoindolines through Aminative Domino Cyclization of 2-Alkynylbenzonitriles. *European Journal of Organic Chemistr*: 2016; pp 453-458.

(98) Sakthivel, K.; Srinivasan, K. Synthesis of naphthalene amino esters by the Blaise reaction of o-alkynylarenenitriles. *The Journal of Organic Chemistry* **2014**, *79* (7), 3244-3248.

(99) Ye, P.; Shao, Y.; Xie, L.; Shen, K.; Cheng, T.; Chen, J. Lanthanide-Catalyzed Tandem Insertion of Secondary Amines with 2-Alkynylbenzonitriles: Synthesis of Aminoisoindoles. *Chemistry An Asian Journal* **2018**, *13* (23), 3681-3690.

(100) Shen, H.; Xie, Z. Atom-Economical Synthesis of N-Heterocycles via Cascade Inter-/Intramolecular C− N Bond-Forming Reactions Catalyzed by Ti Amides. *Journal of the American Chemical Society* **2010**, *132* (33), 11473-11480.

(101) Yang, D.; Burugupalli, S.; Daniel, D.; Chen, Y. Microwave-assisted one-pot synthesis of isoquinolines, furopyridines, and thienopyridines by palladium-catalyzed sequential Coupling–Imination–Annulation of 2-bromoarylaldehydes with terminal acetylenes and ammonium acetate. *The Journal of Organic Chemistry* **2012**, *77* (9), 4466-4472.

(102) Long, Y.; She, Z.; Liu, X.; Chen, Y. Synthesis of 1-aminoisoquinolines by gold (III)-mediated domino reactions from 2-alkynylbenzamides and ammonium acetate. *The Journal of Organic Chemistry* **2013**, *78* (6), 2579-2588.

(103) Tsai, C.-W.; Yang, S.-C.; Liu, Y.-M.; Wu, M.-J. Microwave-assisted cycloadditions of 2-alkynylbenzonitriles with sodium azide: selective synthesis of tetrazolo [5, 1-a] pyridines and 4, 5-disubstituted-2H-1, 2, 3-triazoles. *Tetrahedron* **2009**, *65* (40), 8367-8372.

(104) Golubev, P. R.; Pankova, A. S.; Kuznetsov, M. A. Transition-Metal-Free Approach to 4-Ethynylpyrimidines via Alkenynones. *European Journal of Organic Chemistry* **2014**, *2014* (17), 3614-3621.

(105) Chow, H.-F.; Wan, C.-W.; Low, K.-H.; Yeung, Y.-Y. A highly selective synthesis of diarylethynes and their oligomers by a palladium-catalyzed Sonogashira coupling reaction under phase transfer conditions. *The Journal of Organic Chemistry* **2001**, *66* (5), 1910-1913.

(106) Díaz-Moscoso, A.; Tizzard, G. J.; Coles, S. J.; Cammidge, A. N. Synthesis of meso-Substituted Tetrabenzotriazaporphyrins: Easy Access to Hybrid Macrocycles. *Angewandte Chemie* **2013**, *125* (41), 10984-10987.

(107) Moussa, Z.; Romo, D. Mild deprotection of primary N-(p-toluenesulfonyl) amides with SmI2 following trifluoroacetylation. *Synlett* **2006**, *2006* (19), 3294-3298.

(108) Xiao, W.; He, Z.; Remiro-Buenamañana, S.; Turner, R. J.; Xu, M.; Yang, X.; Jing, X.; Cammidge, A. N. A π-Extended Donor–Acceptor–Donor Triphenylene Twin Linked via a Pyrazine Bridge. *Organic letters* **2015**, *17* (13), 3286-3289.

(109) Remiro-Buenamañana, S.; Díaz-Moscoso, A.; Hughes, D. L.; Bochmann, M.; Tizzard, G. J.; Coles, S. J.; Cammidge, A. N. Synthesis of Meso-Substituted Subphthalocyanine–Subporphyrin Hybrids: Boron Subtribenzodiazaporphyrins. *Angewandte Chemie International Edition* **2015**, *54* (26), 7510-7514.

(110) Remiro Buenamanana, S. Contracted phthalocyanine macrocycles: Conjugation with nanoparticles and the first synthesis of meso-substituted Boron SubTriBenzoDiAzaPorphyrin hybrids (SubTBDAPs). University of East Anglia, 2015.

(111) Bukowska, P.; Piechowska, J.; Loska, R. Azine-imidazole aza-BODIPY analogues with large Stokes shift. *Dyes and Pigments* **2017**, *137*, 312-321.

(112) Chakraborti, A. K.; Sharma, L.; Nayak, M. K. Demand-based thiolate anion generation under virtually neutral conditions: Influence of steric and electronic factors on chemo-and regioselective cleavage of aryl alkyl ethers. *The Journal of Organic Chemistry* **2002**, *67* (18), 6406-6414.

(113) Liu, S.-T.; Reddy, K. V.; Lai, R.-Y. Oxidative cleavage of alkenes catalyzed by a water/organic soluble manganese porphyrin complex. *Tetrahedron* **2007**, *63* (8), 1821-1825.

(114) Yamashita, J.; Inoue, Y.; Kondo, T.; Hashimoto, H. Ullmann-type coupling reaction of aryl trifluoromethanesulfonates catalyzed by in situ-generated low valent nickel complexes. *Chemistry Letters* **1986**, *15* (3), 407-408.

(115) Li, N.-N.; Zhang, Y.-L.; Mao, S.; Gao, Y.-R.; Guo, D.-D.; Wang, Y.-Q. Palladium-catalyzed C–H homocoupling of furans and thiophenes using oxygen as the oxidant. *Organic Letters* **2014**, *16* (10), 2732-2735.

(116) Ravikanth, M.; Chandrashekar, T. Nonplanar porphyrins and their biological relevance: ground and excited state dynamics. *Coordination Chemistry* **1995**, 105-188.

(117) Jaratjaroonphong, J.; Tuengpanya, S.; Saeeng, R.; Udompong, S.; Srisook, K. Green synthesis and anti-inflammatory studies of a series of 1, 1-bis (heteroaryl) alkane derivatives. *European Journal of Medicinal Chemistry* **2014**, *83*, 561-568.

(118) Marciniak, B.; Rozycka-Sokolowska, E.; Pavlyuk, V. 2-Naphthalenol. *Acta Crystallographica Section E: Structure Reports Online* **2003**, *59* (1), o52-o53.

Appendix

^{1}H NMR (500 MHz, Chloroform-*d*) of compound **155**

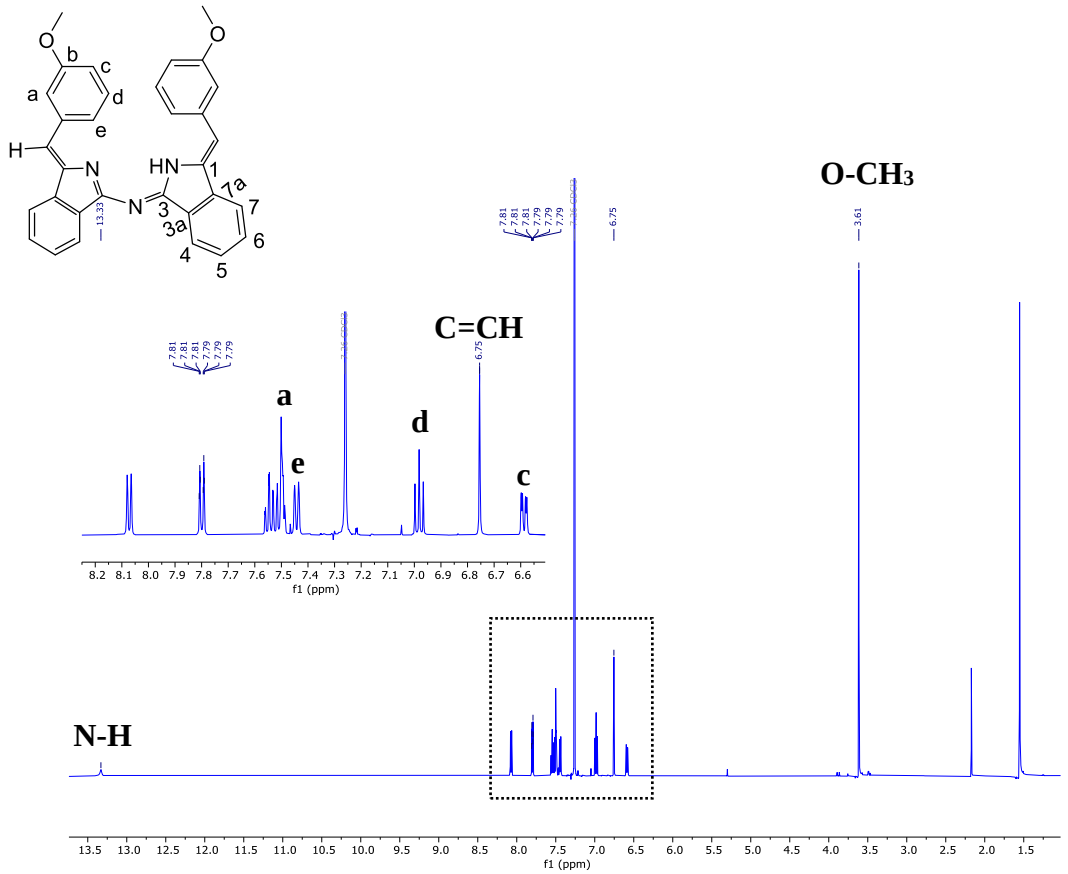

^{13}C NMR (126 MHz, Chloroform-*d*) of compound **155**

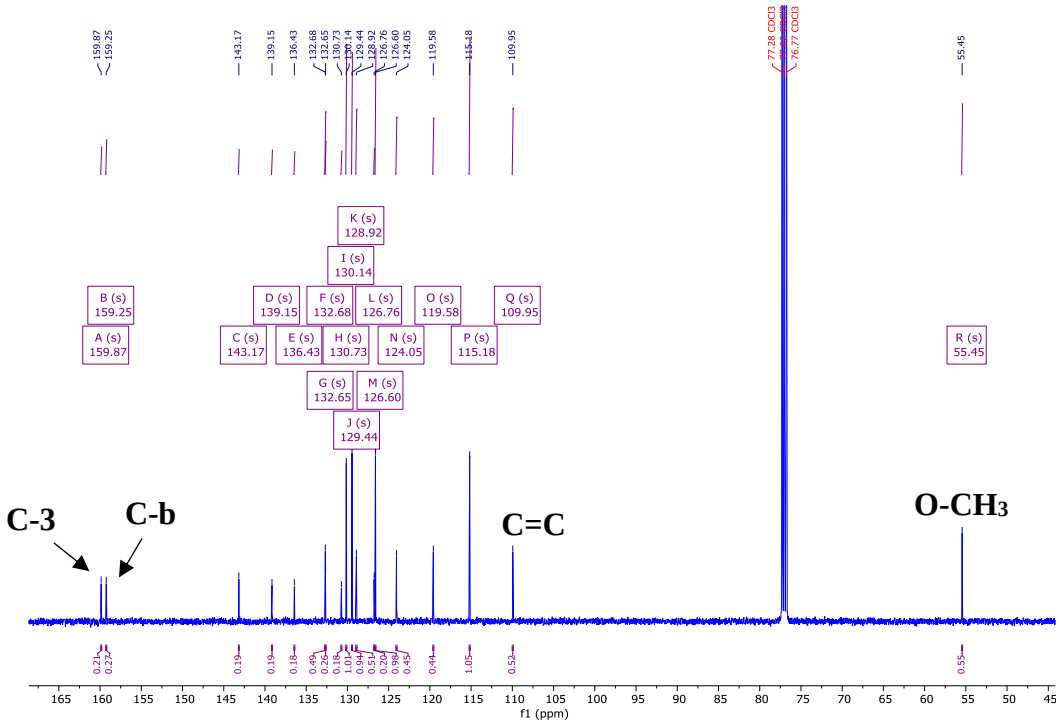

^{1}H NMR (400 MHz, Methylene Chloride-d_2) of compound **156**

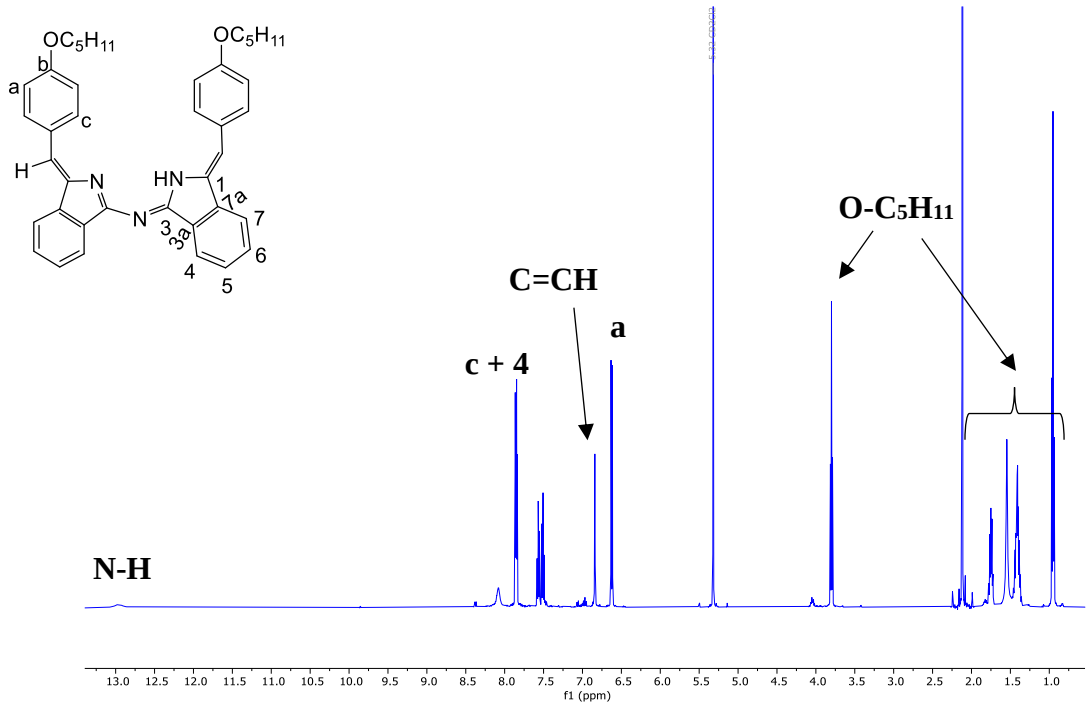

^{13}C NMR (126 MHz, Chloroform-*d*) of compound **156**

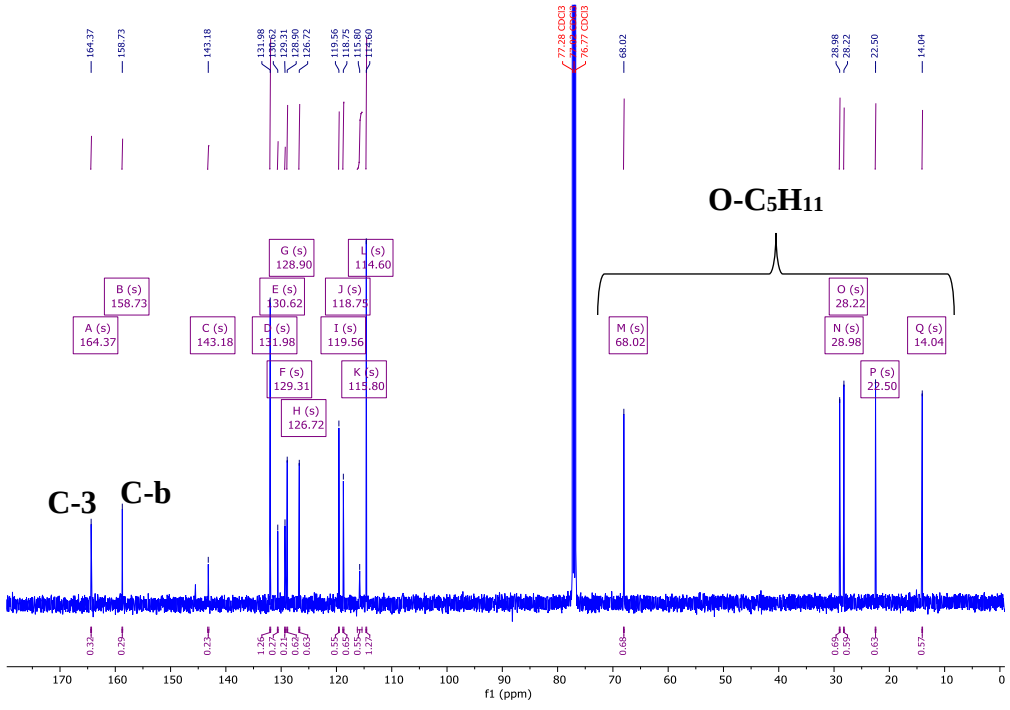

^{1}H NMR (500 MHz, Acetone-d_6) δ) of compound **162**

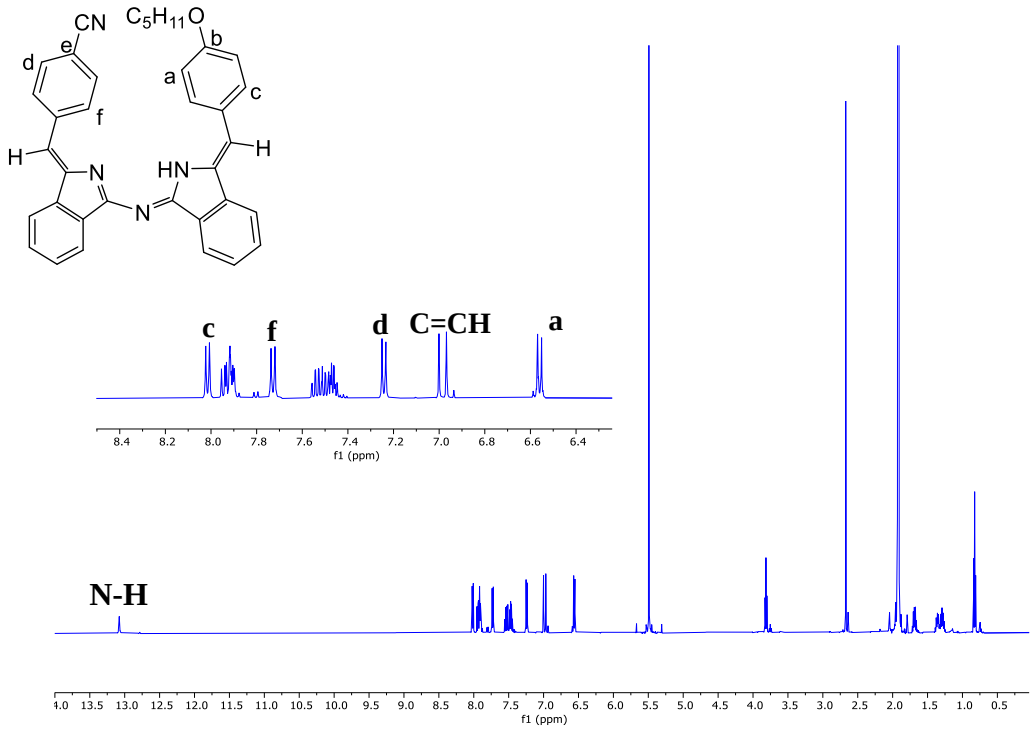

^{13}C NMR (126 MHz, Chloroform-*d*) of compound **160**

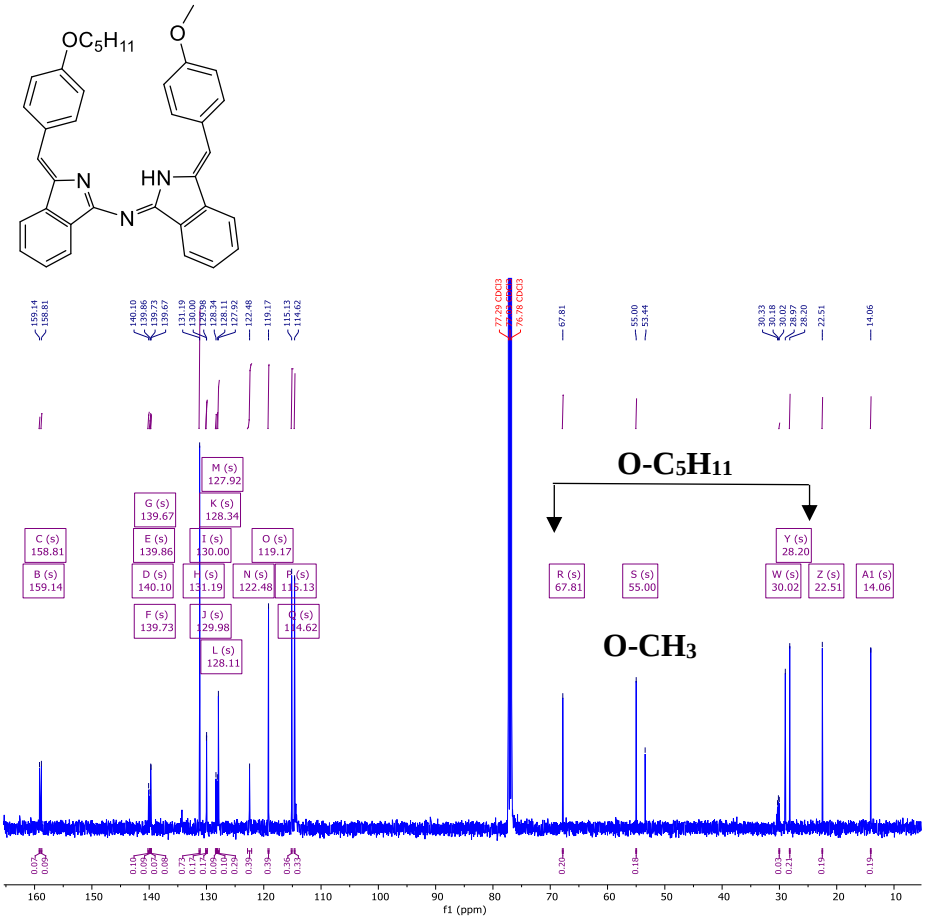

^{1}H NMR (500 MHz, Chloroform-*d*) of compound **164**

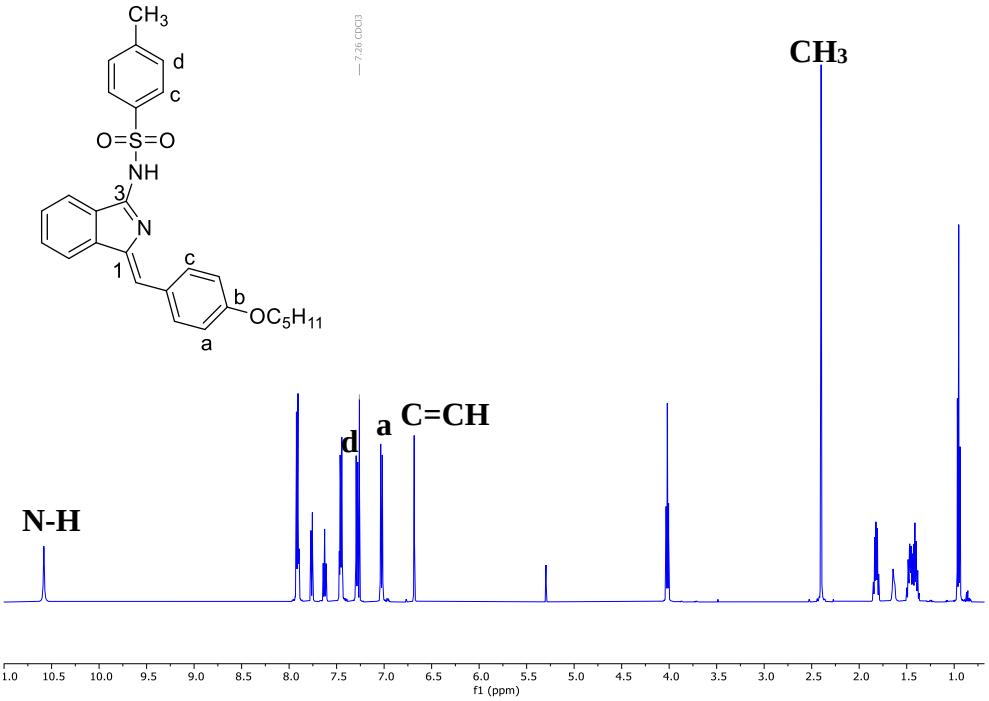

^{13}C NMR (126 MHz, Chloroform-*d*) of compound **164**

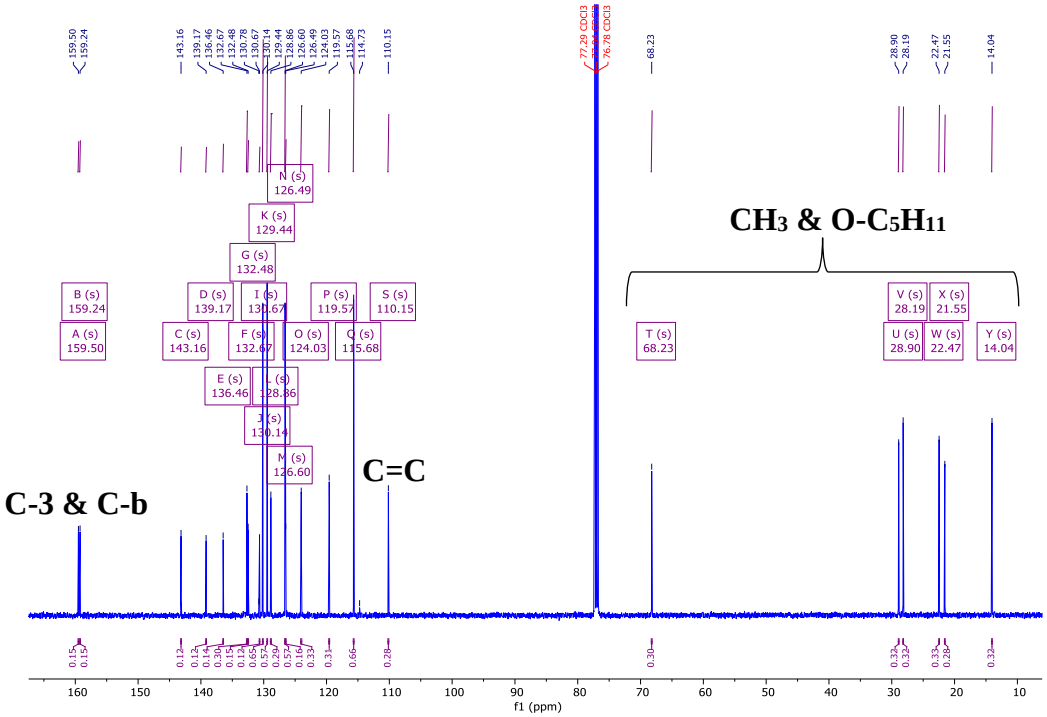

^{1}H NMR (400 MHz, Chloroform-*d*) of compound **165**

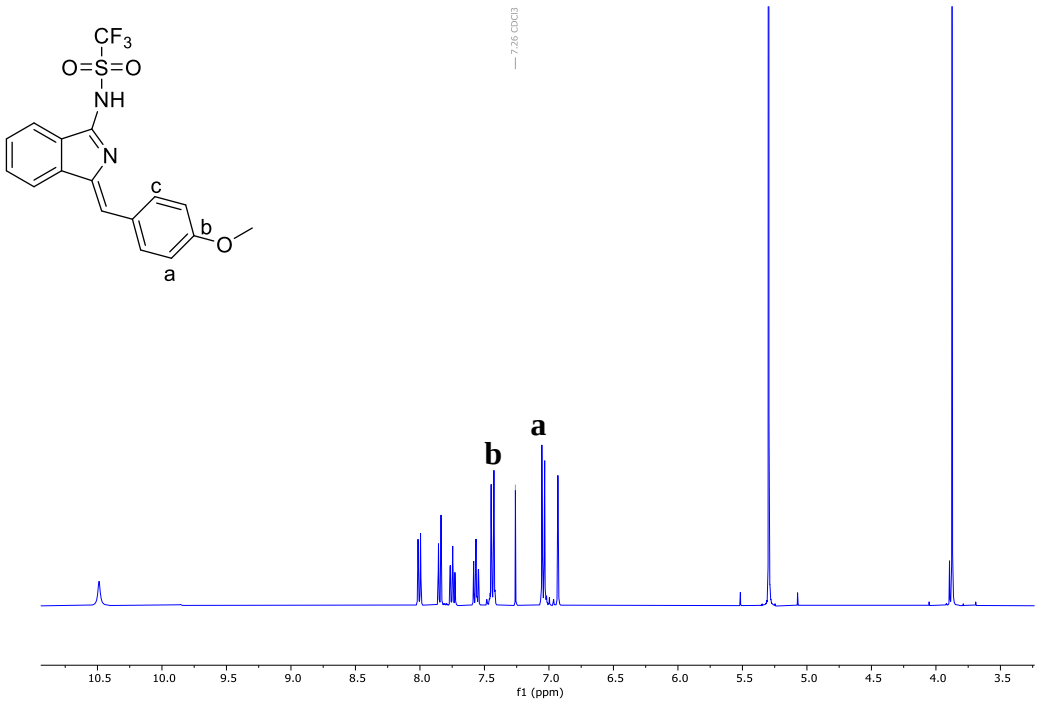

^{13}C NMR (101 MHz, Chloroform-*d*) compound **165**

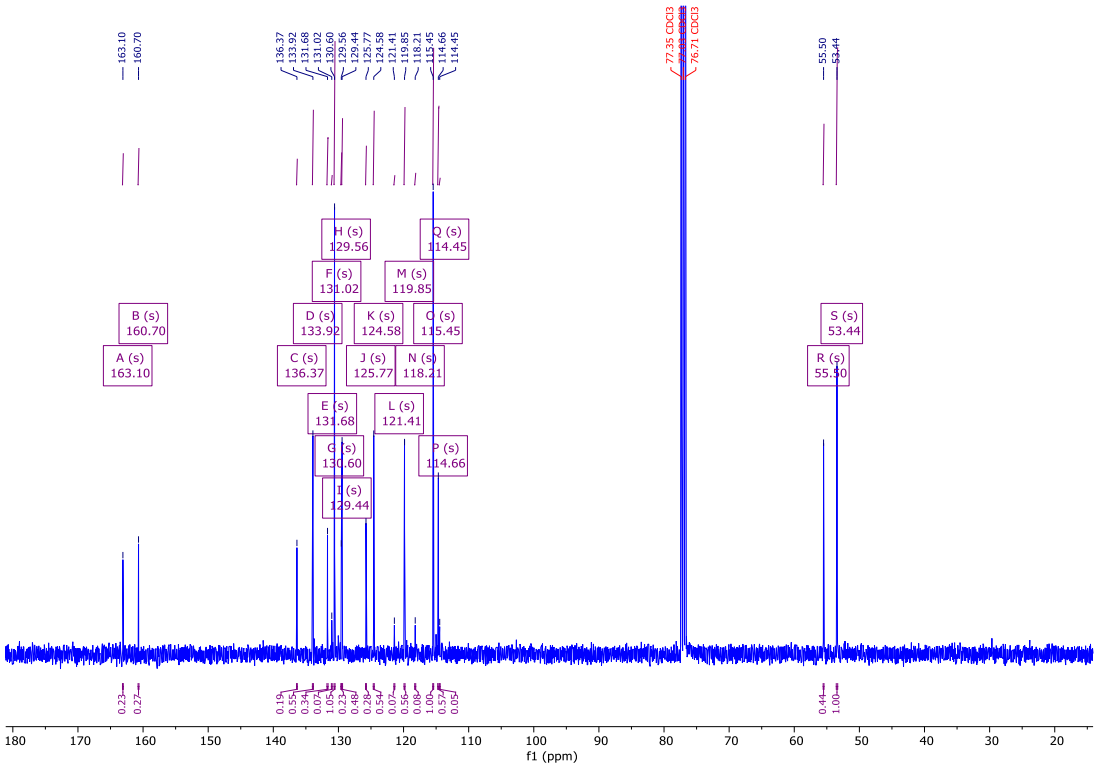

^{13}C NMR (126 MHz, Chloroform-d) of compound **172**

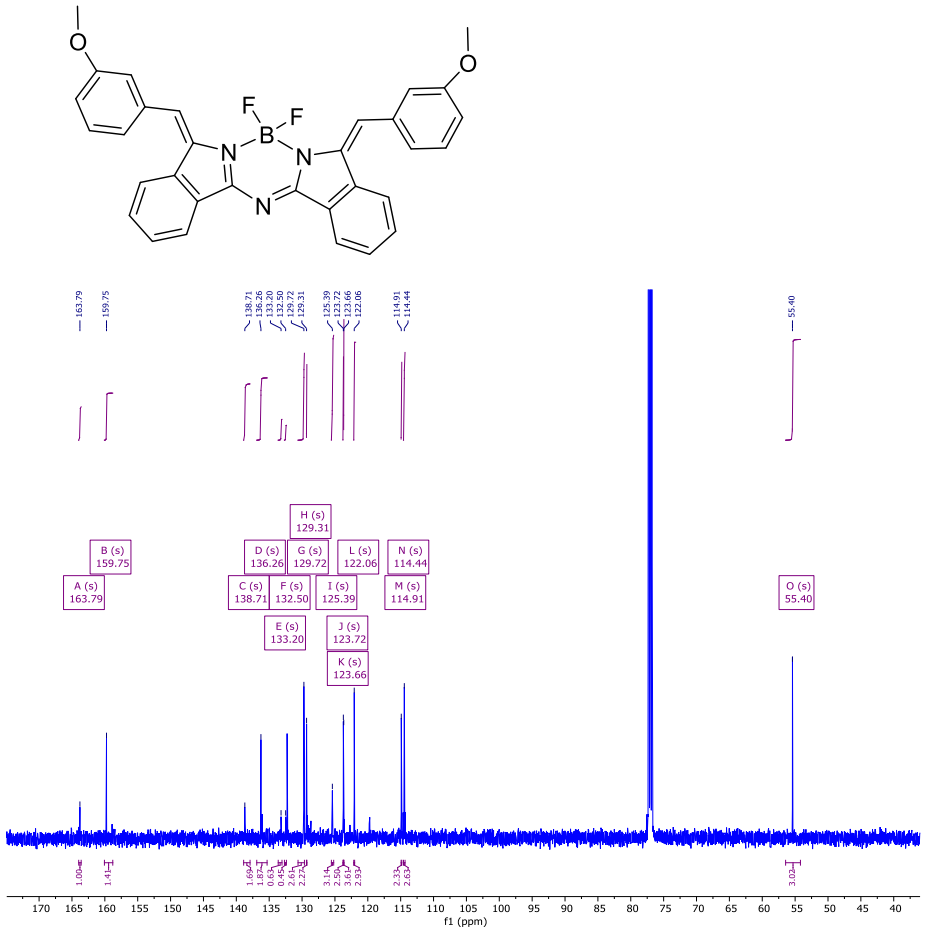

^{1}H NMR (500 MHz, Methylene Chloride-d_2) of compound **173**

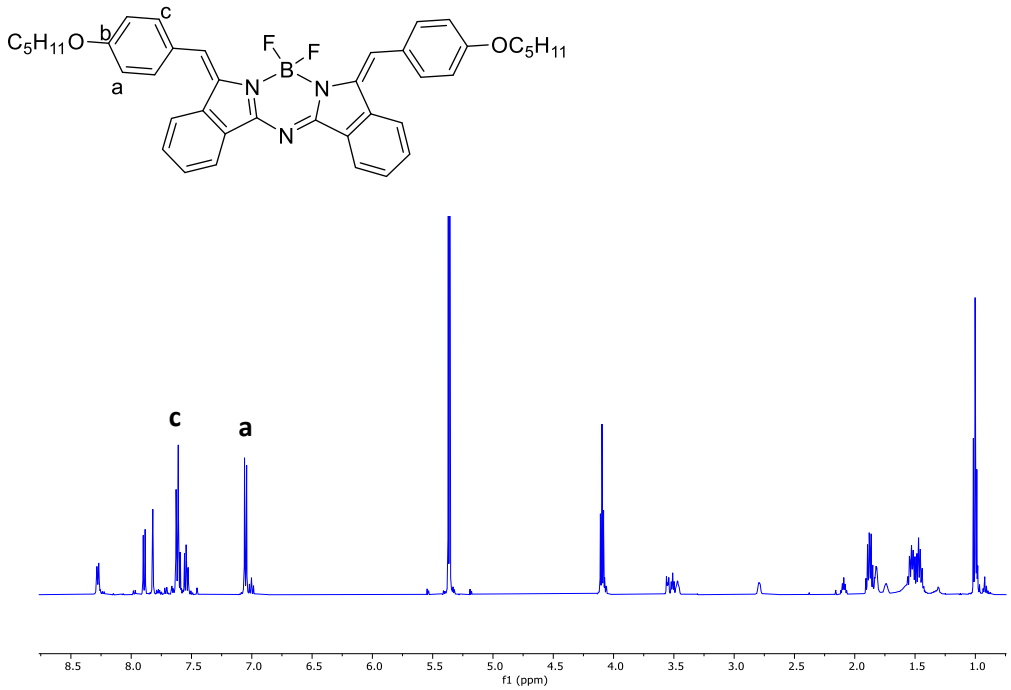

^{1}H NMR (400 MHz, Chloroform-*d*) compound **174**

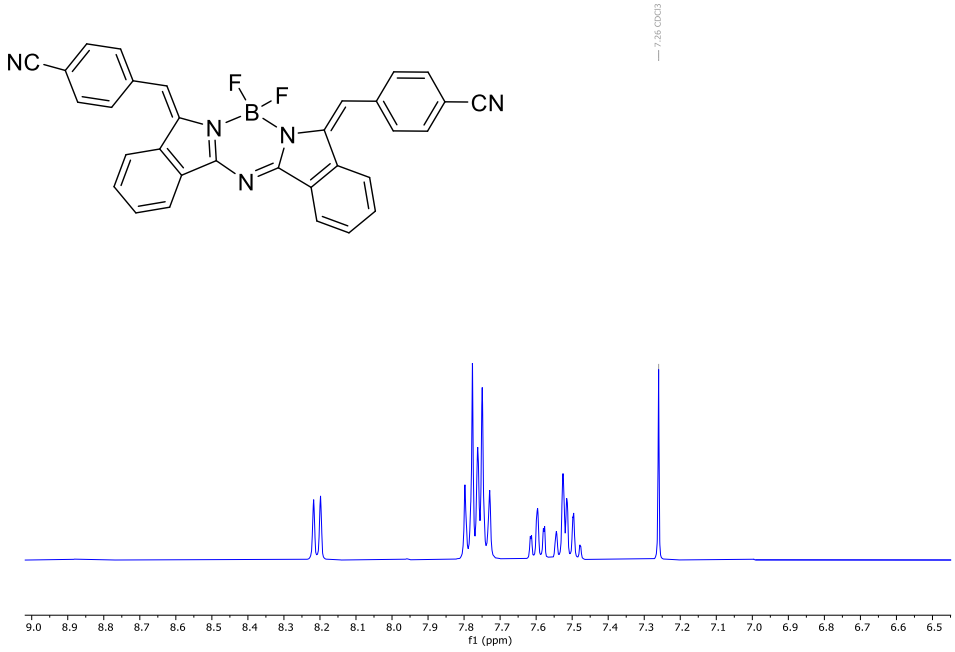

^{19}F NMR (376 MHz, Chloroform-*d*) of compound **174**

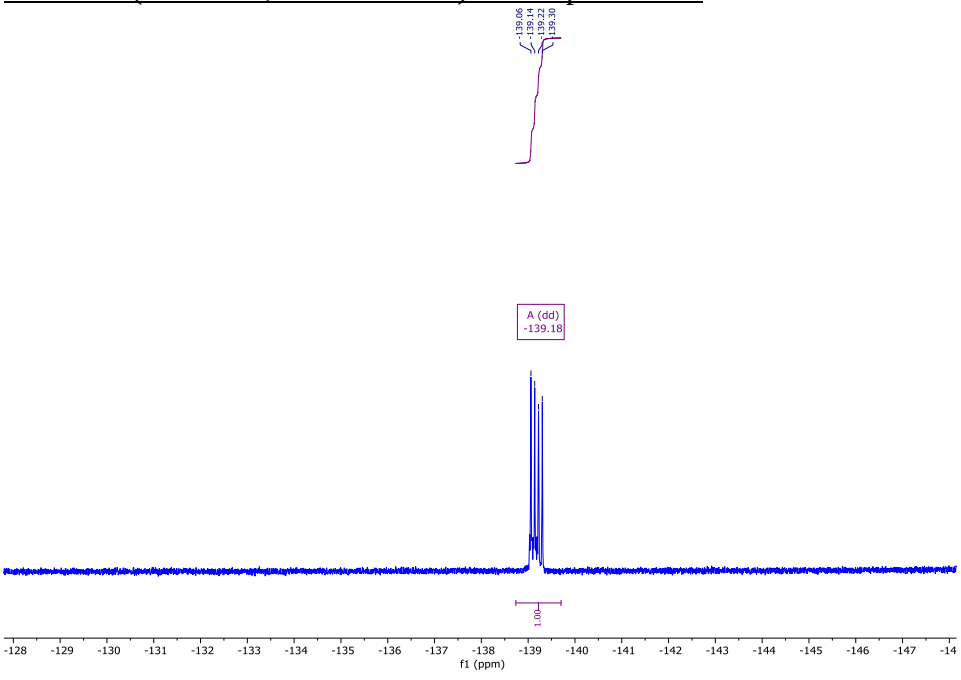

^{13}C NMR (126 MHz, Chloroform-*d*) of compound **174**

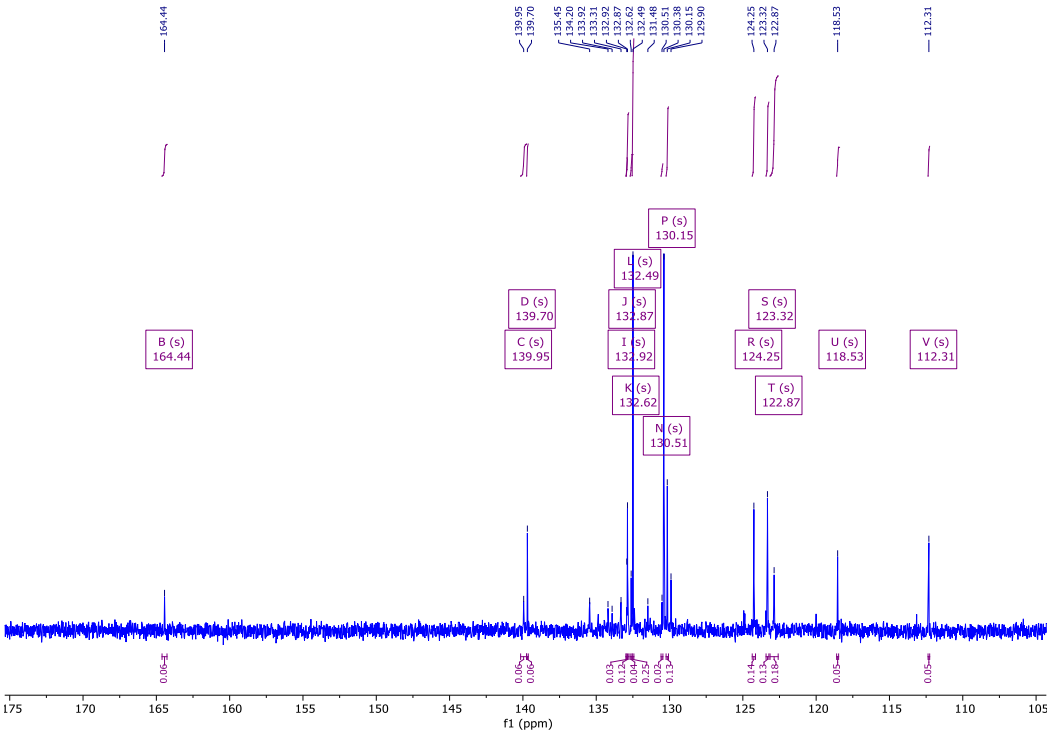

^{1}H NMR (500 MHz, Methylene Chloride-d_2) compound **175**

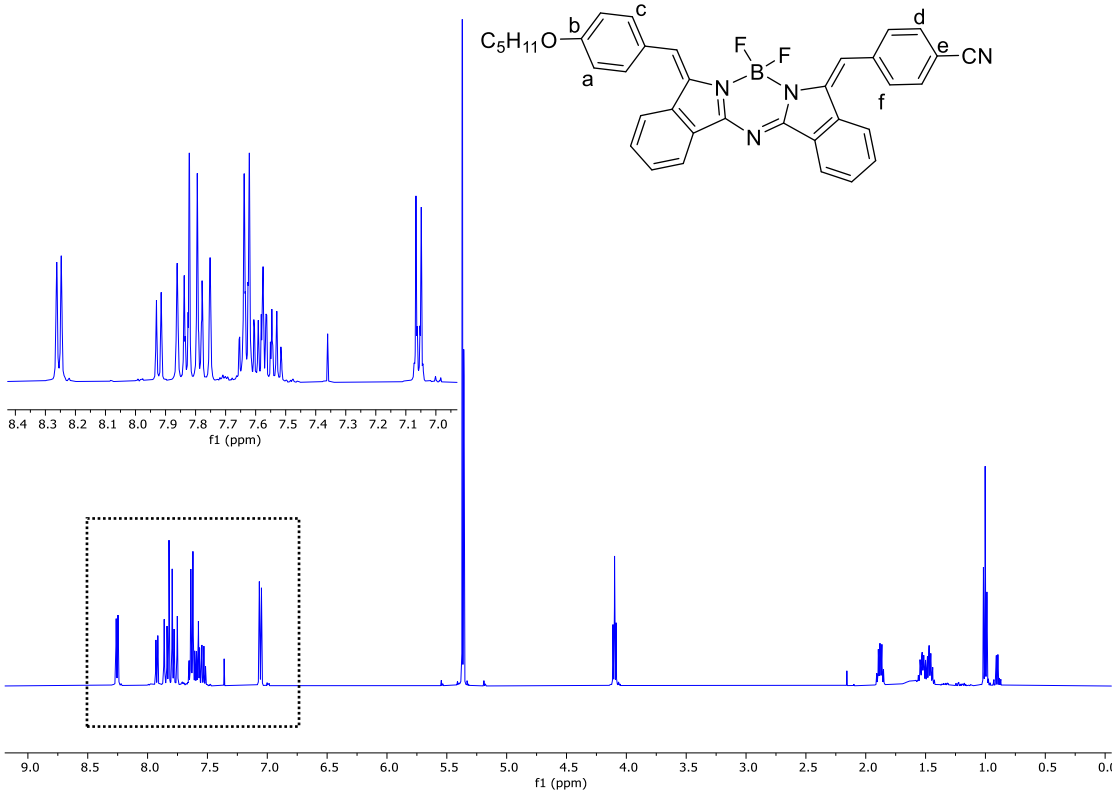

^{19}F NMR (376 MHz, Methylene Chloride-d_2) of compound **175**

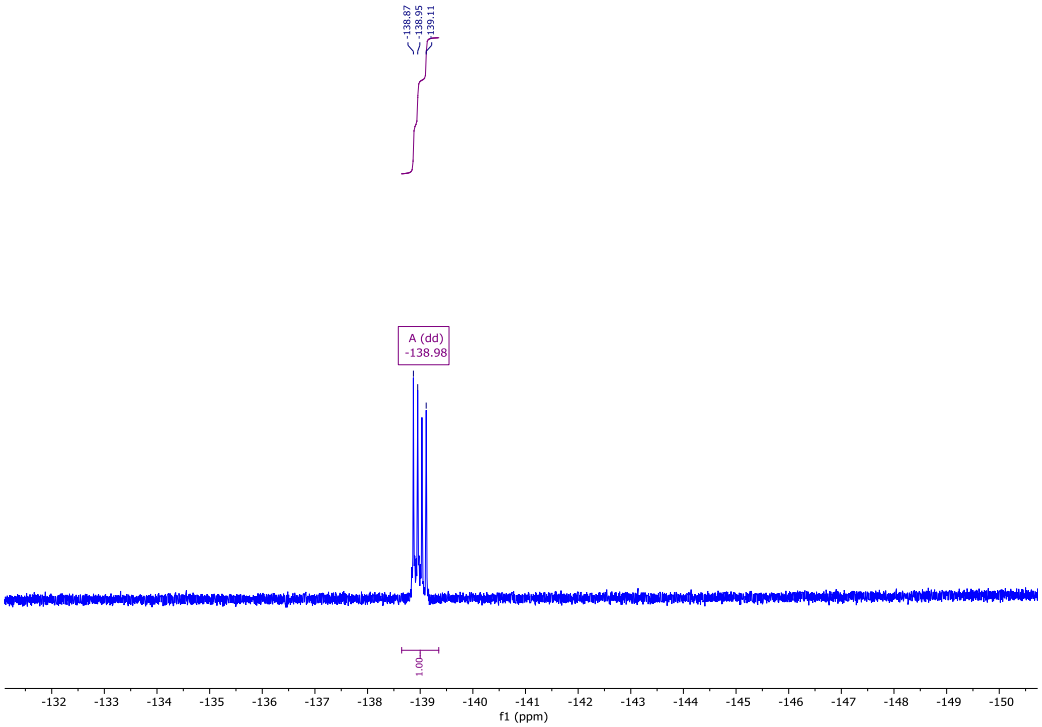

^{13}C NMR (126 MHz, Methylene Chloride-d_2) of compound **175**

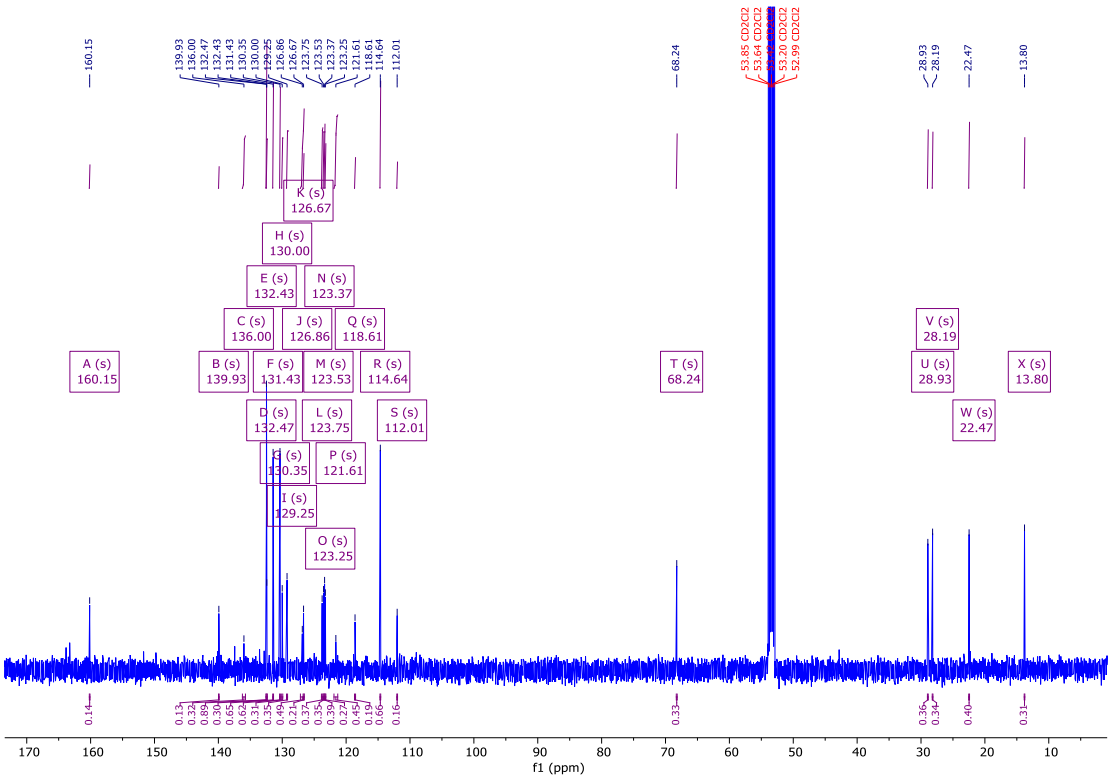

^{1}H NMR (400 MHz, Acetone-d_6) of compound **177**

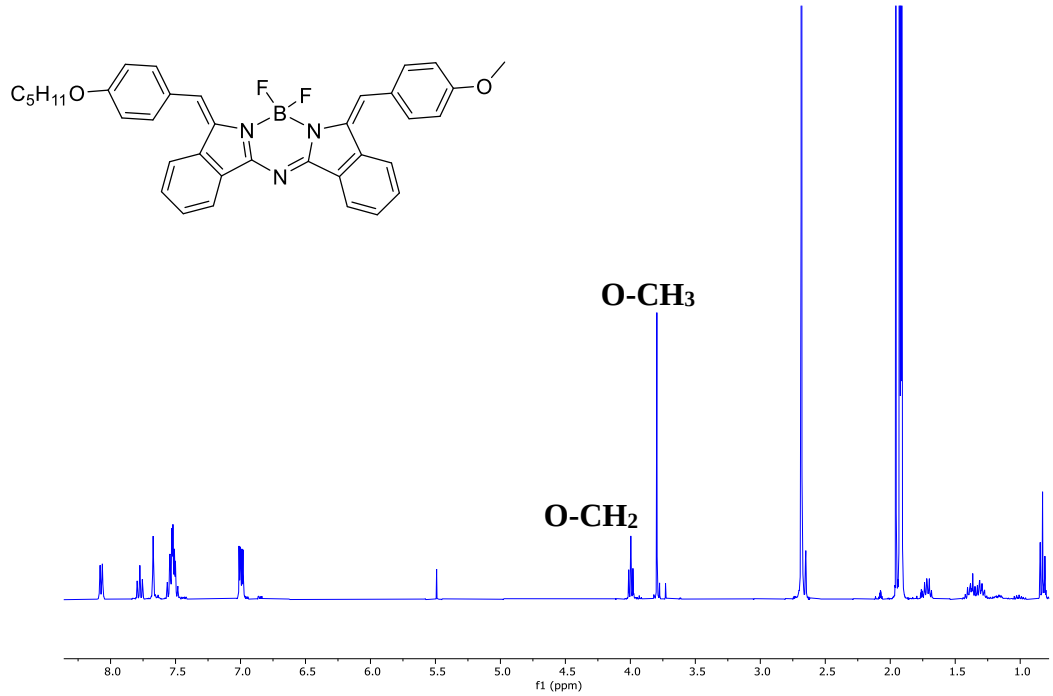

^{19}F NMR (376 MHz, Acetone-d_6) of compound **177**

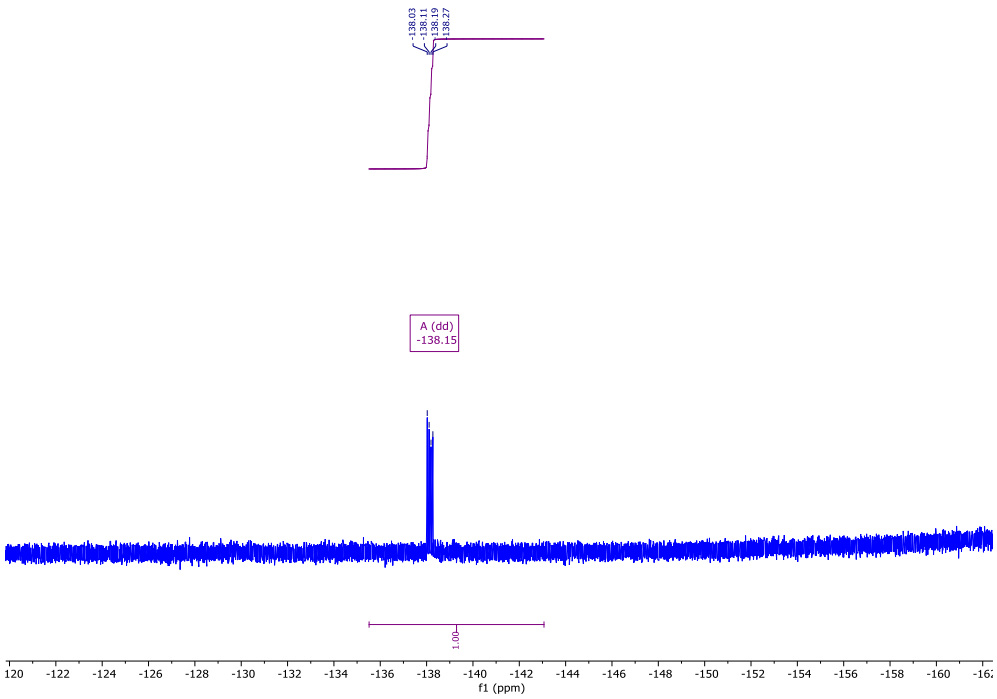

^{13}C NMR (126 MHz, Acetone-d_6) of compound **177**

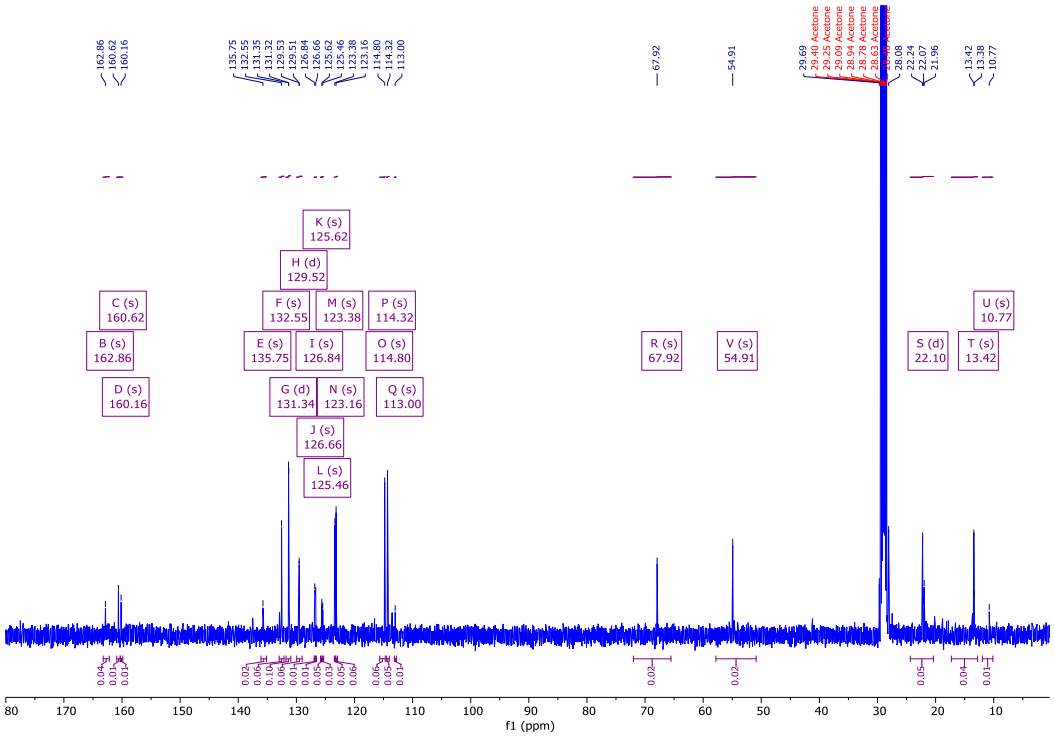

Crystal data and structure refinement for 3-*n*-butyl-isoquinolin-1-amine

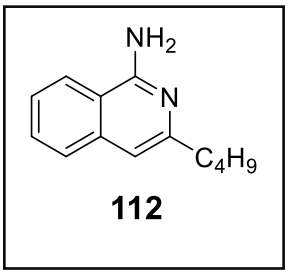

112

Identification code	**112**
Elemental formula	C13 H16 N2
Formula weight	200.28
Crystal system, space group	Monoclinic, P $2_1/c$ (no. 14)
Unit cell dimensions	a = 10.5288(4) Å α = 90 ° b = 5.4244(2) Å β = 103.423(4) ° c = 19.3720(7) Å γ = 90 °
Volume	1076.16(7) $Å^3$
Z, Calculated density	4, 1.236 Mg/m^3
F(000)	432
Absorption coefficient	0.074 mm^{-1}
Temperature	140(1) K
Wavelength	0.71073 Å
Crystal colour, shape	yellow prism
Crystal size	0.35 x 0.18 x 0.07 mm
Crystal mounting:	on a glass fibre, in oil, fixed in cold N_2 stream
On the diffractometer:	
Theta range for data collection	3.260 to 27.496 °
Limiting indices	-13<=h<=13, -7<=k<=7, -25<=l<=25
Completeness to theta = 25.242	99.8 %
Absorption correction	Semi-empirical from equivalents
Max. and min. transmission	1.000 and 0.742
Reflections collected (not including absences)	15704
No. of unique reflections	2466 [R(int) for equivalents = 0.037]
No. of 'observed' reflections ($I > 2\sigma_I$)	1958
Structure determined by	dual methods, in SHELXT
Refinement:	Full-matrix least-squares on F^2, in SHELXL
Data / restraints / parameters	2466 / 0 / 200
Goodness-of-fit on F^2	1.054
Final R indices ('observed' data)	R_1 = 0.043, wR_2 = 0.099

Final R indices (all data) $R_1 = 0.058$, $wR_2 = 0.104$

Reflections weighted:
$w = [\sigma^2(Fo^2) + (0.0464P)^2 + 0.2192P]^{-1}$ where $P=(Fo^2+2Fc^2)/3$

Extinction coefficient n/a

Largest diff. peak and hole 0.23 and -0.22 e.Å^{-3}

Location of largest difference peak at mid-point of C(1)-C(9) bond

---

Table 1. Atomic coordinates (x 10^5) and equivalent isotropic displacement parameters (Å^2 x 10^4). U(eq) is defined as one third of the trace of the orthogonalized Uij tensor. E.s.ds are in parentheses.

	x	y	z	U(eq)
N(1)	51595(11)	110760(20)	59412(6)	254(3)
C(1)	42381(12)	93320(20)	59512(6)	195(3)
N(2)	39358(9)	78280(19)	53965(5)	199(2)
C(3)	30433(11)	59750(20)	53916(6)	193(3)
C(4)	24699(12)	55740(20)	59464(7)	217(3)
C(5)	21793(13)	68890(20)	71321(7)	244(3)
C(6)	24330(13)	85410(30)	76803(7)	259(3)
C(7)	32913(13)	105210(20)	76811(7)	256(3)
C(8)	38984(13)	107990(20)	71280(7)	234(3)
C(9)	36465(11)	91310(20)	65524(6)	190(3)
C(10)	27646(12)	71650(20)	65458(6)	203(3)
C(31)	27515(13)	44480(20)	47216(7)	218(3)
C(32)	16387(12)	26030(20)	46525(7)	227(3)
C(33)	13372(13)	12410(30)	39442(7)	269(3)
C(34)	2930(14)	-7300(30)	39089(9)	310(3)

Table 2. Molecular dimensions. Bond lengths are in Ångstroms, angles in degrees. E.s.ds are in parentheses.

N(1)-C(1)	1.3585(16)	C(7)-H(7)	0.965(16)
N(1)-H(1A)	0.900(18)	C(8)-C(9)	1.4126(17)
N(1)-H(1B)	0.914(17)	C(8)-H(8)	0.971(15)
C(1)-N(2)	1.3278(16)	C(9)-C(10)	1.4121(17)
C(1)-C(9)	1.4468(16)	C(31)-C(32)	1.5228(18)
N(2)-C(3)	1.3744(15)	C(31)-H(31A)	0.994(14)
C(3)-C(4)	1.3668(17)	C(31)-H(31B)	0.988(15)
C(3)-C(31)	1.5100(17)	C(32)-C(33)	1.5254(18)
C(4)-C(10)	1.4219(17)	C(32)-H(32A)	1.003(14)
C(4)-H(4)	0.975(15)	C(32)-H(32B)	1.018(15)
C(5)-C(6)	1.3676(18)	C(33)-C(34)	1.5237(19)
C(5)-C(10)	1.4201(17)	C(33)-H(33A)	1.020(16)
C(5)-H(5)	0.996(15)	C(33)-H(33B)	0.979(16)
C(6)-C(7)	1.4035(19)	C(34)-H(34A)	0.973(16)
C(6)-H(6)	0.982(15)	C(34)-H(34B)	1.016(17)
C(7)-C(8)	1.3772(18)	C(34)-H(34C)	0.995(18)

C(1)-N(1)-H(1A)	117.5(11)	C(9)-C(10)-C(5)	118.60(11)
C(1)-N(1)-H(1B)	119.1(10)	C(9)-C(10)-C(4)	118.95(11)
H(1A)-N(1)-H(1B)	117.9(15)	C(5)-C(10)-C(4)	122.43(12)
N(2)-C(1)-N(1)	117.02(11)	C(3)-C(31)-C(32)	115.78(10)
N(2)-C(1)-C(9)	122.55(11)	C(3)-C(31)-H(31A)	107.0(8)
N(1)-C(1)-C(9)	120.43(11)	C(32)-C(31)-H(31A)	109.6(8)
C(1)-N(2)-C(3)	119.34(10)	C(3)-C(31)-H(31B)	108.2(8)
C(4)-C(3)-N(2)	122.49(11)	C(32)-C(31)-H(31B)	109.7(8)
C(4)-C(3)-C(31)	123.34(11)	H(31A)-C(31)-H(31B)	106.1(11)
N(2)-C(3)-C(31)	114.17(10)	C(31)-C(32)-C(33)	113.12(10)
C(3)-C(4)-C(10)	119.54(12)	C(31)-C(32)-H(32A)	109.1(8)
C(3)-C(4)-H(4)	120.7(8)	C(33)-C(32)-H(32A)	109.2(8)
C(10)-C(4)-H(4)	119.8(8)	C(31)-C(32)-H(32B)	109.9(8)
C(6)-C(5)-C(10)	120.62(12)	C(33)-C(32)-H(32B)	108.8(8)
C(6)-C(5)-H(5)	120.6(8)	H(32A)-C(32)-H(32B)	106.6(11)
C(10)-C(5)-H(5)	118.7(8)	C(34)-C(33)-C(32)	112.19(11)
C(5)-C(6)-C(7)	120.79(12)	C(34)-C(33)-H(33A)	108.9(8)
C(5)-C(6)-H(6)	120.2(9)	C(32)-C(33)-H(33A)	109.0(9)
C(7)-C(6)-H(6)	119.0(9)	C(34)-C(33)-H(33B)	110.9(9)
C(8)-C(7)-C(6)	119.85(12)	C(32)-C(33)-H(33B)	109.1(9)
C(8)-C(7)-H(7)	118.2(9)	H(33A)-C(33)-H(33B)	106.5(12)
C(6)-C(7)-H(7)	121.9(9)	C(33)-C(34)-H(34A)	109.2(9)
C(7)-C(8)-C(9)	120.54(12)	C(33)-C(34)-H(34B)	110.6(9)
C(7)-C(8)-H(8)	119.9(8)	H(34A)-C(34)-H(34B)	110.0(13)
C(9)-C(8)-H(8)	119.5(8)	C(33)-C(34)-H(34C)	113.0(10)
C(10)-C(9)-C(8)	119.57(11)	H(34A)-C(34)-H(34C)	106.8(13)
C(10)-C(9)-C(1)	117.05(11)	H(34B)-C(34)-H(34C)	107.1(13)
C(8)-C(9)-C(1)	123.37(11)		

Table 3. Anisotropic displacement parameters (Å² x 10⁴) for the expression:

$$\exp\{-2\pi^2(h^2a^{*2}U_{11} + \ldots + 2hka^*b^*U_{12})\}$$

E.s.ds are in parentheses.

	U_{11}	U_{22}	U_{33}	U_{23}	U_{13}	U_{12}
N(1)	287(6)	307(6)	189(6)	-29(5)	97(5)	-72(5)
C(1)	181(6)	233(6)	172(6)	36(5)	40(5)	29(5)
N(2)	191(5)	242(5)	171(5)	7(4)	56(4)	9(4)
C(3)	188(6)	209(6)	183(6)	18(5)	41(5)	34(5)
C(4)	233(6)	222(6)	204(6)	16(5)	69(5)	-10(5)
C(5)	263(6)	272(7)	216(7)	50(5)	93(5)	5(5)
C(6)	299(7)	325(7)	182(6)	36(5)	114(5)	44(6)
C(7)	320(7)	281(7)	171(6)	-18(5)	69(5)	34(5)
C(8)	260(7)	239(7)	206(7)	16(5)	57(5)	-2(5)
C(9)	187(6)	224(6)	159(6)	29(5)	43(4)	47(5)
C(10)	214(6)	229(6)	171(6)	38(5)	57(5)	40(5)
C(31)	231(6)	253(7)	184(7)	3(5)	74(5)	13(5)
C(32)	231(6)	241(6)	220(6)	6(5)	75(5)	17(5)
C(33)	265(7)	296(7)	258(7)	-37(6)	89(6)	-23(6)
C(34)	266(7)	289(7)	377(9)	-42(6)	75(6)	-11(6)

Table 4. Hydrogen coordinates (x 10⁴) and isotropic displacement parameters (Å² x 10³). All hydrogen atoms were located in a difference map and were refined freely.

	x	y	z	U(iso)
H(1A)	5255(16)	12290(30)	6266(9)	42(5)
H(1B)	5390(15)	11410(30)	5524(9)	37(4)
H(4)	1849(14)	4230(30)	5931(7)	27(4)
H(5)	1577(14)	5480(30)	7135(8)	25(4)
H(6)	2013(14)	8360(30)	8080(8)	33(4)
H(7)	3484(14)	11700(30)	8064(8)	34(4)
H(8)	4488(14)	12170(30)	7127(7)	26(4)
H(31A)	2553(13)	5620(30)	4316(8)	26(4)
H(31B)	3559(15)	3580(30)	4687(7)	29(4)
H(32A)	834(14)	3490(30)	4710(7)	25(4)
H(32B)	1858(14)	1350(30)	5052(8)	30(4)
H(33A)	1022(14)	2480(30)	3546(8)	32(4)
H(33B)	2144(15)	520(30)	3864(8)	33(4)
H(34A)	-504(15)	40(30)	3978(8)	34(4)
H(34B)	600(16)	-2040(30)	4286(9)	43(5)
H(34C)	64(16)	-1590(30)	3443(9)	47(5)

Table 5. Torsion angles, in degrees. E.s.ds are in parentheses.

N(1)-C(1)-N(2)-C(3) 177.71(10)	N(1)-C(1)-C(9)-C(8) 5.05(18)
C(9)-C(1)-N(2)-C(3)-1.08(17)	C(8)-C(9)-C(10)-C(5)-1.59(17)
C(1)-N(2)-C(3)-C(4)-1.57(17)	C(1)-C(9)-C(10)-C(5) 179.12(11)
C(1)-N(2)-C(3)-C(31) 178.08(10)	C(8)-C(9)-C(10)-C(4) 176.84(11)
N(2)-C(3)-C(4)-C(10) 2.08(18)	C(1)-C(9)-C(10)-C(4)-2.44(16)
C(31)-C(3)-C(4)-C(10)-177.54(11)	C(6)-C(5)-C(10)-C(9) 2.08(18)
C(10)-C(5)-C(6)-C(7)-1.0(2)	C(6)-C(5)-C(10)-C(4)-176.30(12)
C(5)-C(6)-C(7)-C(8)-0.7(2)	C(3)-C(4)-C(10)-C(9) 0.05(18)
C(6)-C(7)-C(8)-C(9) 1.15(19)	C(3)-C(4)-C(10)-C(5) 178.42(12)
C(7)-C(8)-C(9)-C(10) 0.00(18)	C(4)-C(3)-C(31)-C(32) 7.49(18)
C(7)-C(8)-C(9)-C(1) 179.24(12)	N(2)-C(3)-C(31)-C(32)-172.15(10)
N(2)-C(1)-C(9)-C(10) 3.06(17)	C(3)-C(31)-C(32)-C(33) 176.29(11)
N(1)-C(1)-C(9)-C(10)-175.69(11)	C(31)-C(32)-C(33)-C(34) 175.65(12)
N(2)-C(1)-C(9)-C(8)-176.20(11)	

Table 6. Hydrogen bond, in Ångstroms and degrees.

D-H...A	d(D-H)	d(H...A)	d(D...A)	<(DHA)
N(1)-H(1B)...N(2)#1	0.914(17)	2.108(17)	3.0201(15)	175.8(14)

Symmetry transformation used to generate equivalent atoms:
#1 : 1-x, 2-y, 1-z

Crystal structure analysis of 3-*n*-butyl-isoquinolin-1-amine

Crystal data: $C_{13}H_{16}N_2$, M = 200.28. Monoclinic, space group $P2_1/c$ (no. 14), a = 10.5288(4), b = 5.4244(2), c = 19.3720(7) Å, β = 103.423(4) °, V = 1076.16(7) $Å^3$. Z = 4, Dc = 1.236 g cm^{-3}, F(000) = 432, T = 140(1) K, μ(Mo-Kα) = 0.74 cm^{-1}, λ(Mo-Kα) = 0.71073 Å.

Crystals are yellow prisms. From a sample under oil, one, *ca* 0.07 x 0.18 x 0.35 mm, was mounted on a glass fibre and fixed in the cold nitrogen stream on an Oxford Diffraction Xcalibur-3/Sapphire3-CCD diffractometer, equipped with Mo-Kα radiation and graphite monochromator. Intensity data were measured by thin-slice ω- and φ-scans. Total no. of reflections recorded to θ_{max} = 27.5°, was 15704 of which 2466 were unique (Rint = 0.037); 1958 were 'observed' with $I > 2\sigma_I$.

Data were processed using the CrysAlisPro-CCD and -RED (1) programs. The structure was determined by the intrinsic phasing routines in the SHELXT program (2A) and refined by full-matrix least-squares methods, on F^2's, in SHELXL (2B). The non-hydrogen atoms were refined with anisotropic thermal parameters. Hydrogen atoms were located in a difference map and were refined freely. At the conclusion of the refinement, wR_2 = 0.104 and R_1 = 0.058 (2B) for all 2466 reflections weighted $w = [\sigma^2(F_o^2) + (0.0464P)^2 + 0.2192P]^{-1}$ with $P = (F_o^2 + 2F_c^2)/3$; for the 'observed' data only, R_1 = 0.043.

In the final difference map, the highest peaks (*ca* 0.23 $eÅ^{-3}$) were close to the mid-points of the ring C-C bonds.

Scattering factors for neutral atoms were taken from reference (3). Computer programs used in this analysis have been noted above and were run through WinGX (4) on a Dell Optiplex 780 PC at the University of East Anglia.

References

(1) Programs CrysAlisPro, Rigaku Oxford Diffraction Ltd., Abingdon, UK (2018).

(2) G. M. Sheldrick, Programs for crystal structure determination (SHELXT), *Acta Cryst.* (2015) A**71**, 3-8, and refinement (SHELXL), *Acta Cryst.* (2008) A**64**, 112-122 and (2015) C**71**, 3-8.

(3) *'International Tables for X-ray Crystallography'*, Kluwer Academic Publishers, Dordrecht (1992). Vol. C, pp. 500, 219 and 193.

(4) L. J. Farrugia, *J. Appl. Cryst.* (2012) **45**, 849–854.

Legends for Figures

Figure 1. View of a pair of 3-*n*-butyl-isoquinolin-1-amine molecules linked by hydrogen bonds about a centre of symmetry; the atom numbering scheme is indicated. Thermal ellipsoids are drawn at the 50% probability level.

Figure 2. View along the *b* axis of the packing of the hydrogen-bonded dimer pairs.

Notes on the structure.

All the non-hydrogen atoms of the isoquinoline rings of the title molecule form a good planar group; the carbon atoms of the *n*-butyl group lie close to this plane and show an all-*trans* chain. One of the amino H atoms forms a good hydrogen bond to the pyridine N atom of a neighbouring molecule, and this bonding is repeated about a centre of symmetry, thus forming an eight-membered ring which links the pair of molecules in a dimer unit.

Crystal data and structure refinement for MeO-C_6H_4-CC-C_6H_4-$C(NH_2)_2$, Cl, H_2O

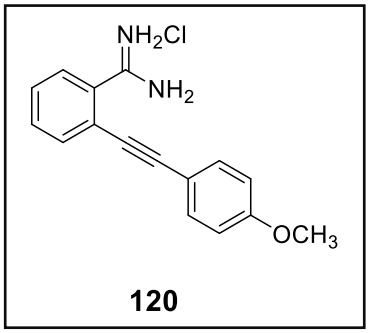

120

Identification code	**120**
Elemental formula	C16 H15 N2 O, H2 O, Cl
Formula weight	304.77
Crystal system, space group	Triclinic, P -1
Unit cell dimensions	a = 8.113(3) Å α = 82.91(2) ° b = 8.133(3) Å β = 83.06(2) ° c = 13.467(3) Å γ = 60.90(3) °
Volume	768.6(4) $Å^3$
Z, Calculated density	2, 1.317 Mg/m^3
F(000)	320
Absorption coefficient	0.254 mm^{-1}
Temperature	140(1) K
Wavelength	0.71073 Å
Crystal colour, shape	colourless plate
Crystal size	0.41 x 0.33 x 0.05 mm
Crystal mounting:	on a glass fibre, in oil, fixed in cold N_2 stream
On the diffractometer:	
Theta range for data collection	3.930 to 19.999 °
Limiting indices	-7<=h<=7, -7<=k<=7, -12<=l<=12
Completeness to theta = 19.999	99.2 %
Absorption correction	Semi-empirical from equivalents
Max. and min. transmission	1.000 and 0.128
Reflections collected (not including absences)	5362
No. of unique reflections	1416 [R(int) for equivalents = 0.186]
No. of 'observed' reflections ($I > 2\sigma_I$)	796
Structure determined by:	dual methods, in SHELXT
Refinement:	Full-matrix least-squares on F^2, in SHELXL

Data / restraints / parameters 1416 / 3 / 200

Goodness-of-fit on F^2 1.075

Final R indices ('observed' data) $R_1 = 0.138$, $wR_2 = 0.311$

Final R indices (all data) $R_1 = 0.213$, $wR_2 = 0.349$

Reflections weighted:
$w = [\sigma^2(Fo^2)+(0.2000P)^2]^{-1}$ where $P=(Fo^2+2Fc^2)/3$

Extinction coefficient n/a

Largest diff. peak and hole 0.68 and -0.46 e.Å^{-3}

Location of largest difference peak close to Cl(1)

Table 1. Atomic coordinates (x 10^4) and equivalent isotropic displacement parameters (Å^2 x 10^3). U(eq) is defined as one third of the trace of the orthogonalized Uij tensor. E.s.ds are in parentheses.

	x	y	z	U(eq)
C(1)	-40(20)	9243(15)	2375(8)	38(3)
C(2)	990(20)	9747(16)	1562(8)	45(4)
C(3)	(20)	11241(17)	882(8)	47(4)
C(4)	-1960(20)	12131(17)	955(8)	43(4)
C(5)	-2960(20)	11652(15)	1722(9)	47(4)
C(6)	-1990(20)	10205(18)	2447(8)	49(4)
C(7)	977(17)	7741(15)	3142(8)	37(3)
C(8)	1726(19)	6545(18)	3761(9)	46(4)
C(9)	2820(20)	4982(16)	4494(8)	38(3)
C(10)	4600(19)	3629(16)	4190(8)	40(3)
C(11)	5650(20)	2128(15)	4861(9)	50(4)
C(12)	4850(20)	2020(18)	5818(9)	44(4)
O(12)	5839(14)	502(11)	6516(5)	51(3)
C(121)	7627(19)	-972(16)	6212(8)	44(3)
C(13)	3090(20)	3354(18)	6132(8)	43(3)
C(14)	2041(19)	4843(16)	5461(9)	46(3)
C(21)	3050(20)	8815(19)	1438(8)	43(3)
N(21)	3998(17)	6913(14)	1522(7)	49(3)
N(22)	3974(16)	9810(13)	1183(6)	52(3)
Cl(1)	2006(5)	4361(4)	1308(2)	52.7(14)
O(51)	7638(15)	6630(12)	932(7)	53(3)

Table 2. Molecular dimensions. Bond lengths are in Ångstroms,angles in degrees. E.s.ds are in parentheses.

C(1)-C(6) 1.382(17)	C(10)-C(11) 1.391(15)
C(1)-C(2) 1.436(17)	C(11)-C(12) 1.383(16)
C(1)-C(7) 1.468(16)	C(12)-C(13) 1.362(16)
C(2)-C(3) 1.383(15)	C(12)-O(12) 1.407(13)
C(2)-C(21) 1.457(17)	O(12)-C(121) 1.413(13)
C(3)-C(4) 1.390(16)	C(13)-C(14) 1.387(16)
C(4)-C(5) 1.373(16)	C(21)-N(22) 1.341(14)
C(5)-C(6) 1.400(16)	C(21)-N(21) 1.349(15)
C(7)-C(8) 1.165(14)	N(21)-H(21A) 0.86(2)
C(8)-C(9) 1.479(18)	O(51)-H(51A) 0.82(2)
C(9)-C(10) 1.372(15)	O(51)-H(51B) 0.82(2)
C(9)-C(14) 1.394(16)	
C(6)-C(1)-C(2) 119.9(11)	C(14)-C(9)-C(8) 120.8(13)
C(6)-C(1)-C(7) 119.8(11)	C(9)-C(10)-C(11) 119.7(11)
C(2)-C(1)-C(7) 120.3(12)	C(12)-C(11)-C(10) 118.7(13)
C(3)-C(2)-C(1) 119.3(14)	C(13)-C(12)-C(11) 122.3(11)
C(3)-C(2)-C(21) 117.5(12)	C(13)-C(12)-O(12) 116.8(11)
C(1)-C(2)-C(21) 123.2(10)	C(11)-C(12)-O(12) 120.9(14)
C(2)-C(3)-C(4) 119.2(12)	C(12)-O(12)-C(121) 119.1(9)
C(5)-C(4)-C(3) 122.0(11)	C(12)-C(13)-C(14) 118.9(11)
C(4)-C(5)-C(6) 119.6(13)	C(13)-C(14)-C(9) 119.7(13)
C(1)-C(6)-C(5) 119.9(11)	N(22)-C(21)-N(21) 120.4(13)
C(8)-C(7)-C(1) 177.6(13)	N(22)-C(21)-C(2) 121.2(11)
C(7)-C(8)-C(9) 175.3(14)	N(21)-C(21)-C(2) 118.3(11)
C(10)-C(9)-C(14) 120.7(11)	C(21)-N(21)-H(21A) 115(8)
C(10)-C(9)-C(8) 118.5(11)	H(51A)-O(51)-H(51B) 118(10)

Table 3. Anisotropic displacement parameters ($Å^2$ x 10^3) for the expression: exp $\{-2\pi^2(h^2a^{*2}U_{11} + ... + 2hka^*b^*U_{12})\}$ E.s.ds are in parentheses.

	U_{11}	U_{22}	U_{33}	U_{23}	U_{13}	U_{12}
C(1)	26(11)	32(7)	41(8)	0(6)	-4(7)	-2(7)
C(2)	62(13)	37(7)	41(8)	17(6)	-19(8)	-28(8)
C(3)	58(13)	51(8)	45(8)	19(7)	-13(7)	-38(9)
C(4)	47(12)	46(8)	45(8)	23(6)	-15(7)	-32(8)
C(5)	54(10)	28(7)	54(8)	7(6)	-11(8)	-18(7)
C(6)	55(12)	49(8)	52(8)	3(7)	1(8)	-35(9)
C(7)	39(10)	30(7)	34(7)	5(7)	0(7)	-12(7)
C(8)	42(10)	46(8)	45(8)	12(7)	-1(7)	-21(8)
C(9)	38(11)	33(8)	44(8)	16(6)	-7(7)	-20(8)
C(10)	23(10)	33(7)	51(8)	-1(7)	6(7)	-6(8)
C(11)	75(12)	36(8)	50(9)	18(7)	-31(8)	-35(8)
C(12)	53(12)	56(9)	27(8)	21(7)	-20(7)	-30(9)
O(12)	60(8)	41(5)	44(5)	17(4)	-14(5)	-21(6)
C(121)	39(10)	39(8)	48(7)	17(6)	-14(7)	-17(8)
C(13)	28(10)	43(8)	40(8)	18(7)	7(7)	-9(8)
C(14)	40(10)	43(8)	56(8)	11(7)	-8(7)	-22(7)
C(21)	33(11)	54(10)	42(7)	15(6)	-22(7)	-21(8)
N(21)	59(9)	36(7)	47(6)	19(5)	-20(6)	-20(7)
N(22)	86(10)	49(7)	44(6)	22(5)	-24(6)	-52(7)
Cl(1)	52(3)	45(2)	61(2)	19.3(16)	-19.2(18)	-25(2)
O(51)	44(8)	54(6)	61(6)	10(5)	-14(6)	-24(6)

Table 4. Hydrogen coordinates (x 10^4) and isotropic displacement parameters ($Å^2$ x 10^3). The water and amino hydrogen atoms were located in difference maps; their O-H and N-H distances were constrained as were the Uiso parameters of two of these atoms. All remaining hydrogen atoms were included in idealised positions with U(iso)'s set at 1.2*U(eq) or, for the methyl group hydrogen atoms, 1.5*U(eq) of the parent carbon atoms.

	x	y	z	U(iso)
H(3)	649	11647	381	57
H(4)	-2617	13080	470	52
H(5)	-4279	12285	1759	56
H(6)	-2662	9892	2978	59
H(10)	5099	3714	3539	48
H(11)	6869	1216	4670	60
H(12A)	8120	-1897	6765	66
H(12B)	7501	-1551	5667	66
H(12C)	8477	-470	5998	66
H(13)	2605	3268	6786	52
H(14)	820	5744	5654	55
H(21A)	5120(70)	6430(150)	1720(80)	60
H(51A)	7510(190)	6560(160)	340(30)	60
H(51B)	8710(70)	6280(150)	1100(80)	50(40)

Table 5. Torsion angles, in degrees. E.s.ds are in parentheses.

C(6)-C(1)-C(2)-C(3) 2.4(16)
C(7)-C(1)-C(2)-C(3) -176.1(10)
C(6)-C(1)-C(2)-C(21) 179.3(11)
C(7)-C(1)-C(2)-C(21) 0.8(16)
C(1)-C(2)-C(3)-C(4) -4.9(16)
C(21)-C(2)-C(3)-C(4) 178.1(10)
C(2)-C(3)-C(4)-C(5) 4.3(17)
C(3)-C(4)-C(5)-C(6) -1.0(17)
C(2)-C(1)-C(6)-C(5) 0.8(16)
C(7)-C(1)-C(6)-C(5) 179.3(9)
C(4)-C(5)-C(6)-C(1) -1.5(16)
C(14)-C(9)-C(10)-C(11) -1.7(16)
C(8)-C(9)-C(10)-C(11) -179.1(10)
C(9)-C(10)-C(11)-C(12) 1.4(16)
C(10)-C(11)-C(12)-C(13) -1.6(17)
C(10)-C(11)-C(12)-O(12) 178.2(9)
C(13)-C(12)-O(12)-C(121) 176.6(10)
C(11)-C(12)-O(12)-C(121) -3.2(14)
C(11)-C(12)-C(13)-C(14) 2.0(18)
O(12)-C(12)-C(13)-C(14) -177.8(9)
C(12)-C(13)-C(14)-C(9) -2.2(17)
C(10)-C(9)-C(14)-C(13) 2.1(17)
C(8)-C(9)-C(14)-C(13) 179.5(10)
C(3)-C(2)-C(21)-N(22) 40.1(16)
C(1)-C(2)-C(21)-N(22) -136.8(11)
C(3)-C(2)-C(21)-N(21) -135.6(11)
C(1)-C(2)-C(21)-N(21) 47.5(16)

Table 6. Hydrogen bonds, in Ångstroms and degrees.

D-H...A	d(D-H)	d(H...A)	d(D...A)	<(DHA)
N(21)-H(21)A...O(51)	0.857	2.256	128.32	2.867
O(51)-H(51)A...Cl(1)#1	0.824	2.360	164.22	3.161
O(51)-H(51)B...Cl(1)#2	0.823	2.384	160.43	3.171

Symmetry operations: #1 : 1-x, 1-y, -z #2 : x+1, y, z

Crystal structure analysis of MeO-C_6H_4-CC-C_6H_4-$C(NH_2)_2$, Cl, H_2O

Crystal data: $C_{16}H_{15}N_2O$, H_2O, Cl, M = 304.77. Triclinic, space group P-1 (no. 2), a = 8.113(3), b = 8.133(3), c = 13.467(3) Å, α = 82.91(2), β = 83.06(2), γ = 60.90(3) °, V = 768.6(4) $Å^3$. Z = 2, Dc = 1.317 g cm^{-3}, F(000) = 320, T = 140(1) K, μ(Mo-Kα) = 2.54 cm^{-1}, λ(Mo-Kα) = 0.71073 Å.

Crystals are colourless plates. From a sample under oil, one, *ca* 0.05 x 0.33 x 0.41 mm, was mounted on a glass fibre and fixed in the cold nitrogen stream on an Oxford Diffraction Xcalibur-3/Sapphire3-CCD diffractometer, equipped with Mo-Kα radiation and graphite monochromator. Intensity data were measured by thin-slice ω- and φ-scans. Total no. of reflections recorded to θ_{max} = 20°, was 5362 of which 1416 were unique (Rint = 0.19); 796 were 'observed' with $I > 2\sigma_I$.

Data were processed using the CrysAlisPro-CCD and -RED (1) programs. The structure was determined by the intrinsic phasing routines in the SHELXT program (2A) and refined by full-matrix least-squares methods, on F^2's, in SHELXL (2B). The non-hydrogen atoms were refined with anisotropic thermal parameters. The two water hydrogen atoms and one of the amino hydrogens were located in difference maps and were included in the refinement process but with constrained O/N-H distances; the Uiso values for two of these atoms were fixed. The remaining hydrogen atoms were included in idealised positions and their Uiso values were set to ride on the Ueq values of the parent carbon atoms. The intensity data were rather diffuse and weak and the $2\theta_{max}$ value for inclusion in the refinement process was set at 40°. At the conclusion of the refinement, wR_2 = 0.35 and R_1 = 0.21 (2B) for all 1416 reflections weighted $w = [\sigma^2(F_o^2) + (0.20P)^2]^{-1}$ with $P = (F_o^2 + 2F_c^2)/3$; for the 'observed' data only, R_1 = 0.138.

In the final difference map, the highest peaks (to *ca* 0.7 $eÅ^{-3}$) were close to the chloride ion atom.

Scattering factors for neutral atoms were taken from reference (3). Computer programs used in this analysis have been noted above, and were run through WinGX (4) on a Dell Optiplex 780 PC at the University of East Anglia.

References

(5) Programs CrysAlisPro, Rigaku Oxford Diffraction Ltd., Abingdon, UK (2018).

(6) G. M. Sheldrick, Programs for crystal structure determination (SHELXT), *Acta Cryst.* (2015) A**71**, 3-8, and refinement (SHELXL), *Acta Cryst.* (2008) A**64**, 112-

122 and (2015) C**71**, 3-8.

(7) *'International Tables for X-ray Crystallography'*, Kluwer Academic Publishers, Dordrecht (1992). Vol. C, pp. 500, 219 and 193.

(8) L. J. Farrugia, *J. Appl. Cryst.* (2012) **45**, 849–854.

Legends for Figures

Figure 1. View of the moieties of MeO-C_6H_4-CC-C_6H_4-$C(NH_2)_2$, Cl, H_2O, indicating the atom numbering scheme. Thermal ellipsoids are drawn at the 50% probability level.

Figure 2. View showing the probable hydrogen bonds connecting the ions and water molecules in the crystal.

Figure 3. Packing viewed along the *b* axis.

Crystal data and structure refinement for $C_{16}H_{12}NO\text{-}N{=}C_{16}H_{13}NO$

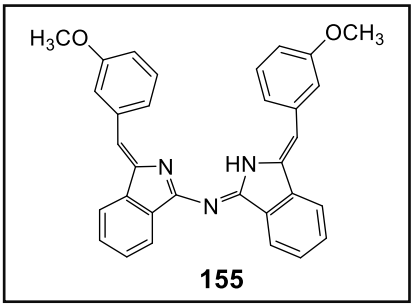

155

Identification code	**155**
Elemental formula	C32 H25 N3 O2
Formula weight	483.55
Crystal system, space group	Triclinic, P -1 (no. 2)
Unit cell dimensions	a = 7.47981(11) Å α = 101.5042(12) ° b = 11.99860(18) Å β = 95.5867(11) ° c = 14.03558(19) Å γ = 103.8877(13) °
Volume	1184.22(3) $Å^3$
Z, Calculated density	2, 1.356 Mg/m^3
F(000)	508
Absorption coefficient	0.679 mm^{-1}
Temperature	100.01(10) K
Wavelength	1.54184 Å
Crystal colour, shape	deep red plate
Crystal size	0.185 x 0.14 x 0.04 mm
Crystal mounting:	on a small loop, in oil, fixed in cold N_2 stream
On the diffractometer:	
Theta range for data collection	3.251 to 69.994 °
Limiting indices	-8<=h<=9, -14<=k<=14, -17<=l<=17
Completeness to theta = 67.684	99.6 %
Absorption correction	Semi-empirical from equivalents
Max. and min. transmission	1.00000 and 0.78261
Reflections collected (not including absences)	35660
No. of unique reflections	4473 [R(int) for equivalents = 0.045]
No. of 'observed' reflections ($I > 2\sigma_I$)	4170
Structure determined by:	dual methods, in SHELXT
Refinement:	Full-matrix least-squares on F^2, in SHELXL
Data / restraints / parameters	4473 / 0 / 340
Goodness-of-fit on F^2	1.057

Final R indices ('observed' data)	R_1 = 0.045, wR_2 = 0.102
Final R indices (all data)	R_1 = 0.047, wR_2 = 0.103
Reflections weighted: $w = [\sigma^2(Fo^2)+(0.0380P)^2+0.8695P]^{-1}$ where $P=(Fo^2+2Fc^2)/3$	
Extinction coefficient	n/a
Largest diff. peak and hole	0.25 and -0.23 e.Å^{-3}
Location of largest difference peak	near C(29)-C(23) bond

Table 1. Atomic coordinates (x 10^5) and equivalent isotropic displacement parameters ($Å^2$ x 10^4). U(eq) is defined as one third of the trace of the orthogonalized Uij tensor. E.s.ds are in parentheses.

	x	y	z	U(eq)
N(1)	75077(16)	51663(10)	53486(9)	180(3)
C(1)	79368(18)	41107(12)	52659(10)	172(3)
N(2)	80062(16)	33605(10)	44441(9)	175(3)
C(3)	85005(19)	23936(12)	47152(10)	177(3)
C(4)	91100(20)	19054(13)	64443(11)	212(3)
C(5)	92530(20)	23859(14)	74446(11)	240(3)
C(6)	90030(20)	35068(14)	77887(11)	238(3)
C(7)	85610(20)	41696(13)	71383(11)	206(3)
C(8)	83967(19)	36783(12)	61418(10)	182(3)
C(9)	86783(19)	25710(12)	57925(10)	183(3)
C(10)	88501(19)	14826(12)	40916(11)	184(3)
C(11)	89997(19)	13456(12)	30459(10)	181(3)
C(12)	95540(20)	23147(12)	26314(10)	193(3)
C(13)	97510(20)	21501(13)	16402(11)	197(3)
O(13)	103138(16)	31664(9)	13213(8)	257(2)
C(131)	106940(20)	30562(14)	3381(11)	258(3)
C(14)	93830(20)	10207(13)	10461(11)	213(3)
C(15)	88480(20)	581(13)	14634(11)	224(3)
C(16)	86760(20)	2065(12)	24483(11)	205(3)
C(21)	69917(18)	54830(12)	45460(10)	174(3)
N(22)	67310(16)	48656(10)	35944(9)	179(3)
C(23)	62378(19)	55134(12)	29299(11)	184(3)
C(24)	58380(20)	76519(12)	32964(11)	209(3)
C(25)	58760(20)	85965(13)	40566(12)	232(3)
C(26)	62610(20)	85527(13)	50413(12)	229(3)
C(27)	66290(20)	75565(12)	52879(11)	205(3)
C(28)	66098(19)	66180(12)	45228(11)	180(3)
C(29)	62111(19)	66526(12)	35404(11)	189(3)
C(30)	58480(20)	51529(13)	19450(11)	208(3)
C(31)	56801(19)	39820(13)	13311(11)	197(3)
C(32)	50760(20)	29497(13)	16701(10)	196(3)
C(33)	48930(20)	18535(13)	10584(11)	203(3)
O(33)	43202(15)	8035(9)	13216(8)	250(2)
C(331)	39650(20)	8411(13)	23059(11)	247(3)
C(34)	52870(20)	17633(13)	972(11)	229(3)
C(35)	58490(20)	27786(14)	-2385(11)	233(3)
C(36)	60470(20)	38823(13)	3656(11)	221(3)

Table 2. Molecular dimensions. Bond lengths are in Ångstroms, angles in degrees. E.s.ds are in parentheses.

N(1)-C(1) 1.3655(18)	N(1)-C(21) 1.3112(18)
C(1)-N(2) 1.3279(18)	C(21)-N(22) 1.3623(18)
C(1)-C(8) 1.4685(19)	C(21)-C(28) 1.4627(19)
N(2)-C(3) 1.4079(18)	N(22)-C(23) 1.4036(18)
C(3)-C(10) 1.353(2)	C(23)-C(30) 1.344(2)
C(3)-C(9) 1.4725(19)	C(23)-C(29) 1.4671(19)
C(4)-C(5) 1.390(2)	C(24)-C(25) 1.386(2)
C(4)-C(9) 1.392(2)	C(24)-C(29) 1.392(2)
C(5)-C(6) 1.399(2)	C(25)-C(26) 1.398(2)
C(6)-C(7) 1.390(2)	C(26)-C(27) 1.389(2)
C(7)-C(8) 1.386(2)	C(27)-C(28) 1.389(2)
C(8)-C(9) 1.395(2)	C(28)-C(29) 1.393(2)
C(10)-C(11) 1.462(2)	C(30)-C(31) 1.464(2)
C(11)-C(12) 1.396(2)	C(31)-C(36) 1.396(2)
C(11)-C(16) 1.405(2)	C(31)-C(32) 1.405(2)
C(12)-C(13) 1.393(2)	C(32)-C(33) 1.388(2)
C(13)-O(13) 1.3684(17)	C(33)-O(33) 1.3655(17)
C(13)-C(14) 1.390(2)	C(33)-C(34) 1.398(2)
O(13)-C(131) 1.4228(18)	O(33)-C(331) 1.4261(18)
C(14)-C(15) 1.389(2)	C(34)-C(35) 1.380(2)
C(15)-C(16) 1.381(2)	C(35)-C(36) 1.389(2)
	N(22)-H(22) 0.90(2)
C(21)-N(1)-C(1)118.93(12)	
N(2)-C(1)-N(1) 127.36(13)	C(8)-C(7)-C(6) 117.31(14)
N(2)-C(1)-C(8) 111.63(12)	C(7)-C(8)-C(9) 122.13(13)
N(1)-C(1)-C(8) 121.02(12)	C(7)-C(8)-C(1) 131.96(13)
C(1)-N(2)-C(3) 107.43(12)	C(9)-C(8)-C(1) 105.90(12)
C(10)-C(3)-N(2) 125.43(13)	C(4)-C(9)-C(8) 120.50(13)
C(10)-C(3)-C(9) 125.63(13)	C(4)-C(9)-C(3) 133.39(13)
N(2)-C(3)-C(9) 108.86(12)	C(8)-C(9)-C(3) 106.05(12)
C(5)-C(4)-C(9) 117.68(14)	C(3)-C(10)-C(11) 128.51(13)
C(4)-C(5)-C(6) 121.41(14)	C(12)-C(11)-C(16) 118.71(13)
C(7)-C(6)-C(5) 120.95(14)	C(12)-C(11)-C(10) 121.99(13)

C(16)-C(11)-C(10) 119.21(13)
C(13)-C(12)-C(11) 120.39(13)
O(13)-C(13)-C(14) 124.35(13)
O(13)-C(13)-C(12) 114.98(12)
C(14)-C(13)-C(12) 120.67(13)
C(13)-O(13)-C(131) 117.50(11)
C(15)-C(14)-C(13) 118.77(13)
C(16)-C(15)-C(14) 121.26(13)
C(15)-C(16)-C(11) 120.16(13)

N(1)-C(21)-N(22) 128.45(13)
N(1)-C(21)-C(28) 124.73(13)
N(22)-C(21)-C(28) 106.82(12)
C(21)-N(22)-C(23) 112.00(12)
C(30)-C(23)-N(22) 126.98(13)
C(30)-C(23)-C(29) 127.65(13)
N(22)-C(23)-C(29) 105.36(12)
C(25)-C(24)-C(29) 117.99(14)
C(24)-C(25)-C(26) 121.44(14)
C(27)-C(26)-C(25) 120.76(14)
C(26)-C(27)-C(28) 117.54(14)
C(27)-C(28)-C(29) 121.95(13)
C(27)-C(28)-C(21) 130.26(13)
C(29)-C(28)-C(21) 107.79(12)
C(24)-C(29)-C(28) 120.32(14)
C(24)-C(29)-C(23) 131.72(14)
C(28)-C(29)-C(23) 107.95(12)
C(23)-C(30)-C(31) 128.37(13)
C(36)-C(31)-C(32) 118.90(13)
C(36)-C(31)-C(30) 119.17(13)
C(32)-C(31)-C(30) 121.86(13)
C(33)-C(32)-C(31) 120.19(13)
O(33)-C(33)-C(32) 124.46(13)
O(33)-C(33)-C(34) 115.05(13)
C(32)-C(33)-C(34) 120.49(13)
C(33)-O(33)-C(331) 117.61(11)
C(35)-C(34)-C(33) 119.13(14)
C(34)-C(35)-C(36) 121.09(14)
C(35)-C(36)-C(31) 120.18(14)
C(21)-N(22)-H(22) 118.8(13)
C(23)-N(22)-H(22) 129.0(13)

Table 3. Anisotropic displacement parameters ($Å^2$ x 10^4) for the expression:exp {$-2\pi^2(h^2a^{*2}U_{11} + ... + 2hka^*b^*U_{12})$} E.s.ds are in parentheses.

	U_{11}	U_{22}	U_{33}	U_{23}	U_{13}	U_{12}
N(1)	176(6)	160(6)	200(6)	37(5)	31(5)	39(5)
C(1)	126(6)	167(7)	210(7)	42(5)	19(5)	19(5)
N(2)	166(6)	158(6)	208(6)	43(5)	31(5)	52(5)
C(3)	144(6)	183(7)	205(7)	63(5)	20(5)	29(5)
C(4)	191(7)	213(7)	246(7)	72(6)	31(6)	64(6)
C(5)	234(7)	272(8)	238(8)	113(6)	17(6)	71(6)
C(6)	229(7)	279(8)	184(7)	40(6)	21(6)	39(6)
C(7)	188(7)	197(7)	215(7)	32(6)	26(6)	29(5)
C(8)	133(6)	186(7)	216(7)	53(5)	22(5)	16(5)
C(9)	130(6)	200(7)	210(7)	49(6)	28(5)	27(5)
C(10)	162(7)	167(7)	229(7)	63(5)	21(5)	43(5)
C(11)	143(6)	191(7)	213(7)	41(6)	17(5)	62(5)
C(12)	205(7)	166(7)	207(7)	19(5)	26(6)	72(5)
C(13)	186(7)	197(7)	229(7)	69(6)	29(6)	72(5)
O(13)	382(6)	198(5)	223(5)	75(4)	97(5)	95(5)
C(131)	295(8)	286(8)	220(7)	100(6)	65(6)	88(6)
C(14)	221(7)	244(7)	180(7)	29(6)	29(6)	90(6)
C(15)	231(7)	168(7)	250(8)	-7(6)	23(6)	62(6)
C(16)	188(7)	173(7)	265(8)	61(6)	41(6)	59(5)

C(21)	133(6)	162(7)	210(7)	30(5)	36(5)	15(5)
N(22)	192(6)	155(6)	190(6)	35(5)	18(5)	52(5)
C(23)	158(7)	159(7)	237(7)	59(6)	33(5)	34(5)
C(24)	180(7)	181(7)	268(8)	74(6)	24(6)	37(5)
C(25)	183(7)	166(7)	352(8)	78(6)	45(6)	41(6)
C(26)	198(7)	170(7)	299(8)	6(6)	52(6)	43(6)
C(27)	169(7)	191(7)	236(7)	23(6)	28(6)	31(5)
C(28)	134(6)	160(7)	237(7)	46(5)	35(5)	20(5)
C(29)	134(6)	177(7)	246(7)	50(6)	34(5)	20(5)
C(30)	213(7)	190(7)	232(7)	77(6)	21(6)	54(6)
C(31)	178(7)	204(7)	208(7)	38(6)	-1(5)	66(5)
C(32)	192(7)	219(7)	176(7)	41(6)	11(5)	68(6)
C(33)	190(7)	197(7)	232(7)	59(6)	5(6)	73(6)
O(33)	338(6)	177(5)	238(5)	39(4)	55(4)	79(4)
C(331)	288(8)	215(7)	252(8)	76(6)	47(6)	71(6)
C(34)	230(7)	238(8)	211(7)	3(6)	6(6)	101(6)
C(35)	233(7)	297(8)	183(7)	51(6)	29(6)	100(6)
C(36)	212(7)	240(7)	226(7)	83(6)	24(6)	69(6)

Table 4. Hydrogen coordinates (x 10^4) and isotropic displacement parameters ($Å^2$ x 10^3). The amino hydrogen atom, H(22), was located in a difference map and was refined freely and isotropically. All remaining hydrogen atoms were included in idealised positions with U(iso)'s set at 1.2*U(eq) or, for the methyl group hydrogen atoms, 1.5*U(eq) of the parent carbon atoms.

	x	y	z	U(iso)
H(4)	9297	1165	6219	25
H(5)	9520	1953	7894	29
H(6)	9134	3813	8462	29
H(7)	8383	4913	7363	25
H(10)	9017	862	4364	22
H(12)	9793	3075	3019	23
H(13A)	11054	3825	201	39
H(13B)	9597	2586	-109	39
H(13C)	11687	2683	259	39
H(14)	9493	912	382	26
H(15)	8602	-701	1072	27
H(16)	8345	-449	2717	25
H(24)	5571	7684	2643	25
H(25)	5640	9274	3909	28
H(26)	6271	9198	5537	28
H(27)	6878	7519	5941	25
H(30)	5660	5720	1610	25
H(32)	4798	3001	2306	23
H(33A)	3684	57	2415	37
H(33B)	2925	1165	2408	37
H(33C)	5046	1326	2757	37
H(34)	5172	1029	-311	27
H(35)	6100	2723	-880	28
H(36)	6426	4557	126	27
H(22)	6980(30)	4153(19)	3469(15)	42(6)

Table 5. Torsion angles, in degrees. E.s.ds are in parentheses.

C(21)-N(1)-C(1)-N(2) 4.4(2)
C(21)-N(1)-C(1)-C(8)-175.74(12)
N(1)-C(1)-N(2)-C(3)-179.84(13)
C(8)-C(1)-N(2)-C(3) 0.26(15)
C(1)-N(2)-C(3)-C(10)-174.78(13)
C(1)-N(2)-C(3)-C(9) 2.03(15)
C(9)-C(4)-C(5)-C(6)-1.0(2)
C(4)-C(5)-C(6)-C(7) 1.4(2)
C(5)-C(6)-C(7)-C(8)-0.5(2)
C(6)-C(7)-C(8)-C(9)-0.7(2)
C(6)-C(7)-C(8)-C(1) 179.23(14)
N(2)-C(1)-C(8)-C(7) 177.53(14)
N(1)-C(1)-C(8)-C(7)-2.4(2)
N(2)-C(1)-C(8)-C(9)-2.53(16)
N(1)-C(1)-C(8)-C(9) 177.56(12)
C(5)-C(4)-C(9)-C(8)-0.2(2)
C(5)-C(4)-C(9)-C(3) 176.61(14)
C(7)-C(8)-C(9)-C(4) 1.1(2)
C(1)-C(8)-C(9)-C(4)-178.86(12)
C(7)-C(8)-C(9)-C(3)-176.50(12)
C(1)-C(8)-C(9)-C(3) 3.55(14)
C(10)-C(3)-C(9)-C(4)-3.9(3)
N(2)-C(3)-C(9)-C(4) 179.29(15)
C(10)-C(3)-C(9)-C(8) 173.22(13)
N(2)-C(3)-C(9)-C(8)-3.58(15)
N(2)-C(3)-C(10)-C(11) 7.3(2)
C(9)-C(3)-C(10)-C(11)-169.03(13)
C(3)-C(10)-C(11)-C(12) 27.2(2)
C(3)-C(10)-C(11)-C(16)-156.33(14)
C(16)-C(11)-C(12)-C(13) 1.0(2)
C(10)-C(11)-C(12)-C(13) 177.49(13)
C(11)-C(12)-C(13)-O(13)-179.55(12)
C(11)-C(12)-C(13)-C(14) 0.6(2)
C(14)-C(13)-O(13)-C(131)-5.4(2)
C(12)-C(13)-O(13)-C(131) 174.72(12)
O(13)-C(13)-C(14)-C(15) 178.99(13)
C(12)-C(13)-C(14)-C(15)-1.2(2)
C(13)-C(14)-C(15)-C(16) 0.1(2)
C(14)-C(15)-C(16)-C(11) 1.5(2)
C(12)-C(11)-C(16)-C(15)-2.1(2)
C(10)-C(11)-C(16)-C(15)-178.64(13)
C(1)-N(1)-C(21)-N(22) 3.2(2)
C(1)-N(1)-C(21)-C(28)-175.85(12)
N(1)-C(21)-N(22)-C(23)-177.91(13)
C(28)-C(21)-N(22)-C(23) 1.23(15)
C(21)-N(22)-C(23)-C(30)-178.54(14)
C(21)-N(22)-C(23)-C(29) 0.56(15)
C(29)-C(24)-C(25)-C(26)-0.5(2)
C(24)-C(25)-C(26)-C(27) 0.4(2)
C(25)-C(26)-C(27)-C(28) 0.4(2)
C(26)-C(27)-C(28)-C(29)-1.0(2)
C(26)-C(27)-C(28)-C(21) 177.98(14)
N(1)-C(21)-C(28)-C(27)-2.5(2)
N(22)-C(21)-C(28)-C(27) 178.30(14)
N(1)-C(21)-C(28)-C(29) 176.54(13)
N(22)-C(21)-C(28)-C(29)-2.64(15)
C(25)-C(24)-C(29)-C(28) 0.0(2)
C(25)-C(24)-C(29)-C(23) 178.27(14)
C(27)-C(28)-C(29)-C(24) 0.8(2)
C(21)-C(28)-C(29)-C(24)-178.35(12)
C(27)-C(28)-C(29)-C(23)-177.86(13)
C(21)-C(28)-C(29)-C(23) 2.98(15)
C(30)-C(23)-C(29)-C(24)-1.6(3)
N(22)-C(23)-C(29)-C(24) 179.30(14)
C(30)-C(23)-C(29)-C(28) 176.86(14)
N(22)-C(23)-C(29)-C(28)-2.23(15)
N(22)-C(23)-C(30)-C(31) 5.8(2)
C(29)-C(23)-C(30)-C(31)-173.08(14)
C(23)-C(30)-C(31)-C(36)-153.14(15)
C(23)-C(30)-C(31)-C(32) 29.9(2)
C(36)-C(31)-C(32)-C(33) 1.5(2)
C(30)-C(31)-C(32)-C(33) 178.48(13)
C(31)-C(32)-C(33)-O(33) 179.87(13)
C(31)-C(32)-C(33)-C(34)-0.7(2)
C(32)-C(33)-O(33)-C(331)-2.8(2)
C(34)-C(33)-O(33)-C(331) 177.69(12)
O(33)-C(33)-C(34)-C(35) 179.06(13)
C(32)-C(33)-C(34)-C(35)-0.5(2)
C(33)-C(34)-C(35)-C(36) 0.7(2)
C(34)-C(35)-C(36)-C(31) 0.1(2)
C(32)-C(31)-C(36)-C(35)-1.2(2)
C(30)-C(31)-C(36)-C(35)-178.29(13)

Table 6. Hydrogen bond, in Ångstroms and degrees.

D-H...A	d(D-H)	d(H...A)	d(D...A)	<(DHA)
N(22)-H(22)...N(2)	0.90(2)	2.01(2)	2.6567(16)	127.3(17)

Crystal structure analysis of $C_{16}H_{12}NO$-N=$C_{16}H_{13}NO$

Crystal data: $C_{32}H_{25}N_3O_2$, M = 483.55. Triclinic, space group P-1 (no. 2), a = 7.47981(11), b = 11.99860(18), c = 14.03558(19) Å, α = 101.5042(12), β = 95.5867(11), γ = 103.8877(13) °, V = 1184.22(3) $Å^3$. Z = 2, Dc = 1.356 g cm^{-3}, F(000) = 508, T = 100.01(10) K, μ(Cu-Kα) = 6.8 cm^{-1}, λ(Cu-Kα) = 1.54184 Å.

The crystals were deep red plates. One, *ca* 0.04 x 0.14 x 0.185 mm, was mounted in oil on a small loop and fixed in the cold nitrogen stream on a Rigaku Oxford Diffraction XtaLAB Synergy diffractometer, equipped with Cu-Kα radiation, HyPix detector and mirror monochromator. Intensity data were measured by thin-slice ω-scans. Total no. of reflections recorded, to θ_{max} = 70.0°, was 35660 of which 4473 were unique (Rint = 0.045); 4170 were 'observed' with $I > 2\sigma_I$.

Data were processed using the CrysAlisPro-CCD and -RED (1) programs. The structure was determined by the intrinsic phasing routines in the SHELXT program (2A) and refined by full-matrix least-squares methods, on F^2's, in SHELXL (2B). The non-hydrogen atoms were refined with anisotropic thermal parameters. The hydrogen atom on N(22) was located in a difference map and was refined freely. The remaining hydrogen atoms were included in idealised positions and their Uiso values were set to ride on the Ueq values of the parent carbon atoms. At the conclusion of the refinement, wR_2 = 0.103 and R_1 = 0.047 (2B) for all 4473 reflections weighted $w = [\sigma^2(F_o^2) + (0.0380\ P)^2 + 0.8695\ P]^{-1}$ with $P = (F_o^2 + 2F_c^2)/3$.

In the final difference map, the highest peak (*ca* 0.25 $eÅ^{-3}$) was near the C(29)-C(23) bond.

Scattering factors for neutral atoms were taken from reference (3). Computer programs used in this analysis have been noted above, and were run through WinGX (4) on a Dell Optiplex 780 PC at the University of East Anglia.

References

(9) Programs CrysAlisPro, Rigaku Oxford Diffraction Ltd., Abingdon, UK (2018).

(10) G. M. Sheldrick, Programs for crystal structure determination (SHELXT), *Acta Cryst.* (2015) A**71**, 3-8, and refinement (SHELXL), *Acta Cryst.* (2008) A**64**, 112-122 and (2015) C**71**, 3-8.

(11) *'International Tables for X-ray Crystallography'*, Kluwer Academic Publishers, Dordrecht (1992). Vol. C, pp. 500, 219 and 193.

(12) L. J. Farrugia, *J. Appl. Cryst.* (2012) **45**, 849–854.

Legends for Figures

Figure 1. View of a molecule of $C_{16}H_{12}NO\text{-}N{=}C_{16}H_{13}NO$, indicating the atom numbering scheme. Thermal ellipsoids are drawn at the 50% probability level.

Figure 2. View of the packing of molecules, along the *a* axis.

Notes on the structure

The molecule shows pseudo-twofold symmetry about N(1); the major distortions from real symmetry are (1) in the hydrogen bond in N(22)-H(22)…N(2) and (2) in the alignment of the methoxy groups.

The hydrogen atom of the hydrogen bond was located clearly in a difference map and was refined freely, isotropically and satisfactorily. The bond distances and angles in the chain between N(2) and N(22) are in agreement with the arrangement of single- and double-bonds of the formula.

The two bicyclic C_8N moieties are essentially coplanar, with the CHC_6H_4 groups veering away to opposite sides of the plane. There are rotations about the C(10)-C(11) and C(30)-C(31) bonds of about 28° which allow the two phenyl rings to lie almost parallel with C(13) and C(33) overlaid at a distance of 3.562 Å. The O-Me bonds are diametrically opposed, with O(13)-C(131) pointing away from N(1) and O(33)-C(331) towards the N(1) centre.

Molecules are stacked in columns parallel to the *a* axis, each molecule involved with three π…π columns; the central bis-bicyclic rings have centrosymmetrically groups on each side at a distance of *ca* 3.5 Å, and each of the C_6H_4OMe groups has, on one side, the other C_6H_4OMe group of the same molecule and, on the other side, the second C_6H_4OMe group of the next molecule along the *a* axis.

Crystal data and structure refinement for F_2BN-{(C_8H_4N)=CH-C_6H_4OMe}$_2$

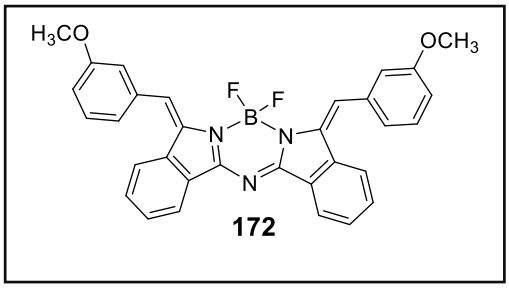

172

Identification code	**172**
Elemental formula	2(C32 H24 B1 F2 N3 O2)
Formula weight	1062.70
Crystal system, space group	Orthorhombic, $P2_12_12$ (no. 18)
Unit cell dimensions	a = 22.0145(8) Å α = 90 ° b = 27.0662(9) Å β = 90 ° c = 8.6554(4) Å γ = 90 °
Volume	5157.3(3) Å^3
Z, Calculated density	4, 1.369 Mg/m^3
F(000)	2208
Absorption coefficient	0.784 mm^{-1}
Temperature	100.01(10) K
Wavelength	1.54184 Å
Crystal colour, shape	yellow prism
Crystal size	0.02 x 0.05 x 0.18 mm
Crystal mounting:	on a small loop, in oil, fixed in cold N_2 stream
On the diffractometer:	
Theta range for data collection	6.343 to 52.066 °
Limiting indices	-22<=h<=22, -27<=k<=27, -8<=l<=8
Completeness to theta = 52.066	99.2 %
Absorption correction	Semi-empirical from equivalents
Max. and min. transmission	1.00000 and 0.62028
Reflections collected (not including absences)	54700
No. of unique reflections	5729 [R(int) for equivalents = 0.108]
No. of 'observed' reflections ($I > 2\sigma_I$)	5047
Structure determined by:	dual methods, in SHELXT
Refinement:	Full-matrix least-squares on F^2, in SHELXL
Data / restraints / parameters	5729 / 0 / 721

Goodness-of-fit on F^2	0.991
Final R indices ('observed' data)	R_1 = 0.039, wR_2 = 0.093
Final R indices (all data)	R_1 = 0.046, wR_2 = 0.095
Reflections weighted: $w = [\sigma^2(Fo^2)+(0.0680P)^2]^{-1}$ where $P=(Fo^2+2Fc^2)/3$	
Absolute structure parameter	0.02(9)
Extinction coefficient	n/a
Largest diff. peak and hole	0.19 and -0.21 e.Å^{-3}
Location of largest difference peak	near C(62)

Table 1. Atomic coordinates (x 10^5) and equivalent isotropic displacement parameters ($Å^2$ x 10^4). U(eq) is defined as one third of the trace of the orthogonalized Uij tensor. E.s.ds are in parentheses.

	x	y	z	U(eq)
B(1)	41790(20)	33917(18)	61840(60)	291(13)
F(11)	38164(10)	36050(8)	73310(30)	345(6)
F(12)	44305(10)	37708(8)	52990(30)	343(6)
N(1)	38071(14)	30337(12)	51850(40)	296(9)
N(2)	43222(15)	22962(12)	59590(40)	303(9)
C(2)	38910(18)	25395(15)	51900(50)	293(11)
C(3)	34477(18)	23128(15)	41880(50)	271(11)
C(4)	33400(20)	18142(16)	39050(50)	333(11)
C(5)	28710(20)	16948(16)	28980(50)	349(12)
C(6)	25220(20)	20643(17)	22270(50)	356(12)
C(7)	26220(20)	25620(15)	25310(50)	325(12)
C(8)	30956(18)	26855(15)	35190(50)	284(11)
C(9)	33211(18)	31584(16)	41610(50)	302(11)
C(10)	31403(18)	36318(15)	40090(50)	301(11)
C(11)	27028(19)	38541(15)	29590(50)	307(11)
C(12)	23647(18)	42610(15)	34950(60)	325(11)
C(13)	19652(18)	45152(15)	25370(50)	301(11)
O(13)	16670(13)	49024(10)	31990(30)	361(8)
C(17)	12010(20)	51377(17)	23070(60)	483(14)
C(14)	18946(19)	43677(16)	10020(50)	335(12)
C(15)	22352(19)	39698(15)	4520(60)	358(12)
C(16)	26324(19)	37176(16)	14010(50)	325(11)
N(21)	46805(14)	30695(12)	69160(40)	287(9)
C(22)	46987(19)	25749(16)	67860(50)	285(11)
C(23)	52079(19)	23886(16)	76750(50)	298(11)
C(24)	53836(19)	19018(16)	79480(50)	334(12)
C(25)	58750(20)	18259(18)	89170(50)	384(12)
C(26)	61646(19)	22227(17)	96260(60)	383(12)
C(27)	59862(18)	27074(16)	93690(50)	342(11)
C(28)	55044(18)	27921(15)	83490(50)	300(11)
C(29)	51653(18)	32391(16)	78820(50)	308(11)
C(30)	52115(18)	37225(16)	82580(50)	320(11)
C(31)	56891(19)	39808(15)	91080(50)	315(11)
C(32)	55183(19)	43742(15)	100590(50)	333(11)
C(33)	59600(20)	46566(16)	108150(60)	362(12)
C(34)	65710(20)	45466(16)	106330(60)	384(12)
C(35)	67420(20)	41620(16)	96710(60)	381(12)
C(36)	63105(18)	38802(17)	89120(50)	358(12)
O(33)	57339(13)	50377(11)	116800(40)	459(8)
C(37)	61540(20)	53720(18)	123380(60)	527(14)
B(41)	14980(20)	65362(18)	10990(60)	297(13)
F(41)	17664(9)	61701(8)	1890(30)	339(6)
F(42)	11391(10)	63023(8)	22090(30)	348(6)
N(41)	19807(14)	68673(12)	18510(40)	291(9)
N(42)	16108(15)	76381(12)	8760(40)	298(9)
C(42)	19927(18)	73640(15)	17170(50)	295(11)
C(43)	24890(20)	75602(16)	26220(50)	305(11)
C(44)	26490(20)	80473(16)	29040(50)	333(12)
C(45)	31360(20)	81331(17)	38880(50)	375(12)
C(46)	34335(19)	77436(17)	45980(60)	376(12)
C(47)	32676(19)	72542(17)	43300(50)	357(12)
C(48)	27901(18)	71623(15)	32980(50)	301(11)
C(49)	24719(18)	67113(16)	28090(50)	309(11)
C(50)	25434(19)	62298(16)	31490(50)	328(11)
C(51)	30250(20)	59854(15)	40290(50)	326(11)
C(52)	28640(20)	55928(15)	49630(50)	367(12)
C(53)	32980(20)	53308(16)	57900(60)	403(12)
C(54)	39040(20)	54576(17)	56580(60)	444(13)
C(55)	40690(20)	58414(18)	46910(60)	435(13)
C(56)	36423(19)	61057(18)	38770(60)	403(13)
O(53)	30768(15)	49565(11)	66810(40)	515(9)

C(57)	35160(30)	46530(18)	74500(60)	572(15)
N(61)	11102(14)	68930(12)	1100(40)	291(9)
C(62)	11848(18)	73881(15)	1090(50)	285(11)
C(63)	7351(18)	76088(15)	-8920(50)	293(11)
C(64)	6270(20)	81064(16)	-11910(50)	318(11)
C(65)	1579(19)	82186(16)	-21950(50)	323(11)
C(66)	-1901(19)	78497(17)	-28360(50)	352(12)
C(67)	-850(20)	73536(17)	-25220(50)	343(12)
C(68)	3889(19)	72309(15)	-15470(50)	294(11)
C(69)	6264(18)	67606(15)	-9080(50)	296(11)
C(70)	4661(18)	62838(16)	-10770(50)	326(11)
C(71)	140(20)	60539(15)	-20900(50)	305(11)
C(72)	-3129(18)	56517(15)	-15130(50)	304(11)
C(73)	-7341(19)	54023(15)	-23960(50)	319(11)
C(74)	-8390(20)	55484(16)	-39140(60)	376(12)
C(75)	-5060(20)	59418(16)	-45100(60)	403(12)
C(76)	-794(19)	61926(16)	-36320(50)	357(11)
O(73)	-10246(13)	50147(10)	-16870(30)	365(7)
C(77)	-14560(20)	47396(17)	-25790(60)	477(14)

Table 2. Molecular dimensions. Bond lengths are in Ångstroms, angles in degrees. E.s.ds are in parentheses.

B(1)-F(12)	1.395(5)
B(1)-F(11)	1.399(5)
B(1)-N(1)	1.536(6)
B(1)-N(21)	1.542(6)
N(1)-C(2)	1.350(5)
N(1)-C(9)	1.430(5)
N(2)-C(22)	1.330(5)
N(2)-C(2)	1.333(5)
C(2)-C(3)	1.442(6)
C(3)-C(4)	1.392(6)
C(3)-C(8)	1.398(6)
C(4)-C(5)	1.390(6)
C(5)-C(6)	1.388(6)
C(6)-C(7)	1.390(6)
C(7)-C(8)	1.390(6)
C(8)-C(9)	1.481(6)
C(9)-C(10)	1.348(6)
C(10)-C(11)	1.454(6)
C(11)-C(16)	1.407(6)
C(11)-C(12)	1.408(6)
C(12)-C(13)	1.391(6)
C(13)-O(13)	1.363(5)
C(13)-C(14)	1.396(6)
O(13)-C(17)	1.433(5)
C(14)-C(15)	1.396(6)
C(15)-C(16)	1.380(6)
N(21)-C(22)	1.344(5)
N(21)-C(29)	1.431(5)
C(22)-C(23)	1.450(6)
C(23)-C(24)	1.394(6)
C(23)-C(28)	1.400(6)
C(24)-C(25)	1.385(6)
C(25)-C(26)	1.391(6)
C(26)-C(27)	1.387(6)
C(27)-C(28)	1.399(6)
C(28)-C(29)	1.478(6)
C(29)-C(30)	1.352(6)
C(30)-C(31)	1.461(6)
C(31)-C(32)	1.398(6)
C(31)-C(36)	1.405(6)
C(32)-C(33)	1.399(6)
C(33)-O(33)	1.368(5)
C(33)-C(34)	1.388(6)
C(34)-C(35)	1.385(6)
C(35)-C(36)	1.384(6)
O(33)-C(37)	1.414(5)
B(41)-F(42)	1.395(5)
B(41)-F(41)	1.397(5)
B(41)-N(41)	1.535(6)
B(41)-N(61)	1.547(6)
N(41)-C(42)	1.350(5)
N(41)-C(49)	1.427(5)
N(42)-C(62)	1.334(5)
N(42)-C(42)	1.337(5)
C(42)-C(43)	1.444(6)
C(43)-C(44)	1.387(6)
C(43)-C(48)	1.394(6)
C(44)-C(45)	1.389(6)
C(45)-C(46)	1.385(6)
C(46)-C(47)	1.393(6)
C(47)-C(48)	1.401(6)
C(48)-C(49)	1.470(6)
C(49)-C(50)	1.345(6)
C(50)-C(51)	1.463(6)
C(51)-C(52)	1.382(6)
C(51)-C(56)	1.404(6)

C(52)-C(53)
1.389(6)
C(53)-O(53)
1.364(5)
C(53)-C(54)
1.382(7)
C(54)-C(55)
1.382(6)
C(55)-C(56)
1.375(6)
O(53)-C(57)
1.432(5)
N(61)-C(62)
1.350(5)
N(61)-C(69)
1.428(5)
C(62)-C(63)
1.445(6)
C(63)-C(64)
1.392(6)
C(63)-C(68)
1.396(6)
C(64)-C(65)
1.383(6)
C(65)-C(66)
1.375(6)

F(12)-B(1)-F(11)
108.2(3)
F(12)-B(1)-N(1)
111.5(4)
F(11)-B(1)-N(1)
110.8(3)
F(12)-B(1)-N(21)
111.0(3)
F(11)-B(1)-N(21)
110.5(4)
N(1)-B(1)-N(21)
104.8(3)
C(2)-N(1)-C(9)
109.8(4)
C(2)-N(1)-B(1)
123.4(4)
C(9)-N(1)-B(1)
126.8(3)
C(22)-N(2)-C(2)
115.6(4)
N(2)-C(2)-N(1)
126.0(4)
N(2)-C(2)-C(3)
124.9(4)
N(1)-C(2)-C(3)
109.1(4)
C(4)-C(3)-C(8)
122.2(4)
C(4)-C(3)-C(2)
129.3(4)
C(8)-C(3)-C(2)
108.5(4)
C(5)-C(4)-C(3)
117.5(4)
C(6)-C(5)-C(4)
120.4(4)
C(5)-C(6)-C(7)
122.1(4)
C(8)-C(7)-C(6)
117.9(4)
C(7)-C(8)-C(3)
119.9(4)
C(7)-C(8)-C(9)
133.7(4)

C(66)-C(67)
1.390(6)
C(67)-C(68)
1.382(6)
C(68)-C(69)
1.483(6)
C(69)-C(70)
1.346(6)
C(70)-C(71)
1.465(6)
C(71)-C(72)
1.397(6)
C(71)-C(76)
1.401(6)
C(72)-C(73)
1.378(6)
C(73)-O(73)
1.373(5)
C(73)-C(74)
1.392(6)
C(74)-C(75)
1.391(6)
C(75)-C(76)
1.387(6)
O(73)-C(77)
1.433(5)

F(42)-B(41)-F(41)
107.8(3)
F(42)-B(41)-N(41)
111.4(4)
F(41)-B(41)-N(41)
111.1(3)
F(42)-B(41)-N(61)
110.6(3)
F(41)-B(41)-N(61)
111.3(4)
N(41)-B(41)-N(61)
104.6(3)
C(42)-N(41)-C(49)
109.2(3)
C(42)-N(41)-B(41)
124.0(4)
C(49)-N(41)-B(41)
126.8(3)
C(62)-N(42)-C(42)
115.6(4)
C(3)-C(8)-C(9)
106.4(4)
C(10)-C(9)-N(1)
120.4(4)
C(10)-C(9)-C(8)
133.3(4)
N(1)-C(9)-C(8)
106.2(3)
C(9)-C(10)-C(11)
130.5(4)
C(16)-C(11)-C(12)
117.6(4)
C(16)-C(11)-C(10)
124.3(4)
C(12)-C(11)-C(10)
117.9(4)
C(13)-C(12)-C(11)
121.7(4)
O(13)-C(13)-C(12)
115.7(4)
O(13)-C(13)-C(14)
124.5(4)
C(12)-C(13)-C(14)
119.7(4)

C(13)-O(13)-C(17) 117.4(3)
C(13)-C(14)-C(15) 119.0(4)
C(16)-C(15)-C(14) 121.3(4)
C(15)-C(16)-C(11) 120.7(4)
C(22)-N(21)-C(29) 110.2(4)
C(22)-N(21)-B(1) 123.4(4)
C(29)-N(21)-B(1) 126.3(3)
N(2)-C(22)-N(21) 126.2(4)
N(2)-C(22)-C(23) 124.8(4)
N(21)-C(22)-C(23) 109.0(4)
C(24)-C(23)-C(28) 122.5(4)
C(24)-C(23)-C(22) 129.3(4)
C(28)-C(23)-C(22) 108.1(4)
C(25)-C(24)-C(23) 117.4(4)
C(24)-C(25)-C(26) 120.7(4)
C(27)-C(26)-C(25) 122.0(4)
C(26)-C(27)-C(28) 118.1(4)
C(27)-C(28)-C(23) 119.3(4)
C(27)-C(28)-C(29) 133.6(4)
C(23)-C(28)-C(29) 106.8(4)
C(30)-C(29)-N(21) 120.5(4)
C(30)-C(29)-C(28) 133.5(4)
N(21)-C(29)-C(28) 105.9(4)
C(29)-C(30)-C(31) 129.7(4)
C(32)-C(31)-C(36) 118.7(4)
C(32)-C(31)-C(30) 117.9(4)
C(36)-C(31)-C(30) 123.2(4)
C(31)-C(32)-C(33) 120.3(4)
O(33)-C(33)-C(34) 125.2(4)
O(33)-C(33)-C(32) 114.5(4)
C(34)-C(33)-C(32) 120.3(4)
C(35)-C(34)-C(33) 119.5(4)
C(36)-C(35)-C(34) 120.9(4)
C(35)-C(36)-C(31) 120.3(4)
C(33)-O(33)-C(37) 117.7(3)
N(42)-C(42)-N(41) 126.0(4)
N(42)-C(42)-C(43) 124.5(4)
N(41)-C(42)-C(43) 109.5(4)
C(44)-C(43)-C(48) 122.6(4)
C(44)-C(43)-C(42) 129.6(4)
C(48)-C(43)-C(42) 107.7(4)
C(43)-C(44)-C(45) 117.6(4)
C(46)-C(45)-C(44) 120.7(4)
C(45)-C(46)-C(47) 121.7(4)
C(46)-C(47)-C(48) 118.1(4)
C(43)-C(48)-C(47) 119.2(4)
C(43)-C(48)-C(49) 107.1(4)
C(47)-C(48)-C(49) 133.5(4)
C(50)-C(49)-N(41) 120.2(4)
C(50)-C(49)-C(48) 133.3(4)
N(41)-C(49)-C(48) 106.4(4)
C(49)-C(50)-C(51) 129.5(4)
C(52)-C(51)-C(56) 118.8(4)
C(52)-C(51)-C(50) 117.8(4)
C(56)-C(51)-C(50) 123.2(4)
C(51)-C(52)-C(53) 121.1(4)
O(53)-C(53)-C(54) 125.2(4)
O(53)-C(53)-C(52) 115.1(4)
C(54)-C(53)-C(52) 119.7(5)
C(53)-C(54)-C(55) 119.3(4)
C(56)-C(55)-C(54) 121.5(4)
C(55)-C(56)-C(51) 119.5(5)
C(53)-O(53)-C(57) 116.6(4)
C(62)-N(61)-C(69) 109.8(3)
C(62)-N(61)-B(41) 123.6(4)
C(69)-N(61)-B(41) 126.6(3)
N(42)-C(62)-N(61) 126.1(4)
N(42)-C(62)-C(63) 124.8(4)
N(61)-C(62)-C(63) 109.1(4)
C(64)-C(63)-C(68) 122.7(4)

C(64)-C(63)-C(62)	129.0(4)	C(69)-C(70)-C(71)	130.6(4)
C(68)-C(63)-C(62)	108.3(4)	C(72)-C(71)-C(76)	118.3(4)
C(65)-C(64)-C(63)	117.2(4)	C(72)-C(71)-C(70)	117.8(4)
C(66)-C(65)-C(64)	120.6(4)	C(76)-C(71)-C(70)	123.7(4)
C(65)-C(66)-C(67)	122.0(4)	C(73)-C(72)-C(71)	122.0(4)
C(68)-C(67)-C(66)	118.5(4)	O(73)-C(73)-C(72)	116.1(4)
C(67)-C(68)-C(63)	118.9(4)	O(73)-C(73)-C(74)	124.2(4)
C(67)-C(68)-C(69)	134.4(4)	C(72)-C(73)-C(74)	119.7(4)
C(63)-C(68)-C(69)	106.6(4)	C(75)-C(74)-C(73)	118.7(4)
C(70)-C(69)-N(61)	120.2(4)	C(76)-C(75)-C(74)	121.9(4)
C(70)-C(69)-C(68)	133.6(4)	C(75)-C(76)-C(71)	119.4(4)
N(61)-C(69)-C(68)	106.1(3)	C(73)-O(73)-C(77)	117.7(3)

Table 3. Anisotropic displacement parameters ($Å^2$ x 10^4) for the expression: exp $\{-2\pi^2(h^2a^{*2}U_{11} + ... + 2hka^*b^*U_{12})\}$ E.s.ds are in parentheses.

	U_{11}	U_{22}	U_{33}	U_{23}	U_{13}	U_{12}
B(1)	290(30)	270(30)	310(30)	10(30)	20(30)	-20(20)
F(11)	344(13)	318(14)	373(16)	-22(12)	7(12)	37(11)
F(12)	335(13)	308(13)	387(15)	44(12)	-35(12)	-17(11)
N(1)	270(19)	270(20)	350(20)	30(18)	5(19)	2(16)
N(2)	310(20)	290(20)	310(20)	18(18)	13(19)	15(19)
C(2)	300(30)	290(30)	290(30)	0(20)	70(20)	0(20)
C(3)	260(20)	270(30)	280(30)	0(20)	60(20)	-20(20)
C(4)	340(30)	330(30)	330(30)	-10(20)	70(20)	10(20)
C(5)	400(30)	320(30)	320(30)	-40(20)	40(20)	-60(20)
C(6)	360(30)	380(30)	330(30)	-30(20)	20(20)	-70(20)
C(7)	310(30)	330(30)	340(30)	40(20)	50(30)	-40(20)
C(8)	270(20)	290(30)	280(30)	20(20)	60(20)	-20(20)
C(9)	260(20)	360(30)	290(30)	10(20)	50(20)	-20(20)
C(10)	270(20)	300(30)	330(30)	-10(20)	10(20)	-10(20)
C(11)	280(20)	270(30)	370(30)	30(20)	10(20)	-70(20)
C(12)	330(20)	290(30)	360(30)	-30(20)	-10(20)	-40(20)
C(13)	320(30)	230(20)	350(30)	0(20)	30(20)	-30(20)
O(13)	413(17)	283(16)	387(19)	18(15)	-14(16)	90(15)
C(17)	490(30)	390(30)	560(40)	20(30)	-30(30)	160(20)
C(14)	300(30)	320(30)	380(30)	50(20)	-40(20)	-30(20)
C(15)	380(30)	340(30)	360(30)	10(20)	-10(20)	-10(20)
C(16)	340(30)	270(20)	360(30)	0(20)	10(20)	-20(20)
N(21)	280(20)	270(20)	310(20)	-2(17)	9(18)	15(16)
C(22)	280(30)	300(30)	280(30)	30(20)	40(20)	10(20)
C(23)	270(20)	350(30)	270(30)	30(20)	60(20)	50(20)
C(24)	350(30)	300(30)	360(30)	10(20)	70(20)	40(20)
C(25)	350(30)	370(30)	440(30)	60(30)	40(30)	60(20)
C(26)	290(20)	440(30)	420(30)	90(30)	20(20)	60(20)
C(27)	290(30)	390(30)	340(30)	70(20)	0(20)	-10(20)
C(28)	250(20)	340(30)	310(30)	40(20)	70(20)	20(20)
C(29)	270(20)	370(30)	280(30)	30(20)	40(20)	-10(20)
C(30)	270(20)	310(30)	370(30)	30(20)	-20(20)	10(20)
C(31)	350(30)	280(30)	310(30)	50(20)	-10(20)	0(20)
C(32)	280(20)	290(20)	440(30)	50(20)	-30(20)	0(20)
C(33)	370(30)	280(30)	430(30)	50(20)	-30(30)	0(20)
C(34)	380(30)	350(30)	420(30)	40(30)	-100(30)	-80(20)
C(35)	280(30)	400(30)	470(30)	90(30)	0(20)	-30(20)

C(36)	330(30)	350(30)	400(30)	70(20)	-10(20)	40(20)
O(33)	426(18)	353(18)	600(20)	-96(19)	-106(18)	-36(16)
C(37)	560(30)	450(30)	570(40)	-40(30)	-170(30)	-120(30)
B(41)	260(30)	310(30)	320(30)	-10(30)	50(30)	-10(30)
F(41)	330(13)	310(13)	376(15)	-44(13)	-29(12)	27(11)
F(42)	324(13)	327(14)	393(16)	-8(12)	1(12)	-2(11)
N(41)	270(20)	310(20)	300(20)	-17(17)	-9(18)	31(17)
N(42)	280(20)	310(20)	310(20)	-18(18)	21(19)	-5(19)
C(42)	290(30)	310(30)	280(30)	0(20)	90(20)	0(20)
C(43)	270(30)	350(30)	290(30)	-20(20)	50(20)	-20(20)
C(44)	320(30)	330(30)	350(30)	-10(20)	60(20)	-30(20)
C(45)	350(30)	380(30)	400(30)	-80(20)	60(30)	-80(20)
C(46)	290(20)	450(30)	390(30)	-120(30)	30(20)	-40(20)
C(47)	290(20)	430(30)	350(30)	-30(20)	40(20)	20(20)
C(48)	260(20)	370(30)	270(30)	-60(20)	50(20)	-50(20)
C(49)	300(30)	340(30)	290(30)	-20(20)	30(20)	-10(20)
C(50)	300(30)	370(30)	320(30)	-20(20)	-20(20)	-40(20)
C(51)	350(30)	300(30)	330(30)	-40(20)	-20(20)	10(20)
C(52)	350(30)	350(30)	400(30)	-90(30)	-60(20)	30(20)
C(53)	540(30)	280(30)	390(30)	-70(20)	-30(30)	-10(30)
C(54)	440(30)	380(30)	510(40)	-130(30)	-190(30)	110(30)
C(55)	370(30)	440(30)	490(30)	-100(30)	-90(30)	50(20)
C(56)	400(30)	370(30)	440(30)	-80(20)	0(30)	10(20)
O(53)	640(20)	354(19)	550(20)	45(19)	-130(20)	37(17)
C(57)	810(40)	430(30)	470(30)	0(30)	-90(30)	230(30)
N(61)	240(20)	290(20)	340(20)	-24(19)	4(19)	-28(16)
C(62)	260(20)	290(30)	300(30)	-50(20)	90(20)	10(20)
C(63)	250(20)	310(30)	320(30)	0(20)	70(20)	20(20)
C(64)	330(30)	290(30)	330(30)	-40(20)	100(20)	-20(20)
C(65)	320(30)	320(30)	320(30)	40(20)	30(20)	50(20)
C(66)	310(30)	370(30)	380(30)	40(20)	20(20)	70(20)
C(67)	280(30)	380(30)	370(30)	-30(20)	-10(20)	50(20)
C(68)	280(20)	330(30)	270(30)	-10(20)	70(20)	0(20)
C(69)	250(20)	310(30)	330(30)	-10(20)	20(20)	0(20)
C(70)	280(20)	340(30)	360(30)	10(20)	10(20)	20(20)
C(71)	290(20)	270(30)	350(30)	10(20)	0(20)	50(20)
C(72)	310(20)	310(30)	290(30)	-20(20)	-20(20)	40(20)
C(73)	310(20)	280(30)	360(30)	0(20)	0(30)	40(20)
C(74)	400(30)	320(30)	410(30)	-50(20)	-80(20)	-60(20)
C(75)	470(30)	390(30)	360(30)	20(20)	-20(30)	-30(20)
C(76)	370(30)	300(30)	400(30)	20(20)	20(20)	0(20)
O(73)	366(17)	309(17)	420(20)	15(17)	-2(16)	-81(15)
C(77)	530(30)	420(30)	480(30)	0(30)	-80(30)	-210(30)

Table 4. Hydrogen coordinates (x 10^4) and isotropic displacement parameters ($Å^2$ x 10^3). All hydrogen atoms were included in idealised positions with U(iso)'s set at 1.2*U(eq) or, for the methyl group hydrogen atoms, 1.5*U(eq) of the parent carbon atoms.

	x	y	z	U(iso)
H(4)	3573	1570	4373	40
H(5)	2790	1365	2671	42
H(6)	2211	1976	1553	43
H(7)	2379	2805	2086	39
H(10)	3326	3852	4685	36
H(12)	2410	4362	4515	39
H(17A)	1027	5403	2895	72
H(17B)	1374	5267	1372	72
H(17C)	891	4901	2057	72
H(14)	1624	4532	355	40
H(15)	2194	3873	-573	43
H(16)	2856	3455	1006	39
H(24)	5179	1638	7498	40
H(25)	6014	1506	9096	46
H(26)	6487	2161	10292	46
H(27)	6181	2968	9861	41
H(30)	4891	3920	7926	38
H(32)	5109	4449	10190	40
H(34)	6865	4730	11153	46
H(35)	7152	4092	9533	46
H(36)	6432	3623	8270	43
H(37A)	5939	5620	12912	79
H(37B)	6423	5196	13017	79
H(37C)	6385	5527	11531	79
H(44)	2438	8307	2451	40
H(45)	3264	8455	4072	45
H(46)	3752	7810	5272	45
H(47)	3468	6996	4821	43
H(50)	2243	6022	2768	39
H(52)	2457	5502	5040	44
H(54)	4198	5287	6214	53
H(55)	4477	5923	4588	52
H(56)	3762	6362	3230	48
H(57A)	3311	4403	8040	86
H(57B)	3774	4499	6697	86
H(57C)	3757	4854	8127	86
H(64)	860	8353	-735	38
H(65)	77	8547	-2440	39
H(66)	-505	7935	-3500	42
H(67)	-328	7110	-2958	41
H(70)	677	6064	-448	39
H(72)	-244	5549	-502	36
H(74)	-1126	5386	-4519	45
H(75)	-572	6039	-5527	48
H(76)	143	6450	-4061	43
H(77A)	-1626	4481	-1955	72
H(77B)	-1775	4956	-2920	72
H(77C)	-1257	4598	-3461	72

Table 5. Torsion angles, in degrees. E.s.ds are in parentheses.

F(12)-B(1)-N(1)-C(2) 127.6(4)
F(11)-B(1)-N(1)-C(2) -111.8(4)
N(21)-B(1)-N(1)-C(2) 7.5(5)
F(12)-B(1)-N(1)-C(9) -54.0(5)
F(11)-B(1)-N(1)-C(9) 66.6(5)
N(21)-B(1)-N(1)-C(9) -174.2(3)
C(22)-N(2)-C(2)-N(1) -0.1(6)
C(22)-N(2)-C(2)-C(3) 178.0(4)

C(9)-N(1)-C(2)-N(2)
176.8(4)
B(1)-N(1)-C(2)-N(2)-4.6(7)
C(9)-N(1)-C(2)-C(3)-1.5(5)
B(1)-N(1)-C(2)-C(3)
177.0(4)
N(2)-C(2)-C(3)-C(4)
5.6(7)
N(1)-C(2)-C(3)-C(4)-176.0(4)
N(2)-C(2)-C(3)-C(8)-176.5(4)
N(1)-C(2)-C(3)-C(8)
1.8(5)
C(8)-C(3)-C(4)-C(5)
1.2(6)
C(2)-C(3)-C(4)-C(5)
178.7(4)
C(3)-C(4)-C(5)-C(6)-0.9(6)
C(4)-C(5)-C(6)-C(7)-0.3(7)
C(5)-C(6)-C(7)-C(8)
1.2(7)
C(6)-C(7)-C(8)-C(3)-0.9(6)
C(6)-C(7)-C(8)-C(9)-176.8(4)
C(4)-C(3)-C(8)-C(7)-0.3(6)
C(2)-C(3)-C(8)-C(7)-178.3(4)
C(4)-C(3)-C(8)-C(9)
176.7(4)
C(2)-C(3)-C(8)-C(9)-1.3(4)
C(2)-N(1)-C(9)-C(10)
177.7(4)
B(1)-N(1)-C(9)-C(10)-0.9(6)
C(2)-N(1)-C(9)-C(8)
0.7(4)
B(1)-N(1)-C(9)-C(8)-177.8(4)
C(7)-C(8)-C(9)-C(10)
0.4(8)
C(3)-C(8)-C(9)-C(10)-176.0(5)
C(7)-C(8)-C(9)-N(1)
176.8(4)
C(3)-C(8)-C(9)-N(1)
0.4(4)
N(1)-C(9)-C(10)-C(11)
173.8(4)
C(8)-C(9)-C(10)-C(11)-10.2(8)
C(9)-C(10)-C(11)-C(16)-
38.9(7)
C(9)-C(10)-C(11)-C(12)
147.0(5)
C(16)-C(11)-C(12)-C(13)
1.3(6)
C(10)-C(11)-C(12)-C(13)
175.8(4)
C(11)-C(12)-C(13)-O(13)-
179.9(4)
C(11)-C(12)-C(13)-C(14)-
0.2(6)
C(12)-C(13)-O(13)-C(17)-
173.0(4)
C(14)-C(13)-O(13)-C(17)
7.3(6)
O(13)-C(13)-C(14)-C(15)
178.8(4)
C(12)-C(13)-C(14)-C(15)-
0.9(6)
C(13)-C(14)-C(15)-C(16)
0.8(6)
C(14)-C(15)-C(16)-C(11)
0.3(6)
C(12)-C(11)-C(16)-C(15)-
1.4(6)
C(10)-C(11)-C(16)-C(15)-
175.5(4)
F(12)-B(1)-N(21)-C(22)-
127.8(4)
F(11)-B(1)-N(21)-C(22)
112.1(4)
N(1)-B(1)-N(21)-C(22)-7.3(5)
F(12)-B(1)-N(21)-C(29)
55.8(5)
F(11)-B(1)-N(21)-C(29)-
64.2(5)
N(1)-B(1)-N(21)-C(29)
176.4(3)
C(2)-N(2)-C(22)-N(21)
0.3(6)
F(42)-B(41)-N(41)-C(42)-
114.3(4)
F(41)-B(41)-N(41)-C(42)
125.4(4)
N(61)-B(41)-N(41)-C(42)
5.2(5)
F(42)-B(41)-N(41)-C(49)
64.2(5)
F(41)-B(41)-N(41)-C(49)-
56.0(5)
N(61)-B(41)-N(41)-C(49)-
176.2(3)
C(62)-N(42)-C(42)-N(41)-
0.1(6)
C(62)-N(42)-C(42)-C(43)
179.4(4)
C(49)-N(41)-C(42)-N(42)
178.2(4)
B(41)-N(41)-C(42)-N(42)-
3.0(7)
C(49)-N(41)-C(42)-C(43)-
1.4(5)
B(41)-N(41)-C(42)-C(43)
177.4(4)
N(42)-C(42)-C(43)-C(44)
4.9(7)
N(41)-C(42)-C(43)-C(44)-
175.5(4)
N(42)-C(42)-C(43)-C(48)-
178.5(4)
N(41)-C(42)-C(43)-C(48)
1.1(5)
C(48)-C(43)-C(44)-C(45)
0.9(7)
C(42)-C(43)-C(44)-C(45)
177.0(4)
C(43)-C(44)-C(45)-C(46)-
2.2(6)
C(44)-C(45)-C(46)-C(47)
1.5(7)
C(45)-C(46)-C(47)-C(48)
0.6(7)
C(44)-C(43)-C(48)-C(47)
1.3(7)
C(42)-C(43)-C(48)-C(47)-
175.6(4)
C(44)-C(43)-C(48)-C(49)
176.5(4)
C(42)-C(43)-C(48)-C(49)-
0.3(5)
C(46)-C(47)-C(48)-C(43)-
2.0(6)
C(46)-C(47)-C(48)-C(49)-
175.7(4)
C(42)-N(41)-C(49)-C(50)
178.1(4)
B(41)-N(41)-C(49)-C(50)-
0.7(6)

C(42)-N(41)-C(49)-C(48)
1.2(4)
B(41)-N(41)-C(49)-C(48)-
177.6(4)
C(43)-C(48)-C(49)-C(50)-
176.8(5)
C(47)-C(48)-C(49)-C(50)-
2.5(8)
C(43)-C(48)-C(49)-N(41)-
0.5(5)
C(47)-C(48)-C(49)-N(41)
173.8(4)
N(41)-C(49)-C(50)-C(51)
176.5(4)
C(48)-C(49)-C(50)-C(51)-
7.6(9)
C(49)-C(50)-C(51)-C(52)
143.2(5)
C(49)-C(50)-C(51)-C(56)-
41.9(7)
C(56)-C(51)-C(52)-C(53)
2.4(7)
C(50)-C(51)-C(52)-C(53)
177.6(4)
C(51)-C(52)-C(53)-O(53)
179.2(4)
C(51)-C(52)-C(53)-C(54)-
1.2(7)
O(53)-C(53)-C(54)-C(55)
179.0(4)
C(2)-N(2)-C(22)-C(23)-
178.3(4)
C(29)-N(21)-C(22)-N(2)-
178.9(4)
B(1)-N(21)-C(22)-N(2)
4.2(7)
C(29)-N(21)-C(22)-C(23)-
0.2(5)
B(1)-N(21)-C(22)-C(23)-
177.0(4)
N(2)-C(22)-C(23)-C(24)-5.2(7)
N(21)-C(22)-C(23)-C(24)
176.0(4)
N(2)-C(22)-C(23)-C(28)
178.4(4)
N(21)-C(22)-C(23)-C(28)-
0.4(5)
C(28)-C(23)-C(24)-C(25)-
0.7(6)
C(22)-C(23)-C(24)-C(25)-
176.6(4)
C(23)-C(24)-C(25)-C(26)
2.3(6)
C(24)-C(25)-C(26)-C(27)-
1.6(7)
C(25)-C(26)-C(27)-C(28)-
0.7(7)
C(26)-C(27)-C(28)-C(23)
2.3(6)
C(26)-C(27)-C(28)-C(29)
174.8(4)
C(24)-C(23)-C(28)-C(27)-
1.7(6)
C(22)-C(23)-C(28)-C(27)
175.0(4)
C(24)-C(23)-C(28)-C(29)-
176.0(4)
C(22)-C(23)-C(28)-C(29)
0.7(5)
C(22)-N(21)-C(29)-C(30)-
175.6(4)
C(52)-C(53)-C(54)-C(55)-
0.6(7)
C(53)-C(54)-C(55)-C(56)
1.1(7)
C(54)-C(55)-C(56)-C(51)
0.1(7)
C(52)-C(51)-C(56)-C(55)-
1.9(7)
C(50)-C(51)-C(56)-C(55)-
176.8(4)
C(54)-C(53)-O(53)-C(57)-
4.5(7)
C(52)-C(53)-O(53)-C(57)
175.1(4)
F(42)-B(41)-N(61)-C(62)
114.6(4)
F(41)-B(41)-N(61)-C(62)-
125.5(4)
N(41)-B(41)-N(61)-C(62)-
5.4(5)
F(42)-B(41)-N(61)-C(69)-
64.7(5)
F(41)-B(41)-N(61)-C(69)
55.1(5)
N(41)-B(41)-N(61)-C(69)
175.2(3)
C(42)-N(42)-C(62)-N(61)-
0.1(6)

B(1)-N(21)-C(29)-C(30)
1.2(6)
C(22)-N(21)-C(29)-C(28)
0.6(5)
B(1)-N(21)-C(29)-C(28)
177.4(4)
C(27)-C(28)-C(29)-C(30)
1.5(8)
C(23)-C(28)-C(29)-C(30)
174.7(5)
C(27)-C(28)-C(29)-N(21)-
174.0(4)
C(23)-C(28)-C(29)-N(21)-
0.8(4)
N(21)-C(29)-C(30)-C(31)-
174.4(4)
C(28)-C(29)-C(30)-C(31)
10.7(8)
C(29)-C(30)-C(31)-C(32)-
145.4(5)
C(29)-C(30)-C(31)-C(36)
40.1(7)
C(36)-C(31)-C(32)-C(33)-
0.9(6)
C(30)-C(31)-C(32)-C(33)-
175.5(4)
C(31)-C(32)-C(33)-O(33)
178.5(4)
C(31)-C(32)-C(33)-C(34)-
0.3(7)
O(33)-C(33)-C(34)-C(35)-
177.3(4)
C(32)-C(33)-C(34)-C(35)
1.4(7)
C(33)-C(34)-C(35)-C(36)-
1.2(7)
C(34)-C(35)-C(36)-C(31)
0.0(7)
C(32)-C(31)-C(36)-C(35)
1.0(6)

C(30)-C(31)-C(36)-C(35) 175.4(4)
C(34)-C(33)-O(33)-C(37) 5.6(7)
C(32)-C(33)-O(33)-C(37)- 173.1(4)
C(42)-N(42)-C(62)-C(63)- 178.6(4)
C(69)-N(61)-C(62)-N(42)- 177.0(4)
B(41)-N(61)-C(62)-N(42) 3.5(6)
C(69)-N(61)-C(62)-C(63) 1.6(4)
B(41)-N(61)-C(62)-C(63)- 177.8(4)
N(42)-C(62)-C(63)-C(64)- 4.2(7)
N(61)-C(62)-C(63)-C(64) 177.1(4)
N(42)-C(62)-C(63)-C(68) 177.1(4)
N(61)-C(62)-C(63)-C(68)- 1.6(5)
C(68)-C(63)-C(64)-C(65)- 0.7(6)
C(62)-C(63)-C(64)-C(65)- 179.3(4)
C(63)-C(64)-C(65)-C(66) 1.3(6)
C(64)-C(65)-C(66)-C(67)- 0.7(7)
C(65)-C(66)-C(67)-C(68)- 0.7(7)
C(66)-C(67)-C(68)-C(63) 1.3(6)
C(66)-C(67)-C(68)-C(69) 177.6(4)
C(64)-C(63)-C(68)-C(67)- 0.6(6)
C(62)-C(63)-C(68)-C(67) 178.2(4)
C(64)-C(63)-C(68)-C(69)- 177.9(4)
C(62)-C(63)-C(68)-C(69) 0.9(4)
C(62)-N(61)-C(69)-C(70)- 179.2(4)
B(41)-N(61)-C(69)-C(70) 0.2(6)
C(62)-N(61)-C(69)-C(68)- 1.0(4)
B(41)-N(61)-C(69)-C(68) 178.4(4)
C(67)-C(68)-C(69)-C(70) 1.2(8)
C(63)-C(68)-C(69)-C(70) 177.8(5)
C(67)-C(68)-C(69)-N(61)- 176.6(4)
C(63)-C(68)-C(69)-N(61) 0.0(4)
N(61)-C(69)-C(70)-C(71)- 176.6(4)
C(68)-C(69)-C(70)-C(71) 5.8(8)
C(69)-C(70)-C(71)-C(72)- 143.4(5)
C(69)-C(70)-C(71)-C(76) 41.0(7)
C(76)-C(71)-C(72)-C(73)- 2.2(6)
C(70)-C(71)-C(72)-C(73)- 178.0(4)
C(71)-C(72)-C(73)-O(73)- 179.8(4)
C(71)-C(72)-C(73)-C(74) 0.5(6)
O(73)-C(73)-C(74)-C(75)- 178.8(4)
C(72)-C(73)-C(74)-C(75) 0.9(6)
C(73)-C(74)-C(75)-C(76)- 0.5(7)
C(74)-C(75)-C(76)-C(71)- 1.2(6)
C(72)-C(71)-C(76)-C(75) 2.5(6)
C(70)-C(71)-C(76)-C(75) 178.0(4)
C(72)-C(73)-O(73)-C(77)- 178.7(4)
C(74)-C(73)-O(73)-C(77) 1.0(6)

Table 6. Hydrogen bonds, in Ångstroms and degrees.

D-H...A	d(D-H)	d(H...A)	d(D...A)	<(DHA)
C(10)-H(10)...F(12)	0.93	2.50	3.075(5)	120.3
C(17)-H(17A)...F(42)	0.96	2.52	3.156(5)	123.9
C(14)-H(14)...O(73)#1	0.93	2.52	3.447(5)	171.3
C(30)-H(30)...F(12)	0.93	2.52	3.088(5)	119.4
C(50)-H(50)...F(41)	0.93	2.50	3.085(5)	121.2
C(70)-H(70)...F(41)	0.93	2.48	3.081(5)	122.6
C(74)-H(74)...O(13)#3	0.93	2.44	3.325(6)	160.0

Symmetry transformations used to generate equivalent atoms:
#1 : -x, 1-y, z #2 : -x, 1-y, z-1

Crystal structure analysis of F_2BN-{(C_8H_4N)=CH-C_6H_4OMe}$_2$

Crystal data: 2($C_{32}H_{24}BF_2N_3O_2$), M = 1062.70. Orthorhombic, space group $P2_12_12$ (no. 18), a = 22.0145(8), b = 27.0662(9), c = 8.6554(4) Å, V = 5157.3(3) Å^3. Z = 4, Dc = 1.369 g cm^{-3}, F(000) = 2208, T = 100.01(10) K, μ(Cu-Kα) = 7.84 cm^{-1}, λ(Cu-Kα) = 1.54184 Å.

The crystal was a fine yellow prism. One crystal, *ca* 0.02 x 0.06 x 0.18 mm, was mounted, in oil, on a small loop and fixed in the cold nitrogen stream on a Rigaku Oxford Diffraction XtaLAB Synergy diffractometer, equipped with Cu-Kα radiation, HyPix detector and mirror monochromator. Intensity data were measured by thin-slice ω-scans. Total no. of reflections recorded, to θ_{max} = 52.066°, was 54700 of which 5729 were unique (Rint = 0.108); 5047 were 'observed' with I > 2σ_I.

Data were processed using the CrysAlisPro-CCD and -RED (1) programs. The structure was determined by the intrinsic phasing routines in the SHELXT program (2A) and refined by full-matrix least-squares methods, on F^2's, in SHELXL (2B). There are two independent molecules in this crystal. The non-hydrogen atoms were refined with anisotropic thermal parameters. The hydrogen atoms were included in idealised positions and their Uiso values were set to ride on the Ueq values of the parent carbon atoms. At the conclusion of the refinement, wR_2 = 0.095 and R_1 = 0.046 (2B) for all 5729 reflections weighted w = $[\sigma^2(F_o^2) + (0.0680\ P)^2]^{-1}$ with P = $(F_o^2 + 2F_c^2)/3$; for the 'observed' data only, R_1 = 0.039. The Flack (absolute structure) parameter is 0.02(9) and the correct absolute configuration is shown in the Figures.

In the final difference map, the highest peak (*ca* 0.2 eÅ^{-3}) was near C(62).

Scattering factors for neutral atoms were taken from reference (3). Computer programs used in this analysis have been noted above, and were run through WinGX (4) on a Dell Optiplex 780 PC at the University of East Anglia.

References

(13) Programs CrysAlisPro, Rigaku Oxford Diffraction Ltd., Abingdon, UK (2018).

(14) G. M. Sheldrick, Programs for crystal structure determination (SHELXT), *Acta Cryst.* (2015) A**71**, 3-8, and refinement (SHELXL), *Acta Cryst.* (2008) A**64**, 112-122 and (2015) C**71**, 3-8.

(15) *'International Tables for X-ray Crystallography'*, Kluwer Academic Publishers,

Dordrecht (1992). Vol. C, pp. 500, 219 and 193.

(16) L. J. Farrugia, *J. Appl. Cryst.* (2012) **45**, 849–854.

Legends for Figures

Figure 1. View of the two independent molecules of F_2BN-{(C_8H_4N)=CH-C_6H_4OMe}$_2$ indicating the atom numbering scheme. Thermal ellipsoids are drawn at the 50% probability level.

Figure 2. Side-on view of the two molecules.

Figure 3. Similar view as Figure 2, showing the stacking of one set of columns of isoindoline rings.

Figure 4. View along the *b* axis of the same set of isoindoline columns.

Notes on the structure

There are two independent molecules in this crystal, Figure 1; they are related by a pseudo-twofold symmetry axis. Each molecule shows pseudo-symmetry about the plane containing the boron atom, the two fluorine atoms and the N(2) or N(22) atom; the symmetry does not extend beyond this particular molecule.

These molecules are very similar in conformation; the central C_2N_3B ring in each molecule has a shallow envelope shape with B(1) and B(41) displaced 0.102(5) and 0.073(5) Å from the good mean-planes of the other five ring atoms. The normals to these two planes, related by the pseudo-symmetry, are 9.2(2)° apart. In each molecule, the adjoining isoindoline groups are essentially coplanar with the central C_2N_3B rings. In every case (in these two adjoining molecules), there is rotation about the C(10)–C(11) type bond by *ca* 45°; this brings the four O atoms out of the general molecular plane, and they all lie on the same side of that plane and are displaced *ca* 1.3 Å from the plane, Figure 2.

The central C_2N_3B rings are essentially planar and show aromatic mean dimensions, viz. B–N 1.538, (B)–N–C 1.438, C–N_{BH} 1.333 Å, and in the isoindoline-phenyl ring link, as C(9)–C(10) and C(10)–C(11) 1.348 and 1.461 Å, respectively.

Crystal data and structure refinement for N(C_8NH_5-CH-C_6H_4-CN)(C_8NH_4-CH-C_6H_4-CN)

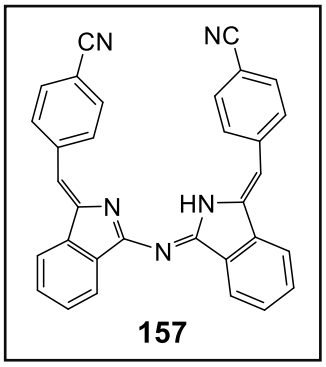

157

Identification code	**157**
Elemental formula	C32 H19 N5
Formula weight	473.52
Crystal system, space group	Monoclinic, $P2_1/n$ (eqiv. to no. 14)
Unit cell dimensions	a = 12.5809(2) Å α = 90 ° b = 8.0343(2) Å β = 95.576(2) ° c = 23.6089(4) Å γ = 90 °
Volume	2375.07(8) $Å^3$
Z, Calculated density	4, 1.324 Mg/m^3
F(000)	984
Absorption coefficient	0.632 mm^{-1}
Temperature	100.01(10) K
Wavelength	1.54184 Å
Crystal colour, shape	dark red needle
Crystal size	0.3 x 0.1 x 0.05 mm
Crystal mounting:	on a Micro-mount, in oil, fixed in cold N_2 stream
On the diffractometer:	
Theta range for data collection	7.688 to 72.478 °
Limiting indices	-15<=h<=13, -9<=k<=9, -29<=l<=27
Completeness to theta = 67.684	99.4 %
Absorption correction	Semi-empirical from equivalents
Max. and min. transmission	1.00000 and 0.81773
Reflections collected (not including absences)	17294
No. of unique reflections	4624 [R(int) for equivalents = 0.032]
No. of 'observed' reflections ($I > 2\sigma_I$)	4049
Structure determined by:	dual methods, in SHELXT
Refinement:	Full-matrix least-squares on F^2, in SHELXL

Data / restraints / parameters	4624 / 0 / 343
Goodness-of-fit on F^2	1.044
Final R indices ('observed' data)	R_1 = 0.037, wR_2 = 0.091
Final R indices (all data)	R_1 = 0.043, wR_2 = 0.094
Reflections weighted: $w = [\sigma^2(Fo^2)+(0.0436P)^2+0.5908P]^{-1}$ where $P=(Fo^2+2Fc^2)/3$	
Extinction coefficient	n/a
Largest diff. peak and hole	0.17 and -0.18 e.Å^{-3}
Location of largest difference peak	near midpoint of C(1)-C(9) bond

Table 1. Atomic coordinates (x 10^5) and equivalent isotropic displacement parameters ($Å^2$ x 10^4). U(eq) is defined as one third of the trace of the orthogonalized Uij tensor. E.s.ds are in parentheses.

	x	y	z	U(eq)
C(1)	58408(9)	38330(15)	46837(5)	257(3)
N(2)	61216(9)	51094(13)	43534(4)	267(2)
C(3)	54936(9)	51422(16)	38276(5)	269(3)
C(4)	47756(9)	37017(15)	38332(5)	264(3)
C(5)	39913(10)	30917(16)	34312(5)	307(3)
C(6)	34144(10)	17062(17)	35750(5)	321(3)
C(7)	36077(10)	9541(17)	41086(5)	315(3)
C(8)	43748(10)	15812(16)	45123(5)	285(3)
C(9)	49587(9)	29462(15)	43660(5)	253(2)
C(10)	55222(10)	62889(16)	34143(5)	290(3)
C(11)	61033(9)	78643(16)	34365(5)	277(3)
C(12)	63844(10)	87181(16)	39473(5)	306(3)
C(13)	68849(10)	102452(17)	39524(5)	309(3)
C(14)	71258(10)	109696(17)	34426(5)	302(3)
C(15)	68490(11)	101449(18)	29272(5)	354(3)
C(16)	63344(11)	86248(17)	29282(5)	332(3)
C(17)	76550(10)	125618(18)	34537(5)	332(3)
N(18)	80820(10)	138250(16)	34653(5)	413(3)
C(21)	71533(9)	42315(15)	54242(5)	257(2)
N(22)	77576(8)	52623(13)	51527(4)	266(2)
C(23)	86345(9)	57393(15)	55300(5)	252(2)
C(24)	85050(9)	49943(15)	60897(5)	254(2)
C(25)	90904(10)	51118(16)	66183(5)	302(3)
C(26)	87278(11)	42296(17)	70680(5)	329(3)
C(27)	78083(10)	32482(16)	69945(5)	306(3)
C(28)	72238(10)	31256(15)	64671(5)	272(3)
C(29)	75826(9)	40208(15)	60192(5)	250(2)
C(30)	94852(10)	66381(15)	54000(5)	266(3)
C(31)	97118(9)	73646(15)	48589(5)	256(2)
C(32)	90760(10)	71419(16)	43426(5)	295(3)
C(33)	93088(10)	79559(17)	38546(5)	309(3)
C(34)	101906(10)	90073(16)	38655(5)	289(3)
C(35)	108588(10)	91957(16)	43688(5)	302(3)
C(36)	106228(10)	83748(16)	48537(5)	288(3)
C(37)	104102(10)	98984(17)	33617(6)	330(3)
N(38)	105795(10)	106297(16)	29607(5)	420(3)
N(41)	62650(8)	34125(13)	51973(4)	276(2)

Table 2. Molecular dimensions. Bond lengths are in Ångstroms, angles in degrees. E.s.ds are in parentheses.

C(1)-N(41)	1.3204(15)	C(21)-N(22)	1.3302(16)
C(1)-N(2)	1.3557(16)	C(21)-N(41)	1.3611(16)
C(1)-C(9)	1.4628(17)	C(21)-C(29)	1.4650(16)
N(2)-C(3)	1.4056(15)	N(22)-C(23)	1.4023(15)
N(2)-H(2)	0.878(19)	N(22)-H(22)	0.91(5)
C(3)-C(10)	1.3449(18)	C(23)-C(30)	1.3509(18)
C(3)-C(4)	1.4690(18)	C(23)-C(24)	1.4741(17)
C(4)-C(5)	1.3902(17)	C(24)-C(25)	1.3894(17)
C(4)-C(9)	1.3956(17)	C(24)-C(29)	1.3959(17)
C(5)-C(6)	1.3890(19)	C(25)-C(26)	1.3898(18)
C(6)-C(7)	1.3972(19)	C(26)-C(27)	1.3968(19)
C(7)-C(8)	1.3837(18)	C(27)-C(28)	1.3867(17)
C(8)-C(9)	1.3824(18)	C(28)-C(29)	1.3901(17)
C(10)-C(11)	1.4601(18)	C(30)-C(31)	1.4575(17)
C(11)-C(16)	1.4020(18)	C(31)-C(32)	1.4030(17)
C(11)-C(12)	1.4024(17)	C(31)-C(36)	1.4055(17)
C(12)-C(13)	1.3786(19)	C(32)-C(33)	1.3806(18)
C(13)-C(14)	1.3965(18)	C(33)-C(34)	1.3926(18)
C(14)-C(15)	1.3995(18)	C(34)-C(35)	1.3955(18)
C(14)-C(17)	1.4412(19)	C(34)-C(37)	1.4377(18)
C(15)-C(16)	1.382(2)	C(35)-C(36)	1.3784(18)
C(17)-N(18)	1.1474(18)	C(37)-N(38)	1.1516(18)

C(1)-N(41)-C(21)	118.75(11)		
N(41)-C(1)-N(2)	128.10(11)	C(5)-C(4)-C(3)	131.90(11)
N(41)-C(1)-C(9)	124.40(11)	C(9)-C(4)-C(3)	107.64(10)
N(2)-C(1)-C(9)	107.50(10)	C(6)-C(5)-C(4)	117.96(12)
C(1)-N(2)-C(3)	111.51(10)	C(5)-C(6)-C(7)	121.18(11)
C(1)-N(2)-H(2)	120.8(11)	C(8)-C(7)-C(6)	120.81(12)
C(3)-N(2)-H(2)	126.5(11)	C(9)-C(8)-C(7)	117.96(11)
C(10)-C(3)-N(2)	126.96(11)	C(8)-C(9)-C(4)	121.67(11)
C(10)-C(3)-C(4)	127.30(11)	C(8)-C(9)-C(1)	130.80(11)
N(2)-C(3)-C(4)	105.70(10)	C(4)-C(9)-C(1)	107.51(11)
C(5)-C(4)-C(9)	120.40(12)	C(3)-C(10)-C(11)	128.05(11)

C(16)-C(11)-C(12) 117.83(12)
C(16)-C(11)-C(10) 119.45(11)
C(12)-C(11)-C(10) 122.58(11)
C(13)-C(12)-C(11) 121.31(12)
C(12)-C(13)-C(14) 120.03(12)
C(13)-C(14)-C(15) 119.71(12)
C(13)-C(14)-C(17) 119.52(11)
C(15)-C(14)-C(17) 120.77(12)
C(16)-C(15)-C(14) 119.59(12)
C(15)-C(16)-C(11) 121.51(12)
N(18)-C(17)-C(14) 179.51(16)
N(22)-C(21)-N(41) 126.67(11)
N(22)-C(21)-C(29) 111.06(10)
N(41)-C(21)-C(29) 122.26(11)
C(21)-N(22)-C(23) 108.37(10)
C(21)-N(22)-H(22) 120(3)
C(23)-N(22)-H(22) 130(3)
C(30)-C(23)-N(22) 126.41(11)
C(30)-C(23)-C(24) 125.43(11)
N(22)-C(23)-C(24) 108.05(10)
C(25)-C(24)-C(29) 120.48(11)
C(25)-C(24)-C(23) 133.05(11)
C(29)-C(24)-C(23) 106.47(10)
C(24)-C(25)-C(26) 117.82(12)
C(25)-C(26)-C(27) 121.50(11)
C(28)-C(27)-C(26) 120.80(12)
C(27)-C(28)-C(29) 117.60(11)
C(28)-C(29)-C(24) 121.79(11)
C(28)-C(29)-C(21) 132.26(11)
C(24)-C(29)-C(21) 105.93(10)
C(23)-C(30)-C(31) 129.78(11)
C(32)-C(31)-C(36) 117.55(11)
C(32)-C(31)-C(30) 124.53(11)
C(36)-C(31)-C(30) 117.91(10)
C(33)-C(32)-C(31) 121.02(12)
C(32)-C(33)-C(34) 120.34(11)
C(33)-C(34)-C(35) 119.63(11)
C(33)-C(34)-C(37) 120.24(11)
C(35)-C(34)-C(37) 120.13(12)
C(36)-C(35)-C(34) 119.66(12)
C(35)-C(36)-C(31) 121.69(11)
N(38)-C(37)-C(34) 179.13(15)

Table 3. Anisotropic displacement parameters ($Å^2$ x 10^4) for the expression: exp {$-2\pi^2(h^2a^{*2}U_{11} + ... + 2hka^*b^*U_{12})$} E.s.ds are in parentheses.

	U_{11}	U_{22}	U_{33}	U_{23}	U_{13}	U_{12}
C(1)	244(6)	293(6)	234(6)	-19(5)	22(4)	23(5)
N(2)	257(5)	304(6)	233(5)	12(4)	-19(4)	-2(4)
C(3)	254(6)	322(6)	225(6)	-29(5)	-10(4)	38(5)
C(4)	256(6)	284(6)	249(6)	-29(5)	6(5)	47(5)
C(5)	326(6)	340(7)	242(6)	-40(5)	-29(5)	28(5)
C(6)	297(6)	363(7)	292(6)	-85(5)	-23(5)	-14(5)
C(7)	287(6)	319(7)	343(7)	-50(5)	49(5)	-22(5)
C(8)	287(6)	313(6)	255(6)	-7(5)	32(5)	26(5)
C(9)	236(6)	285(6)	235(6)	-36(5)	10(4)	44(5)
C(10)	295(6)	347(7)	220(6)	-17(5)	-20(5)	29(5)
C(11)	255(6)	320(6)	250(6)	16(5)	-4(4)	47(5)
C(12)	350(6)	337(7)	232(6)	10(5)	23(5)	43(5)
C(13)	318(6)	347(7)	254(6)	-33(5)	-6(5)	49(5)
C(14)	282(6)	322(7)	297(6)	-11(5)	5(5)	27(5)
C(15)	418(7)	391(8)	248(6)	21(5)	15(5)	-29(6)
C(16)	386(7)	376(7)	222(6)	-7(5)	-31(5)	-20(6)
C(17)	339(7)	385(8)	273(6)	-27(5)	28(5)	14(6)
N(18)	454(7)	422(7)	363(6)	-60(5)	39(5)	-72(6)
C(21)	273(6)	248(6)	245(6)	-9(5)	-10(5)	38(5)

N(22)	255(5)	280(5)	254(5)	0(4)	-21(4)	13(4)
C(23)	273(6)	245(6)	230(6)	-18(4)	-13(4)	37(5)
C(24)	269(6)	242(6)	248(6)	-19(4)	5(4)	44(5)
C(25)	312(6)	314(7)	269(6)	-20(5)	-22(5)	-14(5)
C(26)	361(7)	389(7)	222(6)	-6(5)	-40(5)	-4(6)
C(27)	350(6)	326(7)	238(6)	21(5)	17(5)	15(5)
C(28)	276(6)	265(6)	271(6)	-4(5)	8(5)	13(5)
C(29)	259(6)	243(6)	243(6)	-23(4)	-4(4)	44(5)
C(30)	271(6)	280(6)	234(6)	-32(5)	-36(4)	20(5)
C(31)	252(6)	243(6)	271(6)	-19(5)	9(4)	33(5)
C(32)	276(6)	310(7)	295(6)	4(5)	4(5)	-20(5)
C(33)	290(6)	359(7)	270(6)	4(5)	-21(5)	6(5)
C(34)	302(6)	276(6)	293(6)	2(5)	52(5)	44(5)
C(35)	271(6)	295(6)	344(6)	-34(5)	56(5)	-16(5)
C(36)	263(6)	314(7)	280(6)	-41(5)	-10(5)	3(5)
C(37)	337(7)	331(7)	321(7)	-5(5)	23(5)	9(5)
N(38)	470(7)	439(7)	348(6)	56(5)	31(5)	-50(6)
N(41)	272(5)	305(5)	241(5)	11(4)	-29(4)	-8(4)

Table 4. Hydrogen coordinates (x 10^4) and isotropic displacement parameters ($Å^2$ x 10^3). The two part-amino-hydrogen atoms were located in difference maps and were refined freely. The remaining hydrogen atoms were included in idealised positions with U(iso)'s set at 1.2*U(eq) of the parent carbon atoms.

	x	y	z	U(iso)	S.o.f.#
H(5)	3857	3596	3077	37	
H(6)	2890	1271	3311	38	
H(7)	3216	21	4194	38	
H(8)	4494	1099	4871	34	
H(10)	5122	6049	3072	35	
H(12)	6230	8245	4289	37	
H(13)	7062	10793	4296	37	
H(15)	7010	10617	2586	42	
H(16)	6137	8094	2584	40	
H(25)	9705	5760	6670	36	
H(26)	9106	4294	7426	39	
H(27)	7585	2670	7303	37	
H(28)	6614	2468	6415	33	
H(30)	10005	6821	5701	32	
H(32)	8489	6435	4329	35	
H(33)	8874	7801	3517	37	
H(35)	11460	9872	4377	36	
H(36)	11078	8492	5186	35	
H(2)	6710(15)	5680(20)	4445(7)	5(6)	0.64(4)
H(22)	7510(40)	5700(60)	4810(20)	50(18)	0.36(4)

- site occupancy, if different from 1.

Table 5. Torsion angles, in degrees. E.s.ds are in parentheses.

N(41)-C(1)-N(2)-C(3) 179.03(12)
C(9)-C(1)-N(2)-C(3)-0.55(13)
C(1)-N(2)-C(3)-C(10) 176.20(12)
C(1)-N(2)-C(3)-C(4)-1.78(13)
C(10)-C(3)-C(4)-C(5) 2.8(2)
N(2)-C(3)-C(4)-C(5)-179.23(13)
C(10)-C(3)-C(4)-C(9)- 174.47(12)
N(2)-C(3)-C(4)-C(9) 3.50(13)
C(9)-C(4)-C(5)-C(6)-0.86(18)
C(3)-C(4)-C(5)-C(6)-177.84(12)
C(4)-C(5)-C(6)-C(7) 0.54(19)
C(5)-C(6)-C(7)-C(8) 0.7(2)
C(6)-C(7)-C(8)-C(9)-1.51(18)
C(7)-C(8)-C(9)-C(4) 1.20(18)
C(7)-C(8)-C(9)-C(1)-176.94(12)
C(5)-C(4)-C(9)-C(8)-0.01(18)
C(3)-C(4)-C(9)-C(8) 177.63(11)
C(5)-C(4)-C(9)-C(1) 178.51(11)
C(3)-C(4)-C(9)-C(1)-3.85(13)
N(41)-C(1)-C(9)-C(8) 1.5(2)
N(2)-C(1)-C(9)-C(8)-178.86(12)
N(41)-C(1)-C(9)-C(4)- 176.80(11)
N(2)-C(1)-C(9)-C(4) 2.80(13)
N(2)-C(3)-C(10)-C(11)-8.3(2)
C(4)-C(3)-C(10)-C(11) 169.21(12)
C(3)-C(10)-C(11)-C(16) 158.68(13)
C(3)-C(10)-C(11)-C(12)-25.6(2)
C(16)-C(11)-C(12)-C(13)- 0.87(18)
C(10)-C(11)-C(12)-C(13)- 176.63(12)
C(11)-C(12)-C(13)-C(14)- 0.25(19)
C(12)-C(13)-C(14)-C(15) 0.53(19)
C(12)-C(13)-C(14)-C(17)- 179.62(12)
C(13)-C(14)-C(15)-C(16) 0.3(2)
C(17)-C(14)-C(15)-C(16)- 179.50(12)
C(14)-C(15)-C(16)-C(11)-1.5(2)
C(12)-C(11)-C(16)-C(15) 1.77(19)
C(10)-C(11)-C(16)-C(15) 177.67(12)
N(41)-C(21)-N(22)-C(23)- 175.70(11)
C(29)-C(21)-N(22)-C(23) 2.56(13)
C(21)-N(22)-C(23)-C(30) 172.76(12)
C(21)-N(22)-C(23)-C(24)- 3.54(13)
C(30)-C(23)-C(24)-C(25) 7.4(2)
N(22)-C(23)-C(24)-C(25)- 176.23(13)
C(30)-C(23)-C(24)-C(29)- 173.16(12)
N(22)-C(23)-C(24)-C(29) 3.18(13)
C(29)-C(24)-C(25)-C(26) 0.17(18)
C(23)-C(24)-C(25)-C(26) 179.52(13)
C(24)-C(25)-C(26)-C(27) 0.3(2)
C(25)-C(26)-C(27)-C(28)-0.1(2)
C(26)-C(27)-C(28)-C(29)- 0.45(18)
C(27)-C(28)-C(29)-C(24) 0.89(18)
C(27)-C(28)-C(29)-C(21)- 177.34(12)
C(25)-C(24)-C(29)-C(28)- 0.77(18)
C(23)-C(24)-C(29)-C(28) 179.73(11)
C(25)-C(24)-C(29)-C(21) 177.87(11)
C(23)-C(24)-C(29)-C(21)- 1.63(12)
N(22)-C(21)-C(29)-C(28) 177.92(12)
N(41)-C(21)-C(29)-C(28)-3.7(2)
N(22)-C(21)-C(29)-C(24)- 0.51(13)
N(41)-C(21)-C(29)-C(24) 177.84(11)
N(22)-C(23)-C(30)-C(31) 1.5(2)
C(24)-C(23)-C(30)-C(31) 177.13(12)
C(23)-C(30)-C(31)-C(32)-4.7(2)
C(23)-C(30)-C(31)-C(36) 174.48(12)
C(36)-C(31)-C(32)-C(33)- 3.26(18)
C(30)-C(31)-C(32)-C(33) 175.96(12)
C(31)-C(32)-C(33)-C(34) 0.6(2)
C(32)-C(33)-C(34)-C(35) 1.96(19)
C(32)-C(33)-C(34)-C(37)- 177.84(12)
C(33)-C(34)-C(35)-C(36)- 1.76(19)
C(37)-C(34)-C(35)-C(36) 178.04(12)
C(34)-C(35)-C(36)-C(31)- 1.02(19)
C(32)-C(31)-C(36)-C(35) 3.48(18)
C(30)-C(31)-C(36)-C(35)- 175.79(11)
N(2)-C(1)-N(41)-C(21)-6.19(19)
C(9)-C(1)-N(41)-C(21) 173.33(11)

N(22)-C(21)-N(41)-C(1)	-	C(29)-C(21)-N(41)-C(1)		
11.13(18)		170.79(11)		

Table 6. Hydrogen bonds, in Ångstroms and degrees.

D-H...A	d(D-H)	d(H...A)	d(D...A)	<(DHA)
N(2)-H(2)...N(22)	0.878(19)	2.053(17)	2.6565(14)	125.1(14)
N(22)-H(22)...N(2)	0.91(5)	2.02(5)	2.6565(14)	126(4)

Crystal structure analysis of $N(C_8NH_5\text{-}CH\text{-}C_6H_4\text{-}CN)(C_8NH_4\text{-}CH\text{-}C_6H_4\text{-}CN)$

Crystal data: $C_{32}H_{19}N_5$, M = 473.52. Monoclinic, space group $P2_1/n$ (equiv. to no. 14), a = 12.5809(2), b = 8.0343(2), c = 23.6089(4) Å, β = 95.576(2) °, V = 2375.07(8) $Å^3$. Z = 4, Dc = 1.324 g cm^{-3}, F(000) = 984, T = 100.01(10) K, μ(Cu-Kα) = 6.32 cm^{-1}, λ(Cu-Kα) = 1.54184 Å.

The crystal was a dark red needle. From a sample under oil, one, *ca* 0.05 x 0.1 x 0.3 mm, was mounted on a small loop and fixed in the cold nitrogen stream on a Rigaku Oxford Diffraction XtaLAB Synergy diffractometer, equipped with Cu-Kα radiation, HyPix detector and mirror monochromator. Intensity data were measured by thin-slice ω-scans. Total no. of reflections recorded, to θ_{max} = 72.5°, was 17294 of which 4624 were unique (Rint = 0.032); 4049 were 'observed' with $I > 2\sigma_I$.

Data were processed using the CrysAlisPro-CCD and -RED (1) programs. The structure was determined by the intrinsic phasing routines in the SHELXT program (2A) and refined by full-matrix least-squares methods, on F^2's, in SHELXL (2B). The non-hydrogen atoms were refined with anisotropic thermal parameters. The amino hydrogen atom was disordered over the two nitrogen atoms, N(2) and N(22), located in difference maps and both were refined freely. The remaining hydrogen atoms were included in idealised positions and their Uiso values were set to ride on the Ueq values of the parent carbon atoms. At the conclusion of the refinement, wR_2 = 0.094 and R_1 = 0.043 (2B) for all 4624 reflections weighted $w = [\sigma^2(F_o^2) + (0.0436\ P)^2 + 0.591\ P]^{-1}$ with $P = (F_o^2 + 2F_c^2)/3$; for the 'observed' data only, R_1 = 0.037.

In the final difference map, the highest peak (*ca* 0.17 $eÅ^{-3}$) was near the midpoint of the C(1)-C(9) bond.

Scattering factors for neutral atoms were taken from reference (3). Computer programs used in this analysis have been noted above, and were run through WinGX (4) on a Dell Optiplex 780 PC at the University of East Anglia.

References

(17) Programs CrysAlisPro, Rigaku Oxford Diffraction Ltd., Abingdon, UK (2018).

(18) G. M. Sheldrick, Programs for crystal structure determination (SHELXT), *Acta Cryst.* (2015) A**71**, 3-8, and refinement (SHELXL), *Acta Cryst.* (2008) A**64**, 112-122 and (2015) C**71**, 3-8.

(19) *'International Tables for X-ray Crystallography'*, Kluwer Academic Publishers, Dordrecht (1992). Vol. C, pp. 500, 219 and 193.

(20) L. J. Farrugia, *J. Appl. Cryst.* (2012) **45**, 849–854.

Legends for Figures

Figure 1. View of a molecule of the N-bis-isoindole derivative, indicating the atom numbering scheme. Thermal ellipsoids are drawn at the 50% probability level.

Figure 2. View of the molecule with the normal to the three N atoms N(2), N(22) and N(41), vertical in the plane of the paper.

Figure 3. Overlap of a N-bis-isoindole unit by its inverted neighbour.

Figure 4. The packing of molecules, along the *110* axis.

Notes on the structure.

The two isoindole groups, connected through the central N(41) atom, Figure 1, are essentially identical in dimensions except in the rotation of the phenyl group planes about the C(10)-C(11) and C(30)-C(31) bonds; the benzyl isoindole group of C(21) to N(38) is approximately planar whereas there is a rotation of *ca* 29.9 ° about the C(10)-C(11) bond in the group of C(1) to N(18).

All the bonds in the chain of N(2)-C(1)-N(41)-C(21)-N(22) are very similar, at *ca* 1.34 Å, suggesting delocalisation. However, the amino nitrogen atoms are different - the hydrogen on N(2) comes up strongly in early difference maps while the H on N(22) appears weaker. I am assuming that there is only one H atom here, shared unequally between the two N atoms - certainly the refinement is best this way! After refinement, the ratio of H(2):H(22) is *ca* 0.64:0.36. Both these hydrogen atoms are involved in hydrogen bonds - to the opposite N atom in the molecule. There is a hint of a spiralling of the atoms along this chain, and this feature is followed to the end of the group at N(38), but is interrupted by the rotation about the C(10)-C(11) bond in the other group, Figure 2.

Molecules are stacked in pairs about centres of symmetry: the ring of C(4)-C(9) lies over that of C(21'),N(22'),C(23'-24'),C(29'), with N(41') over the centre of the adjoining

pyrazole ring of N(2), and C(1) and C(1') are almost directly superimposed, 3.292 Å apart, Figure 3. The phenyl rings of C(31-36) and C(31"-36") are overlapping with a C(36)-C(36") distance of 3.156 Å. Molecules are stacked parallel to the *b* axis through these π…π interactions,

Crystal data and structure refinement for a BF_2-linked N(bis-isoindoline) derivative

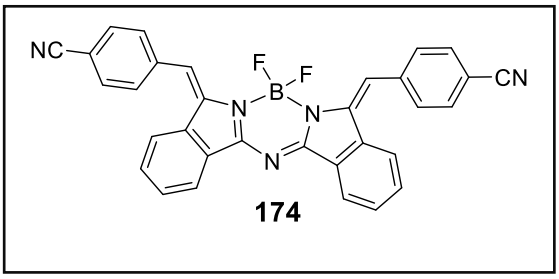

174

Identification code	**174**
Elemental formula	C32 H18 B F2 N5, 0.5(C H2 Cl2)
Formula weight	563.79
Crystal system, space group	Orthorhombic, Pbca (no, 61)
Unit cell dimensions	a = 16.2443(2) Å α = 90 ° b = 15.9943(2) Å β = 90 ° c = 20.3605(2) Å γ = 90 °
Volume	5289.99(11) $Å^3$
Z, Calculated density	8, 1.416 Mg/m^3
F(000)	2312
Absorption coefficient	1.783 mm^{-1}
Temperature	100.01(10) K
Wavelength	1.54184 Å
Crystal colour, shape	dark yellow block
Crystal size	0.45 x 0.35 x 0.3 mm
Crystal mounting:	on a small loop, in oil, fixed in cold N_2 stream
On the diffractometer:	
Theta range for data collection	7.775 to 72.496 °
Limiting indices	-16<=h<=20, -16<=k<=19, -25<=l<=23
Completeness to theta = 67.684	99.5 %
Absorption correction	Semi-empirical from equivalents
Max. and min. transmission	1.00000 and 0.59544
Reflections collected (not including absences)	21805
No. of unique reflections	5148 [R(int) for equivalents = 0.033]
No. of 'observed' reflections ($I > 2\sigma_I$)	4449
Structure determined by:	dual methods, in SHELXT
Refinement:	Full-matrix least-squares on F^2, in SHELXL
Data / restraints / parameters	5148 / 0 / 388

Goodness-of-fit on F^2	1.057
Final R indices ('observed' data)	R_1 = 0.043, wR_2 = 0.110
Final R indices (all data)	R_1 = 0.050, wR_2 = 0.113
Reflections weighted: $w = [\sigma^2(Fo^2)+(0.0521P)^2+3.0672P]^{-1}$ where $P=(Fo^2+2Fc^2)/3$	
Extinction coefficient	0.00022(7)
Largest diff. peak and hole	0.54 and -0.44 e.Å^{-3}
Location of largest difference peak	near N(28)

Table 1. Atomic coordinates (x 10^5) and equivalent isotropic displacement parameters ($Å^2$ x 10^4). U(eq) is defined as one third of the trace of the orthogonalized Uij tensor. E.s.ds are in parentheses.

	x	y	z	U(eq)	S.o.f.#
C(1)	35837(10)	40447(10)	51837(7)	226(3)	
N(2)	34704(8)	41431(8)	58344(6)	214(3)	
C(3)	32111(9)	33761(10)	61224(8)	219(3)	
C(4)	31521(10)	27692(11)	55778(8)	240(3)	
C(5)	28822(11)	19411(12)	55350(9)	304(4)	
C(6)	28682(12)	15711(13)	49184(10)	382(4)	
C(7)	31120(12)	19963(13)	43524(9)	376(4)	
C(8)	33672(11)	28190(12)	43875(8)	304(4)	
C(9)	33786(10)	31925(11)	50053(8)	250(3)	
B	36067(12)	49791(11)	62000(8)	230(4)	
F(1)	41389(7)	48792(6)	67256(4)	301(2)	
F(2)	28578(6)	52882(6)	64209(5)	328(2)	
N(10)	38345(9)	46296(9)	47632(6)	246(3)	
C(11)	40115(10)	53695(10)	50274(7)	229(3)	
N(12)	39765(8)	55657(8)	56720(6)	222(3)	
C(13)	42106(10)	64170(10)	57659(8)	231(3)	
C(14)	43859(10)	67520(10)	51055(8)	239(3)	
C(15)	46529(10)	75314(11)	48814(8)	275(4)	
C(16)	47785(11)	76294(12)	42113(9)	311(4)	
C(17)	46533(11)	69744(12)	37717(8)	320(4)	
C(18)	44032(11)	61970(12)	39880(8)	289(4)	
C(19)	42708(10)	61021(11)	46606(8)	246(3)	
C(20)	30159(10)	33323(10)	67682(8)	228(3)	
C(21)	28261(10)	25749(10)	71455(8)	231(3)	
C(22)	32952(10)	18480(11)	70729(8)	268(4)	
C(23)	31114(11)	11372(11)	74247(9)	288(4)	
C(24)	24506(11)	11364(11)	78575(8)	304(4)	
C(25)	19977(11)	18672(12)	79594(8)	316(4)	
C(26)	21977(10)	25830(11)	76146(8)	262(3)	
C(27)	22383(13)	3608(14)	81749(11)	439(5)	
N(28)	20818(13)	-2725(14)	83992(13)	684(7)	
C(30)	42878(10)	67532(10)	63675(8)	254(3)	
C(31)	44686(10)	76390(10)	65080(7)	241(3)	
C(32)	51139(11)	78495(11)	69276(8)	279(4)	
C(33)	52896(12)	86762(11)	70682(8)	300(4)	
C(34)	48023(11)	93076(10)	68035(8)	252(3)	
C(35)	41332(10)	91073(11)	64031(8)	267(4)	
C(36)	39796(10)	82763(11)	62521(8)	266(4)	
C(37)	49871(10)	101760(11)	69278(8)	273(4)	
N(38)	51216(9)	108725(9)	70137(7)	312(3)	
C(51)	7880(30)	-1090(30)	97480(30)	542(12)	0.5
Cl(52)	15618(6)	6576(6)	97791(5)	432(2)	0.5
Cl(53)	-1891(6)	2455(7)	99504(6)	512(3)	0.5

- site occupancy, if different from 1.
* - U(iso) ($Å^2$ x 10^4)

Table 2. Molecular dimensions. Bond lengths are in Ångstroms, angles in degrees. E.s.ds are in parentheses.

C(1)-N(10)	1.332(2)	C(14)-C(15)	1.397(2)
C(1)-N(2)	1.3467(19)	C(15)-C(16)	1.389(2)
C(1)-C(9)	1.449(2)	C(16)-C(17)	1.393(3)
N(2)-C(3)	1.423(2)	C(17)-C(18)	1.380(3)
N(2)-B	1.546(2)	C(18)-C(19)	1.395(2)
C(3)-C(20)	1.354(2)	C(20)-C(21)	1.467(2)
C(3)-C(4)	1.477(2)	C(21)-C(22)	1.398(2)
C(4)-C(9)	1.397(2)	C(21)-C(26)	1.398(2)
C(4)-C(5)	1.398(2)	C(22)-C(23)	1.376(2)
C(5)-C(6)	1.388(2)	C(23)-C(24)	1.389(3)
C(6)-C(7)	1.395(3)	C(24)-C(25)	1.397(3)
C(7)-C(8)	1.381(3)	C(24)-C(27)	1.441(3)
C(8)-C(9)	1.393(2)	C(25)-C(26)	1.382(2)
B-F(1)	1.385(2)	C(27)-N(28)	1.140(3)
B-F(2)	1.388(2)	C(30)-C(31)	1.475(2)
B-N(12)	1.548(2)	C(31)-C(36)	1.393(2)
N(10)-C(11)	1.331(2)	C(31)-C(32)	1.394(2)
C(11)-N(12)	1.3506(19)	C(32)-C(33)	1.383(2)
C(11)-C(19)	1.452(2)	C(33)-C(34)	1.392(2)
N(12)-C(13)	1.427(2)	C(34)-C(35)	1.396(2)
C(13)-C(30)	1.343(2)	C(34)-C(37)	1.443(2)
C(13)-C(14)	1.475(2)	C(35)-C(36)	1.387(2)
C(14)-C(19)	1.391(2)	C(37)-N(38)	1.149(2)
N(10)-C(1)-N(2)	126.30(15)	C(9)-C(4)-C(5)	119.33(15)
N(10)-C(1)-C(9)	124.73(14)	C(9)-C(4)-C(3)	106.90(14)
N(2)-C(1)-C(9)	108.97(14)	C(5)-C(4)-C(3)	133.62(16)
C(1)-N(2)-C(3)	110.18(13)	C(6)-C(5)-C(4)	117.74(17)
C(1)-N(2)-B	123.72(13)	C(5)-C(6)-C(7)	122.30(18)
C(3)-N(2)-B	126.10(13)	C(8)-C(7)-C(6)	120.44(16)
C(20)-C(3)-N(2)	120.92(14)	C(7)-C(8)-C(9)	117.35(17)
C(20)-C(3)-C(4)	132.82(15)	C(8)-C(9)-C(4)	122.82(16)
N(2)-C(3)-C(4)	106.04(13)	C(8)-C(9)-C(1)	129.26(16)

C(4)-C(9)-C(1) 107.90(14)
F(1)-B-F(2) 109.74(13)
F(1)-B-N(2) 111.20(13)
F(2)-B-N(2) 109.79(14)
F(1)-B-N(12) 111.36(14)
F(2)-B-N(12) 110.44(13)
N(2)-B-N(12) 104.20(12)
C(11)-N(10)-C(1) 115.51(13)
N(10)-C(11)-N(12) 126.15(15)
N(10)-C(11)-C(19) 124.91(14)
N(12)-C(11)-C(19) 108.94(14)
C(11)-N(12)-C(13) 109.92(13)
C(11)-N(12)-B 123.39(14)
C(13)-N(12)-B 126.06(13)
C(30)-C(13)-N(12) 121.95(14)
C(30)-C(13)-C(14) 131.87(15)
N(12)-C(13)-C(14) 106.02(13)
C(19)-C(14)-C(15) 119.73(15)
C(19)-C(14)-C(13) 107.22(14)
C(15)-C(14)-C(13) 133.00(16)
C(16)-C(15)-C(14) 117.87(17)
C(15)-C(16)-C(17) 121.67(17)
C(18)-C(17)-C(16) 121.04(15)
C(17)-C(18)-C(19) 117.17(17)
C(14)-C(19)-C(18) 122.51(16)
C(14)-C(19)-C(11) 107.88(14)

C(51)-Cl(53) 1.735(5)
C(51)-Cl(52) 1.757(5)

C(18)-C(19)-C(11) 129.61(16)
C(3)-C(20)-C(21) 126.89(15)
C(22)-C(21)-C(26) 118.55(15)
C(22)-C(21)-C(20) 121.12(15)
C(26)-C(21)-C(20) 120.23(15)
C(23)-C(22)-C(21) 120.91(16)
C(22)-C(23)-C(24) 119.91(16)
C(23)-C(24)-C(25) 120.04(16)
C(23)-C(24)-C(27) 118.06(17)
C(25)-C(24)-C(27) 121.87(17)
C(26)-C(25)-C(24) 119.61(16)
C(25)-C(26)-C(21) 120.75(16)
N(28)-C(27)-C(24) 176.7(3)
C(13)-C(30)-C(31) 125.45(15)
C(36)-C(31)-C(32) 118.77(15)
C(36)-C(31)-C(30) 121.11(15)
C(32)-C(31)-C(30) 120.05(15)
C(33)-C(32)-C(31) 120.88(16)
C(32)-C(33)-C(34) 119.76(16)
C(33)-C(34)-C(35) 120.16(15)
C(33)-C(34)-C(37) 120.81(16)
C(35)-C(34)-C(37) 119.02(15)
C(36)-C(35)-C(34) 119.31(16)
C(35)-C(36)-C(31) 121.04(16)
N(38)-C(37)-C(34) 178.28(19)

Cl(53)-C(51)-Cl(52) 114.7(3)

Table 3. Anisotropic displacement parameters ($Å^2$ x 10^4) for the expression: exp {$-2\pi^2(h^2a^{*2}U_{11}$ + ... + $2hka^*b^*U_{12})$} E.s.ds are in parentheses.

	U_{11}	U_{22}	U_{33}	U_{23}	U_{13}	U_{12}
C(1)	222(7)	254(8)	203(7)	-23(6)	-8(6)	47(6)
N(2)	232(6)	221(7)	189(6)	-3(5)	5(5)	7(5)
C(3)	193(7)	209(7)	253(7)	-13(6)	-5(6)	0(6)
C(4)	191(7)	271(8)	259(8)	-46(7)	-9(6)	4(6)
C(5)	276(8)	305(9)	331(9)	-61(7)	26(7)	-65(7)
C(6)	392(10)	348(10)	407(10)	-131(8)	27(8)	-123(8)
C(7)	417(11)	404(11)	306(9)	-160(8)	-6(8)	-63(9)
C(8)	313(9)	346(10)	253(8)	-69(7)	-5(7)	5(7)
C(9)	210(7)	285(9)	254(8)	-36(7)	-20(6)	30(7)
B	302(9)	199(8)	191(8)	10(7)	29(7)	8(7)
F(1)	478(6)	230(5)	193(4)	20(4)	-57(4)	-50(4)
F(2)	396(6)	233(5)	355(5)	8(4)	157(4)	38(4)
N(10)	288(7)	263(7)	187(6)	-10(5)	-2(5)	45(6)
C(11)	225(8)	267(8)	194(7)	7(6)	4(6)	56(6)
N(12)	264(7)	217(7)	185(6)	9(5)	11(5)	13(5)
C(13)	239(8)	221(8)	234(7)	42(6)	17(6)	8(6)
C(14)	214(7)	275(8)	228(7)	52(6)	15(6)	34(6)
C(15)	260(8)	295(9)	269(8)	66(7)	23(7)	7(7)
C(16)	273(8)	353(10)	305(9)	131(7)	61(7)	41(7)
C(17)	324(9)	422(10)	215(8)	106(7)	59(7)	99(8)
C(18)	298(9)	366(9)	204(8)	36(7)	30(7)	87(7)
C(19)	231(8)	285(8)	224(8)	43(6)	19(6)	64(7)
C(20)	235(8)	203(7)	247(8)	-25(6)	4(6)	-8(6)
C(21)	233(7)	237(8)	223(7)	-13(6)	-26(6)	-36(6)
C(22)	269(8)	251(8)	284(8)	-24(7)	12(7)	-26(7)
C(23)	295(9)	227(8)	342(9)	-6(7)	-49(7)	-16(7)
C(24)	294(9)	299(9)	320(8)	67(7)	-48(7)	-62(7)
C(25)	300(9)	371(10)	276(8)	53(7)	31(7)	-10(8)
C(26)	289(8)	253(8)	244(8)	-1(6)	22(7)	12(7)
C(27)	342(10)	423(12)	554(12)	175(10)	-11(9)	-25(9)
N(28)	523(12)	544(13)	984(17)	442(13)	12(11)	-48(10)
C(30)	305(8)	234(8)	222(7)	43(6)	15(6)	-21(7)
C(31)	298(8)	241(8)	183(7)	20(6)	47(6)	-20(7)
C(32)	382(10)	238(8)	218(8)	15(6)	-35(7)	25(7)
C(33)	370(9)	278(9)	251(8)	16(7)	-71(7)	-15(7)
C(34)	309(9)	222(8)	227(7)	20(6)	22(6)	-24(7)
C(35)	266(8)	245(8)	290(8)	33(7)	7(7)	10(7)
C(36)	244(8)	277(8)	278(8)	7(7)	-5(6)	-32(7)
C(37)	290(8)	278(9)	251(8)	40(7)	-12(7)	9(7)
N(38)	352(8)	251(8)	335(8)	41(6)	-31(6)	-16(6)
C(51)	400(20)	450(30)	770(30)	-210(20)	-90(20)	20(20)
Cl(52)	417(5)	419(5)	459(5)	-104(4)	56(4)	25(4)
Cl(53)	392(7)	563(7)	581(6)	-221(6)	-37(5)	-59(4)

Table 4. Hydrogen coordinates (x 10^4) and isotropic displacement parameters ($Å^2$ x 10^3). All hydrogen atoms were included in idealised positions with U(iso)'s set at 1.2*U(eq) or, for the methyl group hydrogen atoms, 1.5*U(eq) of the parent carbon atoms.

	x	y	z	U(iso)	S.o.f.#
H(5)	2718	1648	5907	36	
H(6)	2690	1021	4881	46	
H(7)	3103	1724	3949	45	
H(8)	3525	3112	4013	36	
H(15)	4744	7971	5172	33	
H(16)	4950	8146	4052	37	
H(17)	4740	7062	3325	38	
H(18)	4326	5755	3697	35	
H(20)	3001	3836	6997	27	
H(22)	3738	1845	6783	32	
H(23)	3429	658	7373	35	
H(25)	1564	1872	8258	38	
H(26)	1911	3076	7695	31	
H(30)	4222	6398	6725	30	
H(32)	5430	7428	7116	34	
H(33)	5732	8810	7339	36	
H(35)	3794	9527	6239	32	
H(36)	3543	8142	5976	32	
H(51A)	772	-340	9308	65	0.5
H(51B)	935	-558	10046	65	0.5

- site occupancy, if different from 1.

Table 5. Torsion angles, in degrees. E.s.ds are in parentheses.

N(10)-C(1)-N(2)-C(3-	
179.15(15)	
C(9)-C(1)-N(2)-C(3)	
1.51(17)	
N(10)-C(1)-N(2)-B	
1.0(2)	
C(9)-C(1)-N(2)-B	-178.39(14)
C(1)-N(2)-C(3)-C(20)-	
176.46(14)	
B-N(2)-C(3)-C(20)	
3.4(2)	
C(1)-N(2)-C(3)-C(4)	-1.16(17)
B-N(2)-C(3)-C(4)	
178.74(14)	
C(20)-C(3)-C(4)-C(9)	
174.85(17)	
N(2)-C(3)-C(4)-C(9)	
0.34(17)	
C(20)-C(3)-C(4)-C(5)	-0.5(3)
N(2)-C(3)-C(4)-C(5)-	
175.00(18)	
C(9)-C(4)-C(5)-C(6)	
1.3(3)	
C(3)-C(4)-C(5)-C(6)	
176.14(18)	
C(4)-C(5)-C(6)-C(7)	
0.0(3)	
C(5)-C(6)-C(7)-C(8)	-1.1(3)
C(6)-C(7)-C(8)-C(9)	
0.8(3)	
C(7)-C(8)-C(9)-C(4)	
0.5(3)	
C(7)-C(8)-C(9)-C(1)-	
177.29(17)	
C(5)-C(4)-C(9)-C(8)	-1.6(3)
C(3)-C(4)-C(9)-C(8)-	
177.72(15)	
C(5)-C(4)-C(9)-C(1)	
176.66(15)	
C(3)-C(4)-C(9)-C(1)	
0.52(17)	
N(10)-C(1)-C(9)-C(8)	-2.5(3)
N(2)-C(1)-C(9)-C(8)	
176.82(16)	
N(10)-C(1)-C(9)-C(4)	
179.37(15)	
N(2)-C(1)-C(9)-C(4)	-1.27(18)
C(1)-N(2)-B-F(1)	-126.44(15)
C(3)-N(2)-B-F(1)	
53.7(2)	
C(1)-N(2)-B-F(2)	
111.92(16)	
C(3)-N(2)-B-F(2)	-67.96(19)
C(1)-N(2)-B-N(12)	-6.4(2)
C(3)-N(2)-B-N(12)	
173.76(13)	
N(2)-C(1)-N(10)-C(11)	
2.3(2)	
C(9)-C(1)-N(10)-C(11)-	
178.45(15)	
C(1)-N(10)-C(11)-N(12)	
1.6(2)	
C(1)-N(10)-C(11)-C(19)-	
178.02(15)	
N(10)-C(11)-N(12)-C(13)	
179.97(15)	
C(19)-C(11)-N(12)-C(13)-	
0.39(18)	
N(10)-C(11)-N(12)-B	-8.6(2)
C(19)-C(11)-N(12)-B	
171.07(14)	
F(1)-B-N(12)-C(11)	
129.76(15)	
F(2)-B-N(12)-C(11)-	
108.04(16)	
N(2)-B-N(12)-C(11)	
9.8(2)	
F(1)-B-N(12)-C(13)-	60.2(2)
F(2)-B-N(12)-C(13)	
62.0(2)	
N(2)-B-N(12)-C(13)	
179.85(13)	
C(11)-N(12)-C(13)-C(30)-	
174.91(15)	
B-N(12)-C(13)-C(30)	
13.9(2)	
C(11)-N(12)-C(13)-C(14)	
1.03(17)	
B-N(12)-C(13)-C(14)-	
170.15(14)	
C(30)-C(13)-C(14)-C(19)	
174.09(18)	
N(12)-C(13)-C(14)-C(19)-	
1.28(17)	
C(30)-C(13)-C(14)-C(15)-	
3.3(3)	
N(12)-C(13)-C(14)-C(15)-	
178.63(17)	
C(19)-C(14)-C(15)-C(16)	
1.3(2)	
C(13)-C(14)-C(15)-C(16)	
178.34(17)	
C(14)-C(15)-C(16)-C(17)-	
0.7(3)	
C(15)-C(16)-C(17)-C(18)-	
0.4(3)	
C(16)-C(17)-C(18)-C(19)	
0.9(3)	
C(15)-C(14)-C(19)-C(18)	-
0.8(2)	
C(13)-C(14)-C(19)-C(18)	-
178.52(15)	
C(15)-C(14)-C(19)-C(11)	
178.83(14)	
C(13)-C(14)-C(19)-C(11)	
1.06(17)	
C(17)-C(18)-C(19)-C(14)	-
0.4(2)	
C(17)-C(18)-C(19)-C(11)	-
179.84(16)	
N(10)-C(11)-C(19)-C(14)	
179.20(15)	
N(12)-C(11)-C(19)-C(14)	-
0.45(18)	
N(10)-C(11)-C(19)-C(18)	-
1.3(3)	
N(12)-C(11)-C(19)-C(18)	
179.09(16)	
N(2)-C(3)-C(20)-C(21)-	
172.98(14)	
C(4)-C(3)-C(20)-C(21)	
13.2(3)	
C(3)-C(20)-C(21)-C(22)	
43.4(2)	
C(3)-C(20)-C(21)-C(26)-	
140.28(17)	

C(26)-C(21)-C(22)-C(23) 4.1(2)
C(20)-C(21)-C(22)-C(23)-179.56(15)
C(21)-C(22)-C(23)-C(24) 0.2(3)
C(22)-C(23)-C(24)-C(25)-3.1(3)
C(22)-C(23)-C(24)-C(27) 174.99(17)
C(23)-C(24)-C(25)-C(26) 1.7(3)
C(27)-C(24)-C(25)-C(26)-176.31(18)
C(24)-C(25)-C(26)-C(21) 2.6(3)
C(22)-C(21)-C(26)-C(25)-5.5(2)
C(20)-C(21)-C(26)-C(25) 178.12(15)
N(12)-C(13)-C(30)-C(31)-175.40(15)
C(14)-C(13)-C(30)-C(31) 9.8(3)
C(13)-C(30)-C(31)-C(36) 54.9(2)
C(13)-C(30)-C(31)-C(32)-128.13(19)
C(36)-C(31)-C(32)-C(33)-2.6(2)
C(30)-C(31)-C(32)-C(33)-179.62(16)
C(31)-C(32)-C(33)-C(34) 1.9(3)
C(32)-C(33)-C(34)-C(35) 0.7(3)
C(32)-C(33)-C(34)-C(37)-178.23(16)
C(33)-C(34)-C(35)-C(36)-2.5(2)
C(37)-C(34)-C(35)-C(36) 176.45(15)
C(34)-C(35)-C(36)-C(31) 1.8(2)
C(32)-C(31)-C(36)-C(35) 0.8(2)
C(30)-C(31)-C(36)-C(35) 177.74(15)

Table 6. Hydrogen bonds (?), in Ångstroms and degrees.

D-H...A	d(D-H)	d(H...A)	d(D...A)	<(DHA)
C(20)-H(20)...F(1)	0.93	2.55	3.0751(19)	116.0
C(20)-H(20)...F(2)	0.93	2.61	3.2175(19)	123.2
C(30)-H(30)...F(1)	0.93	2.43	3.0943(19)	128.1

Crystal structure analysis of a BF_2-linked N(bis-isoindoline) derivative

Crystal data: $C_{32}H_{18}BF_2N_5$, 0.5(CH_2Cl_2), M = 563.79. Orthorhombic, space group Pbca (no. 61), a = 16.2443(2), b = 15.9943(2), c = 20.3605(2) Å, V = 5289.99(11) $Å^3$. Z = 8, Dc = 1.416 g cm^{-3}, F(000) = 2312, T = 100.01(10) K, μ(Cu-Kα) = 17.83 cm^{-1}, λ(Cu-Kα) = 1.54184 Å.

The crystals were dark yellow blocks. From a sample under oil, one, *ca* 0.3 x 0.35 x 0.45 mm, was mounted on a small loop and fixed in the cold nitrogen stream on a Rigaku Oxford Diffraction XtaLAB Synergy diffractometer, equipped with Cu-Kα radiation, HyPix detector and mirror monochromator. Intensity data were measured by thin-slice ω-scans. Total no. of reflections recorded, to θ_{max} = 72.5°, was 21805 of which 5148 were unique (Rint = 0.033); 4449 were 'observed' with $I > 2\sigma_I$.

Data were processed using the CrysAlisPro-CCD and -RED (1) programs. The structure was determined by the intrinsic phasing routines in the SHELXT program (2A) and refined by full-matrix least-squares methods, on F^2's, in SHELXL (2B). The principal molecule was clear and well-defined. A solvent (CH_2Cl_2) molecule was found, disordered about a centre of symmetry. All the non-hydrogen atoms were refined with anisotropic thermal parameters. The hydrogen atoms were included in idealised positions and their Uiso values were set to ride on the Ueq values of the parent carbon atoms. At the conclusion of the refinement, wR_2 = 0.113 and R_1 = 0.050 (2B) for all 5148 reflections weighted $w = [\sigma^2(F_o^2) + (0.0521\ P)^2 + 3.067\ P]^{-1}$ with $P = (F_o^2 + 2F_c^2)/3$; for the 'observed' data only, R_1 = 0.043.

In the final difference map, the highest peak (*ca* 0.54 $eÅ^{-3}$) was near N(28).

Scattering factors for neutral atoms were taken from reference (3). Computer programs used in this analysis have been noted above, and were run through WinGX (4) on a Dell Optiplex 780 PC at the University of East Anglia.

References

(21) Programs CrysAlisPro, Rigaku Oxford Diffraction Ltd., Abingdon, UK (2021).

(22) G. M. Sheldrick, Programs for crystal structure determination (SHELXT), *Acta Cryst.* (2015) A**71**, 3-8, and refinement (SHELXL), *Acta Cryst.* (2008) A**64**, 112-122 and (2015) C**71**, 3-8.

(23) *'International Tables for X-ray Crystallography'*, Kluwer Academic Publishers,

Dordrecht (1992). Vol. C, pp. 500, 219 and 193.

(24) L. J. Farrugia, *J. Appl. Cryst.* (2012) **45**, 849–854.

Legends for Figures

Figure 1. View of a molecule of the BF_2-linked N(bis-isoindoline) derivative, indicating the atom numbering scheme. Thermal ellipsoids are drawn at the 50% probability level.

Figure 2. View of the packing of molecules, along the *b* axis. Molecules are linked through N-H…O hydrogen bonds in chains parallel to the *c* axis.

Notes on the structure.

The BF_2-linked N(bis-isoindoline) derivative molecule has a three-plane structure. The central plane comprises the two isoindole groups and the N(10) and B atoms that link them; the isoindole rings are tilted only slightly from the mean-plane of the central six-membered ring. The two phenyl rings are rotated from the isoindole rings, about the C(20)-C(21) and C(30)-C(31) bonds, by 52.2 and 61.8 ° respectively.

The solvent molecule, CH_2Cl_2, is disordered and lies close to a centre of symmetry with Cl(53') 0.66 A from the C(51)-Cl(53) bond.

There are several short intramolecular contacts, e.g. H(15)-C(22) and, correspondingly, H(5)-H(36), both at 2.57 Å. Most of the intermolecular contacts are close to van der Waals' distances.

Crystal data and structure refinement for C_8H_5N-NSO_2CF_3-1,CHC_6H_4OMe-3

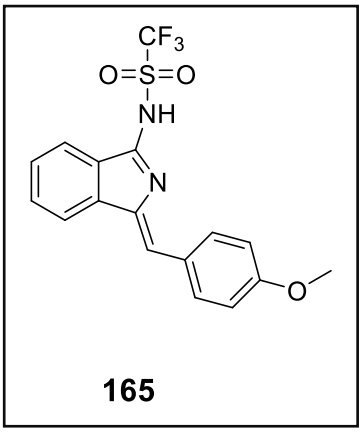

165

Identification code	**165**
Elemental formula	C17 H13 F3 N2 O3 S
Formula weight	382.35
Crystal system, space group	Triclinic, P -1
Unit cell dimensions	a = 7.0556(3) Å α = 107.878(4) ° b = 10.5060(5) Å β = 103.794(4) ° c = 12.6271(5) Å γ = 101.674(4) °
Volume	825.77(7) $Å^3$
Z, Calculated density	2, 1.538 Mg/m^3
F(000)	392
Absorption coefficient	2.242 mm^{-1}
Temperature	100.01(10) K
Wavelength	1.54184 Å
Crystal colour, shape	? ?
Crystal size	? x ? x ? mm
Crystal mounting:	on a glass fibre, in oil, fixed in cold N_2 stream
On the diffractometer:	
Theta range for data collection	7.769 to 69.908 °
Limiting indices	-8<=h<=8, -12<=k<=12, -15<=l<=13
Completeness to theta = 67.684	98.2 %
Absorption correction	Semi-empirical from equivalents
Max. and min. transmission	1.00000 and 0.68226
Reflections collected (not including absences)	7870
No. of unique reflections	3042 [R(int) for equivalents = 0.048]
No. of 'observed' reflections ($I > 2\sigma_I$)	2659
Structure determined by:	dual methods, in SHELXT
Refinement:	Full-matrix least-squares on F^2, in SHELXL

Data / restraints / parameters	3042 / 0 / 235
Goodness-of-fit on F^2	1.074
Final R indices ('observed' data)	R_1 = 0.055, wR_2 = 0.153
Final R indices (all data)	R_1 = 0.060, wR_2 = 0.157
Reflections weighted: $w = [\sigma^2(Fo^2)+(0.1025P)^2+0.2160P]^{-1}$ where $P=(Fo^2+2Fc^2)/3$	
Extinction coefficient	n/a
Largest diff. peak and hole	0.55 and -0.57 e.Å^{-3}
Location of largest difference peak	near C(13)

Table 1. Atomic coordinates (x 10^5) and equivalent isotropic displacement parameters ($Å^2$ x 10^4). U(eq) is defined as one third of the trace of the orthogonalized Uij tensor. E.s.ds are in parentheses.

	x	y	z	U(eq)
C(1)	88220(30)	63890(20)	60185(19)	249(5)
N(2)	76650(30)	62378(18)	49530(16)	252(4)
C(3)	66440(30)	48130(20)	42221(19)	249(5)
C(4)	67480(30)	26050(20)	47370(20)	293(5)
C(5)	75930(40)	21780(20)	56170(20)	321(5)
C(6)	89550(40)	31470(30)	67110(20)	314(5)
C(7)	94810(30)	45750(20)	69400(20)	281(5)
C(8)	86200(30)	49940(20)	60530(20)	253(5)
C(9)	72610(30)	40340(20)	49569(19)	255(5)
N(11)	99930(30)	75513(19)	69228(17)	282(4)
O(121)	85500(30)	91070(17)	59508(15)	420(5)
O(122)	121910(30)	98472(19)	71226(17)	468(5)
S(12)	101316(9)	90602(5)	68759(5)	313(2)
C(13)	95620(40)	98730(20)	82280(20)	314(5)
F(131)	77320(20)	91919(15)	81895(13)	410(4)
F(132)	96120(30)	111876(15)	83793(14)	463(4)
F(133)	109490(20)	98972(17)	91558(12)	443(4)
C(30)	54000(30)	42900(20)	31020(20)	264(5)
C(31)	47540(30)	49670(20)	22887(19)	259(5)
C(32)	56640(30)	63520(20)	24410(20)	287(5)
C(33)	50000(30)	69110(20)	16210(20)	286(5)
C(34)	33740(30)	60780(20)	5910(20)	279(5)
C(35)	24250(30)	47030(20)	4190(20)	297(5)
C(36)	30960(30)	41550(20)	12456(19)	273(5)
O(37)	26190(20)	65245(18)	-2805(15)	337(4)
C(38)	36840(40)	78840(30)	-1930(20)	352(6)

Table 2. Molecular dimensions. Bond lengths are in Ångstroms, angles in degrees. E.s.ds are in parentheses.

C(1)-N(11)	1.328(3)	O(122)-S(12)	1.4255(19)
C(1)-N(2)	1.340(3)	S(12)-C(13)	1.838(2)
C(1)-C(8)	1.459(3)	C(13)-F(133)	1.325(3)
N(2)-C(3)	1.417(3)	C(13)-F(131)	1.325(3)
C(3)-C(30)	1.345(3)	C(13)-F(132)	1.327(3)
C(3)-C(9)	1.462(3)	C(30)-C(31)	1.458(3)
C(4)-C(5)	1.374(3)	C(31)-C(32)	1.399(3)
C(4)-C(9)	1.392(3)	C(31)-C(36)	1.415(3)
C(5)-C(6)	1.406(4)	C(32)-C(33)	1.375(3)
C(6)-C(7)	1.389(3)	C(33)-C(34)	1.399(3)
C(7)-C(8)	1.380(3)	C(34)-O(37)	1.361(3)
C(8)-C(9)	1.404(3)	C(34)-C(35)	1.389(3)
N(11)-S(12)	1.589(2)	C(35)-C(36)	1.374(3)
O(121)-S(12)	1.431(2)	O(37)-C(38)	1.431(3)

N(11)-C(1)-N(2)	129.4(2)	O(122)-S(12)-O(121)	119.12(13)
N(11)-C(1)-C(8)	122.8(2)	O(122)-S(12)-N(11)	111.47(12)
N(2)-C(1)-C(8)	107.76(18)	O(121)-S(12)-N(11)	115.41(10)
C(1)-N(2)-C(3)	112.39(19)	O(122)-S(12)-C(13)	103.40(11)
C(30)-C(3)-N(2)	128.0(2)	O(121)-S(12)-C(13)	105.09(12)
C(30)-C(3)-C(9)	127.6(2)	N(11)-S(12)-C(13)	99.14(11)
N(2)-C(3)-C(9)	104.47(18)	F(133)-C(13)-F(131)	108.6(2)
C(5)-C(4)-C(9)	118.3(2)	F(133)-C(13)-F(132)	107.66(18)
C(4)-C(5)-C(6)	121.4(2)	F(131)-C(13)-F(132)	108.4(2)
C(7)-C(6)-C(5)	120.8(2)	F(133)-C(13)-S(12)	110.55(17)
C(8)-C(7)-C(6)	117.4(2)	F(131)-C(13)-S(12)	111.64(15)
C(7)-C(8)-C(9)	122.2(2)	F(132)-C(13)-S(12)	109.82(17)
C(7)-C(8)-C(1)	130.8(2)	C(3)-C(30)-C(31)	131.7(2)
C(9)-C(8)-C(1)	106.92(19)	C(32)-C(31)-C(36)	116.9(2)
C(4)-C(9)-C(8)	119.9(2)	C(32)-C(31)-C(30)	125.4(2)
C(4)-C(9)-C(3)	131.7(2)	C(36)-C(31)-C(30)	117.7(2)
C(8)-C(9)-C(3)	108.45(19)	C(33)-C(32)-C(31)	122.2(2)
C(1)-N(11)-S(12)	121.78(17)	C(32)-C(33)-C(34)	119.6(2)

O(37)-C(34)-C(35)	C(36)-C(35)-C(34)
116.19(19)	120.3(2)
O(37)-C(34)-C(33)	C(35)-C(36)-C(31)
124.3(2)	121.4(2)
C(35)-C(34)-C(33)	C(34)-O(37)-C(38)
119.6(2)	117.80(17)

Table 3. Anisotropic displacement parameters ($Å^2$ x 10^4) for the expression: exp $\{-2\pi^2(h^2a^{*2}U_{11} + ... + 2hka^*b^*U_{12})\}$ E.s.ds are in parentheses.

	U_{11}	U_{22}	U_{33}	U_{23}	U_{13}	U_{12}
C(1)	229(10)	212(10)	244(11)	24(9)	80(9)	26(8)
N(2)	266(9)	169(8)	234(9)	27(7)	30(7)	17(7)
C(3)	224(10)	174(10)	273(11)	26(8)	58(9)	17(8)
C(4)	256(11)	202(11)	317(12)	20(9)	66(9)	4(9)
C(5)	331(12)	224(11)	382(13)	89(10)	119(10)	62(9)
C(6)	319(12)	309(12)	306(12)	127(10)	84(10)	76(10)
C(7)	250(11)	278(11)	252(11)	48(9)	59(9)	53(9)
C(8)	223(10)	209(10)	262(11)	43(9)	64(9)	13(8)
C(9)	221(10)	218(10)	262(11)	42(9)	68(9)	17(8)
N(11)	299(10)	201(9)	238(9)	18(7)	37(8)	10(7)
O(121)	644(12)	211(8)	276(9)	50(7)	32(8)	61(8)
O(122)	498(11)	259(9)	463(11)	-37(8)	221(9)	-83(8)
S(12)	394(4)	180(3)	247(3)	5(2)	79(3)	-10(2)
C(13)	369(12)	201(10)	290(12)	35(9)	79(10)	34(9)
F(131)	395(8)	294(7)	440(9)	28(6)	161(7)	31(6)
F(132)	704(11)	196(7)	427(8)	44(6)	210(8)	86(7)
F(133)	495(9)	462(9)	247(7)	30(6)	40(6)	139(7)
C(30)	231(10)	199(10)	275(11)	25(9)	60(9)	3(8)
C(31)	241(10)	232(11)	228(11)	21(9)	57(9)	35(8)
C(32)	242(10)	251(11)	242(11)	17(9)	10(9)	13(9)
C(33)	259(11)	216(10)	272(12)	24(9)	31(9)	8(9)
C(34)	251(10)	267(11)	239(11)	37(9)	45(9)	42(9)
C(35)	253(11)	273(11)	238(11)	12(9)	23(9)	11(9)
C(36)	238(10)	211(10)	246(11)	1(9)	27(9)	2(8)
O(37)	306(8)	306(9)	287(9)	85(7)	-11(7)	26(7)
C(38)	400(13)	272(12)	327(13)	109(10)	48(10)	71(10)

Table 4. Hydrogen coordinates (x 10^4) and isotropic displacement parameters ($Å^2$ x 10^3). All hydrogen atoms were included in idealised positions with U(iso)'s set at 1.2*U(eq) or, for the methyl group hydrogen atoms, 1.5*U(eq) of the parent carbon atoms.

	x	y	z	U(iso)
H(2)	7551	6943	4732	30
H(4)	5838	1942	3998	35
H(5)	7248	1207	5482	39
H(6)	9523	2821	7301	38
H(7)	10397	5237	7678	34
H(30)	4839	3299	2783	32
H(32)	6777	6925	3134	34
H(33)	5642	7858	1753	34
H(35)	1305	4138	-273	36
H(36)	2434	3212	1114	33
H(38A)	2985	8074	-872	53
H(38B)	3709	8592	532	53
H(38C)	5088	7918	-179	53

Table 5. Torsion angles, in degrees. E.s.ds are in parentheses.

N(11)-C(1)-N(2)-C(3) 179.6(2)	O(122)-S(12)-C(13)-F(133)- 54.0(2)
C(8)-C(1)-N(2)-C(3) 0.0(2)	O(121)-S(12)-C(13)-F(133)- 179.57(15)
C(1)-N(2)-C(3)-C(30)-178.8(2)	N(11)-S(12)-C(13)-F(133) 60.85(18)
C(1)-N(2)-C(3)-C(9) 0.8(2)	O(122)-S(12)-C(13)-F(131)- 175.03(17)
C(9)-C(4)-C(5)-C(6)-0.5(4)	O(121)-S(12)-C(13)-F(131) 59.4(2)
C(4)-C(5)-C(6)-C(7) 0.4(4)	N(11)-S(12)-C(13)-F(131)- 60.22(19)
C(5)-C(6)-C(7)-C(8)-0.2(3)	O(122)-S(12)-C(13)-F(132) 64.7(2)
C(6)-C(7)-C(8)-C(9) 0.1(3)	O(121)-S(12)-C(13)-F(132)- 60.93(19)
C(6)-C(7)-C(8)-C(1) 178.7(2)	N(11)-S(12)-C(13)-F(132) 179.49(16)
N(11)-C(1)-C(8)-C(7) 0.7(4)	N(2)-C(3)-C(30)-C(31) 1.9(4)
N(2)-C(1)-C(8)-C(7) -179.7(2)	C(9)-C(3)-C(30)-C(31)-177.5(2)
N(11)-C(1)-C(8)-C(9) 179.5(2)	C(3)-C(30)-C(31)-C(32) 14.2(4)
N(2)-C(1)-C(8)-C(9)-0.9(2)	C(3)-C(30)-C(31)-C(36)-167.1(2)
C(5)-C(4)-C(9)-C(8) 0.4(3)	C(36)-C(31)-C(32)-C(33)-0.2(4)
C(5)-C(4)-C(9)-C(3) 179.8(2)	C(30)-C(31)-C(32)-C(33) 178.4(2)
C(7)-C(8)-C(9)-C(4)-0.2(3)	C(31)-C(32)-C(33)-C(34)-0.5(4)
C(1)-C(8)-C(9)-C(4)- 179.13(19)	C(32)-C(33)-C(34)-O(37)- 179.2(2)
C(7)-C(8)-C(9)-C(3)-179.7(2)	C(32)-C(33)-C(34)-C(35) 1.2(4)
C(1)-C(8)-C(9)-C(3) 1.3(2)	O(37)-C(34)-C(35)-C(36) 179.3(2)
C(30)-C(3)-C(9)-C(4)-1.2(4)	C(33)-C(34)-C(35)-C(36)-1.0(4)
N(2)-C(3)-C(9)-C(4) 179.2(2)	C(34)-C(35)-C(36)-C(31) 0.2(4)
C(30)-C(3)-C(9)-C(8) 178.3(2)	C(32)-C(31)-C(36)-C(35) 0.4(3)
N(2)-C(3)-C(9)-C(8)-1.3(2)	C(30)-C(31)-C(36)-C(35)- 178.4(2)
N(2)-C(1)-N(11)-S(12) 2.4(3)	C(35)-C(34)-O(37)-C(38)- 173.8(2)
C(8)-C(1)-N(11)-S(12)- 178.05(16)	C(33)-C(34)-O(37)-C(38) 6.5(3)
C(1)-N(11)-S(12)-O(122)- 124.11(19)	
C(1)-N(11)-S(12)-O(121) 15.9(2)	
C(1)-N(11)-S(12)-C(13) 127.5(2)	

Table 6. Hydrogen bonds, in Ångstroms and degrees.

D-H...A	d(D-H)	d(H...A)	d(D...A)	<(DHA)
N(2)-H(2)...O(121)	0.88	2.17	2.756(2)	123.3
C(30)-H(30)...F(131)#1	0.95	2.59	3.503(3)	162.1
C(33)-H(33)...O(122)#2	0.95	2.35	3.240(3)	155.1
C(38)-H(38A)...F(133)#3	0.98	2.61	3.292(3)	126.5

Symmetry transformations used to generate equivalent atoms:
#1 : 1-x, 1-y, 1-z #2 : 2-x, 2-y, 2-z #3 : x-1, y, z-1

Crystal structure analysis of C_8H_5N-NSO_2CF_3-1,CHC_6H_4OMe-3

Crystal data: $C_{17}H_{13}F_3N_2O_3S$, M = 382.35. Triclinic, space group P-1 (no. 2), a = 7.0556(3), b = 10.5060(5), c = 12.6271(5) Å, α = 107.878(4), β = 103.794(4), γ = 101.674(4) °, V = 825.77(7) $Å^3$. Z = 2, Dc = 1.538 g cm^{-3}, F(000) = 392, T = 100.01(10) K, μ(Cu-Kα) = 22.4 cm^{-1}, λ(Cu-Kα) = 1.54184 Å.

The crystal was a colourless shard. From a sample under oil, one, *ca* 0. x 0. x 0. mm, was mounted on a small loop and fixed in the cold nitrogen stream on a Rigaku Oxford Diffraction XtaLAB Synergy diffractometer, equipped with Cu-Kα radiation, HyPix detector and mirror monochromator. Intensity data were measured by thin-slice ω-scans. Total no. of reflections recorded, to θ_{max} = 70.0°, was 7870 of which 3042 were unique (Rint = 0.048); 2659 were 'observed' with $I > 2\sigma_I$.

Data were processed using the CrysAlisPro-CCD and -RED (1) programs. The structure was determined by the intrinsic phasing routines in the SHELXT program (2A) and refined by full-matrix least-squares methods, on F^2's, in SHELXL (2B). The non-hydrogen atoms were refined with anisotropic thermal parameters. The hydrogen atom on N(2) was located in a difference map. All the hydrogen atoms were included in idealised positions and their Uiso values were set to ride on the Ueq values of the parent carbon or nitrogen atoms. At the conclusion of the refinement, wR_2 = 0.157 and R_1 = 0.060 (2B) for all 3042 reflections weighted $w = [\sigma^2(F_o^2) + (0.1025\ P)^2 + 0.2160\ P]^{-1}$ with $P = (F_o^2 + 2F_c^2)/3$; for the 'observed' data only, R_1 = 0.055.

In the final difference map, the highest peak (*ca* 0.55 $eÅ^{-3}$) was near C(13).

Scattering factors for neutral atoms were taken from reference (3). Computer programs used in this analysis have been noted above, and were run through WinGX (4) on a Dell Optiplex 780 PC at the University of East Anglia.

References

(25) Programs CrysAlisPro, Rigaku Oxford Diffraction Ltd., Abingdon, UK (2018).

(26) G. M. Sheldrick, Programs for crystal structure determination (SHELXT), *Acta Cryst.* (2015) A**71**, 3-8, and refinement (SHELXL), *Acta Cryst.* (2008) A**64**, 112-122 and (2015) C**71**, 3-8.

(27) *'International Tables for X-ray Crystallography'*, Kluwer Academic Publishers, Dordrecht (1992). Vol. C, pp. 500, 219 and 193.

(28) L. J. Farrugia, *J. Appl. Cryst.* (2012) **45**, 849–854.

Legends for Figures

Figure 1. View of a molecule of C_8H_5N-NSO_2CF_3-1,CHC_6H_4OMe-3, indicating the atom numbering scheme. Thermal ellipsoids are drawn at the 50% probability level.

Figure 2. View of the packing of molecules, along the *b* axis.

Figure 3. Showing the stacking of molecules parallel to the *a* axis.

Notes on the structure.

The isoindole group forms the central plane of the molecule. The normal to the phenyl group is rotated 14.3 ° from that of the isoindole group and the SO_2-CF_3 group provides the only significantly displaced atoms from the major planar units.

The pyrrole hydrogen atom was recognised in difference maps and forms a good intramolecular hydrogen bond with O(121), Figure 1.

Molecules are stacked, principally through the π…π interactions between overlapping isoindole rings, in columns parallel to the *a* axis, Figures 2 and 3, with interplanar distances of 3.000 and 3.319 Å, either side of the isoindole plane. The phenyl ring partially overlaps its symmetry neighbour on one side at a distance of 3.59 Å; there are no π…π interactions on the opposing side.

Crystal data and structure refinement for an isoindoline derivative: C_8H_4NH-{CH-C_6H_4-O$(CH_2)_4$Me},-{NSO_2-C_6H_4Me}

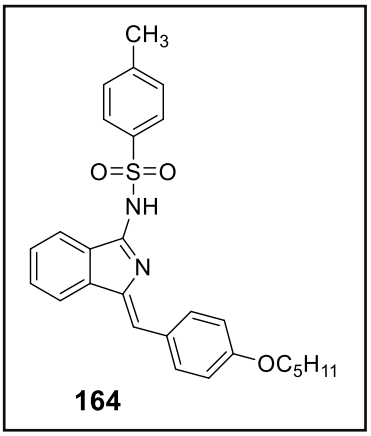

164

Identification code	**164**
Elemental formula	C27 H28 N2 O3 S
Formula weight	460.57
Crystal system, space group	Triclinic, P-1 (no. 2)
Unit cell dimensions	a = 9.72837(12) Å α = 102.8528(10) ° b = 11.21343(12) Å β = 109.6048(12) ° c = 11.52630(15) Å γ = 92.8657(9) °
Volume	1144.13(2) $Å^3$
Z, Calculated density	2, 1.337 Mg/m^3
F(000)	488
Absorption coefficient	0.174 mm^{-1}
Temperature	99.98(15) K
Wavelength	0.71073 Å
Crystal colour, shape	yellow block
Crystal size	0.238 x 0.094 x 0.062 mm
Crystal mounting:	in a small loop, in oil, fixed in cold N_2 stream
On the diffractometer:	
Theta range for data collection	1.880 to 27.497 °
Limiting indices	-12<=h<=12, -14<=k<=14, -14<=l<=14
Completeness to theta = 25.242	100.0 %
Absorption correction	Semi-empirical from equivalents
Max. and min. transmission	1.0000 and 0.9265
Reflections collected (not including absences)	31925
No. of unique reflections	5220 [R(int) for equivalents = 0.024]
No. of 'observed' reflections ($I > 2\sigma_I$)	4840
Structure determined by:	dual methods, in SHELXT

Refinement:	Full-matrix least-squares on F^2, in SHELXL
Data / restraints / parameters	5220 / 0 / 299
Goodness-of-fit on F^2	1.057
Final R indices ('observed' data)	R_1 = 0.031, wR_2 = 0.087
Final R indices (all data)	R_1 = 0.033, wR_2 = 0.088
Reflections weighted: $w = [\sigma^2(Fo^2)+(0.0468P)^2+0.4434P]^{-1}$ where $P=(Fo^2+2Fc^2)/3$	
Extinction coefficient	n/a
Largest diff. peak and hole	0.39 and -0.38 e.Å^{-3}
Location of largest difference peak	near C(21)

Table 1. Atomic coordinates (x 10^5) and equivalent isotropic displacement parameters ($Å^2$ x 10^4). U(eq) is defined as one third of the trace of the orthogonalized Uij tensor. E.s.ds are in parentheses.

	x	y	z	U(eq)
C(1)	58583(11)	59534(9)	66246(10)	149(2)
C(2)	69839(12)	62734(10)	61880(10)	176(2)
C(3)	67899(12)	70116(10)	53503(11)	182(2)
C(4)	54474(12)	74582(9)	48984(10)	157(2)
C(5)	43086(12)	71554(10)	53092(10)	164(2)
C(6)	45257(12)	64189(10)	61637(10)	165(2)
C(10)	61946(11)	51900(9)	75300(10)	153(2)
N(11)	37981(10)	45362(8)	76961(8)	146(2)
C(12)	53349(11)	46014(9)	79924(9)	143(2)
C(13)	58195(12)	38481(9)	89023(9)	145(2)
C(14)	72155(12)	35733(10)	95399(10)	171(2)
C(15)	73151(12)	28242(10)	103689(10)	193(2)
C(16)	60714(13)	23640(10)	105748(10)	196(2)
C(17)	46823(12)	26329(10)	99379(10)	172(2)
C(18)	45828(11)	33751(9)	91016(10)	144(2)
C(19)	32930(12)	38150(9)	83092(9)	143(2)
N(20)	19478(10)	35175(8)	82615(9)	165(2)
S(2)	5529(3)	40241(2)	73698(2)	158.3(8)
O(21)	9698(9)	50971(7)	69885(8)	205(2)
O(22)	-5076(9)	41361(8)	79925(8)	247(2)
C(21)	-2026(11)	28111(10)	59644(10)	159(2)
C(22)	-7005(12)	16494(10)	60329(11)	189(2)
C(23)	-13449(12)	7205(10)	49175(12)	210(2)
C(24)	-14929(12)	9269(11)	37313(11)	216(2)
C(25)	-9907(12)	20987(11)	36908(11)	211(2)
C(26)	-3529(12)	30423(10)	47962(11)	186(2)
C(27)	-21737(14)	-894(12)	25233(12)	293(3)
O(4)	53684(9)	81881(7)	40793(7)	185(2)
C(41)	39867(12)	86423(10)	35936(10)	174(2)
C(42)	41200(13)	94519(10)	27377(10)	183(2)
C(43)	26771(13)	99628(10)	21900(11)	216(2)
C(44)	28044(15)	108479(11)	13849(12)	266(3)
C(45)	14265(16)	114669(13)	9300(14)	373(3)

Table 2. Molecular dimensions. Bond lengths are in Ångstroms, angles in degrees. E.s.ds are in parentheses.

C(1)-C(6)	1.4016(14)
C(1)-C(2)	1.4114(14)
C(1)-C(10)	1.4578(14)
C(2)-C(3)	1.3792(15)
C(3)-C(4)	1.3975(15)
C(4)-O(4)	1.3669(12)
C(4)-C(5)	1.3973(14)
C(5)-C(6)	1.3916(14)
C(10)-C(12)	1.3490(15)
N(11)-C(19)	1.3573(13)
N(11)-C(12)	1.4116(13)
C(12)-C(13)	1.4621(14)
C(13)-C(14)	1.3972(14)
C(13)-C(18)	1.3991(15)
C(14)-C(15)	1.3897(15)
C(15)-C(16)	1.4040(16)
C(16)-C(17)	1.3891(15)
C(17)-C(18)	1.3905(14)
C(18)-C(19)	1.4647(14)
C(19)-N(20)	1.3141(14)
N(20)-S(2)	1.6191(9)
S(2)-O(22)	1.4371(8)
S(2)-O(21)	1.4531(8)
S(2)-C(21)	1.7707(11)
C(21)-C(26)	1.3887(15)
C(21)-C(22)	1.3951(15)
C(22)-C(23)	1.3888(16)
C(23)-C(24)	1.3985(17)
C(24)-C(25)	1.3948(17)
C(24)-C(27)	1.5085(16)
C(25)-C(26)	1.3900(16)
O(4)-C(41)	1.4387(13)
C(41)-C(42)	1.5121(14)
C(42)-C(43)	1.5309(16)
C(43)-C(44)	1.5285(15)
C(44)-C(45)	1.5287(19)

C(6)-C(1)-C(2)	116.84(9)
C(6)-C(1)-C(10)	125.95(9)
C(2)-C(1)-C(10)	117.20(9)
C(3)-C(2)-C(1)	121.84(10)
C(2)-C(3)-C(4)	120.22(10)
O(4)-C(4)-C(5)	124.87(10)
O(4)-C(4)-C(3)	115.76(9)
C(5)-C(4)-C(3)	119.37(10)
C(6)-C(5)-C(4)	119.74(10)
C(5)-C(6)-C(1)	121.98(10)
C(12)-C(10)-C(1)	131.84(10)
C(19)-N(11)-C(12)	112.67(9)
C(10)-C(12)-N(11)	128.85(10)
C(10)-C(12)-C(13)	126.26(10)
N(11)-C(12)-C(13)	104.87(9)
C(14)-C(13)-C(18)	120.41(10)
C(14)-C(13)-C(12)	131.43(10)
C(18)-C(13)-C(12)	108.15(9)
C(15)-C(14)-C(13)	117.44(10)
C(14)-C(15)-C(16)	121.83(10)
C(17)-C(16)-C(15)	120.78(10)
C(16)-C(17)-C(18)	117.33(10)
C(17)-C(18)-C(13)	122.21(10)
C(17)-C(18)-C(19)	129.90(10)
C(13)-C(18)-C(19)	107.89(9)
N(20)-C(19)-N(11)	130.42(10)
N(20)-C(19)-C(18)	123.17(9)
N(11)-C(19)-C(18)	106.40(9)
C(19)-N(20)-S(2)	121.50(8)
O(22)-S(2)-O(21)	117.15(5)

O(22)-S(2)-N(20) 107.00(5)
O(21)-S(2)-N(20) 113.16(5)
O(22)-S(2)-C(21) 107.43(5)
O(21)-S(2)-C(21) 106.68(5)
N(20)-S(2)-C(21) 104.56(5)
C(26)-C(21)-C(22) 120.60(10)
C(26)-C(21)-S(2) 119.48(8)
C(22)-C(21)-S(2) 119.86(8)
C(23)-C(22)-C(21) 119.23(10)
C(22)-C(23)-C(24) 121.21(11)
C(25)-C(24)-C(23) 118.32(11)
C(25)-C(24)-C(27) 120.61(11)
C(23)-C(24)-C(27) 121.07(11)
C(26)-C(25)-C(24) 121.29(11)
C(21)-C(26)-C(25) 119.34(10)
C(4)-O(4)-C(41) 116.40(8)
O(4)-C(41)-C(42) 108.84(9)
C(41)-C(42)-C(43) 111.20(9)
C(44)-C(43)-C(42) 112.45(10)
C(43)-C(44)-C(45) 113.59(11)

Table 3. Anisotropic displacement parameters ($Å^2$ x 10^4) for the expression: exp $\{-2\pi^2(h^2a^{*2}U_{11} + ... + 2hka^*b^*U_{12})\}$ E.s.ds are in parentheses.

	U_{11}	U_{22}	U_{33}	U_{23}	U_{13}	U_{12}
C(1)	157(5)	134(5)	150(5)	36(4)	48(4)	21(4)
C(2)	139(5)	186(5)	205(5)	65(4)	53(4)	40(4)
C(3)	159(5)	195(5)	215(5)	70(4)	85(4)	22(4)
C(4)	182(5)	138(5)	149(5)	49(4)	49(4)	15(4)
C(5)	149(5)	165(5)	187(5)	68(4)	55(4)	41(4)
C(6)	155(5)	174(5)	186(5)	68(4)	72(4)	30(4)
C(10)	143(5)	154(5)	158(5)	42(4)	43(4)	41(4)
N(11)	135(4)	165(4)	150(4)	76(3)	39(3)	38(3)
C(12)	141(5)	143(5)	131(5)	32(4)	27(4)	44(4)
C(13)	167(5)	137(5)	121(5)	27(4)	40(4)	38(4)
C(14)	160(5)	188(5)	155(5)	38(4)	45(4)	42(4)
C(15)	189(5)	213(5)	156(5)	55(4)	20(4)	81(4)
C(16)	241(6)	199(5)	146(5)	81(4)	39(4)	68(4)
C(17)	201(5)	173(5)	144(5)	56(4)	52(4)	30(4)
C(18)	155(5)	139(5)	121(4)	28(4)	28(4)	38(4)
C(19)	168(5)	134(4)	116(4)	33(4)	35(4)	32(4)
N(20)	145(4)	186(4)	167(4)	81(3)	37(3)	32(3)
S(2)	129.1(13)	182.0(14)	169.3(13)	67.6(10)	42.0(10)	45.3(9)
O(21)	186(4)	178(4)	235(4)	93(3)	26(3)	39(3)
O(22)	190(4)	338(5)	246(4)	85(4)	105(3)	94(3)
C(21)	104(4)	191(5)	183(5)	64(4)	38(4)	41(4)
C(22)	152(5)	219(5)	226(5)	109(4)	68(4)	56(4)
C(23)	161(5)	180(5)	292(6)	85(4)	65(4)	47(4)
C(24)	143(5)	231(6)	238(6)	39(4)	27(4)	71(4)
C(25)	181(5)	276(6)	175(5)	89(4)	36(4)	71(4)
C(26)	151(5)	208(5)	215(5)	96(4)	54(4)	41(4)
C(27)	252(6)	267(6)	270(6)	6(5)	12(5)	69(5)
O(4)	188(4)	199(4)	210(4)	115(3)	82(3)	41(3)
C(41)	182(5)	173(5)	177(5)	73(4)	57(4)	36(4)
C(42)	233(5)	158(5)	161(5)	61(4)	63(4)	16(4)
C(43)	243(6)	180(5)	200(5)	80(4)	30(4)	12(4)
C(44)	371(7)	203(5)	211(6)	97(4)	59(5)	36(5)
C(45)	368(7)	259(6)	360(7)	154(6)	-77(6)	-14(6)

Table 4. Hydrogen coordinates (x 10^4) and isotropic displacement parameters ($Å^2$ x 10^3). All hydrogen atoms were included in idealised positions with U(iso)'s set at 1.2*U(eq) or, for the methyl group hydrogen atoms, 1.5*U(eq) of the parent carbon atoms.

	x	y	z	U(iso)
H(2)	7882	5978	6473	21
H(3)	7555	7213	5085	22
H(5)	3409	7445	5013	20
H(6)	3764	6230	6437	20
H(10)	7184	5090	7847	18
H(11)	3242	4913	7183	18
H(14)	8046	3880	9414	21
H(15)	8231	2622	10799	23
H(16)	6179	1873	11144	24
H(17)	3852	2329	10066	21
H(22)	-602	1499	6816	23
H(23)	-1684	-53	4960	25
H(25)	-1084	2252	2909	25
H(26)	-30	3821	4754	22
H(27A)	-2272	-863	2733	44
H(27B)	-1555	-131	2023	44
H(27C)	-3128	79	2045	44
H(41A)	3740	9115	4293	21
H(41B)	3210	7956	3117	21
H(42A)	4376	8975	2046	22
H(42B)	4904	10132	3220	22
H(43A)	1909	9281	1669	26
H(43B)	2392	10392	2884	26
H(44A)	3000	10395	648	32
H(44B)	3638	11482	1882	32
H(45A)	1577	12008	432	56
H(45B)	600	10847	419	56
H(45C)	1238	11934	1653	56

Table 5. Torsion angles, in degrees. E.s.ds are in parentheses.

C(6)-C(1)-C(2)-C(3) 0.17(16)	C(12)-N(11)-C(19)-C(18) 1.18(11)
C(10)-C(1)-C(2)-C(3)- 178.71(10)	C(17)-C(18)-C(19)-N(20)- 1.71(17)
C(1)-C(2)-C(3)-C(4)-0.58(17)	C(13)-C(18)-C(19)-N(20) 178.87(10)
C(2)-C(3)-C(4)-O(4) 179.59(10)	C(17)-C(18)-C(19)-N(11) 178.40(10)
C(2)-C(3)-C(4)-C(5) 0.37(16)	C(13)-C(18)-C(19)-N(11)- 1.02(11)
O(4)-C(4)-C(5)-C(6)- 178.92(10)	N(11)-C(19)-N(20)-S(2)- 0.05(16)
C(3)-C(4)-C(5)-C(6) 0.22(16)	C(18)-C(19)-N(20)-S(2)- 179.92(8)
C(4)-C(5)-C(6)-C(1)-0.63(16)	C(19)-N(20)-S(2)-O(22)- 149.17(9)
C(2)-C(1)-C(6)-C(5) 0.44(16)	C(19)-N(20)-S(2)-O(21)- 18.64(10)
C(10)-C(1)-C(6)-C(5) 179.20(10)	C(19)-N(20)-S(2)-C(21) 97.06(9)
C(6)-C(1)-C(10)-C(12) 11.15(19)	O(22)-S(2)-C(21)-C(26) 123.27(9)
C(2)-C(1)-C(10)-C(12)- 170.09(11)	O(21)-S(2)-C(21)-C(26)- 3.13(10)
C(1)-C(10)-C(12)-N(11) 1.52(19)	N(20)-S(2)-C(21)-C(26)- 123.26(9)
C(1)-C(10)-C(12)-C(13) 179.49(10)	O(22)-S(2)-C(21)-C(22)- 53.90(10)
C(19)-N(11)-C(12)-C(10) 177.43(10)	O(21)-S(2)-C(21)-C(22) 179.71(8)
C(19)-N(11)-C(12)-C(13)- 0.87(11)	N(20)-S(2)-C(21)-C(22) 59.57(9)
C(10)-C(12)-C(13)-C(14) 2.24(18)	C(26)-C(21)-C(22)-C(23) 0.28(16)
N(11)-C(12)-C(13)-C(14)- 179.40(10)	S(2)-C(21)-C(22)-C(23) 177.42(8)
C(10)-C(12)-C(13)-C(18)- 178.19(10)	C(21)-C(22)-C(23)-C(24) 0.47(16)
N(11)-C(12)-C(13)-C(18) 0.18(11)	C(22)-C(23)-C(24)-C(25)- 0.72(16)
C(18)-C(13)-C(14)-C(15)- 0.17(15)	C(22)-C(23)-C(24)-C(27) 179.12(10)
C(12)-C(13)-C(14)-C(15) 179.36(10)	C(23)-C(24)-C(25)-C(26) 0.23(16)
C(13)-C(14)-C(15)-C(16)- 0.55(16)	C(27)-C(24)-C(25)-C(26)- 179.61(10)
C(14)-C(15)-C(16)-C(17) 0.80(17)	C(22)-C(21)-C(26)-C(25)- 0.76(16)
C(15)-C(16)-C(17)-C(18)- 0.31(16)	S(2)-C(21)-C(26)-C(25)- 177.91(8)
C(16)-C(17)-C(18)-C(13)- 0.41(16)	C(24)-C(25)-C(26)-C(21) 0.50(17)
C(16)-C(17)-C(18)-C(19)- 179.76(10)	C(5)-C(4)-O(4)-C(41)-1.58(15)
C(14)-C(13)-C(18)-C(17) 0.66(16)	C(3)-C(4)-O(4)-C(41) 179.26(9)
C(12)-C(13)-C(18)-C(17)- 178.97(9)	C(4)-O(4)-C(41)-C(42) 178.57(8)
C(14)-C(13)-C(18)-C(19)- 179.87(9)	O(4)-C(41)-C(42)-C(43) 179.95(8)
C(12)-C(13)-C(18)-C(19) 0.51(11)	C(41)-C(42)-C(43)-C(44) 176.52(9)
C(12)-N(11)-C(19)-N(20)- 178.70(11)	C(42)-C(43)-C(44)-C(45)- 174.52(10)

Table 6. Hydrogen bonds, in Ångstroms and degrees.

D-H...A	d(D-H)	d(H...A)	d(D...A)	<(DHA)
C(10)-H(10)...O(22)#1	0.93	2.51	3.3890(13)	158.4
N(11)-H(11)...O(21)	0.86	2.17	2.7434(12)	123.7
C(26)-H(26)...O(21)#2	0.93	2.51	3.1860(13)	129.7

Symmetry transformations used to generate equivalent atoms:
#1 : x+1, y, z #2 : -x, 1-y, 1-z

Crystal structure analysis of an isoindoline derivative, C_8H_4NH-{CH-C_6H_4-$O(CH_2)_4Me$},-{NSO_2-C_6H_4Me}

Crystal data: $C_{27}H_{28}N_2O_3S$, M = 460.57. Triclinic, space group P-1 (no. 2), a = 9.72837(12), b = 11.21343(12), c = 11.52630(15) Å, α = 102.8528(10), β = 109.6048(12), γ = 92.8657(9) °, V = 1144.13(2) $Å^3$. Z = 2, Dc = 1.337 g cm^{-3}, F(000) = 488, T = 99.98(15) K, . μ(Mo-Kα) = 1.74 cm^{-1}, λ(Mo-Kα) = 0.71073 Å.

The crystal was a yellow block. From a sample under oil, one, *ca* 0.062 x 0.094 x 0.062 mm, was mounted on a small loop and fixed in the cold nitrogen stream on a Rigaku Oxford Diffraction XtaLAB Synergy diffractometer, equipped with Mo-Kα radiation, HyPix detector and mirror monochromator. Intensity data were measured by thin-slice ω-scans. Total no. of reflections recorded, to θ_{max} = 72.5°, was 31925 of which 5220 were unique (Rint = 0.024); 4840 were 'observed' with $I > 2\sigma_I$.

Data were processed using the CrysAlisPro-CCD and -RED (1) programs. The structure was determined by the intrinsic phasing routines in the SHELXT program (2A) and refined by full-matrix least-squares methods, on F^2's, in SHELXL (2B). The non-hydrogen atoms were refined with anisotropic thermal parameters. The hydrogen atoms were included in idealised positions and their Uiso values were set to ride on the Ueq values of the parent carbon or nitrogen atoms. At the conclusion of the refinement, wR_2 = 0.088 and R_1 = 0.033 (2B) for all 5220 reflections weighted w = $[\sigma^2(F_o^2) + (0.0468\ P)^2 + 0.4434\ P]^{-1}$ with P = $(F_o^2 + 2F_c^2)/3$; for the 'observed' data only, R_1 = 0.031.

In the final difference map, the highest peak (*ca* 0.39 $eÅ^{-3}$) was near C(21).

Scattering factors for neutral atoms were taken from reference (3). Computer programs used in this analysis have been noted above, and were run through WinGX (4) on a Dell Optiplex 780 PC at the University of East Anglia.

References

(29) Programs CrysAlisPro, Rigaku Oxford Diffraction Ltd., Abingdon, UK (2018).

(30) G. M. Sheldrick, Programs for crystal structure determination (SHELXT), *Acta Cryst.* (2015) A**71**, 3-8, and refinement (SHELXL), *Acta Cryst.* (2008) A**64**, 112-122 and (2015) C**71**, 3-8.

(31) *'International Tables for X-ray Crystallography'*, Kluwer Academic Publishers, Dordrecht (1992). Vol. C, pp. 500, 219 and 193.

(32) L. J. Farrugia, *J. Appl. Cryst.* (2012) **45**, 849–854.

Legends for Figures

Figure 1. View of a molecule of the isoindoline derivative, indicating the atom numbering scheme. Thermal ellipsoids are drawn at the 50% probability level.

Figure 2. View of the packing of molecules, along the *b* axis.